Mutually Adaptive Shared Control between Human Operator and Autonomy in Ground Vehicles

by

Yifan Weng

A dissertation submitted in partial fulfillment
of the requirements for the degree of
Doctor of Philosophy
(Mechanical Engineering)
in the University of Michigan
2022

Doctoral Committee:

Associate Research Scientist Tulga Ersal, Co-Chair
Professor Jeffrey L. Stein, Co-Chair
Dr. Mark J. Brudnak
Professor Brent Gillespie
Dr. Paramsothy Jayakumar
Associate Professor Xi Jessie Yang

Yifan Weng

wenyifan@umich.edu

ORCID iD: 0000-0002-3381-8904

For my family.

Acknowledgments

First of all, I would like to express my sincere gratitude to my advisors, Dr. Tulga Ersal and Prof. Jeffrey L. Stein, for their guidance and support in this research. Dr. Tulga Ersal provides very helpful advice with insight as a great mentor. He gives freedom to me to explore different ideas. He is very patient in helping me overcome the difficulties during my research journey, which is very helpful during the pandemic. In addition, he provides great help in improving my technical writing as well as presentation skills, which are critical skills for researchers. Prof. Jeffrey L. Stein has been very helpful during my research journey. I always appreciate his constructive advice, which highlights the major points of the research project. I have learned a lot from his opinions and guidance with kindness. In conclusion, I am privileged to work with Dr. Ersal and Prof. Stein in my career.

I would also express my sincere gratitude to Prof. Xi J. Yang, who provides advice from a field other than the one I am working in. As a collaborator, Prof. Yang gives very professional advice as an expert in human factor. In addition, her support and patience are the keys to the success of this research project.

I am grateful for all the people who have participated in this research and provided critical feedback. It is a pleasure to work with Dr. Paramsothy Jayakumar and Dr. Mark J. Brudnak. They can always provide timely feedback from a different perspective that I can't think about. I want to convey my gratitude to Prof. Brent Gillespie for bringing his expertise and giving constructive suggestions to this work. I also appreciate the help and advice from Dr. Vishnu Desaraju in both the academic area and internship at Toyota Research Institute.

I would like to acknowledge the Automotive Research Center (ARC), Toyota Re-

search Institute, and Rackham Graduate School for supporting and funding this research.

As a member of the Ersal Research Group, I appreciate the help and friendship of my colleagues: Dr. Xinyi Ge, Dr. Yingshi Zheng, Dr. Alireza Goshtasbi, Dr. Huckleberry Febbo, Dr. John Wurts, Dr. James Dallas, Chen Li, Siyuan Yu, Congkai Shen, Zheng Dong, Kshitij Jain, and Yue Tang.

I am grateful for my collaborator in the Interaction and Collaboration Research Lab (ICRL), Dr. Ruikun Luo. I appreciate his fruitful work in the workload estimation area. I have learned a lot from him and enjoy working with him.

Finally, I want to express my deepest gratitude to my family, who have provided endless love and support. In particular, I want to thank my mother, Haiying Gu, and my father, Zhiwei Weng, for their kindness, patience, and love. Their support and impact are the keys to the success of this work.

Table of Contents

List of Tables

List of Figures

Abstract

Semi-autonomous driving can leverage the benefits of self-driving vehicle technologies today, even if the latter may still be limited in scope and reliability for fully autonomous driving. In semi-autonomous driving, the human driver collaborates with autonomy to control the vehicle. Among the various frameworks to enable this collaboration, this thesis focuses on the haptic shared control framework, because it allows for a continuous negotiation between the two agents, which has been shown to be beneficial over discrete transition schemes.

An essential question for shared control is how to allocate the control authority between the two agents. The literature presents static and adaptive schemes, the latter allowing for better driving performance. To date, several vehicle and human factors have been considered for adaptation, but a crucial human factor has been omitted: workload. Workload represents the availability of the driver's mental resources and is important especially when the driver engages in multiple tasks as expected in a semi-autonomous driving setting. Therefore, the overarching goal of this thesis is to develop adaptive haptic shared control schemes for semi-autonomous driving that take workload into account and evaluate their benefits over non-adaptive schemes.

To achieve this goal, this thesis develops workload-adaptive control schemes at two levels. The first adaptation developed is at the control consolidation level, i.e., after the autonomy commands are generated and during their blending with the human's commands. The developed scheme modulates autonomy commands as a function of driver workload. Human subject studies are used to assess the performance of the developed schemes, where the subjects' goal in the driving task is to track a path with the help of autonomy and complete a surveillance task simultaneously. Results

from the human subject studies reveal that compared with the non-adaptive control consolidation, the developed adaptive control consolidation scheme can achieve similar driving performance with less control effort from the human under the conditions when there is a minor disagreement between agents. Under conditions where there are significant disagreements between the two agents in the perception of the path center, the adaptive control consolidation can reduce workload, path tracking error, and control effort while increasing trust.

The second adaptation is developed within the autonomy. It enables adaptation of the autonomy's control commands independent of how they are blended with the human's control command. Results show that, compared with non-adaptive cases with different maximum speed limits, it can balance the driving performance, duration, emergency maneuvering performance, human's control effort under emergency, and self-reported workload while reducing the control effort in the lane-keeping task.

Finally, simultaneous adaptation at both levels is also evaluated through human subject tests. Results show that when both adaptive schemes are used, they can balance driving performance, duration, and workload with less steering effort from the human when compared with the non-adaptive cases. Compared to using adaptive autonomy alone, adding the adaptive control consolidation further reduces the control effort under emergency conditions and the driving duration. Compared to using the adaptive control consolidation alone, adding the adaptive autonomy reduces the control effort in the lane-keeping task and achieves a more robust driving performance.

Therefore, this dissertation makes the following original contributions:

1. A workload-adaptive control consolidation scheme and its performance evaluation.

2. A workload-adaptive autonomy and its performance evaluation.

3. Evaluation when adaptation happens in both control consolidation and autonomy.

Chapter 1

Introduction

This work develops adaptive haptic shared control schemes for semi-autonomous ground vehicles that take the driver's workload into account.

Three bodies of literature research motivate this work and provide the foundation upon which this work stands. They are (1) the shared control consolidation in semi-autonomous vehicles, (2) the definition of the workload and why it is an important human factor to consider in designing shared control systems, and (3) the autonomy used in shared control systems. They are reviewed in detail below.

1.1 Motivation and Background

1.1.1 Shared Control Consolidations in Semi-autonomous Vehicle

Autonomous driving promises a vision that it will offer many benefits, such as allowing the human driver to pay attention to tasks other than driving [1], as well as improving fuel efficiency [2, 3], traffic flow [4], and safety [5, 6].

However, autonomous driving can be used only in limited operational domains so far [7, 8]. Several accidents indicate that autonomous driving is still under development [9]. Furthermore, in [10], researchers who won the DARPA Urban Grand Challenge find that it is still beneficial to include some help from human operators

in the autonomous vehicle they developed, especially when recovering from failure cases. Therefore, the autonomous driving technology is currently limited in scope and reliability.

Alternatively, semi-autonomous driving is a method to bridge the gap and leverage some of the benefits of autonomous driving before fully autonomous driving becomes possible [11]. Both the human driver and autonomy are in the control loop in the semi-autonomous mode. A control consolidation algorithm decides the resultant control commands from the agents' commands. This collaborative control paradigm between the human driver and autonomy belongs to a category of human-machine teaming problem: shared control.

One important research question in shared control of a vehicle is how to allocate control authority between agents when more than one agent generates commands to control the vehicle. When the hierarchy of authority is considered, prior literature on shared control of a vehicle gives two perspectives: supervisory and cooperative.

In supervisory shared control, one agent acts as the supervisor and monitors the other agent's commands. The supervisor has the capability of determining the final control commands. Therefore, the supervisor has the ultimate control authority. A Level 2 automation [12] can be considered supervisory shared control where the human driver acts as the supervisor. The human driver monitors the vehicle's states and decides if the autonomy's driving behavior is satisfactory or if it is necessary for the human to take over. On the other hand, autonomy can act as the supervisor, as well. In [13, 14, 15, 16], autonomy monitors the control commands from the human driver and decides whether it is necessary to make modifications based on its own assessment, which is typically based on safety metrics. As such, supervisory control is a serial framework where the supervisor is the downstream agent whose control decision, including pass-through vs. override [17] or modify [18], is the final decision and executed by the vehicle.

In cooperative shared control, the control commands from both agents influence the vehicle; i.e., both agents have control authority. There are different ways to coordinate the control commands from both agents.

One way is to blend the steering angle commands from both agents to generate the final commands for the vehicle. An arbitrator is used to determine which control commands have more weight in the final command [19, 20, 21, 22, 23, 24, 25]

The arbitrator can be designed using different metrics. For example, in [19, 20, 21], researchers develop the arbitrators using the front wheel sideslip to assess threats. In [24], researchers set the weights of the control commands from both agents based on the difference between the actual human input and desired human input calculated by a parallel driver model. In this type of cooperative shared control scheme, the human operator feels the impact of their commands from the vehicle's response after the final control commands take effect. Therefore, the control loop closes after the steering wheel.

The other way is to merge the torques from both agents through a common steering wheel, which is also called haptic shared control. In this type of shared control, both agents reflect their intention by applying steering torque on the common steering wheel. By sensing the torque from the other one, an agent can infer the other's intention and react correspondingly, which can be considered a process of continuous negotiation. Because the steering wheel is common with a single resultant steering angle, the agents can feel the impact of their decision on the final steering angle command immediately after exerting their torque. Hence, the loop is closed at the steering wheel in this type of shared control.

Considering the potential benefits of such continuous negotiation [26] at the steering wheel, researchers have developed some haptic shared control frameworks and tested their performance [27, 28, 29, 30, 31, 32, 33, 34]. Some typical examples are listed as follows. In [27], researchers demonstrate that the haptic shared control improves the driving performance while reducing visual demand or shortening the reaction time in the secondary task when participants perform a dual-task mission. In [30], researchers design a haptic-shared-control-based assistance system and find that it can reduce drivers' workload and enhance drivers' skills in the backward parking scenario. In [28], researchers develop two haptic shared control schemes with bandwidth guidance as well as continuous guidance. Results show that both schemes help

reduce drivers' errors in the lane-keeping mission. Furthermore, in [29], researchers compare the haptic shared control with supervisory control modes and find the haptic shared control yields better overall performance in an obstacle avoidance scenario. Given these results and the benefit of the continuous negotiation, this dissertation focuses on haptic shared control schemes.

In haptic shared control schemes, the assistance level of the autonomy decides the magnitude of the autonomy's torque applied on the steering wheel. Therefore, it determines how hard it is for the human driver to negotiate with the autonomy. Hence, the autonomy's assistance level offers a means to introduce adaptation into the haptic shared control framework.

Although early research focuses on the haptic shared control schemes with fixed assistance level by designing the haptic interface as a virtual spring with fixed impedance [27, 35], later work starts to focus on varying assistance level schemes. One large group of the varying assistance level designs focuses on the vehicle-performance metrics. For example, in [28], researchers change the impedance of the virtual spring so that the assistance level is changed when the lateral error of the vehicle exceeds a designed threshold. In [36], researchers design the adaptive assistance level based on the time-to-line crossing (TLC).

The other group focuses on human factors. For example, in [37], researchers design the assistance level of the haptic system using driver activity, which is driver's torque. In [38, 39], researchers adopt both attention and human torque as the factors to adapt the assistance level. In [40, 41], the researchers use drowsiness and distraction as the factors. In [42, 43], the researchers state the benefits of taking the neuromuscular behavior into account when designing the haptic shared control system.

These efforts have shown the importance of taking human factors into account in adapting the autonomy's assistance level in shared control. However, one important human factor, namely, workload, has not yet been considered.

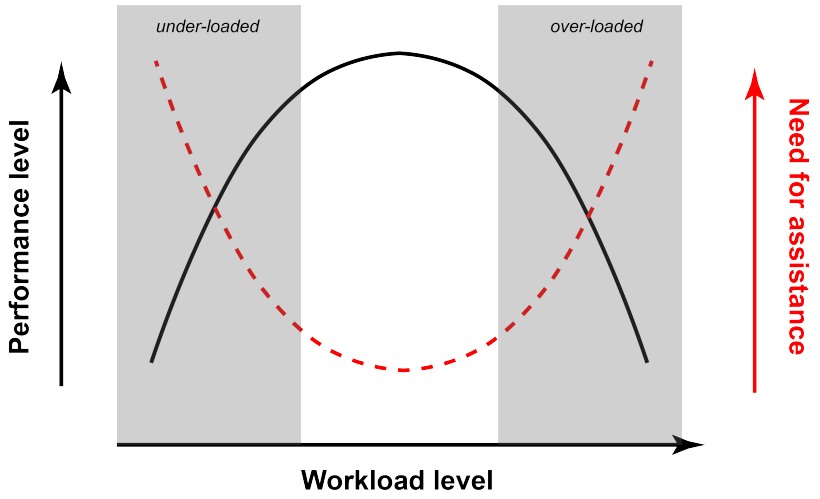

Figure 1.1: The relationship between mission performance (black line) [47, 48, 49, 50, 51]/need for assistance (red dashed line)[48] and workload

1.1.2 Workload

Workload is defined as a relative concept [44]. In [45], researchers claim that the capacity that humans use to process and respond to information is limited. Therefore, the workload is defined as "the portion of the operator's limited capacity actually required to perform a particular task." Another definition of workload is "the relation between the function relating the mental resources demanded by a task and those resources available to be supplied by the human operator" [46].

Workload is an important human factor that impacts performance. In [47, 48, 49], researchers show an inverted "U-shaped" curve to represent the relationship between the performance and the workload as shown in Fig. 1.1. In [50, 51], researchers find that it can be seen as an extension to include workload from Yerkes-Dodson law [52], which initially relates arousal to performance and proposes a similar inverted "U-shaped" curve. Prior literature finds that performance suffers from both under-loaded conditions and over-loaded conditions. On the one hand, in [53, 54, 55], the researchers find a drop in mission performance when the drivers are over-loaded. The worse performance in the over-loaded condition can be explained by inattention or fatigue driving [56, 57]. On the other hand, in [58, 59], researchers argue that the drivers may underestimate the need to maintain task-direct effort, leading to a

performance drop in under-loaded conditions. In [60], researchers also argue that the vigilance decrement leads to sub-optimal performance when the workload of the subject is too low.

The impacts of workload on performance can also be observed when automation systems are involved. In [61], researchers show a performance drop in a supervisory shared control scenario between human and unmanned air vehicles equipped with an autonomy system when the subjects experience high workload conditions and act as the supervisor. In [62], researchers show that in the takeover scheme, workload can impact the takeover performance. Specifically, a high workload condition leads to a lower takeover readiness and worse performance in the takeover scenario. As another example, the performance of the secondary tasks suffers in a dual-task scenario when Tesla's autopilot is on and the human operator is experiencing the under-loaded condition [63]. A moderate workload is therefore preferable to achieve optimal performance [44, 48].

As a result, in [48], researchers suggest that the automation system should assess the state of the driver and provide additional support to relieve the driver in over-loaded and under-loaded conditions in shared control scenarios as shown in Fig. 1.1. However, the way to incorporate workload in shared control design remains an open question.

1.1.3 Autonomy in Shared Control

Not only can the control consolidation be adaptive to improve performance, but the autonomy used in shared control can also be adaptive. In the literature about shared control, two types of autonomy are presented. The first type of autonomy has its own reference trajectory and goal. In [19] where the final commands come from a weighted blend of two input steering angles, the Model Predictive Control method is used to generate the autonomy's steering input. The goal of autonomy is to minimize deviation from the centerline of a corridor and regulate the control commands. In haptic shared control, this type of autonomy can also be found. In [27], a geometric approach is used. The reference steering angle is calculated from the vehicle's position,

heading, and the closest point on the reference trajectory. In [29], the autonomy's control commands are generated from the model predictive control method. The goal of autonomy is to achieve a minimum deviation from the centerline with regulated control commands while avoiding obstacles it perceives.

The second type of autonomy considers the presence of the human operator's input commands. One large group of this type of autonomy can be found in supervisory shared control when autonomy acts as a supervisor. As described in Sec. 1.1.1, autonomy is the downstream agent who considers the commands of the human operator. In [18], the autonomy is designed to achieve a minimum interference from human input in the near future while the autonomy will follow the planned path afterward. In [13], the autonomy is designed to match the human's commands unless it is necessary to generate a significant deviation from the human's commands to ensure the safety of the vehicle. These two methods use the model predictive control method and assume the desired trajectory is known to the autonomy. Others use data-driven methods and learn the model from the data. In [64, 65], researchers use a data-driven method to achieve minimum deviation from the human's input without violating safety constraints. A Koopman operator learns the model, and the control spaces are sampled in these cases.

Autonomy that can incorporate the human operator's commands can also be found in the cooperative shared control. In [66], researchers use another human subject as the autonomy who steers a separate steering wheel, which is called the wizard-of-Oz method. There is a physical link between the human's steering wheel and autonomy's steering wheel. Therefore, the emulated autonomy considers the impact of the human operator's commands when making steering decisions. It can be viewed as a negotiation between two agents. Similar method is observed in [67], while instead of physical link, the researchers use a Proportional-Integral-Derivative (PID) controller to generate the torque using the force-feedback feature of the steering wheel. In [68, 69], researchers design a scheme where the controller tracks a modified trajectory. By considering the driver's torque and attention, the modified trajectory tries to achieve a trade-off between matching the driver's intended trajectory and

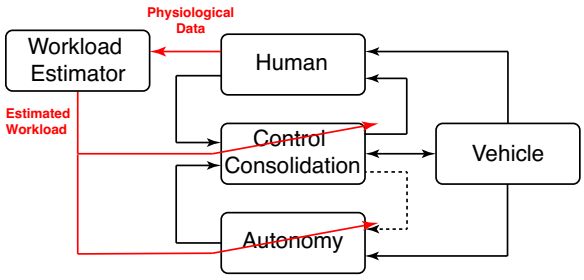

Figure 1.2: Illustration of the overarching goal.

following the original reference track.

In summary, while literature starts to consider the impact of human operators, adaptation to workload is not considered at the autonomy level. Incorporating workload in autonomy design remains an open question in the shared control domain.

1.2 Research Objectives and Research Questions

This dissertation develops and evaluates workload-adaptive haptic shared control schemes. The adaptation happens at both the control consolidation level and autonomy level, as shown in Fig 1.2.

To meet this objective, we pursue the following research questions:

- How can workload be taken into account in adaptive haptic shared control consolidation?
- Does the workload-adaptive haptic shared control consolidation improve mission performance in a multi-tasking driving scenario?
- How can workload be taken into account in the autonomy design within a haptic shared control framework?
- Does the workload-adaptive autonomy improve the mission performance in a multi-tasking driving scenario?
- Do the workload-adaptive control consolidation, and workload-adaptive autonomy improve mission performance when both of them are applied in a multi-tasking driving scenario?

1.3 Research Gaps and Milestones

After recognizing the importance of workload and the lack of its consideration in the existing adaptive shared control schemes, this thesis identifies two research gaps:

1. The state-of-the-art adaptive shared control schemes do not consider workload.
2. Adaptation to workload has not been considered at the autonomy level.

This dissertation fills these gaps by facilitating mutual understanding and adaptation in haptic shared control through novel workload-adaptive haptic shared control schemes at both control consolidation and autonomy levels.

This thesis documents the following milestones to address the research objective and answer the research questions shown in Sec. 1.2.

- Milestone 1: Implement the concept of haptic shared control in a driver-in-the-loop simulator.

  This thesis develops shared control schemes for semi-autonomous driving scenarios based on the haptic shared control framework. This work relies on human subject studies for evaluation. Therefore, a driver-in-the-loop testbed is developed with a force feedback steering wheel and other necessary sensors. It includes a real-time high-fidelity vehicle model, an autonomy that can generate real-time commands, and a visualization station that can emulate the real-time driving environment. The human subjects can use the testbed to finish a simulation-based driving task. Moreover, a secondary task is utilized to control the human driver's workload, forming a part of the dual-task scenario. The secondary task represents a surveillance task that is common in military missions.

- Milestone 2: Develop and evaluate a workload-adaptive haptic control consolidation

  The first adaptive scheme developed in this thesis is the adaptive control consolidation. It determines the assistance level from autonomy based on the driver's

workload, which correspondingly modifies the magnitude of autonomy's torque on the steering wheel. The adaptive control consolidation also considers other factors, such as driver's torque and eyes on road, which are helpful for assistance level modification. Human subject studies are conducted using the testbed from Milestone 1. Subjects are required to finish a mission that includes a driving task. The studies are conducted with the help of the real-time workload estimator developed by our collaborators, Dr. Ruikun Luo and Prof. Jessie Yang. The studies include different workload conditions and different driving conditions. The mission performance of the adaptive control consolidation is evaluated by comparing it to the performance when the baseline consolidation is implemented, i.e., non-adaptive control consolidation.

- Milestone 3: Identify the design parameters of autonomy that can impact the workload

  In the literature, several variables are found to have impacts on drivers' workload in the human driving mode, such as acceleration [70], speed [71], etc. These variables can also potentially impact the human driver's workload in the semi-autonomous driving mode. By changing some design parameters of the autonomy, these variables can be modified and workload managed correspondingly. This thesis identifies the parameter of autonomy with the most significant effect on workload in haptic shared control, namely the maximum speed limit. It becomes a candidate for the tuning parameter of the autonomy to enable the adaptation at the autonomy level. Human subject studies are conducted to validate the selected parameter with at least two different levels to find their relationships with workload.

- Milestone 4: Develop and evaluate a workload-adaptive autonomy whose parameters are identified in Milestone 3

  A workload-adaptive autonomy formulation is developed by leveraging the identified parameter and its relationships with workload from Milestone 3. In this design, the identified parameter adapts to workload as well as some other hu-

man factors, such as the human torque and steering rate. A human subject study is conducted to evaluate the mission performance when the developed workload-adaptive autonomy is implemented using a dual-task scenario for the mission. The study is conducted with the help of the real-time workload estimator, which is developed by our collaborators named above. Different workload conditions and different autonomy settings are included in this study. The mission performance of the adaptive autonomy is assessed by comparing it to the performance when different non-adaptive autonomy settings are implemented. The non-adaptive autonomy settings include different values of the identified parameter shown in Milestone 3.

- Milestone 5: Evaluate the performance of the adaptive schemes where the adaptations happen in both control consolidation level and autonomy level.

  In Milestone 2 and Milestone 4, the workload-adaptive control consolidation and workload-adaptive autonomy are developed separately. Separate human subject studies are conducted to evaluate their effects on mission performance in isolation. In Milestone 5, the combined effect of these schemes is investigated; i.e., the benefits are assessed when both workload-adaptive control consolidation and workload-adaptive autonomy are engaged. A human subject study is used to evaluate the combined performance with the help of the real-time workload estimator. It includes the baseline and the adaptive schemes from both adaptation levels under different workload conditions. For example, when the testbed implements the adaptive control consolidation, the human subjects experience both adaptive autonomy and non-adaptive autonomy. Therefore, the combined effect of two adaptation levels and their separate impacts are studied.

1.4 Original Contributions

Based on the milestones listed in Sec.1.3, the original contributions of this thesis are:

- Development of a workload-adaptive control consolidation and the evaluation

of its performance.

- Development of a workload-adaptive autonomy and the evaluation of its performance.
- The evaluation of the combined framework which includes both workload-adaptive control consolidation and workload-adaptive autonomy.

1.5 Organization of the Dissertation

The rest of the dissertation is organized as follows. Chapter 2 describes the testbed used for the human subject study, which is the main method to evaluate the proposed workload-adaptive control schemes. Chapter 3 introduces the workload-adaptive control consolidation and presents a detailed evaluation of its performance based on the results from two user studies. Chapter 4 presents the validation of the parameter of the autonomy used for adaptation and the corresponding design of the workload-adaptive autonomy. In addition, Chapter 4 also assesses the performance of the adaptive autonomy using a human subject study. Chapter 5 provides the evaluation of the performance when both workload-adaptive control consolidation and workload-adaptive autonomy navigation formulation are utilized. Finally, Chapter 6 concludes the dissertation with a summary of contributions in this dissertation and suggestions for several possible future directions in the research of the mutually adaptive shared control.

Chapter 2

Tele-operated Dual-task Shared Control Platform

The human subject study is the primary method to evaluate the potential benefits of workload adaptation at the control consolidation level and the autonomy level in semi-autonomous driving, as proposed in Chapter 1. Therefore, a real-time human-in-the-loop simulation platform has been developed, which provides support for the experiment and is used to collect data from the participants.

The primary mission in the human subject studies performed in this work is a driving mission. A simulated driving scenario is created for the subjects so that they are able to drive in an environment close to reality without experiencing practical hazardous conditions. Therefore, a vehicle simulation module and a visualization module are embedded to simulate the vehicle's behavior and visualize the vehicle's motion in a simulated environment. In addition, an autonomy module is used to provide assistance when the subjects are driving. A motorized steering wheel with a force feedback feature acts as the hardware interface for the subject to interact with autonomy and the vehicle. Sometimes, the participants are required to conduct a secondary task, namely a surveillance task, besides the driving task. In the surveillance task, participants are instructed to conduct a threat identification on a secondary screen as accurately as possible. Therefore, there is a surveillance module on the secondary screen that supports the surveillance task. During the mission, the

human's torque and workload are collected by using torque sensors and the Tobii glasses. These modules are shown in Fig. 2.1. The detailed introductions of these modules are given below.

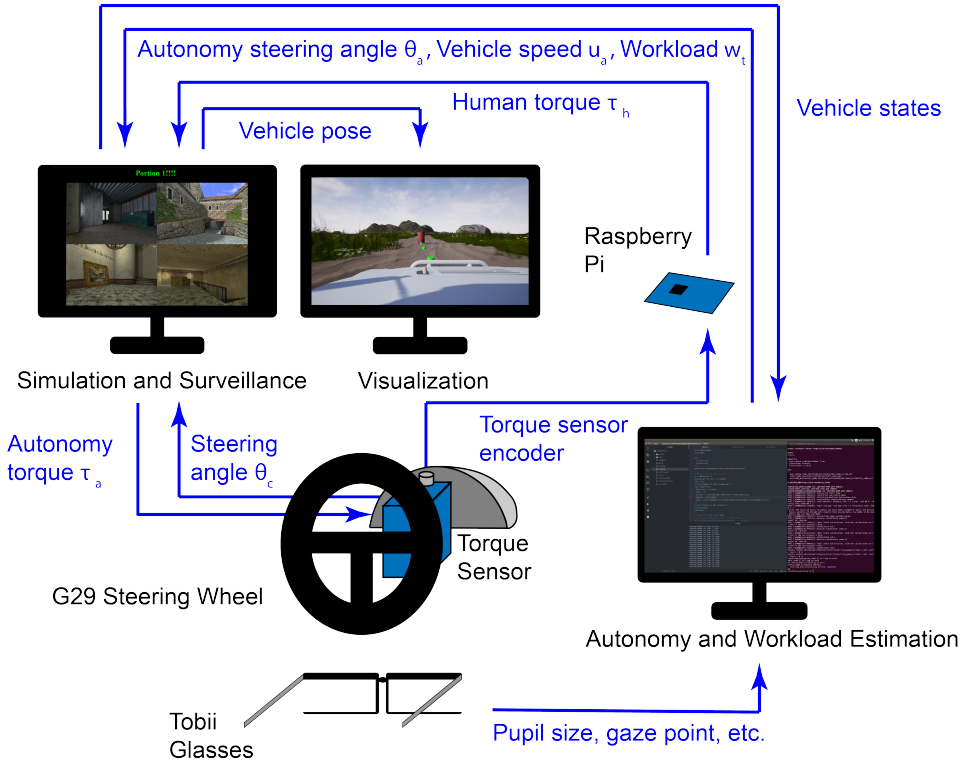

Figure 2.1: The overall structure of the testbed. The modules are labeled by text in black while the signals are labeled by text in blue.

2.1 Vehicle Simulation Module

The vehicle simulation module is developed based on the tele-operated vehicle simulation setup of [72]. In this testbed, a 14 DoF high fidelity model [73] is embedded to simulate the behavior of a military truck, namely, a notional High Mobility Multipurpose Wheeled Vehicle (HMMWV). The simulation is built based on MATLAB® Simulink® Desktop Real-Time [74]. The simulated HMMWV is the ego vehicle to control in an off-road environment. No other vehicle exists in this simulated environment.

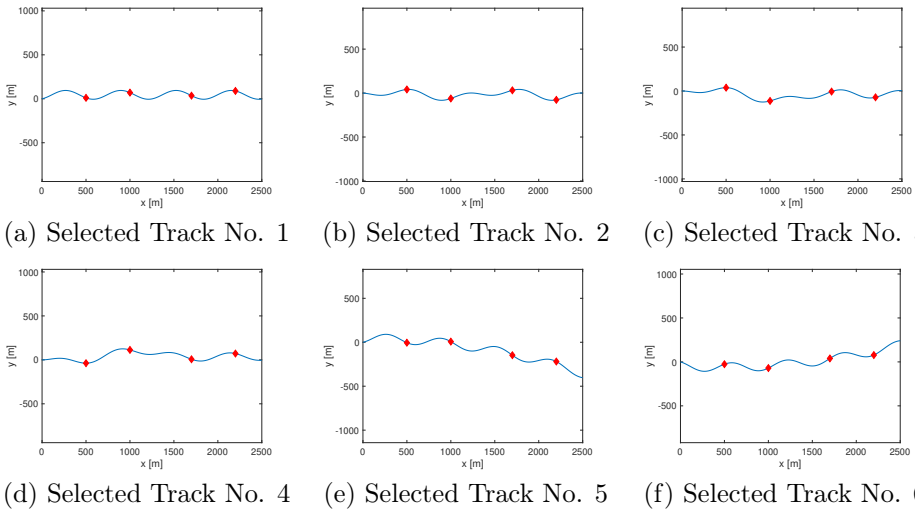

(a) Selected Track No. 1 (b) Selected Track No. 2 (c) Selected Track No. 3

(d) Selected Track No. 4 (e) Selected Track No. 5 (f) Selected Track No. 6

Figure 2.2: The track set selected for the visualization module. The red markers are the positions for the obstacles.

2.2 Visualization Module

The visualization module is created to emulate the vehicle's behavior and the vehicle's interaction with the environment. The major goal of the driving task is to track a centerline in the off-road environment while avoiding obstacles that are located at the centerline. Therefore, in the following subsections, the selection of the track, the representation of the centerline, and the obstacle are introduced.

2.2.1 Track Selection

In the visualization module, six tracks are chosen as the driving environment for participants [75]. They are selected based on two reasons. First, participants report similar difficulty traveling within the track when driving in the simulated shared control environment. Second, participants report similar difficulties across these different tracks. These tracks are shown in Fig. 2.2.

Figure 2.3: Visualization module based on Simulink 3D Animation Toolbox. The highlighted hook is a reference for the subject to find the center of the vehicle.

2.2.2 Visualization Environment 1: Simulink® 3D Animation Toolbox Based Environment

A visualization environment is created based on MATLAB® Simulink® 3D Animation Toolbox [76], which is shown in Fig. 2.3. The tracks mentioned in Sec. 2.2.1 are the centerlines shown on the screen of the visualization module. The centerline is represented as the dashed white line. The road is 20-meter-wide, which is represented as the grey path in the figure. (i.e., 10 meters on each side of the centerline). The green cylinders are the obstacles on the path. In addition, the trees are designed to provide cues to the subjects about the speed of the vehicle.

2.2.3 Visualization Environment 2: Unreal Engine 4 Based Environment

A visualization environment based on Unreal Engine 4 [77] and its extensions [78, 79] has also been developed to provide a better visual effect that can emulate an off-road driving environment. The track set used in this environment is identical to the one described in Sec. 2.2.1.

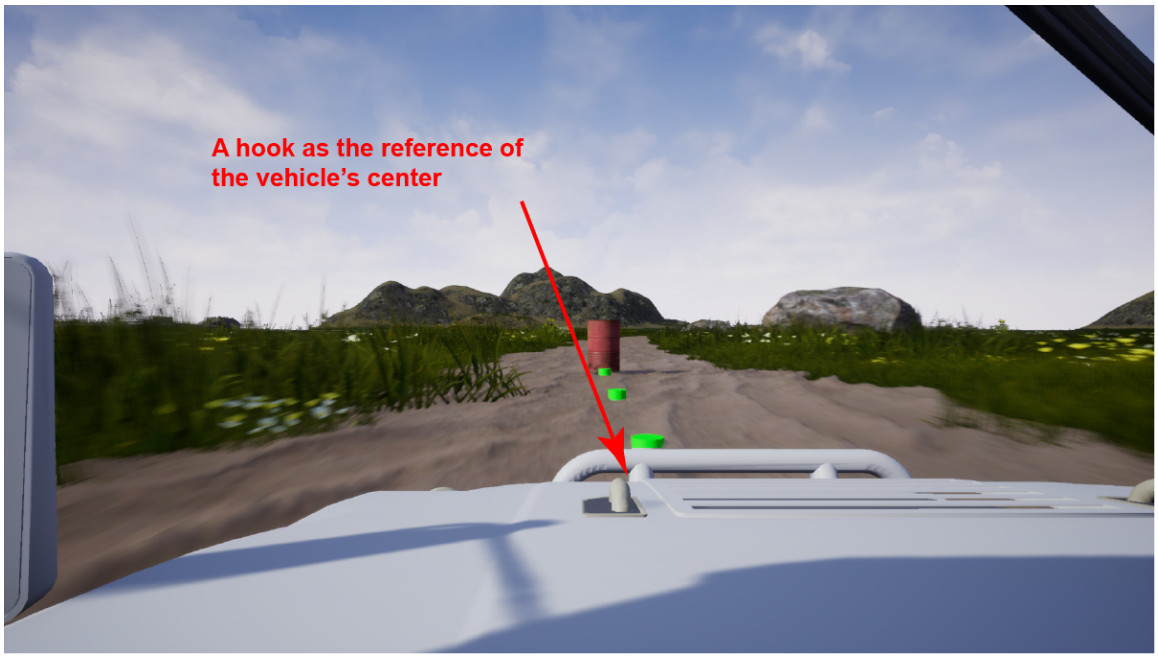

Figure 2.4: Visualization module based on Unreal Engine 4. The highlighted hook is a reference for the subject to find the center of the vehicle.

Unlike the visualization environment shown in Sec. 2.2.2, where the path is represented as a road, a sand road texture is used in the Unreal-Engine-based environment with surrounding grass and rocks. The motion of the grass and rocks indicates the vehicle's speed in this environment. The centerline is represented by a series of green dots, and the obstacles are represented by the red barrels. This visualization environment is shown in Fig. 2.4. When the subject hits an obstacle, an animation showing the explosion of the barrel is presented to the subject, as shown in Fig. 2.5. It is used to create a clear obstacle-hitting alert, which is another difference compared to the Simulink VR visualization environment shown in Sec. 2.2.2.

2.3 Autonomy Module

The autonomy in this testbed provides both reference steering angle commands and speed set-point commands. Nonlinear Model Predictive Control (NMPC) is used in the autonomy module to generate the steering angle and speed commands. In [80, 81], the authors describe the formulation of the Nonlinear Model Predictive Control

Figure 2.5: Visualization when the subject hits an obstacle (barrel) based on Unreal Engine 4. It alerts both the subject and the experimenter that the subject hits an obstacle.

(NMPC) in detail. The cost function varies depending on different experimental designs in this dissertation. In this section, the common components of autonomy used in different human subject studies are described.

2.3.1 NMPC Optimal Control Problem Formulation

The nonlinear optimal control problem (OCP) in the autonomy module, which is a modified version of [80, 81], is

$$\min J(\zeta_i, \xi_i) \tag{2.1}$$

subject to

$$\begin{aligned} \xi_{i+1} &= V(\zeta_i, \xi_i) \\ \xi_{min} &\leq \xi_i \leq \xi_{max}, i = 1...N \\ \zeta_{min} &\leq \zeta_i \leq \zeta_{max}, i = 1...N-1 \end{aligned} \tag{2.2}$$

In this formulation, Eq. 2.1 is the cost function which varies between different human subject studies. ξ represents the vehicle's state vector, while ζ represents the

vehicle's control vector. N is the number of prediction steps in the entire prediction horizon. The first constraint in Eq. 2.2 is the 3 DoF vehicle dynamics [82] the state vectors and control vectors should obey throughout the entire prediction horizon. This model is selected as the prediction model because it can achieve a balance between prediction speed and model fidelity. The second and the third constraints in Eq. 2.2 are the states and control constraints.

Several states constraints are imposed as:

$$\begin{bmatrix} \psi_{min} \\ \delta_{mix} \\ u_{x,min} \\ a_{x,min}(u) \end{bmatrix} \leq \begin{bmatrix} \psi \\ \delta \\ u_x \\ a_x \end{bmatrix} \leq \begin{bmatrix} \psi_{max} \\ \delta_{max} \\ u_{x,max} \\ a_{x,max}(u) \end{bmatrix} \tag{2.3}$$

where ψ is the yaw angle of the vehicle. δ is the steering angle. u_x and a_x are the longitudinal speed and acceleration. The adaptive autonomy introduced in Chapter 4 changes some of these constraints.

2.3.2 Solution Strategy

This dissertation uses the open-source nonlinear optimal control package NLOptControl [83] to solve the described Nonlinear Model Predictive Control (NMPC) problem. The package adopts the Legendre-Gauss-Radau (LGR) collocation method to transfer the described continuous optimal control problem to a nonlinear program problem. Then the nonlinear program solver package IPOPT [84] is used to solve the transferred nonlinear program problem. This optimization process generates a series of steering angles and speed commands throughout the prediction horizon T_P. Then the commands from the first 3 seconds, or the control horizon, are buffered for future use. While executing the previous control command series, the system formulates and solves a new optimal control problem with a new prediction horizon. The resulting new command series are applied as soon as they are ready. Therefore, the update time of the control commands may vary. The median update time is 0.22 second,

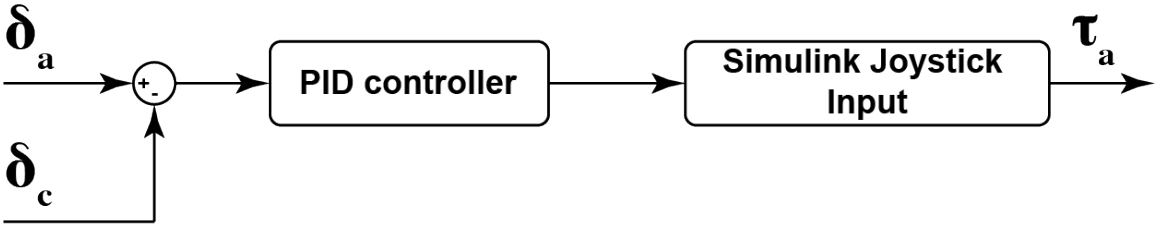

Figure 2.6: Block diagram of the PID controller which generates the autonomy torque τ_a

Table 2.1: PID tunning parameters

Parameters	K_P	K_I	K_D
Value	5.5	3	0.13

while the maximum update time is 0.57 second. Based on the previous literature [80, 81, 85], the update time is considered sufficient.

2.3.3 Autonomy Torque for Force Feedback

The autonomy torque, labeled as τ_a, is calculated through a proportional-integral-derivative (PID) controller. It aimes to track the reference steering angle δ_a resulting from the nonlinear model predictive control (NMPC) problem given the current steering angle from the steering wheel δ_c. The block diagram of the autonomy torque is shown in Fig. 2.6. The PID controller is tuned so that after directly applying autonomy torque τ_a on the steering wheel, the autonomy can track its perceived centerline without any human intervention. The tuned weights of the PID controller are shown in Table 2.1.

2.4 Steering Wheel with Rotatory Torque Sensor

A Logitech® G29 steering wheel and pedal set are used in this testbed to provide the hardware interface for subjects to interact with the autonomy and simulated environment. The speed is controlled by autonomy, and the pedal set is used to provide the signal indicating the starting point of the experiment. Therefore, subjects only need to press the gas pedal once to begin the experiment, and they do not need to

interact with the pedal set during the experiment. In contrast, subjects are required to interact with the steering wheel during the entire experiment. The autonomy is designed to help subjects with the driving missions. By applying the torque corresponding to autonomy's reference signal through its force-feedback feature, the G29 steering wheel creates a haptic interface for subjects to perform shared driving control in steering.

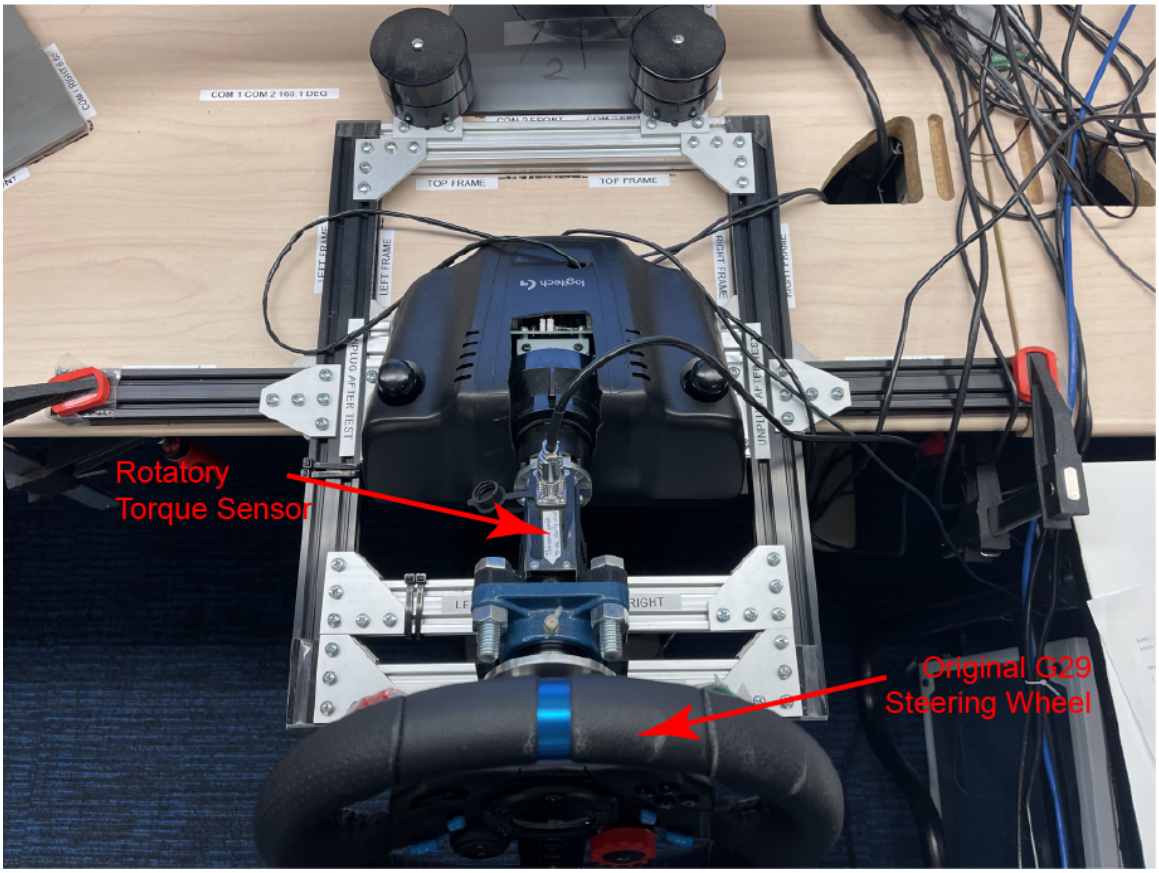

Figure 2.7: The modified G29 steering wheel. A rotatory sensor is added to the middle shaft of the steering wheel.

The steering wheel and pedal set are connected to the simulation module as a joystick. Their data, including the steering angle, force feedback magnitude, and pedal position, are recorded by using the Simulink Block called "Joystick Input", which is part of the Simulink Desktop Real-Time. To obtain the human torque applied on the steering wheel, a rotatory torque sensor is attached to the Logitech steering wheel. This rotatory sensor is connected to a Raspberry Pi that reads the

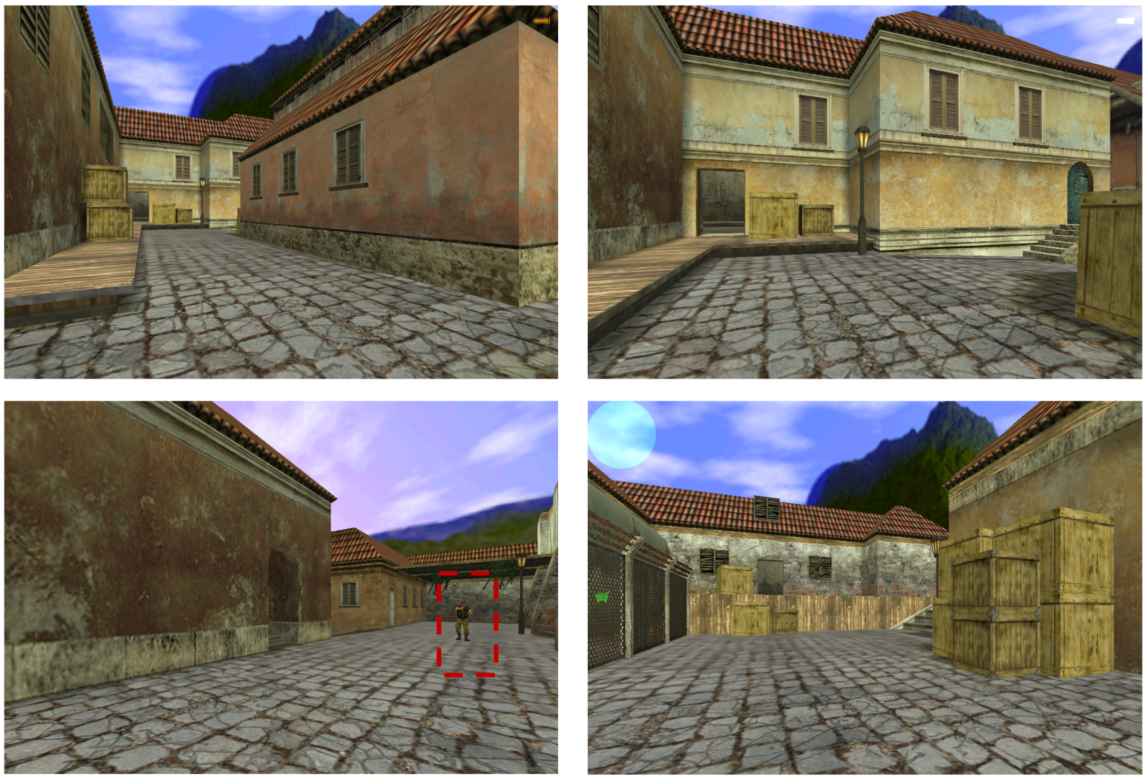

Figure 2.8: Illustration of the surveillance task. Lower left: threat.

torque data from the rotatory sensor and sends the data back to the vehicle simulation module. The modified steering wheel is shown in Fig. 2.7.

2.5 Surveillance Task Module

The surveillance module shares the same computer with the vehicle simulation module. It acts as a secondary task in the human subject study. Our collaborators, Dr. Ruikun Luo and Prof. Jessie X. Yang, have developed the surveillance task testbed [86].

In the surveillance task, the participants receive image feeds and need to identify if potential threats exist in these images. Fig. 2.8 shows one image set of the surveillance task. Participants report “danger" by clicking the red lever (right lever) on the steering wheel if they identify the potential threat in the images. Otherwise, they report “clear" by clicking the green lever (left lever). Due to the need to operate these

Table 2.2: Features and models used in the workload estimation module

Features	Best models to analyze these features
Gaze trajectory	Hidden Markov Model (HMM)
Pupil size	Support-Vector Machine (SVM)
Fixation feature	Support-Vector Machine (SVM)
Fixation trajectory	Gaussian Mixture Model (GMM)

levers, it is inconvenient for subjects to cross their hands during the experiment. To avoid this issue, the operation range of the steering wheel is set to be -90 degrees to 90 degrees.

When a new set of images appears, an alert notifies the subject. The subject needs to finish the threat identification within a fixed amount of time, which is called the pace of the study. After the subject makes the identification or the time for identification is passed without a response from the subject, the images are replaced by a white screen as a transition to the next image feed. The pace is used to control the subject's workload. A rapid pace leads to a high surveillance task urgency, while a slow pace leads to a low surveillance task urgency.

2.6 Online Workload Estimation Module

Our collaborators, Dr. Ruikun Luo and Prof. Jessie X. Yang, have developed the online workload estimation module in [86], [75] and [87]. They use non-intrusive physiological measurements such as pupil size [87, 86], gaze trajectory [86, 75, 87], and fixation features [87]. The features and best models to analyze these features are shown in Table 2.2. In [75], the Hidden Markov Model (HMM), which analyzes the gaze trajectory, can achieve a 0.66 F_1 score, 0.67 precision and 0.66 recall. In [86] and [87], our collaborators use the Bayesian Inference (BI) model to leverage the analysis of the best models. In [87], the Bayesian Inference (BI) model can achieve a 0.82 F_1 score, 0.82 precision and 0.82 recall.

Chapter 3

Workload-adaptive Shared Control Consolidation

3.1 Introduction

This chapter examines the benefit of considering workload at the control consolidation level. Two workload-adaptive control consolidations are developed. Adaptation in these two consolidations is achieved by changing the assistance level of the autonomy's torque. The modification is based on the human driver's (estimated) workload. In addition to workload, other human factors are also considered, such as the human driver's torque, which represents the degree of intervention from the human operator. After designing an adaptive control consolidation, a human subject study in semi-autonomous driving mode is conducted to evaluate the performance with the developed consolidation. Therefore, this chapter includes two sections to describe the designs and evaluations of these two control consolidations. The way to control and estimate the workload is another difference between these evaluations of the two consolidations. In Experiment 1, which evaluates the first developed adaptive control consolidation, the screen refresh rate is used to control the human operator's workload. The workload of the human driver is designed as a piece of known information based on different screen refresh rates. In Experiment 2, where the second adaptive control consolidation is evaluated, the designed surveillance task, which is mentioned

in Sec. 2.5, acts as a secondary task to control the human driver's workload. A real-time workload estimation algorithm based on Hidden Markov Model (HMM), which is developed by our collaborators, Dr. Ruikun Luo and Prof. Jessie X. Yang [75], is used to estimate the human driver's workload.

3.2 Adaptive Shared Control Consolidation Based on Workload and Human's Torque

This section introduces the design of the first adaptive control consolidation. Two human factors are used in the design: the workload and the driver's torque. As shown in Sec. 1.1.2, the workload is used to adjust the level of assistance from autonomy. In addition, the degree of intervention is also important, which is represented by the human driver's torque. One supporting example of taking both workload and torque into account is the minimum intervention from the human operator. If the human operator is at a moderate workload but is not fully engaged, the assistance level should be kept at the highest level to enable the vehicle's driving on its own. This section first introduces the non-adaptive control consolidation in Sec. 3.2.1.1, which works as a benchmark. Then it introduces the design principles of the adaptive control consolidation in Sec. 3.2.1.2.

3.2.1 Control Consolidation Design

3.2.1.1 Non-adaptive Control Consolidation

The block diagram for the (non-adaptive) haptic shared control used in this work is shown in Figure 3.1. It is implemented in the testbed described in Chapter 2. Through this haptic shared control design, the human operator can feel autonomy's assistance torque from the steering wheel and negotiate with it. In this case, the assistance torque applied on the steering wheel equals the autonomy's torque τ_a, whose value is calculated by the PID controller stated in Sec. 2.3.3. Therefore, the resultant torque from the steering wheel τ_c combines both human's torque τ_h and autonomy's torque

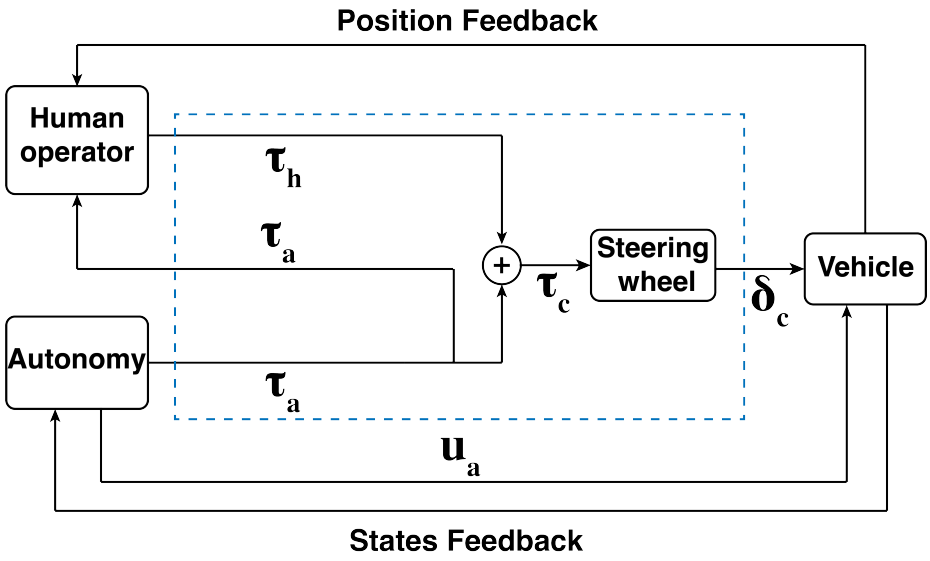

Figure 3.1: Block diagram for (non-adaptive) haptic shared control. τ_{h} and τ_{a} represent the torque from human and autonomy, respectively. τ_{c} and δ_{c} are the resultant torque and actual control steering angle. u_a is the speed from autonomy. The blue dashed box encircles the control consolidation of the system.

τ_a, i.e., $\tau_c = \tau_h + \tau_a$. It determines the final steering control input to the vehicle, namely, the steering angle δ_c.

3.2.1.2 Workload-adaptive Control Consolidation

The block diagram of the adaptive control consolidation is shown in Fig. 3.2. The adaptive scheme is designed based on two human factors: workload of the human operator w_t and the human operator's input torque τ_h. Workload w_t reflects the condition of the human operator, whereas the human's input torque τ_h indicates the human's degree of intervention. The degree of intervention can also reflect the human operator's degree of disagreement with autonomy in the semi-autonomous driving mode.

The resultant torque in Fig. 3.2 is calculated as

$$\tau_{\mathrm{c}} = \tau_{\mathrm{h}} + \beta(w_t, \hat{\tau}_{\mathrm{h}})\tau_{\mathrm{a}}, \tag{3.1}$$

where the term β is referred to as the assistance level. It represents the degree

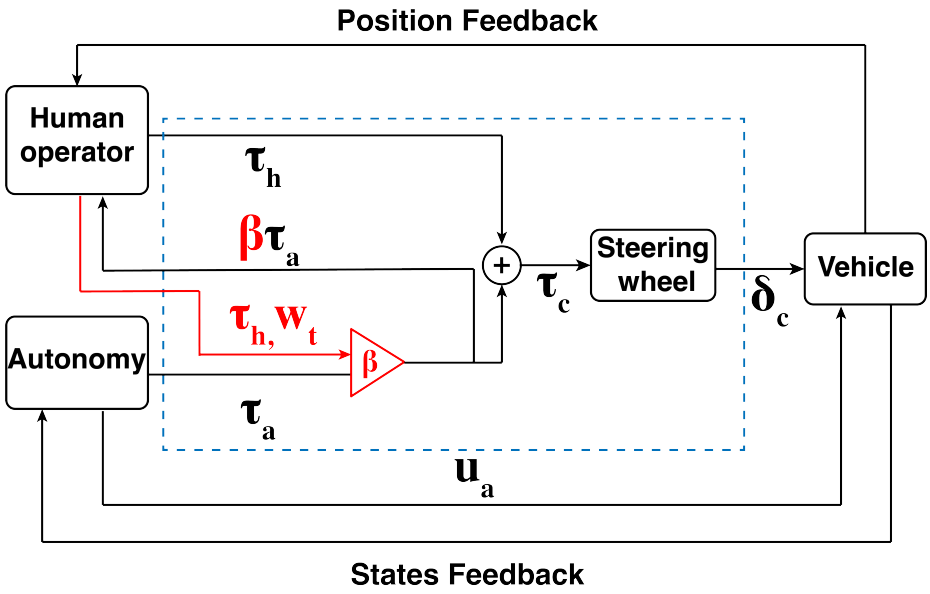

Figure 3.2: Block diagram for workload-adaptive haptic shared control consolidation. τ_{h} and τ_{a} represent the torque from human and autonomy, respectively. The assistance level β is affected by the human's torque τ_h and human's workload w_t. The human operator can feel the assistance torque $\beta\tau_a$ on the steering wheel and exert his/her torque τ_h correspondingly. τ_{c} and δ_{c} are the resultant torque and actual control steering angle. u_a is the speed from autonomy. The blue dashed box encircles the control consolidation of the system.

of assistance from autonomy, thus controlling the assistance torque applied on the steering wheel. $\hat{\tau}_{\mathrm{h}}$ is the human's normalized input torque, which is calculated by dividing the human's torque τ_{h} by an estimate of the maximum value $\tau_{\mathrm{h,max}}$ the human operator can apply. In the testbed, $\tau_{\mathrm{h,max}}$ is set as 1.7 Nm based on pilot human subject studies. By modifying the assistance level β, the magnitude of the assistance torque applied on the steering wheel can be varied in a manner adaptive to the human operator's workload and torque in contrast to a fixed assistance level case. Therefore, in the non-adaptive scheme whose block diagram is shown in Fig. 3.1, the assistance level β is always 1, and the assistance torque always equals autonomy's torque τ_a.

The relationship between the assistance level β, the workload w_t and the normalized human torque $\hat{\tau}_{\mathrm{h}}$ is shown in a 3D plot in Fig. 3.3. The assistance level β is heuristically designed based on two aspects. The first aspect considers human performance under different workload conditions, which is introduced in Sec. 1.1.2. As

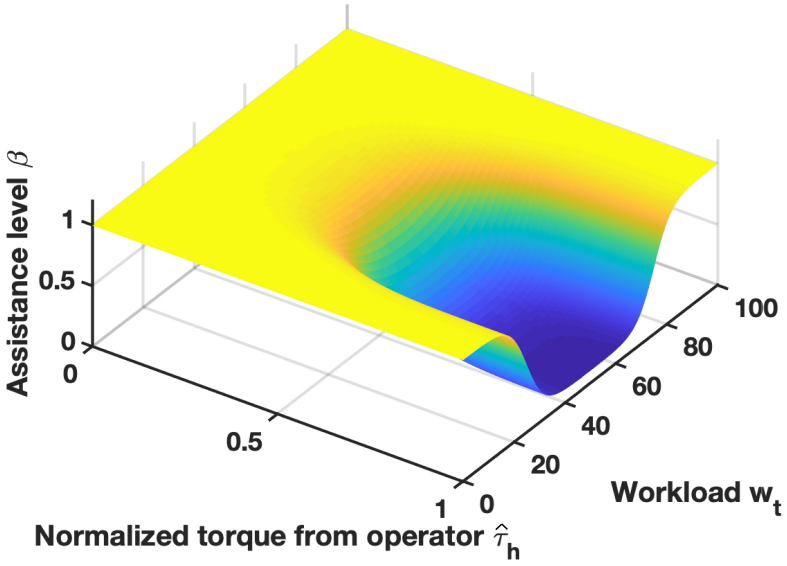

Figure 3.3: The relationship between the assistance level β and the normalized human's torque $\hat{\tau}_{\mathrm{h}}$ as well as human's workload w_t. We define $w_t = 0$ when the human operator is under the under-loaded case and $w_t = 100$ when the human operator is under the over-loaded case.

shown in Fig. 3.4, for a given amount of torque exerted by the human operator, the level of assistance from autonomy varies with the workload of the human. The curve is designed according to the principle described in [48]. It indicates that the human operator should receive less support in the moderate workload condition than in the over-loaded or under-loaded conditions because a moderate workload is considered optimal for human performance.

In the present study, workload w_t is defined such that $w_t = 0$ represents the under-loaded cases, $w_t = 50$ is the moderate workload cases, and $w_t = 100$ is the over-loaded cases. When the human operator has a moderate workload ($w_t = 50$), β is set to be the lowest value among the whole workload spectrum. In particular, a value is chosen that is close to zero but not too small to the extent that the human does not feel the assistance torque and hence cannot feel the intention of the autonomy anymore. Specifically, $\beta = 0.1$ for moderate workload when the human operator exerts the maximum torque. When the human operator is under-loaded ($w_t = 0$) or over-loaded ($w_t = 100$), $\beta = 1$ to provide full support from autonomy. The assistance level of

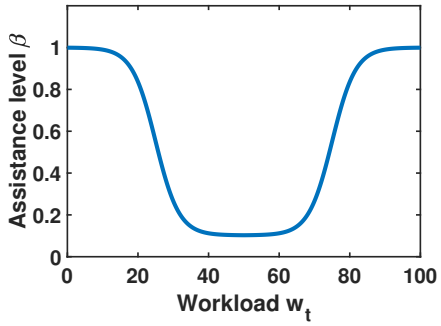

(a) Relationship between assistance level β and workload w_t when human's torque is at its maximum. It is the highlighted section in the 3D plot as shown in Fig. 3.4b.

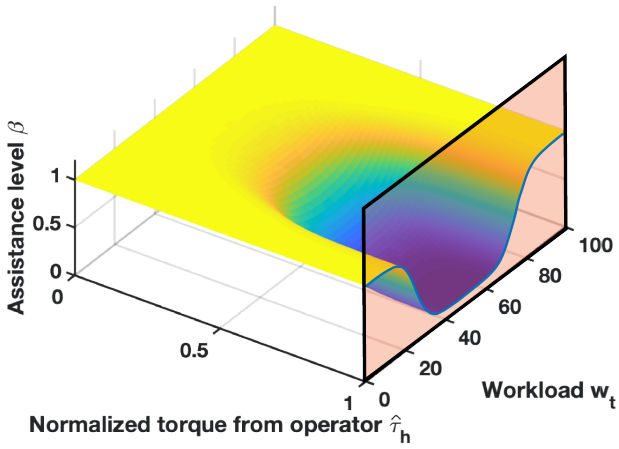

(b) The position of the typical relationship between the assistance level β and workload w_t in the presented 3D relationship between the assistance level β, the workload w_t and the normalized human torque $\hat{\tau}_{\mathrm{h}}$.

Figure 3.4: Illustration of the first design principle of the assistance level β.

the moderate workload condition is obtained from a pilot study. In the pilot study, all possible values from 0.1 to 1 with an increment of 0.1 are investigated. Then the value with the best mission performance is selected. Sigmoid functions are used to connect the moderate workload case and the under-loaded and over-loaded cases smoothly. Using the sigmoid function to connect two known conditions smoothly can also be found in [88, 89].

As for the second design aspect, for a given workload the human operator experiences, larger torque input from the human indicates a stronger disagreement with autonomy. Emergency cases or cases when failure happens in the autonomy system may require such strong interventions. Hence, the assistance level is reduced to make it easier for the human to control the vehicle as he/she applies more torque, as shown in Fig 3.5.

The reduction in the assistance level depends on the human's workload. Since a moderate workload level is considered optimal in the literature [48], when the human operator has a moderate workload, his/her command is considered to be more reliable compared with the over-loaded or under-loaded cases. Therefore, the assistance level β is reduced more when $w_t = 50$ than the cases when $w_t = 0$ or $w_t = 100$. For

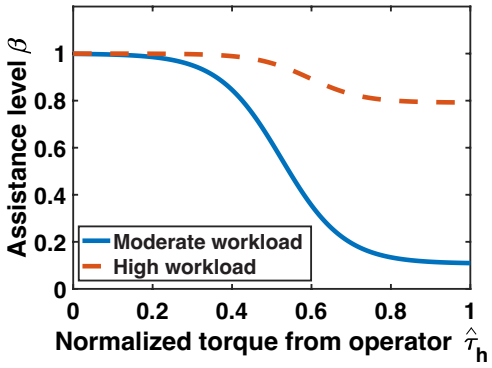

(a) Relationship between assistance level β and normalized human's torque $\hat{\tau}_{\mathrm{h}}$ when human's workload w_t is different. The curves are the section shown in Fig. 3.5b and Fig. 3.5c, respectively.

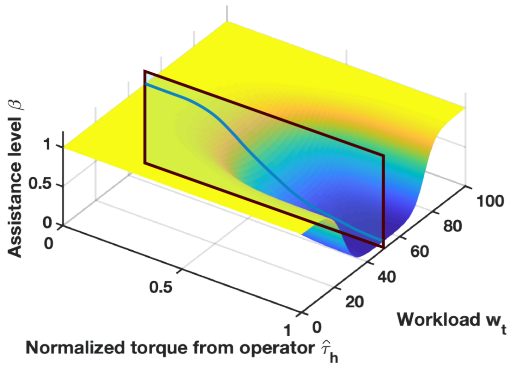

(b) The 3D plot section showing the relationship between the assistance level β and normalized human's torque $\hat{\tau}_{\mathrm{h}}$ under moderate workload cases.

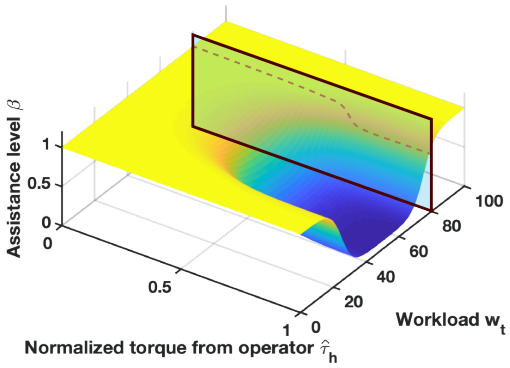

(c) The 3D plot section showing relationship between the assistance level β and normalized human's torque $\hat{\tau}_{\mathrm{h}}$ under relatively high workload cases.

Figure 3.5: Illustration of the second design principle of the assistance level β.

all these cases, β starts from 1 to navigate the vehicle in autonomous mode when the human operator has no input torque. This assistance level is maintained until reaching a threshold to filter out small unintended torques. In the cases when the human operator experiences a moderate workload and completely yields to autonomy, this threshold is set to around 0.04 Nm, and the corresponding normalized torque is calculated to be 0.02. This threshold is obtained from the torque data of pilot human subject studies.

Similarly, the threshold for under and over-loaded cases ($w_t = 0$ or $w_t = 100$) is picked as 0.3. A quadratic function, which is symmetric about $w_t = 50$, connects

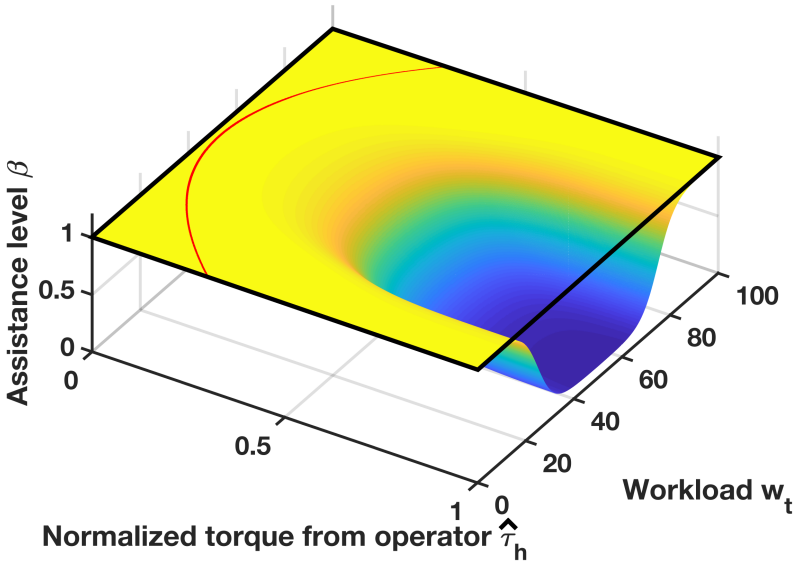

Figure 3.6: The threshold to reduce the assistance level from $\beta = 1$.

these values in three different cases to model the threshold for different workload values w_t. It is shown as the red curve in the 3D plot in Fig. 3.6. Thus, for a given workload, the threshold is calculated, and the minimum assistance level aligns with the corresponding result obtained by the first design principle when the human exerts the maximum torque ($\hat{\tau}_\mathrm{h} = 1$). The smooth transitions along the dimension of normalized human torque are achieved through a sigmoid function.

Combining these two aspects, the assistance level β is calculated as

$$\begin{aligned}\beta(w_t, \hat{\tau}_\mathrm{h}) =& 1 - \left[1 - \left(\frac{0.9e^{0.3(|w_t-50|-25)}}{e^{0.3(|w_t-50|-25)}+1} + 0.1\right)\right] \\ & \left[\frac{e^{\frac{60\hat{\tau}_\mathrm{h}-18.6-8.4(\frac{w_t}{50}-1)^2}{2.9-1.4(\frac{w_t}{50}-1)^2}}}{e^{\frac{60\hat{\tau}_\mathrm{h}-18.6-8.4(\frac{w_t}{50}-1)^2}{2.9-1.4(\frac{w_t}{50}-1)^2}}+1}\right].\end{aligned} \tag{3.2}$$

3.2.2 Evaluation of the Adaptive Control Consolidation: Experiment 1

3.2.2.1 Introduction

The human subject study Experiment 1 is conducted to evaluate the performance of the designed adaptive control consolidation in Sec. 3.2.1.2. There are 8 participants in this human subject study. They are required to control the vehicle and track the centerline collaboratively with autonomy. To introduce the cases where there is a disagreement between the human operator and autonomy, obstacle avoidance and biased scenarios are presented. It is assumed that different screen refresh rates affect the participants' workload. Therefore, in this experiment, the screen refresh rate is used to control the workload of the human operator. There are two screen refresh rates in this study: 20 Hz (fluent mode) and 2.5 Hz (delayed mode). The estimated workload is known directly from the screen refresh rate setting. Both adaptive control consolidation and baseline non-adaptive control consolidation are implemented in this experiment to compare the results.

3.2.2.2 Method

Participants

There are 8 participants in the experiment. All of them are students from the College of Engineering at the University of Michigan. These 8 participants are on average 22.9 years old (SD = 3.6 years) and have an average of 4.1 years of driving experience (SD = 3.5 years). All participants have a normal or corrected-to-normal vision.

Driving Task

In this experiment, subjects use the testbed, whose visualization module is introduced in Sec. 2.2.2. In the driving task, the participant and the autonomy share the steering control of the vehicle, whereas the vehicle's speed is controlled by autonomy. The goal of the task is to complete a track with minimal deviation from the path, as denoted by the centerline, without hitting an obstacle. The autonomy has no obstacle

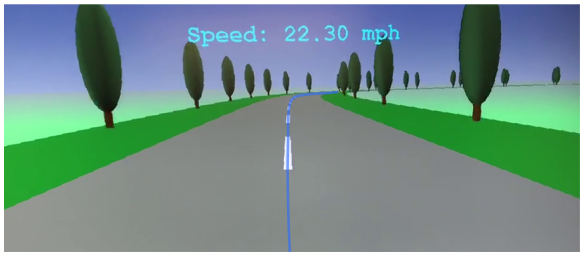

(a) Autonomy with no bias.

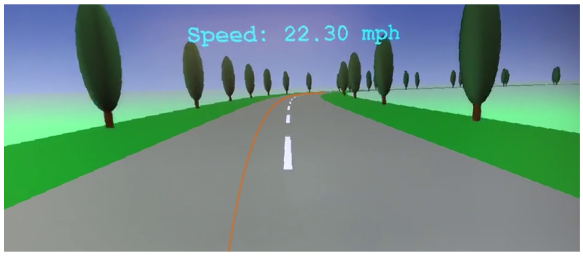

(b) Autonomy with 0.8 m left-sided bias.

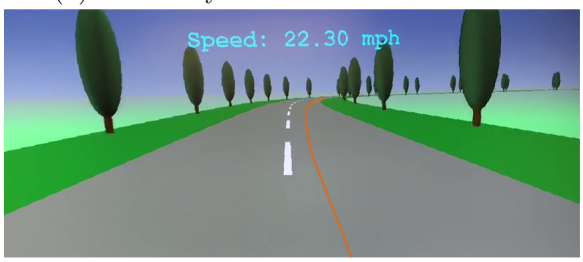

(c) Autonomy with 0.8 m right-sided bias.

Figure 3.7: Illustration of the biased/unbiased autonomy design.

avoidance capability. In some cases, to emulate a perception challenge, an offset is introduced such that the autonomy tracks a path that deviates from the centerline by 0.8 m, which is referred to as biased autonomy. The value of bias is selected to be large enough to differ from the unbiased case clearly, but not too large to render autonomy useless. The illustration of the biased autonomy is shown in Fig. 3.7. The screen refresh rate is assumed to affect the participants' workload. Therefore, in this experiment, two screen refresh rates, 20 Hz and 2.5 Hz, are presented to regulate the subject's workload. The cases where the screen refresh rate is 20 Hz are considered a moderate workload, and the cases with the screen refresh rate of 2.5 Hz are considered a high workload. These two values are picked based on the following reasons. 20 Hz is the maximum screen refresh rate the real-time testbed can achieve, while 2.5 Hz is picked so that the subject feels some difficulty in the driving task but can still control the vehicle. Both non-adaptive shared control consolidation and adap-

Table 3.1: Weights of autonomy in Experiment 1

Parameters	w_1	w_2	w_3	w_4	w_5
Value	0.05	2.0	0.9	0.2	0.001

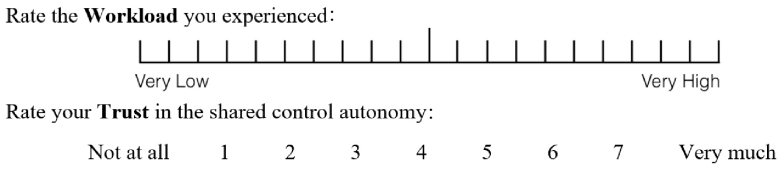

Figure 3.8: The survey which contains uni-dimensional scales for workload and trust.

tive shared control consolidation are used as described in Sec. 3.2.1.1 and Sec. 3.2.1.2, respectively.

Autonomy Formulation

The cost function used in this study is

$$\begin{aligned} J = w_1 T_p + w_2 \int_{t_0}^{t_P} \Big(y_{\text{ref}}(x(t)) - y(t)\Big)^2 dt + w_3 \int_{t_0}^{t_P} \gamma^2 dt \\ + w_4 \int_{t_0}^{t_P} J_x^2 dt + w_5 \int_{t_0}^{t_P} \tanh\Big[-\frac{F_{z,rl} - a}{b}\Big] + \tanh\Big[-\frac{F_{z,rr} - a}{b}\Big] dt. \end{aligned} \tag{3.3}$$

It consists of five terms. The first term is used to control the speed of the vehicle. T_p is the prediction horizon calculated by traveling a constant distance, which is 100 m in this study. The second term penalizes the deviation from the current position of the vehicle $y(t)$ to the given position on the path $y_{\text{ref}}(x(t))$. The third and fourth terms regulate the control inputs of the vehicle, namely, the longitudinal jerk J_x and steering rate γ, for a smooth steering maneuver and acceleration. The fifth term is a soft constraint that increases the cost when one of the vertical tire loads $F_{z,rl}$, $F_{z,rr}$ is close to the lowest allowable threshold. This soft constraint is used to prevent the vehicle from operating at its dynamic limit unnecessarily [80, 85]. Five weights w_1, w_2, w_3, w_4 and w_5 are set to achieve a trade-off between these goals, whose values are listed in Table 3.1.

Experimental Design

The experiment uses a within-subjects design with three independent variables. The first independent variable is the shared control consolidation settings (adaptive

Table 3.2: Eight test conditions in Experiment 1

Condition	Autonomy performance	Screen refresh rate	Shared control consolidation setting
1	Unbiased	20 Hz	Non-adaptive
2	Unbiased	20 Hz	Adaptive
3	Biased	20 Hz	Non-adaptive
4	Biased	20 Hz	Adaptive
5	Unbiased	2.5 Hz	Non-adaptive
6	Unbiased	2.5 Hz	Adaptive
7	Biased	2.5 Hz	Non-adaptive
8	Biased	2.5 Hz	Adaptive

haptic shared control vs. non-adaptive haptic shared control). The second independent variable is the screen refresh rate (20 Hz vs. 2.5 Hz). The third independent variable is the performance of the autonomy (biased vs. unbiased). Each participant experiences 8 tracks in the experiment. On each track, one combination of control consolidation setting, screen refresh rate, and performance of autonomy is used. The resulting eight test conditions are shown in Table 3.2. The presentation of test conditions follows an 8×8 Latin square design to eliminate potential order effects.

Measures

Five dependent variables are collected in the experiment:

- Participants' self-reported workload
- Participants' self-reported trust in the shared control autonomy
- Participants' control effort in the lane-keeping stage
- Driving task performance (in the lane-keeping stage)
- Participants' control effort during the obstacle avoidance maneuver.

In this work, the obstacle-avoidance stage has a similar definition as in [29]. Specifically, the obstacle-avoidance stage is defined as the period when the human subjects deviate at least 1 m from the centerline and avoid the obstacles. The illustration of the obstacle-avoidance stage is shown in Fig. 3.9. The rest of the driving period is defined as the lane-keeping stage.

After each track, participants report their workload and trust using two unidimensional scales, as shown in Fig. 3.8. The NASA TLX survey [90] and the Moray's

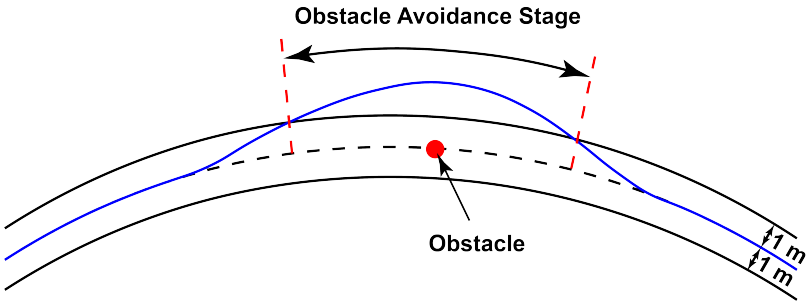

Figure 3.9: The illustration of the definition of obstacle-avoidance stage.

trust survey [91] are presented to the participants before the evaluation stage such that they understand the meaning of workload and trust.

Participants' control effort is calculated as the average torque that a participant applied on the steering wheel. The measurement is acquired at the frequency of 100 Hz by the torque sensor. Driving task performance is evaluated by the path tracking error. The path tracking error is calculated as the mean of the absolute deviation of the vehicle's position from the centerline. The measurement is also acquired at the frequency of 100 Hz.

Experimental Procedure

Participants first provide a signed informed consent form and fill in a demographic survey. During the training session, the participants perform five trials of the driving task under different conditions: one trial with the 20 Hz refresh rate, non-adaptive control consolidation with an unbiased autonomy, and four trials with the 2.5 Hz refresh rate. They experience non-adaptive control consolidation with an unbiased autonomy, adaptive control consolidation with a biased autonomy, adaptive control consolidation with an unbiased autonomy, and non-adaptive control consolidation with a biased autonomy in order. Each trial takes approximately 2.5 min.

During the real experiment, participants perform the driving task on 8 different tracks with the different test cases described in Table 3.2. Each trial takes approximately 1.5 min. After each trial, the participants are asked to fill a post-survey about the workload and trust during the last finished track. If they hit the obstacle, the trial is restarted.

Table 3.3: Mean and standard error (SE) of workload, trust, lane-keeping error, torque during centerline tracking, and torque during obstacle avoidance in Experiment 1

Metrics	N	Screen Refresh Rate							
		20 Hz				2.5 Hz			
		Unbiased Autonomy		Biased Autonomy		Unbiased Autonomy		Biased Autonomy	
		Adaptive	Non-adaptive	Adaptive	Non-adaptive	Adaptive	Non-adaptive	Adaptive	Non-adaptive
Workload	8	4.00 ± 0.94	2.88 ± 0.52	7.63 ± 2.15	9.25 ± 1.39	8.25 ± 1.71	9.13 ± 2.06	11.00 ± 1.50	15.00 ± 1.57
Trust	8	5.88 ± 0.52	6.25 ± 0.25	4.13 ± 0.67	4.00 ± 0.53	5.25 ± 0.56	4.75 ± 0.53	3.63 ± 0.42	3.00 ± 0.46
Centerline tracking error (m)	8	0.19 ± 0.019	0.18 ± 0.022	0.27 ± 0.036	0.32 ± 0.036	0.26 ± 0.039	0.28 ± 0.026	0.48 ± 0.029	0.52 ± 0.047
Torque for centerline tracking stage (Nm)	8	0.19 ± 0.012	0.18 ± 0.011	0.45 ± 0.033	0.99 ± 0.044	0.17 ± 0.024	0.23 ± 0.017	0.44 ± 0.076	0.79 ± 0.084
Torque for obstacle avoidance (Nm)	8	0.35 ± 0.020	0.53 ± 0.036	0.43 ± 0.035	0.76 ± 0.070	0.54 ± 0.049	0.57 ± 0.043	0.73 ± 0.052	1.01 ± 0.095

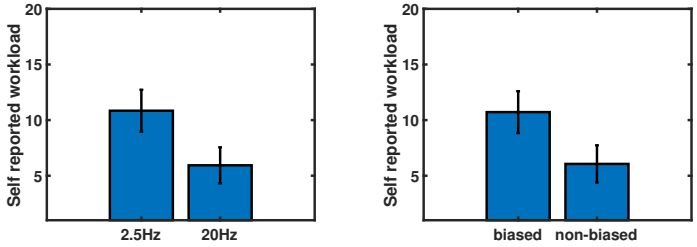

(a) Self-reported workload and screen refresh rate

(b) Self-reported workload and autonomy's performance

Figure 3.10: Mean and standard error (SE) values of self-reported workload with different conditions in Experiment 1

3.2.2.3 Results

Three-way repeated measures Analysis of Variance (ANOVA) is conducted with the control consolidation setting, autonomy performance, and screen refresh rate as the within-subjects variables. Results are reported as significant for a statistical significance level of $\alpha = 0.05$; i.e., if the probability p of observing the difference seen in the experimental data purely due to random effects is less than 5%, the difference is deemed statistically significant. Table 3.3 summarizes the mean and standard error (SE) values of the participants' self-reported workload, self-reported trust, driving task performance, and their exerted torque during the lane-keeping stage and the torque during obstacle avoidance.

Participants' Workload

Both screen refresh rate and autonomy performance have an impact on the participant's self-reported workload, as shown in Fig. 3.10. The effect of different schemes is not significant. With the 20 Hz screen refresh rate, participants report lower workload ($F(1,7) = 20.02,\ p < 0.001$). When there is no bias for autonomy, participants report lower workload ($F(1,7) = 18.03,\ p < 0.001$).

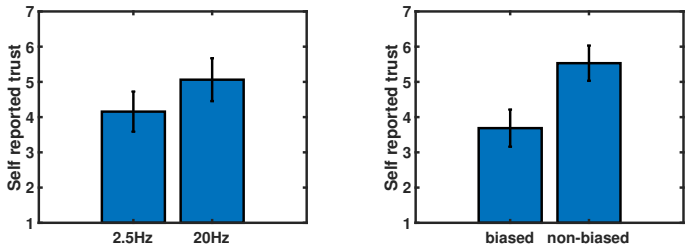

(a) Self-reported trust and screen refresh rate

(b) Self-reported trust and autonomy's performance

Figure 3.11: Mean and standard error (SE) values of trust with different conditions in Experiment 1

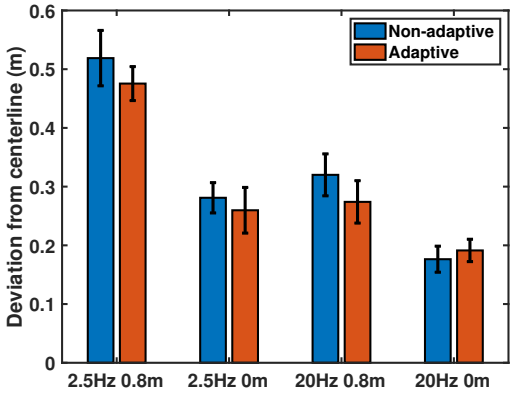

Figure 3.12: Driving task performance in lane-keeping stage for the four conditions of 20 Hz vs. 2.5 Hz refresh rate and 0 m vs. 0.8 m bias in the perception of the path

Trust in Automation

Both screen refresh rate and performance of autonomy have an impact on the participant's self-reported trust as shown in Fig. 3.11. The effect of schemes on trust is not significant. Participants trust the shared control autonomy more when the autonomy is unbiased ($F(1,7) = 27.13,\ p < 0.001$). They also trust the autonomy more when the screen refresh rate is 20 Hz ($F(1,7) = 6.56,\ p = 0.013$).

Driving Task Performance

There is no significance in the path tracking error between two shared control consolidations, as shown in Fig. 3.12. On the other hand, the performance is significantly worse when the low refresh rate is presented compared with the high refresh rate case ($F(1,7) = 38.47,\ p < 0.001$). Moreover, the performance is also worse when a biased autonomy is implemented ($F(1,7) = 54.12,\ p < 0.001$).

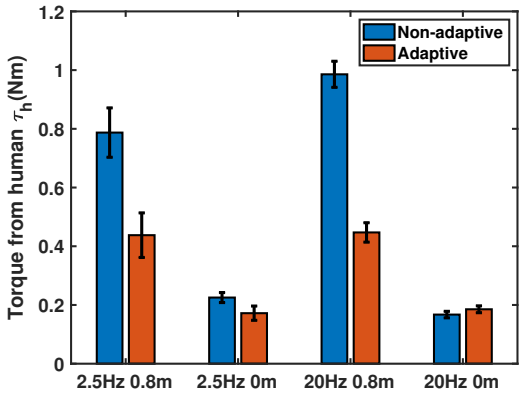

Figure 3.13: Steering control effort in the lane-keeping stage for the four conditions of 20 Hz vs. 2.5 Hz refresh rate and 0 m vs. 0.8 m bias in the perception of the path

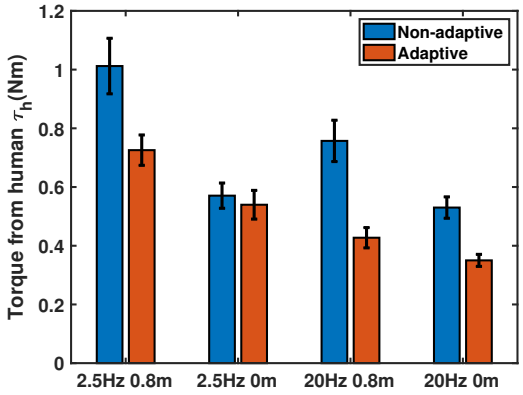

Figure 3.14: Steering control effort in obstacle-avoidance stage for the four conditions of 20 Hz vs. 2.5 Hz refresh rate and 0 m vs. 0.8 m bias in the perception of the path

Participants' Control Effort in Lane-keeping Stage

That the adaptive scheme reduces the torque applied by the human operator compared with the non-adaptive case ($F(1,7) = 47.53, p < 0.001$). Specifically, when the autonomy has a bias, the human exerts significantly less torque compared with the non-adaptive control consolidation, as shown in Fig. 3.13. Moreover, the human participant also needs to apply significantly higher torque in the biased case than in the unbiased case ($F(1,7) = 202.98,\ p < 0.001$), while the impact from the refresh rate is not significant.

Participants' Control Effort in Obstacle Avoidance

That the adaptive scheme reduces the torque applied by the human operator

compared with the non-adaptive case when avoiding obstacles ($F(1,7) = 29.08,\ p < 0.001$). Specifically, when the autonomy has a bias, the human exerts significantly less torque compared with the non-adaptive control consolidation, as shown in Fig. 3.14. The control effort is less when the adaptive scheme is implemented. Moreover, the human operator also needs to apply more torque in the low refresh rate case ($F(1,7) = 26.08,\ p < 0.001$) than in the high refresh rate case. The torque in biased case is also significantly higher ($F(1,7) = 36.9,\ p < 0.001$) than the unbiased case.

3.2.2.4 Discussion

Participants' Workload

Participants report lower workload when experiencing the 20 Hz screen refresh rate or the unbiased autonomy. First, in the cases when the screen refresh rate is 2.5 Hz, the human operator may need to use more mental resources to interpolate between two frames. Therefore, this result verifies the hypothesis that the screen refresh rate affects the workload and validates the proposed method of regulating workload by screen refresh rate in this experiment. Second, the workload reduction from the unbiased autonomy may result from the fact that the human operator may exert more steering effort for fighting with autonomy in the biased case compared with the unbiased cases. Nevertheless, only refresh rate is designed to affect the workload in the experimental design. The workload increase due to bias is not considered, and thus results may improve if the workload due to bias is also taken into account in the adaptive scheme.

Trust in Automation

Participants trust the shared control autonomy more when the autonomy is unbiased or when the screen refresh rate is 20 Hz. On the one hand, since the performance degrades when the autonomy has a bias, the result supports prior research that the human operator's trust in automation depends on the autonomy's performance [92, 93]. On the other hand, the trust increase may result from the fact that information on the environment is abundant in the cases when the screen refresh rate is 20 Hz. Human participants can evaluate the performance of the autonomy better, generating more

trust towards the autonomy.

Driving Task Performance

Results show no significant difference in driving task performance between two shared control consolidation settings, while the performance is significantly worse when the screen refresh rate is low or when the autonomy is biased. The results indicate that different control consolidation settings can achieve similar driving task performance under this condition.

Participants' Control Effort in Lane-keeping Stage

According to the results, adaptive control consolidation can reduce the human's control effort in the lane-keeping stage compared with the non-adaptive cases. Moreover, the reduction is even larger when the autonomy is biased. It can be explained in two aspects. First, when the autonomy has a relatively better performance, the human operator has a higher trust towards the autonomy, leading to the fact that the human operator yields to autonomy more. Therefore, there is almost no difference between these two control consolidations, since in the adaptive scheme, the assistance level is set to be 1 when the torque is small, i.e., when the human yields to autonomy. Second, when the autonomy has some bias, and the human operator needs to intervene to achieve the task objective, the control effort is less when the adaptive scheme is utilized. This observation shows that the adaptive scheme can reduce the control effort, helping the human operator correct the biased guidance from the autonomy easier.

Participants' Control Effort in Obstacle Avoidance

The adaptive control consolidation reduces the torque applied by the human operator compared with the non-adaptive consolidation in the obstacle-avoidance stage. Similar to the previous discussion, the adaptive scheme can reduce the control effort from the autonomy, thereby making it easier for the human to intervene to avoid obstacles.

Effect of Taking Workload into Consideration When Designing Adaptive Control Consolidation

The workload-adaptive control consolidation contains two inputs: the (estimated)

workload w_t from the human operator and the human's torque τ_h. This subsection aims to analyze the impact of the workload, which is the major human factor considered in this dissertation. A torque-adaptive control consolidation is created here, which assumes the human operator always has a moderate workload condition. Therefore, the calculation of its assistance level, which is called re-calculated assistance level and labeled by β_n, is setting the workload $w_t = 50$ in Eq. 3.2 under all circumstances. Under the moderate workload condition, the re-calculated assistance level β_n is identical to the original assistance level β. However, there is a difference between these assistance levels under the over-loaded condition. As shown in Fig. 3.15, the re-calculated assistance level is smaller than the original assistance level. It will lead to a smaller control effort based on the results in Experiment 1. However, a reduced assistance level under the over-loaded condition leads to a worse mission performance, as suggested by [48]. Therefore, the role of the workload in the over-loaded condition is to achieve a good mission performance with more control effort when compared with the consolidation, which does not consider the workload. It is achieved by providing more assistance from autonomy.

3.3 Modified Adaptive Shared Control Consolidation Based on Workload, Human's Torque, and Eyes-On-Road

3.3.1 Modified Adaptive Control Consolidation Design

Compared with the adaptive control consolidation designed in Sec. 3.2.1.2, one more feature is added, namely, eyes-on-road e_t, in the modified adaptive shared control consolidation for the cases when secondary tasks are involved. Eyes-on-road is defined as the percentage of time a subject is looking at the driving task. The intuitive rationale behind adding this human factor is as follows: When the human operator experiences a moderate workload condition, the assistance from autonomy is reduced

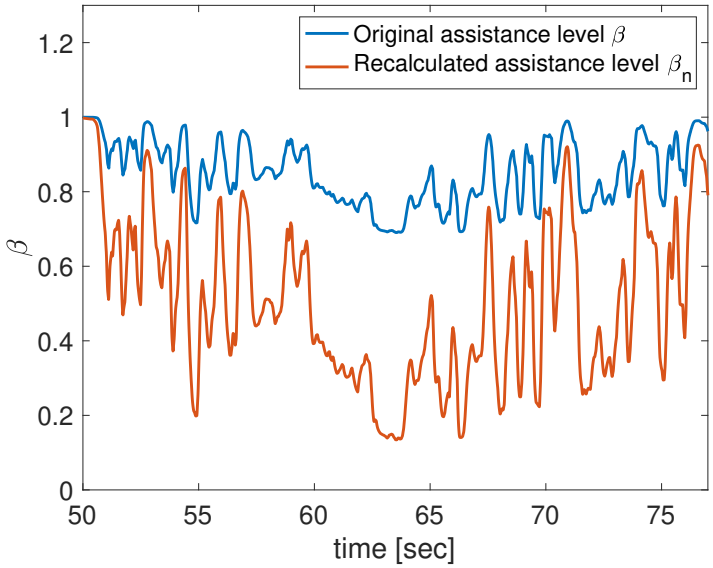

Figure 3.15: Difference between the assistance level in workload-adaptive control consolidation (original assistance level β) and the assistance level in a torque-adaptive control consolidation (recalculated assistance level β_n) under the over-loaded condition.)

in the previous adaptive control consolidation design in Sec. 3.2.1.2. This is not favorable when the subject focuses on tasks other than driving. Therefore, an additional assistance level is added to compensate for this issue. The modified adaptive shared control scheme is designed based on three features: workload, torque from the human operator, and eyes on road. The resultant torque τ_c in the adaptive scheme is $\tau_c = \tau_h + \beta(w_t, e_t, \hat{\tau}_h)\tau_a$, where the term β is the assistance level. Similar to the adaptive control consolidation described in Sec. 3.2.1.2, it also determines the level of assistance from autonomy.

The implementation of the modified adaptive scheme is shown in the block diagram in Fig. 3.16. In the design for the assistance level in modified adaptive control consolidation, β is separated into two parts: base assistance level $\bar{\beta}$ and assistance level increment $\Delta\beta$; i.e., $\beta = \bar{\beta}(w_t, \hat{\tau}_h) + \Delta\beta(w_t, e_t)$. The base assistance level $\bar{\beta}$ considers the impact of workload and input torque from the human operator. The assistance level increment $\Delta\beta$, which is a new component in the modified adaptive control consolidation, considers the combined effect of eyes-on-road and workload.

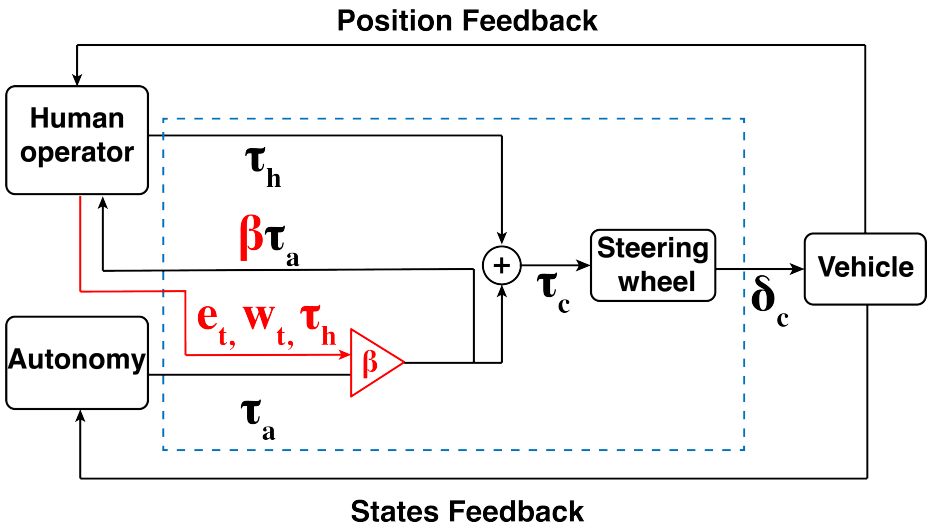

Figure 3.16: Block diagram of the modified adaptive shared control consolidation. τ_{h} and τ_{a} represent the torque from human and autonomy, respectively. The assistance level β is affected by the human's eyes on road e_t, human's workload w_t and the human's torque τ_h. The human operator can feel the assistance torque $\beta\tau_a$ on the steering wheel and exert his/her torque τ_h correspondingly. τ_{c} and δ_{c} are the resultant torque and actual control steering angle while the speed of the vehicle is a constant (15 m/s). The blue dashed box encircles the control consolidation of the system.

Because the base assistance level is already introduced in Sec. 3.2.1.2 in detail, the assistance level increment is detailed in this section.

The relationship between the assistance level increment $\Delta\beta$, the workload w_t and eyes on road e_t is shown in a 3D plot in Fig 3.17. The assistance level increment $\Delta\beta$ is designed based on two design principles.

First, keeping the workload w_t constant, when the subject focuses on the driving task, i.e., e_t is very close to 1, $\Delta\beta$ is very close to 0, which indicates no additional assistance level is provided based on the eyes-on-road metric. When the subject directs their attention to the secondary tasks, i.e., e_t is very close to 0, $\Delta\beta$ increases to a high level, which is illustrated in Fig. 3.18. An exponential function is used to connect these two points. Second, keeping the eyes-on-road e_t constant, when workload w_t is high, the increment $\Delta\beta$ is large, whereas when the workload is moderate, the increment $\Delta\beta$ is small, which is shown in Fig. 3.19. The value of $\Delta\beta$ is set as 0.4 when the subject experiences moderate workload ($w_t = 50$) based on a pilot study. It is set as 0.9 when the subject is over-loaded or under-loaded ($w_t = 100$ or $w_t = 0$).

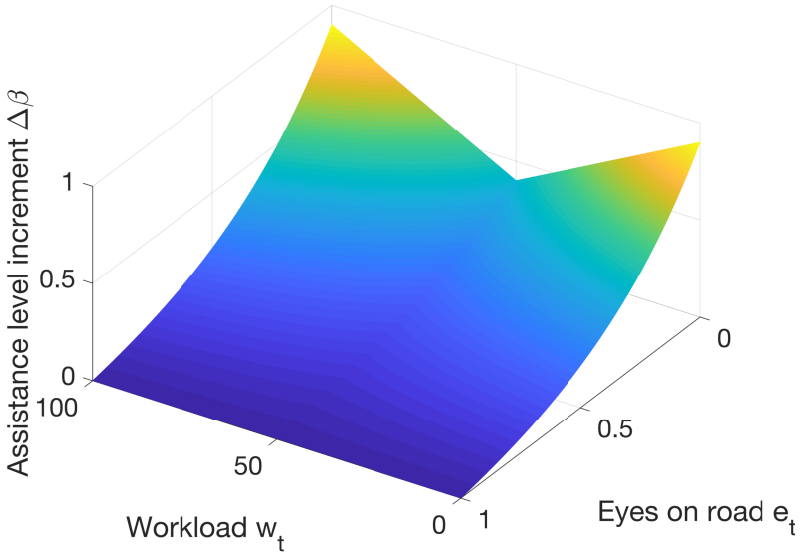

Figure 3.17: The relationship between the assistance level increment $\Delta\beta$, the workload w_t and eyes-on-road e_t. We define $e_t = 0$ when the human operator focuses on the surveillance task while $e_t = 1$ when the human operator focuses on driving.

This value is calculated through linear interpolation when the workload is between these critical values.

Combining these considerations, the formulation of assistance level increment $\Delta\beta$ is obtained as

$$\Delta\beta(w_t, e_t) = 0.1(0.1|w_t - 50| + 5)^{1-e_t} - 0.1 \tag{3.4}$$

Hence, the assistance level β in the modified adaptive control consolidation is a direct sum of the two terms $\bar{\beta}$ and $\Delta\beta$.

3.3.2 Evaluation of the Modified Adaptive Shared Control Consolidation: Experiment 2

3.3.2.1 Introduction

Another human subject study, Experiment 2, is used to evaluate the performance of the modified adaptive control consolidation, which is demonstrated in Sec. 3.3.1. There are 12 subjects in this human subject study. They are required to control the vehicle and track the centerline collaboratively with autonomy. The autonomy has

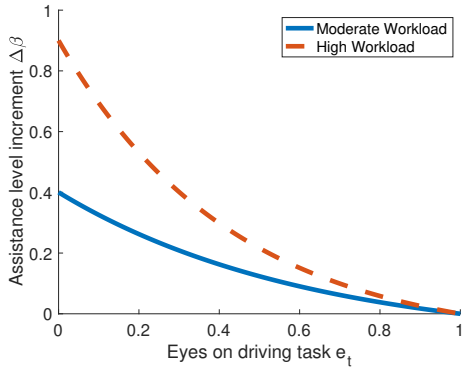

(a) Relationship between assistance level increment $\Delta\beta$ and eyes on road e_t when human's workload w_t is different.The curves are the section shown in Fig. 3.18b and Fig. 3.18c, respectively.

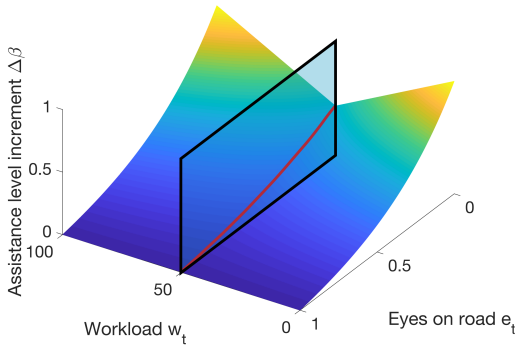

(b) The 3D plot section showing the relationship between the assistance level increment $\Delta\beta$ and eyes on road e_t under moderate workload cases.

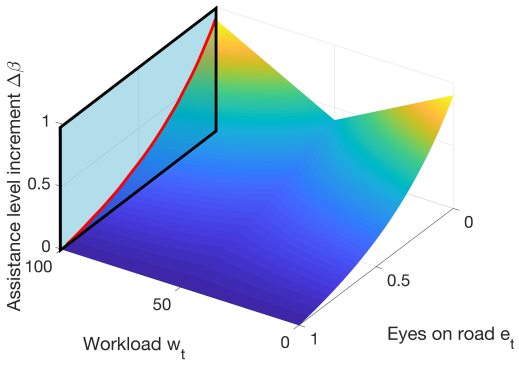

(c) The 3D plot section showing the relationship between the assistance level increment $\Delta\beta$ and eyes on road e_t under high workload cases.

Figure 3.18: Illustration of the first design principle of assistance level increment

a perception bias, which is approximately 1 m. Unlike Experiment 1, no obstacle is presented in the driving task in this experiment. In addition, the participants need to perform a surveillance task in Experiment 2. The surveillance task urgency, introduced in Sec. 2.5, is assumed to impact the participants' workload significantly. Therefore, in this experiment, it is proposed to use different surveillance task urgencies to control the workload of the human operator. There are two surveillance task urgencies: low urgency (6.5 s pace) and high urgency (1.5 s pace). A workload estimator, which is provided by our collaborators, Dr. Ruikun Luo and Prof. Jessie Yang, uses the Hidden Markov Model (HMM) to obtain the workload estimation [75].

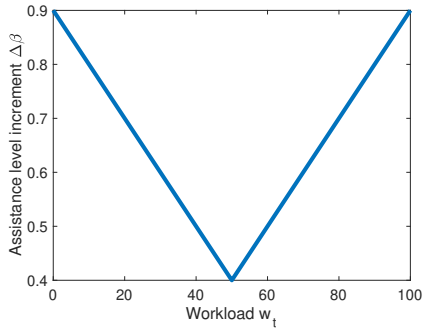

(a) Relationship between assistance level increment $\Delta\beta$ and workload w_t when $e_t = 0$. The curve is the section shown in Fig. 3.19b

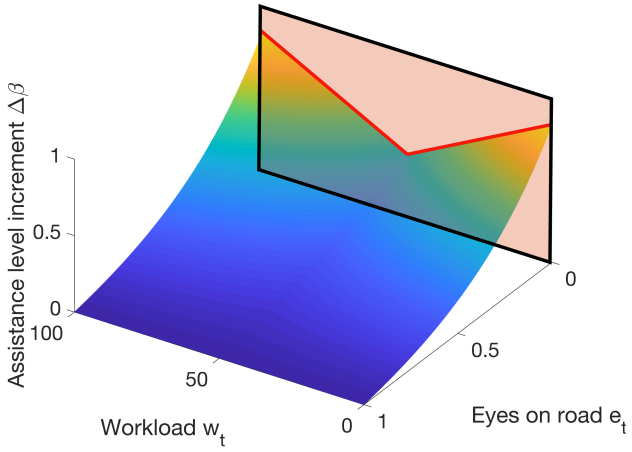

(b) Relationship between assistance level increment $\Delta\beta$ and workload w_t when $e_t = 0$ in 3D plot.

Figure 3.19: Illustration of the second design principle of assistance level increment

It uses the gaze trajectory data obtained from the eye tracker, Tobii Pro Glasses 2. Its F_1 score, precision, and recall are 0.664 ± 0.005, 0.668 ± 0.005 and 0.660 ± 0.005, respectively. Both the modified adaptive control consolidation and the baseline non-adaptive control consolidation are implemented to compare the results.

3.3.2.2 Method

Participants

There are a total of 13 student participants in this experiment. Data of 1 participant are discarded due to the wrong experiment setup. The remaining 12 participants are on average 22.3 years old ($SD = 3.7$ years) and have an average of 5.7 years of driving experience ($SD = 3.9$ years). All participants have a normal or corrected-to-normal vision, and the eye tracker can be calibrated on their eyes.

Apparatus and stimuli

In this experiment, subjects use the testbed, whose visualization module is introduced in Sec. 2.2.2. The driving module is identical to Experiment 1. In the driving task, the participant and the autonomy share the steering control of the vehicle, whereas the vehicle travels at a fixed speed, which is 15 m/s. The goal of the

Table 3.4: Cost function weights in NMPC in Experiment 2

Weight	w_1	w_2	w_3
Value	10.0	1.5	0.001

task is to complete a track with minimal deviation from the path, as denoted by the centerline. To emulate degraded localization due to sensor uncertainty, an offset is introduced such that the autonomy tracks a line that deviates from the centerline by 1 m. Unlike Experiment 1, the surveillance task urgency is used to control the subject's workload in this experiment. There are two surveillance task urgencies: 1.5 s pace and 6.5 pace. They are labeled as high surveillance task urgency and low surveillance task urgency, respectively. In the appendix of [75], the choice of the values of the surveillance task urgency is assessed. Both the non-adaptive shared control consolidation and the modified adaptive shared control consolidation are used in this experiment as described in Sec. 3.2.1.1 and Sec. 3.3.1, respectively. For the workload estimation and eyes on road calculation, the gaze point data from a 4 s time window captured by the eye tracker, Tobii Pro Glasses 2 (30 Hz sampling rate), are used to estimate participants' workload and eyes on road. The calculation method of the estimated workload w_t can be found in [75] using the Hidden Markov Model (HMM). The eyes on road e_t is calculated as the average number of times that a participant's gaze points fall on the driving screen within the time window. Due to the large mass and high center of gravity of the simulated military vehicle, a rapid change of control commands resulting from a rapid change of estimated workload w_t and eyes on road e_t can trigger a rollover. Therefore, a moving average filter is applied with a 1 s time window, and w_t and e_t are down-sampled to 10 Hz.

Autonomy Formulation

The cost function used in this study is

$$\begin{aligned} J =& w_1 \int_{t_0}^{t_P} \left(y_{\text{ref}}(x(t)) - y(t)\right)^2 dt + w_2 \int_{t_0}^{t_P} \gamma^2 dt \\ &+ w_3 \int_{t_0}^{t_P} \left(\tanh\left[\frac{a - F_{z,rl}}{b}\right] + \tanh\left[\frac{a - F_{z,rr}}{b}\right] \right) dt \end{aligned} \tag{3.5}$$

It consists of three terms. As introduced by Sec. 3.2.2.2, they are used to penalize

Table 3.5: Four test conditions in Experiment 2

Condition	Surveillance task urgency		Shared control consolidation setting
	First half of the track	Second half of the track	
1	1.5 s	6.5 s	Non-adaptive
2	1.5 s	6.5 s	(Modified) adaptive
3	6.5 s	1.5 s	Non-adaptive
4	6.5 s	1.5 s	(Modified) adaptive

the deviation from the current line, regulate the control inputs of the vehicle for a smooth steering maneuver, and prevent the vehicle from operating at its dynamic limit unnecessarily. Three weights w_1, w_2, and w_3 are set to achieve a trade-off between these goals, whose values are listed in Table 3.4.

Experimental design

The experiment uses a within-subjects design with two independent variables. The first independent variable is the shared control consolidation setting (modified adaptive haptic shared control vs. non-adaptive haptic shared control). The second independent variable is the surveillance task urgency (1.5 s vs. 6.5 s). Each participant experiences four tracks in the experiment. On each track, one type of haptic shared control consolidation is used. In addition, each track is segmented into two portions, one portion with high urgency surveillance task (1.5 s) and the other with low urgency surveillance task (6.5 s). The resulting four test conditions are shown in Table 3.5. The presentation of test conditions follows a 4×4 Latin square design to eliminate potential order effects.

Measures

Five dependent variables are collected in the experiment:

- Participants' self-reported workload
- Participants' self-reported trust in the shared control autonomy
- Participants' steering control effort
- Driving task performance
- Surveillance task performance

After each track, participants report their workload and trust for the first and the second half of the track using two uni-dimensional scales. The NASA TLX survey [90] and Jian's trust survey [94] are presented to the participants such that they understand the meaning of workload and trust.

Participants' steering control effort is calculated as the average of the absolute value of the torque that a participant applies on the steering wheel. The torque from the human operator is estimated from a nonlinear steering wheel model, which captures the relationship between the torque and steering angle based on experimental data. Driving task performance is evaluated by the lane-keeping error. The lane-keeping error is calculated as the mean of the absolute deviation of the vehicle's position from the centerline. The surveillance task performance is measured using the detection accuracy of the surveillance task.

Experimental procedure

Before the training session starts, participants provide a signed informed consent and fill in a demographic survey. After that, they are assisted in wearing the eye tracker with calibration. With the normal room light and without any specific tasks, the experimenter measures each participant's baseline pupil diameter twice, each about 30 s before the training.

During the training session, the participants first perform two trials of the driving task only, one with the non-adaptive haptic shared control and one with the modified adaptive haptic shared control. Each trial takes approximately 1.5 min. Then the participants perform three trials of the surveillance task only. Each trial takes approximately 60 s. After that, the participants perform four trials of the combined driving and surveillance task.

During the official experiment, participants perform the driving task and the surveillance task on four different tracks with different test cases as described in Table 3.5. Each trial takes approximately 3 min. After each trial, the participants are asked to fill a post-survey about the workload and trust during each portion of the track.

Table 3.6: Mean and standard error (SE) of workload, trust, lane keeping error, detection accuracy and torque in Experiment 2

Metrics	N	Surveillance task urgency			
		1.5 s		6.5 s	
		Adaptive	Non-adaptive	Adaptive	Non-adaptive
Workload	12	13.96 ± 0.82	14.08 ± 0.87	7.83 ± 0.81	8.71 ± 0.97
Trust	12	4.04 ± 0.37	3.63 ± 0.30	3.92 ± 0.32	3.29 ± 0.38
Lane keeping error (m)	12	0.28 ± 0.033	0.36 ± 0.045	0.21 ± 0.03	0.26 ± 0.04
Detection accuracy (%)	12	93.43 ± 1.38	91.86 ± 1.13	94.30 ± 1.77	96.54 ± 1.18
Torque (Nm)	12	0.36 ± 0.03	0.73 ± 0.03	0.30 ± 0.02	0.79 ± 0.01

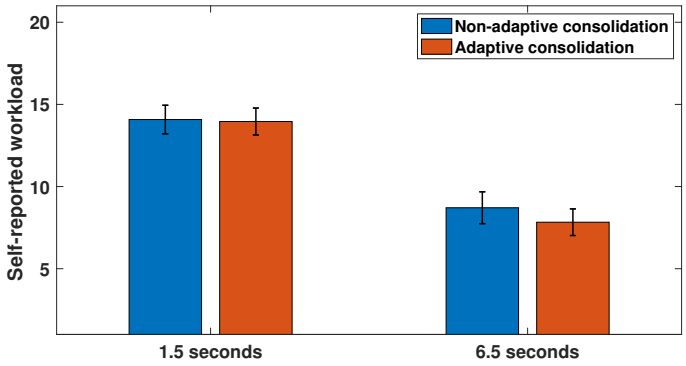

Figure 3.20: Mean and standard error (SE) values of self-reported workload in Experiment 2

3.3.2.3 Results

Two-way repeated-measures Analysis of Variance (ANOVA) is conducted with the shared control consolidation setting and the surveillance task urgency as the within-subjects variables. Results are reported as significant for $\alpha < .05$.

Table 3.6 summarizes the mean and standard error (SE) values of the participants' self-reported workload and trust as well as driving task performance, surveillance task performance, and their exerted torque.

Participants' Workload

Both control consolidation setting and surveillance task urgency influence participants' self-reported workload. With the modified adaptive shared control consolidation, participants report lower workload ($F(1, 11) = 5.18,\ p = .044$). When the surveillance task is less urgent, participants report lower workload ($F(1, 11) = 20.26$, $p < .001$).

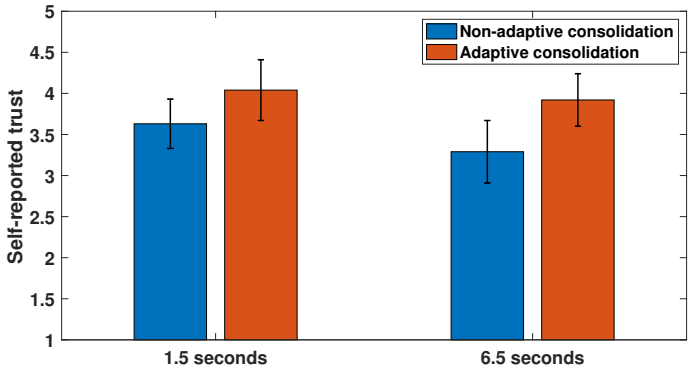

Figure 3.21: Mean and standard error (SE) values of self-reported trust in automation in Experiment 2

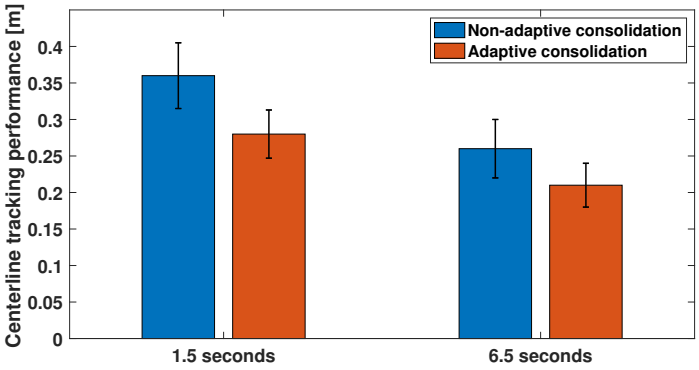

Figure 3.22: Mean and standard error (SE) values of lane keeping error (m) in Experiment 2

Trust in Automation

Participants trust the shared control autonomy more when the control consolidation is adaptive ($F(1, 11) = 12.76,\ p = .004$). The effect of surveillance task urgency on trust is not significant.

Driving Task Performance

The shared control consolidation setting and the surveillance task urgency significantly affect the driving task performance. Participants have smaller lane-keeping errors when using the modified adaptive shared control consolidation ($F(1, 11) = 7.593$, $p = .019$), and when the surveillance task is less urgent ($F(1, 11) = 96.33,\ p < 0.001$) (Fig. 3.22). There is also an interaction effect between the control consolidation setting and surveillance task urgency ($F(1, 11) = 6.141,\ p = .031$). Using modified

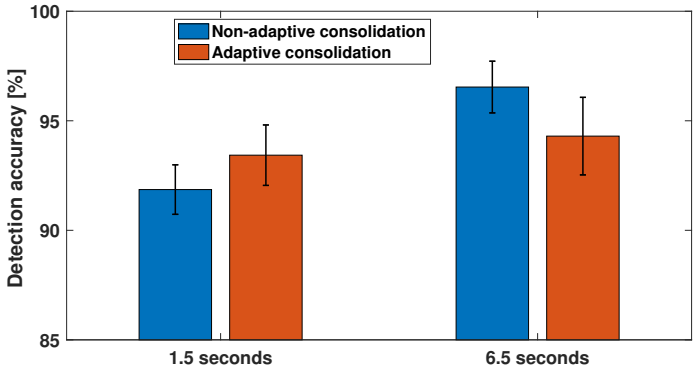

Figure 3.23: Mean and standard error (SE) values of surveillance task detection accuracy (%) in Experiment 2

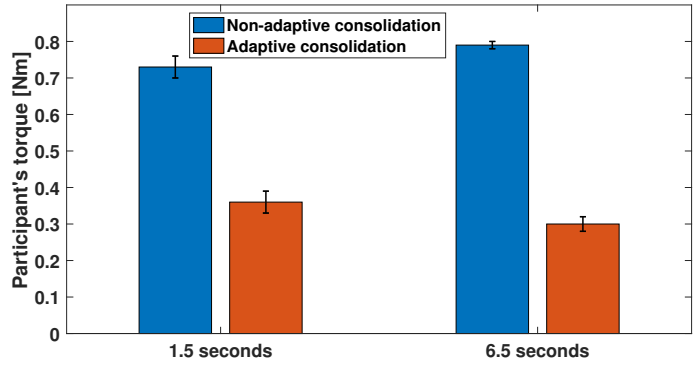

Figure 3.24: Mean and standard error (SE) values of participants' torque (Nm) in Experiment 2

adaptive shared control consolidation leads to a larger reduction in lane-keeping error when the surveillance task is more urgent.

Surveillance Task Performance

For the surveillance task, task urgency significantly influences the detection accuracy ($F(1, 11) = 6.73, \quad p = .025$). Detection accuracy is higher when the task is less urgent. The effect of the shared control consolidation setting is non-significant (Fig. 3.23).

Participants' Steering Control Effort

There is a significant effect of shared control consolidation setting on participants' control effort ($F(1, 11) = 217.66, \ p < .001$). With modified adaptive shared control consolidation, participants exert significantly less control effort. The effect of

surveillance task urgency on participants' control effort is non-significant. In addition, results reveal a significant interaction effect between shared control consolidation setting and surveillance task urgency ($F(1, 11) = 11.42,\ p = .006$). When the surveillance task is less urgent (6.5 s), the modified adaptive shared control consolidation leads to a larger drop in torque.

3.3.2.4 Discussion

Participants' Workload

Participants' self-reported workload decreases when using the modified adaptive shared control consolidation and when the surveillance task becomes less urgent. The results can have resulted from the following reasons. First, the 6.5 s surveillance task urgency imposes a smaller temporal demand on participants, leading to a lower self-reported workload. Therefore, the result validates the proposal of using surveillance task urgency to control the participants' workload. Second, the participants' control effort is smaller with the adaptive control consolidation. Third, participants' driving task performance is higher with the adaptive control consolidation and when the surveillance task is less urgent.

Trust in Automation

This result is consistent with prior research that human operators' trust in automation is determined by the autonomy's performance [92, 93, 95]. Human operators continuously perceive both the driving and the surveillance task performance, based on which they adjust their trust in automation. As the driving task performance increases with the adaptive control consolidation, trust increases accordingly.

Driving Task Performance

The modified adaptive shared control consolidation benefits the driving task performance, especially when participants are under a high workload. Based on the design of the modified adaptive haptic shared control consolidation, with the same input torque, when the human operator has a high workload and focuses on the surveillance task, the assistance level is increased. The increment in the assistance level is expected to aid the driving task and reduce the lane-keeping error. This design

principle is supported by the experimental results.

Surveillance Task Performance

As the surveillance task becomes more urgent and more demanding, the surveillance task performance decreases significantly. This result is consistent with prior research that when workload increases from moderate to high level, task performance decreases [54].

Participants' Steering Control Effort

With the modified adaptive shared control consolidation, participants exert significantly less amount of control effort in both low and high workload conditions. The results can be explained as follows: First, as the participants' trust toward the adaptive shared control scheme is significantly higher than the non-adaptive control scheme, participants have a higher tendency to yield to autonomy, resulting in smaller input torque. Second, according to the design principles of the adaptive shared control consolidation, with the same input torque, when the human operator experiences a moderate workload and focuses on the driving task, the assistance level is reduced. With a reduced assistance level, regardless of whether the human yields to or fights with the autonomy, the human operator's torque is expected to be smaller.

3.4 Conclusion

In this chapter, the concept of workload-adaptive control consolidation is introduced. Two adaptive control consolidations are proposed, and two experiments are conducted to validate these control consolidations, respectively. In Experiment 1, which aims to evaluate the performance of the adaptive control consolidation, the screen refresh rate is used to control the human participant's workload when the driving task is the only task. Results from 8 participants show that the adaptive shared control consolidation can help the human operator exert less control effort during the interventions without sacrificing the driving task performance as characterized by the path tracking error. In Experiment 2, which aims to evaluate the performance of the modified adaptive control consolidation, the surveillance task urgency is used to control the participant's

workload in a driving-surveillance dual-task scenario. In addition, unlike in Experiment 1, where it is assumed the screen refresh rate is known before the trial starts, in Experiment 2, a real-time Hidden Markov Model (HMM)-based workload estimation algorithm is implemented. Results from 12 subjects show that the modified adaptive shared control consolidation can reduce human workload, increase their trust in the system, improve driving performance, and reduce human steering control effort without sacrificing surveillance task performance.

These results reveal the benefit of considering and adapting to workload in shared control problems at the consolidation level. Nevertheless, some limitations exist, and several potential improvements can be made. On the one hand, so far, it is either assumed that the workload estimation is known (Experiment 1) or the Hidden Markov Model is used as the real-time workload estimation (Experiment 2). The performance is yet to be studied when Bayesian Inference, a real-time workload estimation algorithm that is tailored to the dual-task missions, is implemented. This more advanced workload estimation is implemented in Chapter 4 and Chapter 5. On the other hand, the autonomy in this chapter remains to be non-adaptive to workload. The benefit of the workload adaptation is only explored at the control consolidation level. Adapting to workload at the autonomy level can also lead to improvements, and these potential improvements are explored in Chapter 4.

Chapter 4

Workload-adaptive Autonomy Navigation Formulation

4.1 Introduction

This chapter examines the benefit of considering workload and adapting correspondingly at the autonomy level. A pilot study has considered a set of parameters used in the autonomy formulation and identified the vehicle's maximum speed limit as the one with the highest impact on the human driver's workload. Therefore, the first portion of this chapter is to study the impact of the maximum speed limit on the workload thoroughly through a human subject study, namely, Experiment 3. In Experiment 3, participants simultaneously experience both the driving and surveillance tasks. The vehicle's speed is controlled by autonomy in the driving task. In the experiment, the autonomy presents two maximum speed limits. The results indicate that the maximum speed limit significantly impacts workload and several other mission-performance-related metrics. Based on the results from Experiment 3, in the second portion of this chapter, a workload-adaptive autonomy navigation formulation is designed by modifying the maximum speed limit based on the human operator's estimated workload. In addition to workload, other human factors are also considered, such as the human driver's torque, which represents the degree of intervention from the human operator. Another human subject study examines the benefits of the

designed workload-adaptive autonomy, namely, Experiment 4. In Experiment 4, the participants experience both the driving and surveillance tasks with different autonomy settings, and the surveillance task urgency controls the workload of participants. Unlike previous experiments, the real-time workload estimation is achieved using the novel Bayesian Inference (BI) method developed by our collaborators, Dr. Ruikun Luo and Prof. Jessie X. Yang [87].

4.2 Identification of the Autonomy Parameters for Adaptation

The idea of enabling adaption in shared control at the autonomy level relies on changing the autonomy parameters based on the real-time workload estimation. From the prior literature about manual driving, several variables impact drivers' workload, such as acceleration [70] and speed [71]. In addition, the operator's workload is also associated with the obstacles [96, 97] present in the environment. These variables can also potentially impact the human driver's workload in the semi-autonomous driving mode, which is determined by autonomy's parameters in this work. In the shared control driving mode used in the dissertation, the related parameters of autonomy are the autonomy's maximum speed limit, maximum acceleration, headway, and safety margin for obstacle avoidance. According to our pilot user study, participants report that the autonomy's maximum speed limit affects their workload significantly. Therefore, a detailed human subject study is conducted to evaluate and investigate the impact of the autonomy's maximum speed limit on the human operator's workload.

4.2.1 Investigation of the Impact of Autonomy Maximum Speed Limit: Experiment 3

4.2.1.1 Introduction

In this study, the impact of the maximum speed limit on workload is investigated by a human subject study. Different values of the maximum speed limit are adopted as

the autonomy parameter, which is not fixed in the experiment. Based on the subject's reported workload, the impact of the maximum speed limit is obtained. In addition, there is a probability that the impact of the maximum speed limit is different when the subject has different workload conditions. The magnitude of change in workload resulting from different maximum speed limits when the subject has a moderate workload can be different from the one when the subject is over-loaded. Therefore, the sensitivity of this impact is also investigated when the subject has different workload conditions. There are 12 subjects in this human subject study. The driving task for participants is to control the vehicle and track the centerline collaboratively with autonomy. Participants experience two maximum speed limits of autonomy in the driving task: low maximum speed limit (12.5 m/s) and high maximum speed limit (22.5 m/s). Unlike Experiment 1 and Experiment 2, autonomy has no perception bias in this experiment. There are obstacles located at the centerline. The participants also need to perform a surveillance task. The surveillance task urgency, which is introduced in Sec. 2.5, varies in this experiment as well. The surveillance task urgency controls the workload condition of the participant, which helps evaluate the sensitivity of the impact of the maximum speed limit on workload. Two surveillance task urgencies are presented: low urgency (6.5 s pace) and high urgency (1.5 s pace).

4.2.1.2 Method

Participants

There are a total of 12 student participants in the experiment. The participants are on average 25.42 years old (SD = 3.06 years) and have an average of 5.92 years of driving experience (SD = 3.70 years). All participants have a normal or corrected-to-normal vision.

Apparatus and stimuli

Unlike the previous experiments, participants use the testbed introduced in Sec. 2.2.3. They perform two tasks, the driving task and the surveillance task, simultaneously. In the driving task, the participant and the autonomy share the vehicle's steering control, while the vehicle's speed is controlled by autonomy only. The non-adaptive

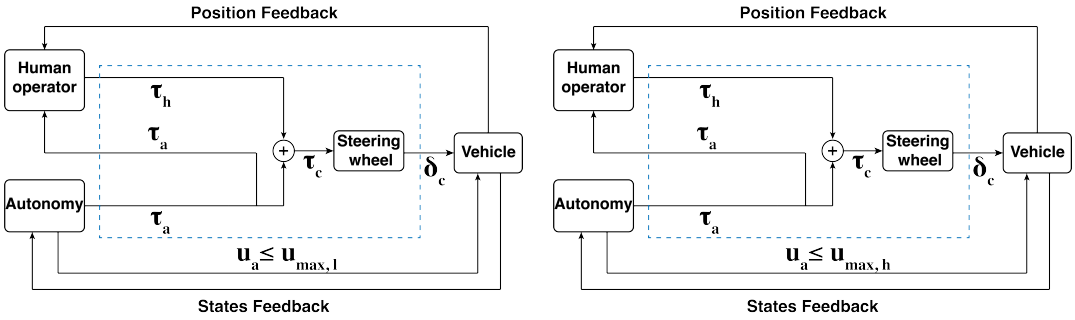

(a) Control block diagram when the low maximum speed limit is implemented.

(b) Control block diagram when the high maximum speed limit is implemented.

Figure 4.1: Control block diagram when different maximum speed limits are implemented. The blue dashed lines highlight the control consolidation where non-adaptive control consolidation is implemented. The term u_a represents the speed of the vehicle is controlled by autonomy only. $u_{max,l}$ and $u_{max,h}$ are the two autonomy maximum speed limits: 12.5 m/s and 22.5 m/s.

control consolidation is used in this experiment, which is shown in Sec. 3.2.1.1, so the impact on workload only comes from the autonomy side. The goal of the driving task is to complete a track with minimal deviation from the centerline while avoiding obstacles on the centerline. The autonomy has no obstacle avoidance capability. This experiment uses two maximum speed limits to study the impact on workload: 12.5 m/s and 22.5 m/s. They are called the low-maximum-speed autonomy and the high-maximum-speed autonomy, respectively. The low-speed limit value for autonomy is selected because it is close to the normal speed restriction of 25 mph (11.18 m/s). The high-speed limit is picked because it is close to 80 km/h (22.22 m/s), the maximum on-road speed for the HMMWV (version M1151 [98]). Besides driving, participants also need to perform the surveillance task. The goal of the surveillance task is to make the identification within the time limit as accurate as possible. The surveillance task urgency is used to control the subject's workload in this experiment, which is helpful for the sensitivity analysis of the maximum speed limit's impact on workload. There are two surveillance task urgencies: 1.5 s pace and 6.5 s pace. They are labeled as high surveillance task urgency and low surveillance task urgency, respectively.

Autonomy Formulation

Table 4.1: Weights of autonomy in Experiment 3

Parameters	w_1	w_2	w_3	w_4	w_5
Value	0.2	10.0	2.4	1.2	5.0

Compared with the autonomy used in Experiment 1 and Experiment 2 shown in Sec. 3.2.2.2 and Sec. 3.3.2.2, a similar autonomy formulation is used in this human subject experiment. The cost function of the autonomy used in this study is

$$\begin{aligned} J =& w_1 x(t_P) + w_2 \int_{t_0}^{t_P} \left(y_{\text{ref}}(x(t)) - y(t)\right)^2 dt + w_3 \int_{t_0}^{t_P} \gamma^2 dt + w_4 \int_{t_0}^{t_P} J_x^2 dt \\ &+ w_5 \int_{t_0}^{t_P} \left(\tanh\left[\frac{a - F_{z,rl}}{b}\right] + \tanh\left[\frac{a - F_{z,rr}}{b}\right] \right) dt \end{aligned} \tag{4.1}$$

The cost function consists of five terms. As introduced by Sec. 3.2.2.2 and Sec. 3.3.2.2, the second to the fifth terms are used to penalize the deviation from the current line, regulate the control inputs of the vehicle for a smooth steering and acceleration maneuver, and prevent the vehicle from operating at its dynamic limit unnecessarily. The first term $w_1 x(t_P)$ is designed to push the vehicle to its speed limit by setting the terminal position as far away as possible. Five weights w_1, w_2, w_3, w_4, and w_5 are set to achieve a trade-off between these goals, whose values are listed in Table 4.1.

In addition, different maximum speed limits are achieved by introducing the additional constraints in the autonomy setting, which is described in Sec. 2.3 as below:

$$u_x \leq u_{x,max}$$

In this experiment, the maximum speed limit $u_{x,max}$ is set to be 12.5 m/s and 22.5 m/s for the low-maximum-speed autonomy and high-maximum-speed autonomy, respectively. The control block diagrams of these two cases are shown in Fig. 4.1.

Experimental design

The experiment adopts a within-subjects design with two independent variables. The first independent variable is the maximum speed limit of autonomy (12.5 m/s

Table 4.2: Four test conditions in Experiment 3

Condition	Surveillance task urgency	Maximum speed limit
1	1.5 s	12.5 m/s
2	1.5 s	22.5 m/s
3	6.5 s	12.5 m/s
4	6.5 s	22.5 m/s

vs. 22.5 m/s). The second independent variable is the surveillance task urgency (1.5 s vs. 6.5 s). Each participant experiences four tracks in the experiment. One combination of a autonomy's maximum speed limit and a surveillance task urgency is presented on each track. The resulting four test conditions are shown in Table 4.2. The presentation of test conditions follows a 4×4 Latin square design to eliminate potential order effects.

Measures

Six dependent variables are collected in the experiment:

- Participants' self-reported workload
- Participants' steering control effort in the lane-keeping task
- Driving task performance
- Participants' steering control effort under emergency
- Emergency maneuvering performance
- Surveillance task performance

In this experiment, the obstacle-avoidance stage has the same definition as in Sec. 3.2.2.2. The obstacle-avoidance stage is defined as the period when the human subjects deviate at least 1 m from the centerline and avoid the obstacles. The remaining part is defined as the lane-keeping stage.

After each track, participants report their workload using the NASA TLX survey [90]. The NASA TLX survey is presented to the participants before the experiment such that they understand the meaning of workload. Similar to previous methods in Sec. 3.2.2.2 and Sec. 3.3.2.2, a participant's steering control effort in the lane-keeping

task is calculated as the average value of the absolute human torque during the lane-keeping stage. Driving task performance is evaluated by lane-keeping error, which is calculated as the mean of the absolute deviation of the vehicle's position from the centerline during the lane-keeping stage. Steering control effort under emergency is calculated as the average of the absolute human torque that the participant applied on the steering wheel during the obstacle avoidance maneuver. Emergency maneuvering performance is evaluated by centerline deviation during the obstacle avoidance maneuver, which uses a similar calculation method as driving task performance but in the obstacle-avoidance stage. The torque from the participant is measured from a steering torque rotatory sensor. The collection rate of driving performance and steering control effort of the lane-keeping and obstacle-avoidance stages is 100 Hz. The surveillance task performance is measured using the detection accuracy of the surveillance task.

Experimental procedure

Participants provide a signed informed consent and fill in a demographic survey before the training session.

During the training session, the participants first perform two trials with the driving task only, one with the low-maximum-speed autonomy and one with the high-maximum-speed autonomy. The trials with the low-maximum-speed autonomy take approximately 5 minutes, while the trials with the high-maximum-speed autonomy take approximately 3 minutes. Then the participants perform a trial with the surveillance task only. It consists of two portions: the low task urgency portion, which comes first, and the high urgency portion, which comes later. The low task urgency portion takes approximately 1 minute, and the high task urgency portion takes approximately 2 minutes. After that, the participants perform two combined driving and surveillance task trials.

During the official experiment, participants perform the driving task and the surveillance task on four different tracks with the test cases described in Table 4.2. The trials with the low-maximum-speed autonomy take approximately 6 minutes, while the trial with the high-maximum-speed autonomy takes approximately 4 min-

Table 4.3: Mean and standard error (SE) of workload, centerline tracking error, centerline tracking torque, deviation under emergency, obstacle avoidance torque, and detection accuracy in Experiment 3

Metrics	N	Surveillance task urgency			
		6.5 s		1.5 s	
		Autonomy's maximum speed limit			
		12.5 m/s	22.5 m/s	12.5 m/s	22.5 m/s
Workload	12	19.940 ± 3.599	32.917 ± 4.951	51.190 ± 3.381	58.333 ± 3.242
Centerline tracking error (m)	12	0.333 ± 0.013	0.568 ± 0.044	0.384 ± 0.017	0.676 ± 0.052
Centerline tracking torque (Nm)	12	0.312 ± 0.018	0.277 ± 0.017	0.309 ± 0.019	0.325 ± 0.023
Deviation under emergency (m)	12	2.778 ± 0.196	3.105 ± 0.211	2.735 ± 0.190	3.145 ± 0.194
Obstacle avoidance torque (Nm)	12	1.486 ± 0.037	0.776 ± 0.049	1.499 ± 0.048	0.809 ± 0.046
Detection accuracy (%)	12	96.035 ± 1.055	93.254 ± 2.212	91.639 ± 1.469	89.794 ± 2.030

utes. After each trial, the participants are asked to fill a post-survey (NASA TLX) about the workload during the last track. If they hit the obstacle, the trial is restarted.

4.2.1.3 Results

Two-way repeated-measures Analysis of Variance (ANOVA) is conducted with the autonomy's maximum speed limit and the surveillance task urgency as the within-subjects variables. Results are reported as significant for $\alpha < .05$.

Table 4.3 summarizes the mean and standard error (SE) values of the participants' self-reported workload, driving task performance, human torque during the lane-keeping stage, emergency maneuvering performance, participants' steering control effort under emergency, and surveillance task performance.

Participants' Self-reported Workload

Both autonomy's maximum speed limit and surveillance task urgency have a significant impact on the self-reported workload, as shown in Fig. 4.2. With a higher maximum speed limit, participants report higher workload value ($F(1, 11) = 61.542$, $p < 0.001$). When the surveillance task is more urgent, participants report higher workload ($F(1, 11) = 37.435,\ p < 0.001$). No significant interaction effect is found between the autonomy's maximum speed limit and surveillance task urgency ($F(1, 11) = 1.289,\ p = 0.280$), as shown in Fig. 4.3.

Driving Task Performance

The autonomy's maximum speed limit and the surveillance task urgency signif-

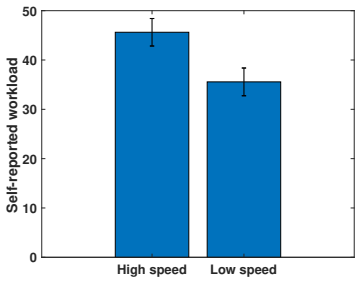

(a) Relationship between self-reported workload and autonomy's maximum speed limit

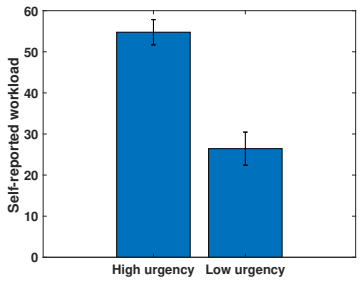

(b) Relationship between self-reported workload and surveillance task urgency

Figure 4.2: Impacts of autonomy's maximum speed limit and surveillance task urgency on participants' self-reported workload in Experiment 3. "High speed" stands for high-maximum-speed autonomy and "Low speed" stands for low-maximum-speed autonomy.

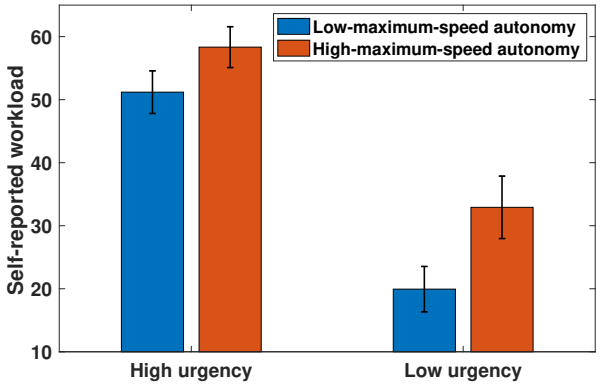

Figure 4.3: Relationship between self-reported workload and different autonomy settings in Experiment 3 under different surveillance task urgencies

icantly affect the driving task performance in the lane-keeping stage. Participants have a smaller centerline tracking error when the autonomy's maximum speed limit is low ($F(1, 11) = 58.171,\ p < 0.001$), and when the surveillance task is less urgent ($F(1, 11) = 9.950,\ p = 0.009$). These results are shown in Fig. 4.4. In addition, no significant interaction effect is observed between autonomy's maximum speed limit and surveillance task urgency ($F(1, 11) = 3.439,\ p = 0.091$), as shown in Fig. 4.5.

Participants' Steering Control Effort During Lane Keeping

No significant effect of the autonomy's maximum speed limit ($F(1, 11) = 0.411$, $p = 0.535$) and surveillance task urgency ($F(1, 11) = 2.445,\ p = 0.146$) on par-

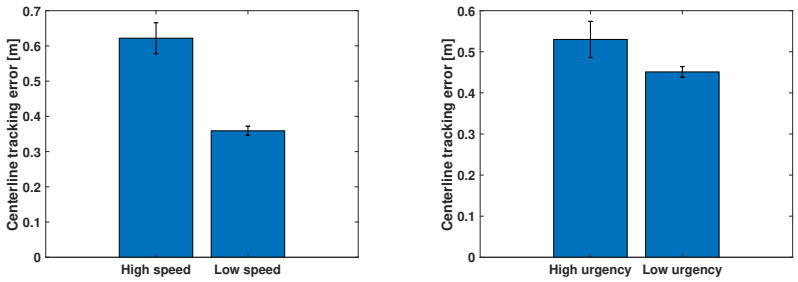

(a) Relationship between centerline tracking error and autonomy's maximum speed limit

(b) Relationship between centerline tracking error and surveillance task urgency

Figure 4.4: Impacts of autonomy's maximum speed limit and surveillance task urgency on centerline tracking error in Experiment 3

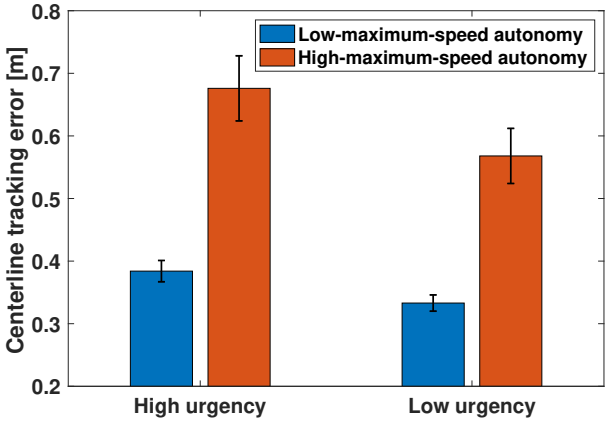

Figure 4.5: Relationship between centerline tracking error in the lane-keeping stage and different autonomy settings in Experiment 3 under different surveillance task urgencies

ticipants' steering control effort during the lane-keeping stage is observed as shown in Fig. 4.6. In addition, the steering control effort during the lane-keeping stage of different autonomy settings under different surveillance task urgencies is shown in Fig. 4.7.

Emergency Maneuvering Performance

The autonomy's maximum speed limit significantly affects the deviation from the centerline in the obstacle-avoidance stage. The participant has a smaller deviation when the autonomy uses lower maximum speed limit ($F(1, 11) = 14.999,\ p = 0.003$) as shown in Fig. 4.8a. The surveillance task urgency has no significant impact on

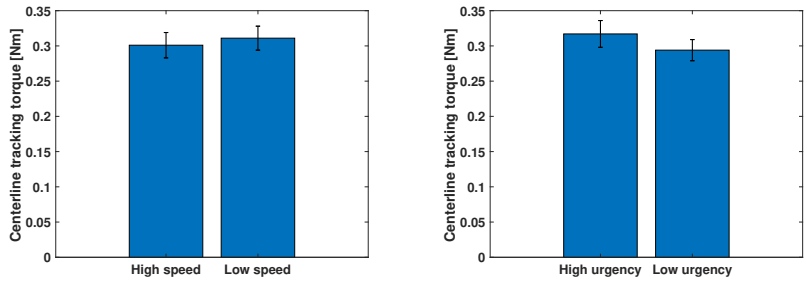

(a) Relationship between centerline tracking torque and autonomy's maximum speed limit

(b) Relationship between centerline tracking torque and surveillance task urgency

Figure 4.6: Impacts of autonomy's maximum speed limit and surveillance task urgency on centerline tracking torque in Experiment 3

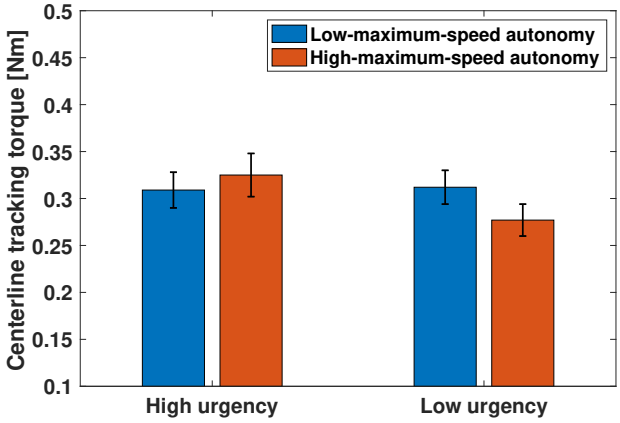

Figure 4.7: Relationship between steering control effort in the lane-keeping stage and different autonomy settings in Experiment 3 under different surveillance task urgencies

deviation from the centerline in the obstacle-avoidance stage ($F(1, 11) = 0.000,\ p = 0.987$), as shown in Fig. 4.8b. In addition, no significant interaction effect is observed ($F(1, 11) = 0.220,\ p = 0.648$), as shown in Fig. 4.9.

Participants' Steering Control Effort Under Emergency

A significant effect of the autonomy's maximum speed limit on participants' steering control effort during the obstacle-avoidance stage is observed ($F(1, 11) = 292.546$, $p < 0.001$). When the high-maximum-speed autonomy is used, the participant exerts less torque in the obstacle-avoidance stage. There is no significant effect of the surveillance task urgency on participants' steering control effort during the obstacle-

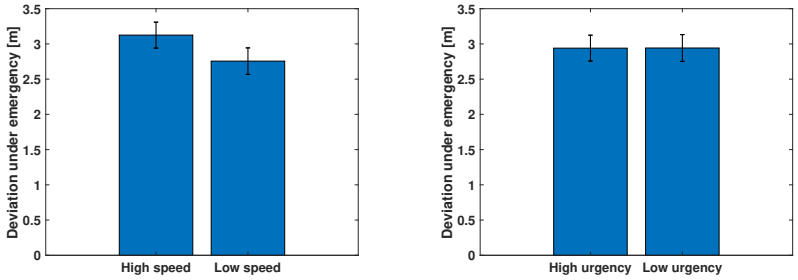

(a) Relationship between autonomy's maximum speed limit and deviation under emergency

(b) Relationship between surveillance task urgency and deviation under emergency

Figure 4.8: Impacts of autonomy's maximum speed limit and surveillance task urgency on deviation under emergency in Experiment 3

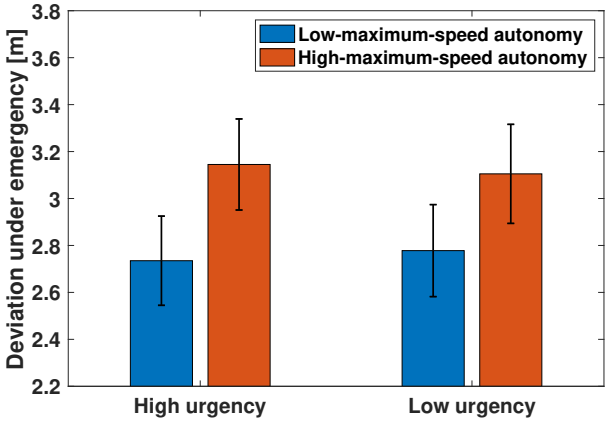

Figure 4.9: Relationship between emergency deviation in the obstacle-avoidance stage and different autonomy settings in Experiment 3 under different surveillance task urgencies

avoidance stage ($F(1, 11) = 0.214,\ p = 0.653$), as shown in Fig. 4.10b. In addition, no significant interaction effect is observed ($F(1, 11) = 0.236,\ p = 0.636$), as shown in Fig. 4.11.

Surveillance Task Performance

Only the surveillance task urgency significantly impacts the detection accuracy of the surveillance task. As shown in Fig. 4.12b, for the surveillance task performance, task urgency significantly influences the detection accuracy ($F(1, 11) = 6.798,\ p = 0.024$). Detection accuracy is higher when the surveillance task is less urgent. The effect of the autonomy's maximum speed limit is non-significant ($F(1, 11) = 4.336,$

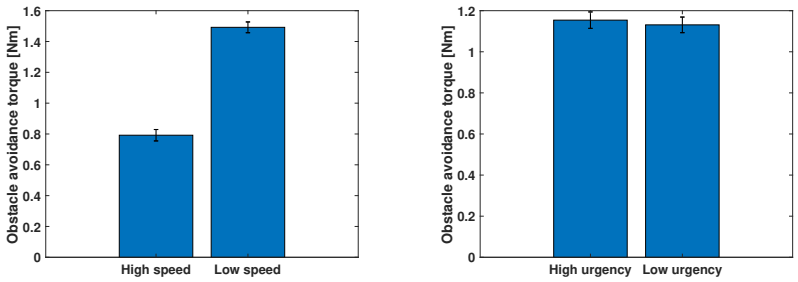

(a) Relationship between autonomy's maximum speed limit and obstacle avoidance torque

(b) Relationship between surveillance task urgency and obstacle avoidance torque

Figure 4.10: Impacts of autonomy's maximum speed limit and surveillance task urgency on obstacle avoidance torque in Experiment 3

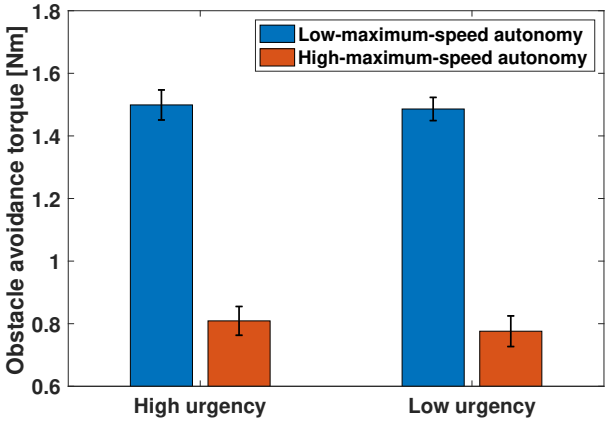

Figure 4.11: Relationship between steering control effort in the obstacle-avoidance stage and different autonomy settings in Experiment 3 under different surveillance task urgencies

$p = 0.061$), as shown in Fig. 4.12a. In addition, no significant interaction effect is observed ($F(1, 11) = 0.134,\ p = 0.721$), as shown in Fig. 4.13.

4.2.1.4 Discussion

Participants' Self-reported Workload

The participants report a higher workload when the high-maximum-speed autonomy is used. It can result from the following reason. Because the autonomy is designed to push the vehicle's speed to its limit, a higher maximum speed limit typically leads to higher vehicle speed. If the vehicle travels faster, which results from

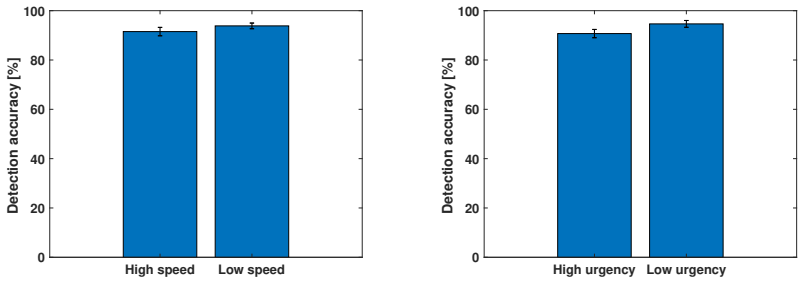

(a) Relationship between autonomy's maximum speed limit and surveillance task accuracy

(b) Relationship between surveillance task urgency and surveillance task accuracy

Figure 4.12: Impacts of autonomy's maximum speed limit and surveillance task urgency on surveillance task accuracy in Experiment 3

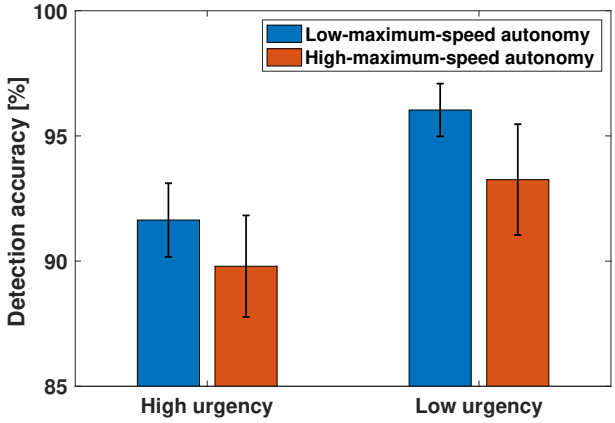

Figure 4.13: Relationship between detection accuracy in the surveillance task and different autonomy settings in Experiment 3 under different surveillance task urgencies

implementing the high-maximum-speed autonomy, the subject has less time to react and increase the workload. These results are consistent with prior research [99] that large speed in haptic shared control leads to a smaller safety margin. In addition, the increase of workload resulting from increasing autonomy's maximum speed limit is similar when the subject has a moderate workload and when the subject is overloaded. It indicates that increasing autonomy's maximum speed limit at this speed range has a similar effect on self-reported workload. On the other hand, participants report a higher workload when the surveillance task is urgent, which aligns with the finding in Sec. 3.3.2.4. It indicates that the surveillance task is able to control the

participants' workload regardless of the autonomy maximum speed settings.

Driving Task Performance

For the driving task performance in the lane-keeping stage, a higher maximum speed limit leads to a higher centerline tracking error. It can result from the same reason as the discussion about the self-reported workload that the high maximum speed autonomy offers a limited safety margin for the human driver. The subject makes more mistakes or unintended maneuvers when the subject has less safety margin to react. In addition, the fast travel speed resulting from the high-maximum-speed autonomy makes the recovery from the mistakes harder.

Steering Control Effort in the Lane-keeping Stage

The human torque in the lane-keeping stage is similar when the autonomy's maximum speed limits are different. It shows that the participants tend to provide a similar amount of intervention under different maximum speed limits. In addition, the centerline tracking torque increases under the high maximum level autonomy cases when switching to an urgent surveillance task. It can be explained by participants trying to interfere more to compensate for the significant increase in centerline tracking error when the surveillance task urgency is high.

Emergency Maneuvering Performance

For the emergency maneuvering performance in the obstacle-avoidance stage, a higher maximum speed limit leads to a higher deviation from the centerline. It can be explained by the following reason. When the high-maximum-speed autonomy is used, the vehicle is very difficult to control (experiencing tire lift-off/rollover) during the obstacle avoidance maneuver. Therefore, subjects tend to choose a gradual path, leading to extra deviation from the centerline.

Participants' Steering Control Effort Under Emergency

For the steering control effort in the obstacle-avoidance stage, a higher maximum speed limit leads to less steering control effort. The reason is very similar to the one provided in the emergency maneuvering performance paragraph. When the high-maximum-speed autonomy is used, the vehicle is very difficult to control (experiencing tire lift-off/rollover) during the obstacle avoidance maneuver. Subjects tend

to interfere less aggressively, so the exerted torque is less.

These characteristics are then used to design the adaptive autonomy showed in the following section.

4.3 Adaptive Autonomy Based on Maximum Speed Limit

4.3.1 Adaptive Autonomy Design

Adaptive autonomy is designed based on three factors: (real-time estimated) workload, steering torque from the human operator, and steering rate of the vehicle. The maximum speed of the adaptive autonomy $u_{x,max}$ is defined as $u_x \leq u_{x,max}(w_t, \tau_h, \hat{\gamma})$, where w_t is the (real-time estimated) workload of the human driver, τ_h is the human torque, and $\hat{\gamma}$ is the normalized steering rate of the vehicle.

In the adaptive autonomy design, the autonomy's maximum speed limit is separated into two parts: base maximum speed $\bar{u}_{x,max}$ and maximum speed reduction $\Delta u_{x,max}$; i.e., $u_{x,max} = \bar{u}_{x,max}(w_t, \tau_h) - \Delta u_{x,max}(w_t, \hat{\gamma})$. The base maximum speed $\bar{u}_{x,max}$ considers the impact of workload and input torque from the human operator. It represents a global trend during the entire driving mission. The maximum speed reduction $\Delta u_{x,max}$ considers the combined effect of steering rate and workload, which considers the transient behavior when there is a rapid change in the steering angle.

The 3D plot showing the relationship between the base maximum speed $\bar{u}_{x,max}$, the workload w_t, and the human torque τ_h is shown in Fig. 4.14. It is designed based on two principles.

The first principle is shown in Fig. 4.15. For a given amount of torque from the human operator, the relationship between the base maximum speed limit and workload is shown in Fig. 4.15a. Based on the conclusion from Experiment 3 (in Sec. 4.2.1.4), a higher maximum speed leads to a higher workload. Therefore, the maximum speed limit under the over-loaded condition is reduced. When the subject has a moderate workload, the maximum speed limit of the autonomy is increased

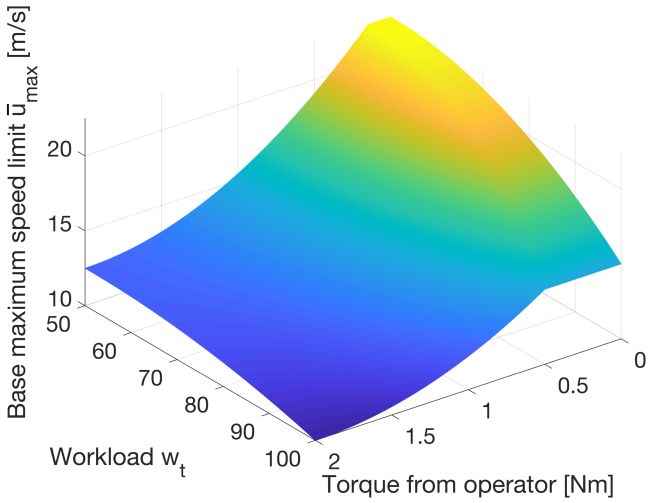

Figure 4.14: Relationship between base maximum speed $\bar{v}_{max}$, workload w_t, and human input torque τ_h.

because the human driver has more mental resources to compensate for the mistakes or unintended maneuvers caused by the high speed. Similar to the definition in the adaptive control consolidation (Sec. 3.2.1.2 and Sec. 3.3.1), the workload value w_t is set as 50 when the subject experiences moderate workload, and 100 when the subject is over-loaded. In the adaptive autonomy design, the base maximum speed limit is 22.5 m/s for the moderate workload ($w_t = 50$) and 15 m/s for the over-loaded condition ($w_t = 100$) when there is no torque applied. The 22.5 m/s is identical to the maximum speed value of the high-maximum-speed autonomy in Sec. 4.2.1.2, and 15 m/s is determined based on pilot human subject studies. A quadratic function is fitted to create the smooth transition from $w_t = 50$ to $w_t = 100$.

The second design principle of the base maximum speed $\bar{u}_{x,max}$ is illustrated in Fig. 4.16. For a given amount of estimated workload from the human operator, a large human intervention torque leads to less base maximum speed. As shown in Fig. 4.16a, the maximum speed limit drops by 10 m/s when the workload is moderate, and human applies maximum torque. In the high workload case, since the maximum speed limit is already low when the human operator applies no torque, it drops by 5 m/s when the human applies the maximum torque. Furthermore, there are two critical properties of the designed curve. Similar to the idea in the adaptive control

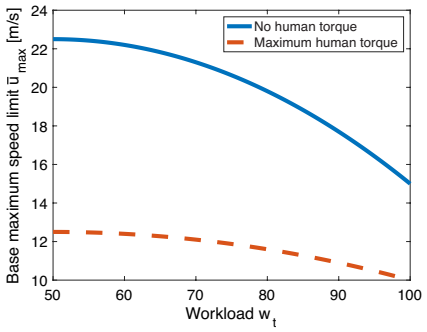

(a) Relationship between base maximum speed $\bar{u}_{x,max}$ and workload w_t for different levels of human's input torque τ_h

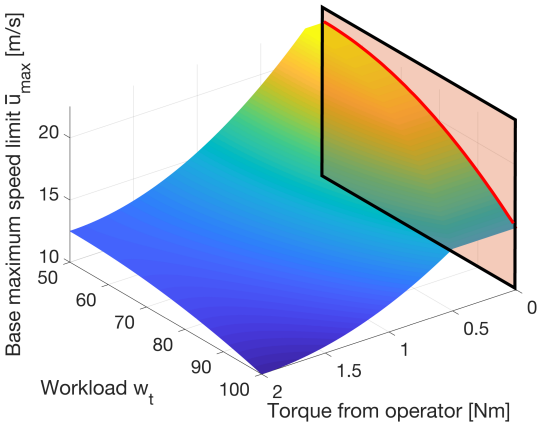

(b) The highlighted section in the 3d plot is the curve in Fig. 4.15a when there is no human torque τ_h applied.

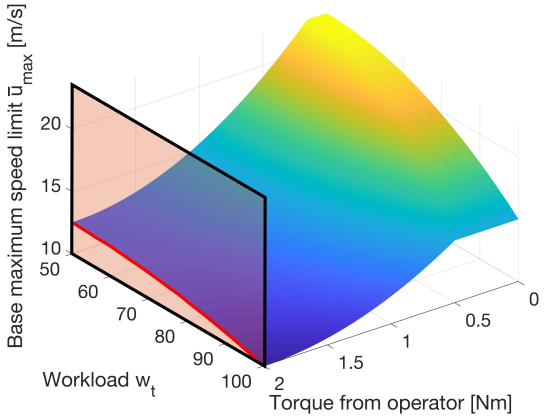

(c) The highlighted section in the 3d plot is the curve in Fig. 4.15a when there the maximum human torque τ_h is applied.

Figure 4.15: Illustration of the first design principle of base maximum speed $\bar{u}_{x,max}$

consolidation design, which is mentioned in Sec. 3.2.1.2, when the human torque is small, the base maximum speed is kept at a constant level to filter out unintended input torque from the human operator. The maximum speed limit starts to drop after the human torque passes a threshold, which increases as workload increases from moderate workload ($w_t = 50$) to high workload ($w_t = 100$). They are labeled as $\tau_{threshold,m}$ and $\tau_{threshold,h}$, respectively. The threshold is smaller when the human operator's workload is moderate. The reason for this design is that, presumably, the human operator makes fewer mistakes at the moderate workload level based on the results in the literature, which shows that under a moderate workload level, the human

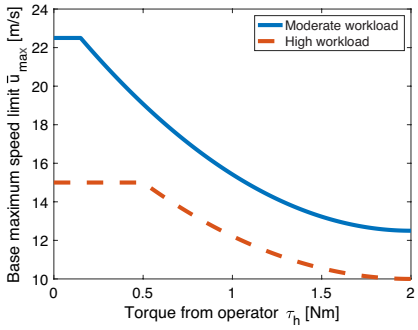

(a) Relationship between base maximum speed $\bar{u}_{x,max}$ and human's input torque τ_h for different levels of human's workload w_t

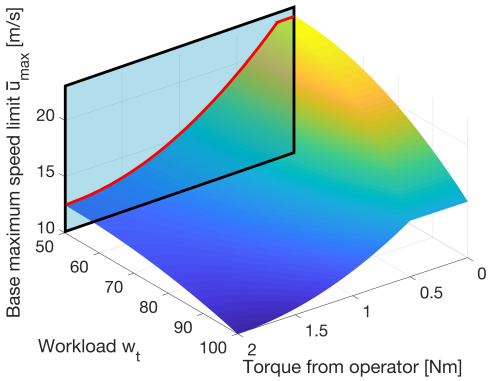

(b) The highlighted section in the 3d plot is the curve in Fig. 4.16a when there the human's workload w_t is moderate.

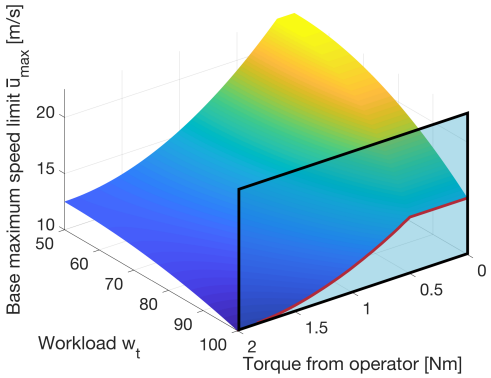

(c) The highlighted section in the 3d plot is the curve in Fig. 4.16a when there the human's workload w_t is high.

Figure 4.16: Illustration of the second design principle of base maximum speed $\bar{u}_{x,max}$

operator's performance is optimal [48]. A quadratic function is fitted to connect the value bounded by the maximum speed limit when there is no torque applied and maximum torque applied under the given workload condition. The quadratic function is selected here based on the results of a pilot human subject study. In the study, the quadratic function outperforms the other curve designs, including the sigmoid function design or linear interpolation.

Combining those two principles, the formulation of the base maximum speed

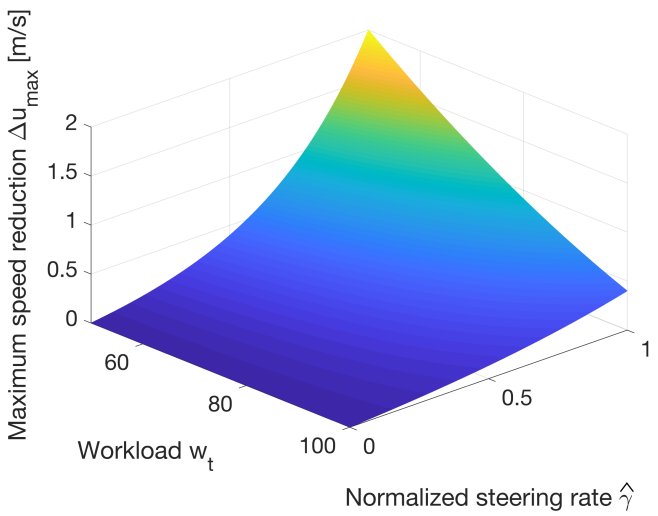

Figure 4.17: Relationship between maximum speed reduction $\Delta u_{x,max}$, workload w_t, and normalized steering rate $\hat{\gamma}$.

$\bar{u}_{x,max}$ is obtained as

$$\bar{u}_{x,max}(w_t, \tau_h) = \begin{cases} f_1 & \tau_h < g \\ (f_1 - f_2)\dfrac{(\tau_{max} - \tau_h)^2}{(\tau_{max} - g)^2} + f_2 & g \leq \tau_h \end{cases} \tag{4.2}$$

where f_1 and f_2 are the function of maximum speed limit when there is no human torque applied, and when maximum human torque is applied under different workload, respectively. They are fitted by the described design principles as $f_1 = -0.003(w_t - 50)^2 + 22.5$ and $f_2 = -0.001(w_t - 50)^2 + 12.5$. The threshold $g(w_t)$ is given by $g(w_t) = (\tau_{threshold,h} - \tau_{threshold,m})\frac{(w_t-50)^2}{2500} + \tau_{threshold,m}$.

The threshold value $\tau_{threshold,m}$ is set as 0.15 Nm when the human operator experiences a moderate workload ($w_t = 50$), while this value $\tau_{threshold,h}$ is 0.5 Nm when the human operator is fully over-loaded ($w_t = 100$) based on results from pilot dual-scenario subject studies. In addition, the maximum human torque τ_{max} is observed using the same method as 2 Nm.

The 3D plot showing the relationship between maximum speed reduction Δv_{max}, the workload w_t and the normalized steering rate $\hat{\gamma}$ is shown in Fig. 4.17. There are two design principles for maximum speed reduction.

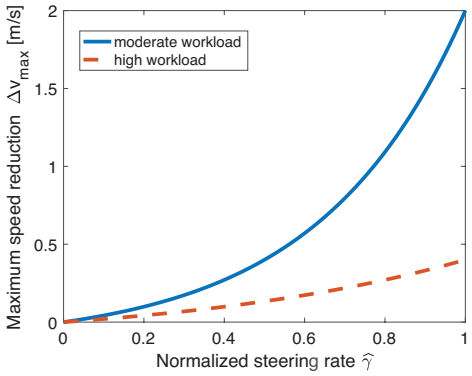

(a) Relationship between maximum speed reduction $\Delta u_{x,max}$ and normalized steering rate $\hat{\gamma}$ for different workloads

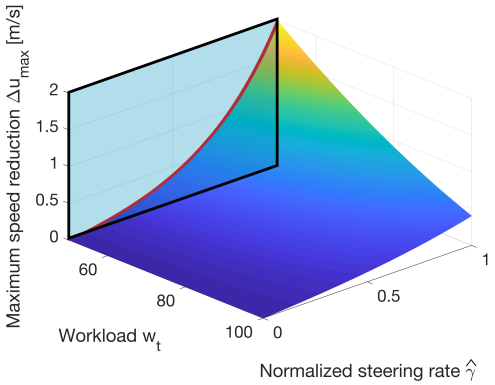

(b) The highlighted section in the 3d plot is the curve in Fig. 4.18a when there the human's workload w_t is moderate.

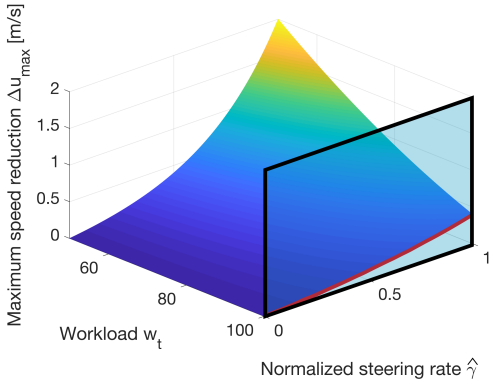

(c) The highlighted section in the 3d plot is the curve in Fig. 4.18a when there the human's workload w_t is high.

Figure 4.18: First design principle of the maximum speed reduction $\Delta u_{x,max}$

First, as shown in Fig. 4.18, keeping the workload constant, when the steering rate is low, i.e., $\hat{\gamma}$ is very close to 0, maximum speed reduction $\Delta u_{x,max}$ is 0. It indicates that no maximum speed reduction is provided, given a low steering rate. When the vehicle has a large steering rate, which indicates a difficulty in controlling the vehicle, maximum speed reduction $\Delta u_{x,max}$ increases to a high level, which is illustrated in Fig. 4.18a. An exponential function is used to connect these two points. On the other hand, as shown in Fig. 4.19, keeping the steering rate constant at the highest level, when workload is high, the maximum speed reduction $\Delta u_{x,max}$ is small because at this point, the maximum speed is already very low. When the workload is moderate, the maximum speed reduction $\Delta u_{x,max}$ is large, which is shown in Fig. 4.19a. The value of maximum speed reduction $\Delta u_{x,max}$ is set as 2 m/s when the

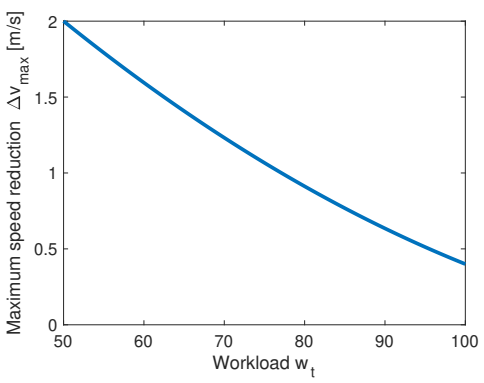

(a) Relationship between maximum speed reduction $\Delta u_{x,max}$ and workload w_t when $\hat{\gamma} = 1$. A quadratic function connects the dots.

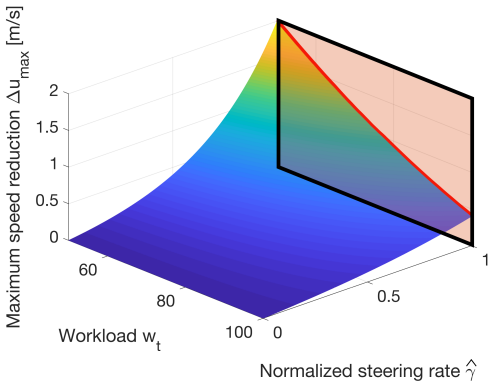

(b) The highlighted section in the 3d plot is the curve in Fig. 4.19a when $\hat{\gamma} = 1$

Figure 4.19: Second design principle of the maximum speed reduction $\Delta u_{x,max}$

subject experiences moderate workload ($w_t = 50$), and as 0.4 m/s when the subject is over-loaded ($w_t = 100$).

Combining these considerations, the formulation of maximum speed reduction $\Delta u_{x,max}$ is obtained as

$$\Delta u_{x,max}(w_t, \hat{\gamma}) = \frac{2}{15}(4 - \frac{1}{25}|w_t - 50|)^{2\hat{\gamma}} - \frac{2}{15} \tag{4.3}$$

Therefore, the maximum speed limit is calculated as $u_{x,max} = \bar{u}_{x,max}(w_t, \tau_h) - \Delta u_{x,max}(w_t, \hat{\gamma})$. Notice that the maximum speed reduction is helpful when the maximum speed is relatively large, the maximum speed $u_{x,max}$ is lower bounded by the function f_2.

4.3.2 Evaluation of the Adaptive Autonomy: Experiment 4

4.3.2.1 Introduction

In this human subject study, namely Experiment 4, the benefits of the proposed adaptive autonomy, which is shown in Sec. 4.3.1, are evaluated. There are 18 participants in this experiment who are asked to perform a dual-task mission, i.e., the driving task and the surveillance task. In the driving task, the subject is required to achieve a centerline tracking with minimum deviation from the centerline with the help of

autonomy. There are obstacles located at the centerline, which are invisible to autonomy. Therefore, it is the subject who should intervene and avoid the obstacles. Three types of autonomy are presented to the subject, including the proposed adaptive autonomy, the low-maximum-speed autonomy, and the high-maximum-speed autonomy, where the latter two are introduced in Sec. 4.2.1.2. In addition to the driving task, the participants also need to perform the surveillance task, whose task urgency, introduced in Sec. 2.5, is used to control the participants' workload. A real-time workload estimator based on Bayesian Inference (BI) is used to estimate participants' workload online [87].

4.3.2.2 Method

Participants

There are 18 students participating in this experiment. The 18 participants are on average 23.61 years old ($SD = 1.88$ years) and had an average of 4.42 years of driving experience ($SD = 2.25$ years). All participants have a normal or corrected-to-normal vision, and the eye tracker can be calibrated on their eyes.

Apparatus and Stimuli

The dual-task shared control simulation platform (introduced in Chapter 2) with the visualization module (introduced in Sec. 2.2.3) is used in this experiment. Participants perform two tasks, the driving task and the surveillance task, simultaneously. In the driving task, the participant and the autonomy share the vehicle's steering control, while the vehicle's speed is controlled by autonomy only. The goal of the driving task is to complete a fixed-length track with minimal deviation from the centerline while avoiding obstacles on the centerline. The autonomy has no obstacle avoidance capability. There are three autonomy settings in this experiment: The adaptive autonomy, which is introduced in Sec. 4.3.1 and the non-adaptive autonomy with a high and a low maximum speed, which is introduced in Sec. 4.2.1.2 and called low-maximum-speed autonomy and high-maximum-speed autonomy, respectively. Both non-adaptive autonomy settings are used as benchmarks. The non-adaptive control consolidation is used in this experiment, which is shown in Sec. 3.2.1.1, so the im-

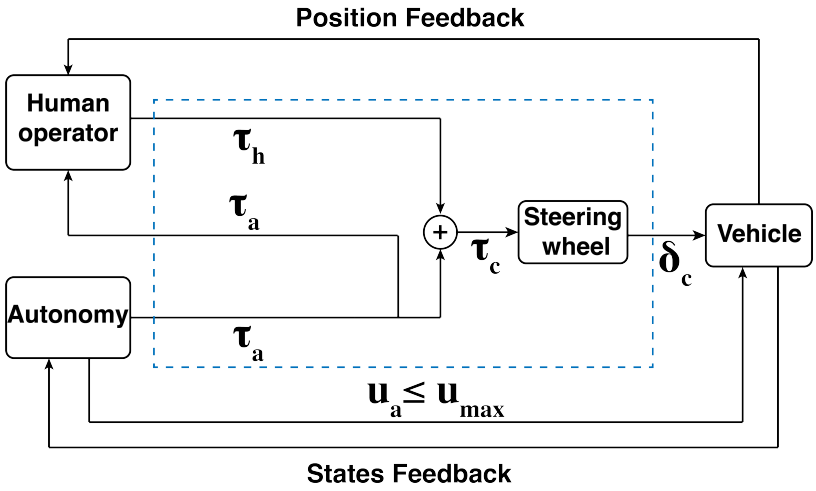

Figure 4.20: Control block diagram when different maximum speed limits are implemented. The blue dashed lines highlight the control consolidation where non-adaptive control consolidation is implemented. The term u_a represents the speed of the vehicle is controlled by autonomy only. u_{max} can assume one of the three autonomy maximum speed limits: 12.5 m/s, 22.5 m/s and adaptive autonomy speed limit $u_{x,max}$.

Table 4.4: Weights of autonomy in Experiment 4

Parameters	w_1	w_2	w_3	w_4	w_5
Value	0.2	10.0	2.4	1.2	5.0

pact on mission performance only comes from the different autonomy settings. The participants also need to perform the surveillance task. The goal of the surveillance task is to make the identification within the time limit as accurate as possible. The surveillance task urgency is used to control the subject's workload in this experiment. There are two surveillance task urgencies: 1.5 s pace and 6.5 s pace. They are labeled as high surveillance task urgency and low surveillance task urgency, respectively. A real-time workload estimator based on Bayesian Inference and developed by our collaborators is used [87]. For the workload estimation, the corresponding data from a 4 s time window captured by the eye tracker, Tobii Pro Glasses 2 (30 Hz sampling rate), are used to estimate participants' workload. The processing of the workload is similar to the method in Experiment 2, which is shown in Sec. 3.3.2.2. A moving average filter is applied with a 1 s time window, and w_t is down-sampled to 10 Hz.

Autonomy Formulation

A similar autonomy formulation compared to Experiment 3 (Sec. 4.2.1.2) is used

in this human subject experiment. The cost function of the autonomy used in this study is

$$\begin{aligned} J =& w_1 x(t_P) + w_2 \int_{t_0}^{t_P} \left(y_{\text{ref}}(x(t)) - y(t)\right)^2 dt + w_3 \int_{t_0}^{t_P} \gamma^2 dt + w_4 \int_{t_0}^{t_P} J_x^2 dt \\ &+ w_5 \int_{t_0}^{t_P} \left(\tanh\left[\frac{a - F_{z,rl}}{b}\right] + \tanh\left[\frac{a - F_{z,rr}}{b}\right] \right) dt \end{aligned} \tag{4.4}$$

The cost function consists of five terms. As introduced by Sec. 4.2.1.2, they are used to push the vehicle to its speed limit and penalize the deviation from the current line, regulate the control inputs of the vehicle for a smooth steering and acceleration maneuver, and prevent the vehicle from operating at its dynamic limit unnecessarily. Five weights w_1, w_2, w_3, w_4, and w_5 are set to achieve a trade-off between these goals, whose values are listed in Table 4.4.

In addition, different maximum speed limits are imposed as additional constraints in the autonomy setting as below:

$$u_x \leq u_{x,max}$$

In this experiment, the maximum speed limit $u_{x,max}$ is set to be 12.5 m/s, 22.5 m/s, and adaptive function $u_{x,max}(w_t, \tau_h, \hat{\gamma})$ for the low-maximum-speed autonomy, high-maximum-speed autonomy, and adaptive autonomy, respectively. Compared with Experiment 3, introduced in Sec. 4.2.1.2, the difference is the additional adaptive autonomy setting. The control block diagrams of these three cases are shown in Fig. 4.20.

Experimental Design

The experiment uses a within-subjects design with two independent variables. The first independent variable is the autonomy settings with different maximum speed limits, i.e., low-maximum-speed (12.5 m/s) vs. high-maximum-speed (22.5 m/s) vs. adaptive. The second independent variable is the surveillance task urgency (1.5 s vs. 6.5 s). Each participant experiences six tracks in the experiment. One combination

Table 4.5: Six test conditions in Experiment 4

Condition	Surveillance task urgency	Autonomy setting
1	1.5 s	Low-maximum-speed (12.5 m/s)
2	1.5 s	High-maximum-speed (22.5 m/s)
3	1.5 s	Adaptive
4	6.5 s	Low-maximum-speed (12.5 m/s)
5	6.5 s	High-maximum-speed (22.5 m/s)
6	6.5 s	Adaptive

of an autonomy setting and a surveillance task urgency is used in each trial. The resulting six test conditions are shown in Table 4.5. The presentation of test conditions follows a 6×6 Latin square design to eliminate potential order effects.

Measures

There are seven dependent variables collected in the experiment:

- Participants' self-reported workload
- Participants' steering control effort in lane-keeping task
- Driving task performance
- Participants' steering control effort under emergency
- Emergency maneuvering performance
- Surveillance task performance
- Time to finish the task

In this experiment, the obstacle-avoidance stage has the same definition as in Sec. 3.2.2.2 and Sec. 4.2.1.2. The obstacle-avoidance stage is defined as the period when the human subjects deviate at least 1 m from the centerline and avoid the obstacles. The remaining part is defined as the lane-keeping stage.

After each track, participants report their workload using the NASA TLX survey [90]. The NASA TLX survey is presented to the participants before the experiment such that they understand the meaning of workload. Similar to previous methods in Sec. 3.2.2.2, Sec. 3.3.2.2 and Sec. 4.2.1.2, a participant's steering control effort in the lane-keeping task is calculated as the average value of the absolute human

torque during the lane-keeping stage. Driving task performance is evaluated by lane-keeping error, which is calculated as the mean of the absolute deviation of the vehicle's position from the centerline during the lane-keeping stage. Steering control effort under emergency is calculated as the average of the absolute human torque that the participant applied on the steering wheel during the obstacle avoidance maneuver. Emergency maneuvering performance is evaluated by centerline deviation during the obstacle avoidance maneuver, which uses a similar calculation method as driving task performance but in the obstacle-avoidance stage. The torque from the participant is measured from a steering torque rotatory sensor. The collection rate of driving performance and steering control effort of the lane-keeping and obstacle-avoidance stages is 100 Hz. The surveillance task performance is measured using the detection accuracy of the surveillance task. In addition, a new metric, the time to finish the mission, is introduced in this experiment. It is the time duration of the mission.

Experimental procedure

Before the training session starts, participants provide a signed informed consent and fill in a demographic survey to report their age and driving experience.

During the training session, the participants first perform three trials of driving tasks only, with the low-maximum-speed autonomy, the high-maximum-speed autonomy, and the adaptive autonomy in order. The trial with the low-maximum-speed autonomy takes approximately 4 minutes, while the trial with the high-maximum-speed autonomy takes approximately 2 minutes. The trial with the adaptive autonomy takes approximately 2 minutes. Then the participants perform a training trial of the surveillance task only. It consists of two portions. The first portion is with the low surveillance task urgency, and it takes approximately 1 minute. The second portion is with the high surveillance task urgency, and it takes approximately 2 minutes. After that, the participants perform three combined driving and surveillance task trials with different surveillance task urgencies and different autonomy settings.

During the official experiment, participants perform the combined driving task and the surveillance task on six tracks with the test cases described in Table 4.5. In each trial, participants travel a fixed distance (around 1200 m). After each trial,

Table 4.6: Mean and standard error (SE) of workload, centerline tracking error, centerline tracking torque, deviation under emergency, obstacle avoidance torque, time to finish the mission and detection accuracy in Experiment 4

Metrics	N	Surveillance task urgency					
		6.5 s			1.5 s		
		Autonomy's maximum speed limit					
		12.5 m/s	22.5 m/s	Adaptive	12.5 m/s	22.5 m/s	Adaptive
Workload	18	17.937 ± 3.118	28.492 ± 4.233	18.651 ± 2.968	33.532 ± 3.838	44.365 ± 4.288	28.175 ± 5.132
Centerline tracking error (m)	18	0.283 ± 0.017	0.472 ± 0.042	0.322 ± 0.023	0.308 ± 0.021	0.513 ± 0.043	0.353 ± 0.023
Centerline tracking torque (Nm)	18	0.361 ± 0.016	0.359 ± 0.020	0.274 ± 0.010	0.321 ± 0.016	0.304 ± 0.015	0.263 ± 0.008
Deviation under emergency (m)	18	2.406 ± 0.100	2.998 ± 0.151	2.803 ± 0.163	2.428 ± 0.136	2.874 ± 0.162	2.623 ± 0.128
Obstacle avoidance torque (Nm)	18	1.489 ± 0.047	0.773 ± 0.059	0.945 ± 0.087	1.511 ± 0.054	0.664 ± 0.047	0.938 ± 0.078
Time to finish the mission (s)	18	122.541 ± 0.015	72.454 ± 0.072	92.824 ± 1.520	122.551 ± 0.017	72.444 ± 0.052	103.898 ± 0.750
Detection accuracy (%)	18	90.850 ± 1.364	92.222 ± 2.499	93.277 ± 1.498	88.662 ± 1.610	86.973 ± 1.516	89.433 ± 1.618

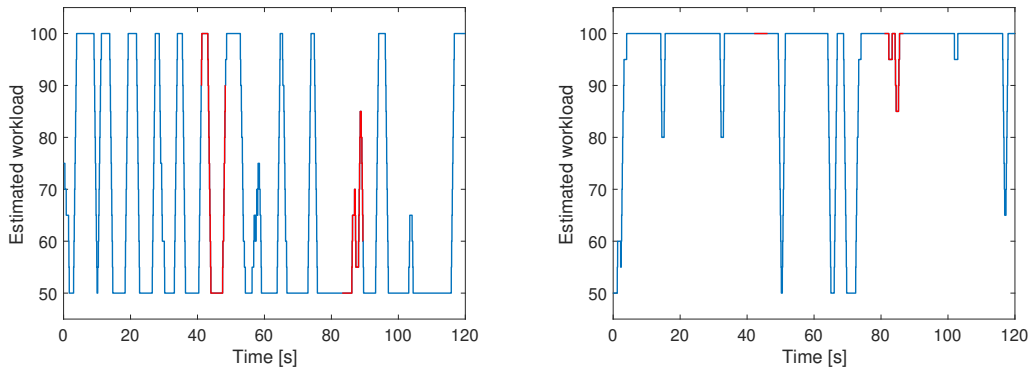

(a) Estimated workload signal in Experiment 4 when the surveillance task urgency is low

(b) Estimated workload signal in Experiment 4 when the surveillance task urgency is high

Figure 4.21: Estimated workload signal provided by Bayesian Inference (BI) estimation algorithm. Red lines indicate the obstacle-avoidance stages.

the participants are required to fill in a post-survey (NASA TLX) [90] to report the workload during the last track. If they hit the obstacle, the trial is restarted.

4.3.2.3 Results

Two-way repeated measures Analysis of Variance (ANOVA) is conducted with the surveillance task urgency and the autonomy settings as the within-subjects variables. Results are reported as significant for $\alpha < .05$.

Table 4.6 summarizes the mean and standard error (SE) values of the participants' self-reported workload, driving task performance, their exerted torque during the lane-keeping stage, emergency maneuvering performance, participants' control effort under emergency, surveillance task performance, and time to finish the mission.

Estimated Workload Signal Illustration

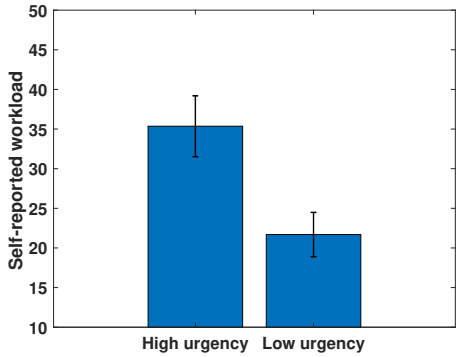

(a) Relationship between surveillance task urgency and participants' self-reported workload in Experiment 4

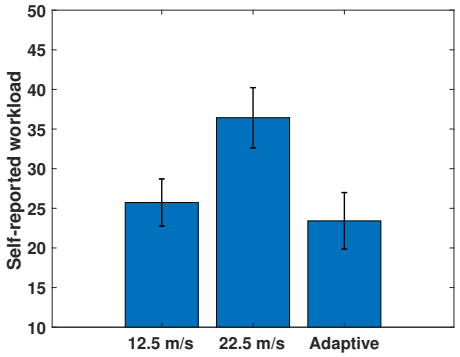

(b) Relationship between autonomy's maximum speed limit and participants' self-reported workload in Experiment 4

Figure 4.22: Relationship between self-reported workload and different independent variables in Experiment 4.

The estimated workload signals under different surveillance task urgencies are shown in Fig. 4.21. These signals are used as the workload w_t in the adaptive autonomy design, which is demonstrated in Sec. 4.3.1. When the subject experiences the under-loaded condition, the workload estimator is able to detect the workload increment brought by the obstacles. In addition, it can also detect the workload increment of the surveillance task, to which the subject allocates some of the resources to handle. When the subject experiences the over-loaded condition, the workload estimator is able to return a signal indicating the subject is over-loaded generally (i.e., $w_t = 100$).

Participants' Self-reported Workload

The participants' self-reported workload is significantly impacted by the surveillance task urgency and the autonomy settings. When the surveillance task urgency is high (1.5 s pace), the participants report a significantly higher workload from the NASA TLX post-survey ($F(1, 17) = 22.689,\ p < 0.001$), as shown in Fig. 4.22a. The autonomy setting also has significant impact ($F(2, 16) = 11.432,\ p < 0.001$), which is shown in Fig. 4.22b. Participants report much higher workload in the high-maximum-speed autonomy cases. Moreover, a pairwise comparison shows a significant difference between the self-reported workload between the high-maximum-speed autonomy cases and low-maximum-speed cases ($p = 0.006$). There is also a significant

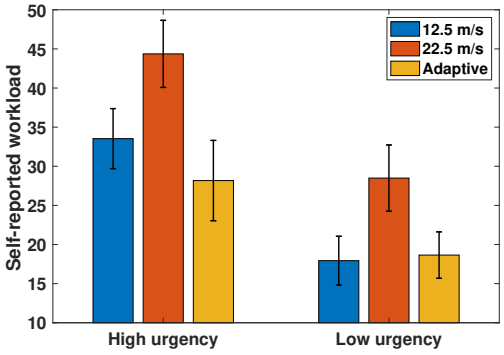

Figure 4.23: Relationship between self-reported workload and different autonomy maximum speed limit in Experiment 4 under different surveillance task urgencies

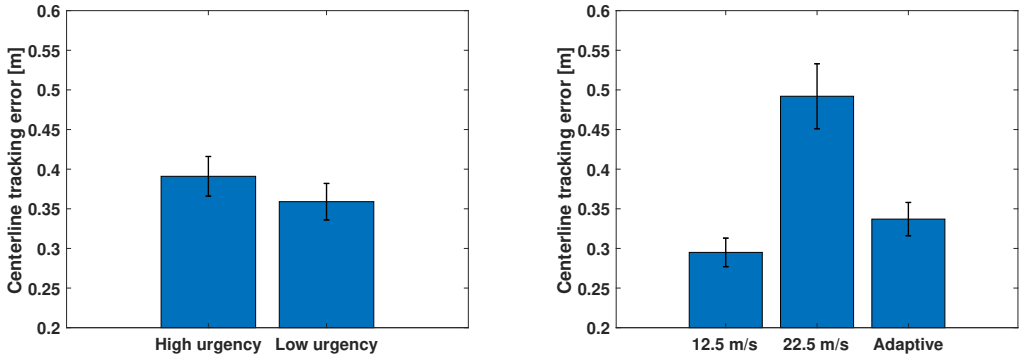

(a) Relationship between surveillance task urgency and centerline tracking error in Experiment 4

(b) Relationship between autonomy's maximum speed limit and centerline tracking error in Experiment 4

Figure 4.24: Relationship between centerline tracking error and different independent variables in Experiment 4.

difference in the self-reported workload between the adaptive autonomy cases and high-maximum-speed autonomy cases ($p < 0.001$). The difference between the adaptive autonomy and low-maximum-speed autonomy is not significant ($p = 0.268$). No interaction effect is found between the surveillance task urgency and the autonomy settings ($F(2, 16) = 1.120,\ p = 0.338$), as shown in Fig. 4.23.

Driving Task Performance

Both surveillance task urgency and autonomy settings significantly impact the driving task performance in the lane-keeping stage. The impact on the centerline tracking error from surveillance task urgency is significant ($F(1, 17) = 9.000,\ p = 0.008$). The centerline tracking error is larger when the urgent surveillance task is

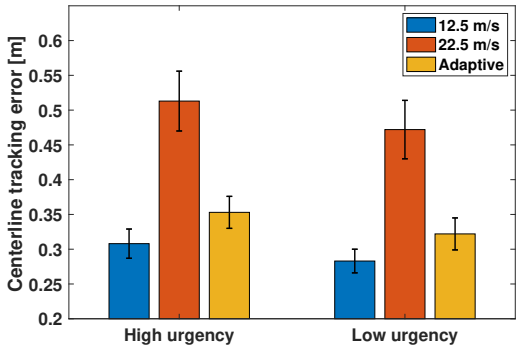

Figure 4.25: Relationship between centerline tracking error and different autonomy maximum speed limit in Experiment 4 under different surveillance task urgencies

used, as shown in Fig. 4.24a.

The autonomy setting has a significant impact on the driving task performance in the lane-keeping stage ($F(2, 16) = 25.771,\ p < 0.001$). Fig. 4.24b shows the centerline tracking error in the lane-keeping stage when three autonomy settings are implemented. The low-maximum-speed autonomy cases achieve the best driving performance, while the centerline tracking error of the high-maximum-speed autonomy cases is the worst. The adaptive autonomy achieves a medium level of driving task performance. Moreover, the pairwise comparisons show several results with significance. First, there is a significant difference between the centerline tracking errors when the low-maximum-speed autonomy and high-maximum speed autonomy are implemented ($p < 0.001$). Second, a significant difference is also observed between the centerline tracking error of the adaptive autonomy and the one of high-maximum-speed autonomy ($p < 0.001$). Third, the difference in the centerline tracking error between the adaptive autonomy cases and the low-maximum-speed autonomy cases is also significant ($p = 0.013$).

In addition, no significant difference ($F(2, 16) = 0.215,\ p = 0.807$) is observed in the interaction effect between the surveillance task urgency and the autonomy settings, as shown in Fig. 4.25.

Participants' Steering Control Effort During Lane Keeping

Both surveillance task urgency and autonomy settings significantly impact the

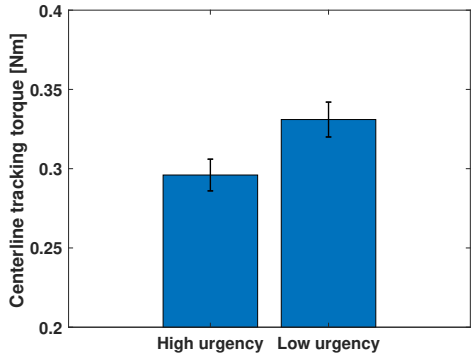

(a) Relationship between surveillance task urgency and centerline tracking torque in Experiment 4

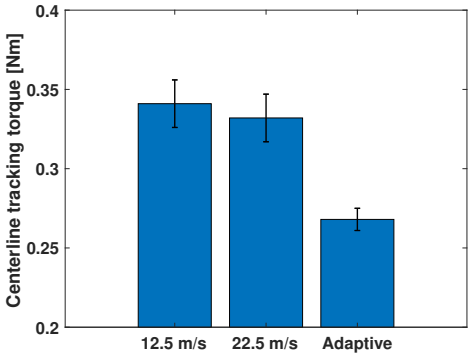

(b) Relationship between autonomy's maximum speed limit and centerline tracking torque in Experiment 4

Figure 4.26: Relationship between centerline tracking torque and different independent variables in Experiment 4.

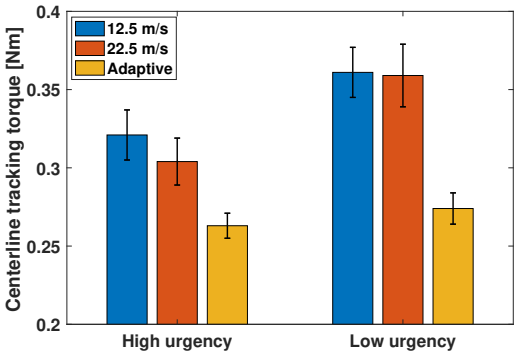

Figure 4.27: Relationship between centerline tracking torque and different autonomy maximum speed limit in Experiment 4 under different surveillance task urgencies

control effort in the lane-keeping stage. With a higher surveillance task urgency, the subjects exert significantly less effort ($F(1, 17) = 18.831,\ p < 0.001$), as shown in Fig. 4.26a.

The autonomy setting significantly impacts the control effort in the lane-keeping stage ($F(2, 16) = 14.553,\ p < 0.001$), as shown in Fig. 4.26b. The adaptive autonomy cases have the least steering control effort. Moreover, the pairwise comparison shows a significant difference between the adaptive autonomy cases and the low-maximum-speed autonomy cases ($p < 0.001$). There is also a significant difference between the adaptive autonomy case and the high-maximum-speed autonomy cases ($p < 0.001$). The difference in the control effort of the lane-keeping stage

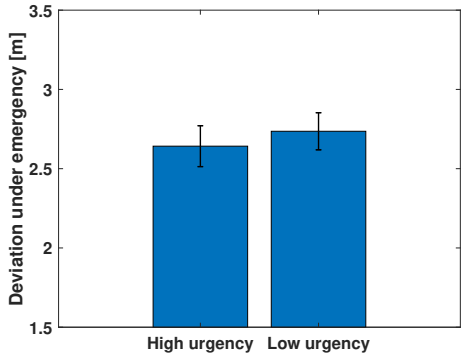

(a) Relationship between surveillance task urgency and deviation from the centerline in the obstacle-avoidance stage in Experiment 4

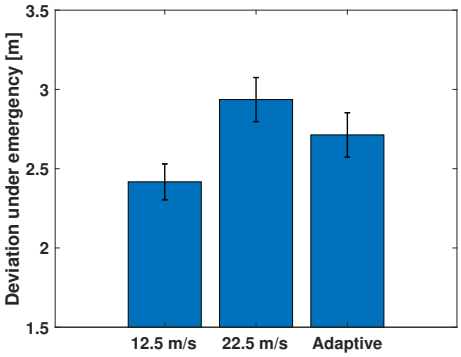

(b) Relationship between autonomy's maximum speed limit and deviation from the centerline in the obstacle-avoidance stage in Experiment 4

Figure 4.28: Relationship between deviation from the centerline in the obstacle-avoidance stage and different independent variables in Experiment 4.

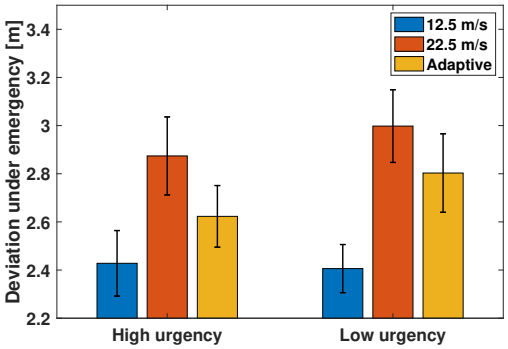

Figure 4.29: Relationship between deviation from the centerline and different autonomy maximum speed limit in Experiment 4 under different surveillance task urgencies

between the low-maximum-speed autonomy cases and high-maximum-speed cases is non-significant ($p = 0.593$).

In addition, no significant interaction effect between the surveillance task urgency and the autonomy setting is observed ($F(2, 16) = 2.365,\ p = 0.109$), as shown in Fig. 4.27.

Emergency Maneuvering Performance

The autonomy setting significantly impacts the deviation from the centerline in the obstacle-avoidance stage ($F(2, 16) = 13.626,\ p < 0.001$), as shown in Fig. 4.28b. The low-maximum-speed autonomy can achieve the best emergency maneuvering

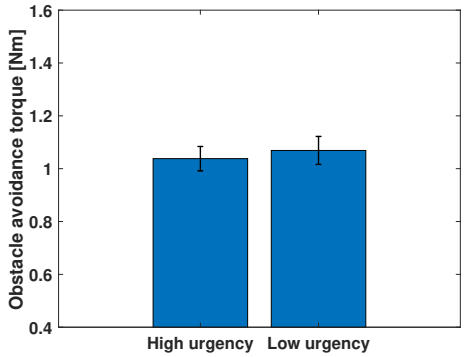

(a) Relationship between surveillance task urgency and emergency steering control effort in Experiment 4

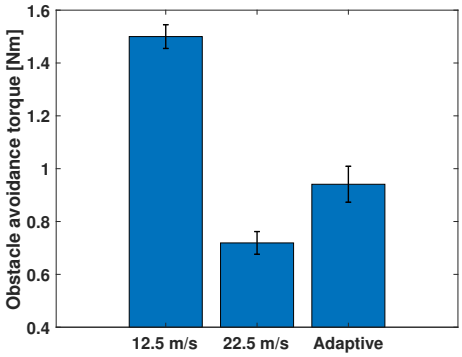

(b) Relationship between autonomy's maximum speed limit and emergency steering control effort in Experiment 4

Figure 4.30: Relationship between emergency steering control effort and different independent variables in Experiment 4.

performance, while the deviation of the centerline in high-maximum-speed autonomy cases is the largest. The emergency maneuvering performance of the adaptive autonomy cases is at a medium level. Moreover, the pairwise comparisons show significant differences between different pairs of autonomy settings. First, there is a significant difference between cases with the low-maximum-speed autonomy and cases with the high-maximum-speed autonomy ($p < 0.001$). Second, there is also a significant difference between the adaptive autonomy case and the high-maximum-speed autonomy cases ($p = 0.042$). Third, there is a significant difference in the deviation between the adaptive autonomy cases and the low-maximum-speed autonomy cases ($p = 0.004$). The impact of the surveillance task urgency on the deviation from the centerline is not significant ($F(1, 17) = 1.860,\ p = 0.190$), as shown in Fig. 4.28a. In addition, no significant interaction effect is found between the surveillance task urgency and the autonomy setting ($F(2, 16) = 1.119,\ p = 0.338$), as shown in Fig. 4.29.

Participants' Steering Control Effort Under Emergency

The autonomy setting has a significant impact on the steering control effort in the obstacle-avoidance stage ($F(2, 16) = 133.264,\ p < 0.001$), as shown in Fig. 4.30b. The cases with the low-maximum-speed autonomy have the highest steering control effort, while the high-maximum-speed autonomy cases have the smallest steering torque. The steering torque of adaptive autonomy cases is at a medium level. More-

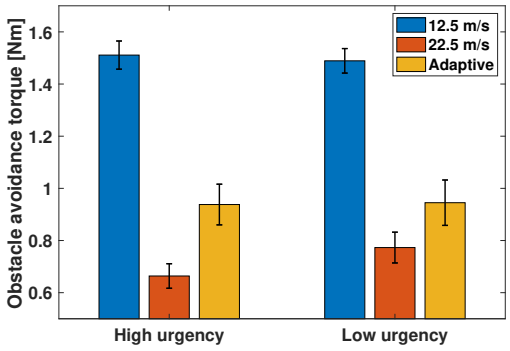

Figure 4.31: Relationship between emergency steering control effort and different autonomy maximum speed limit in Experiment 4 under different surveillance task urgencies

over, the pairwise comparison shows a significant difference in the average steering torque in the obstacle-avoidance stage between the low-maximum-speed autonomy cases and the high-maximum-speed autonomy cases ($p < 0.001$). There is also a significant difference between the adaptive autonomy cases and the high-maximum-speed autonomy cases ($p < 0.001$). A significant difference is also observed between the emergency steering control effort between the adaptive autonomy cases and low-maximum-speed cases ($p < 0.001$). The impact of the surveillance task urgency on the deviation from the centerline is not significant ($F(1, 17) = 0.570,\ p = 0.461$), as shown in Fig. 4.30a. In addition, no interaction effect is observed between the surveillance task urgency and the autonomy setting ($F(2, 16) = 0.991,\ p = 0.382$), as shown in Fig. 4.31.

Surveillance Task Performance

The surveillance task urgency significantly impacts the surveillance task performance ($F(1, 17) = 5.869,\ p = 0.027$), as shown in Fig. 4.32a. The surveillance task performance is better when the surveillance task urgency is low. The impact of the autonomy setting on the surveillance task performance is not significant ($F(2, 16) = 0.945,\ p = 0.399$), as shown in Fig. 4.32b. It indicates that all three autonomy settings have similar surveillance task performance. In addition, no significant interaction effect is found between the surveillance task urgency and the autonomy setting ($F(2, 16) = 0.594,\ p = 0.558$), as shown in Fig. 4.33.

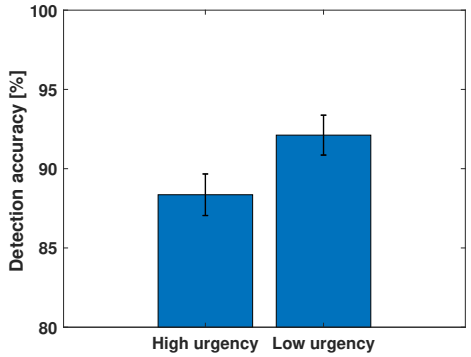

(a) Relationship between surveillance task urgency and detection accuracy in Experiment 4

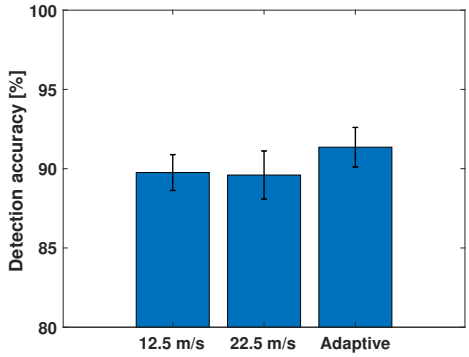

(b) Relationship between autonomy's maximum speed limit and detection accuracy in Experiment 4

Figure 4.32: Relationship between detection accuracy and different independent variables in Experiment 4.

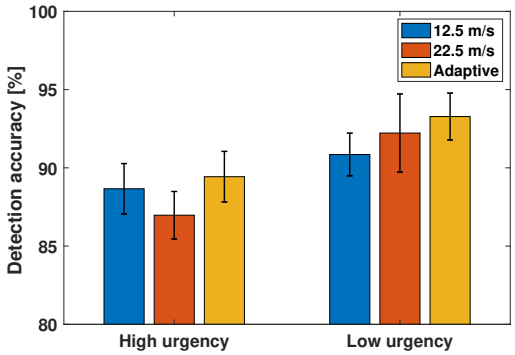

Figure 4.33: Relationship between surveillance task detection accuracy and different autonomy maximum speed limit in Experiment 4 under different surveillance task urgencies

Time to Finish the Mission

Both surveillance task urgency and autonomy setting significantly affect the time to finish the mission. Missions with fixed-length tracks require more time to complete when subjects experience urgent surveillance tasks ($F(1, 17) = 57.823,\ p < 0.001$), as shown in Fig. 4.34a. The autonomy setting also significantly impacts the time to finish the mission ($F(2, 16) = 2045.566,\ p < 0.001$), as shown in Fig. 4.34b. The low-maximum-speed autonomy takes the longest, while the high-maximum-speed autonomy takes the shortest time to complete the mission. The time to finish the mission of the adaptive autonomy is between the two non-adaptive cases. The pairwise

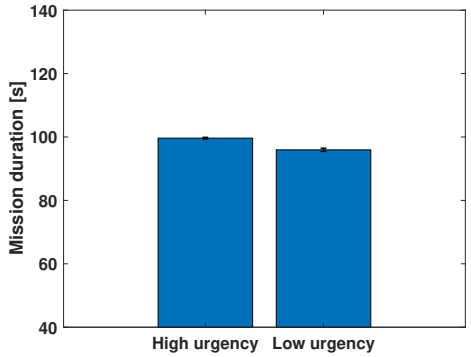

(a) Relationship between surveillance task urgency and mission duration in Experiment 4

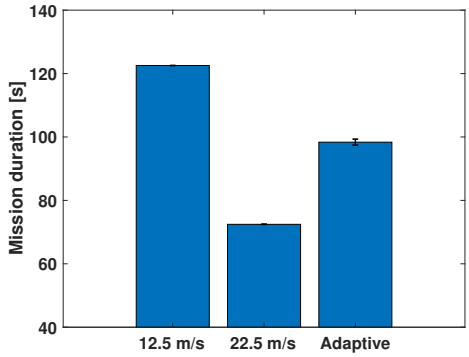

(b) Relationship between autonomy's maximum speed limit and mission duration in Experiment 4

Figure 4.34: Relationship between mission duration and different independent variables in Experiment 4.

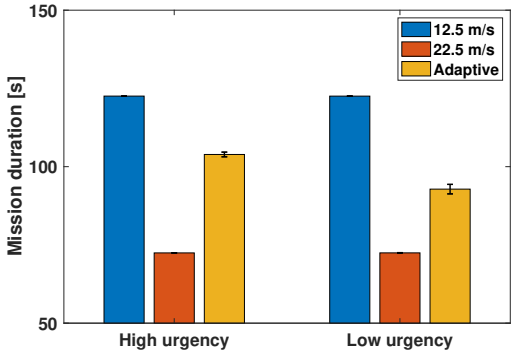

Figure 4.35: Relationship between mission duration and different autonomy maximum speed limit in Experiment 4 under different surveillance task urgencies

comparison shows that each pair of different autonomy settings has a significant difference with $p < 0.001$. The results also indicate a significant interaction effect between the surveillance task urgency and the autonomy setting ($F(2, 16) = 57.133$, $p < 0.001$). Analysis shows an increase in time to finish the mission when adaptive autonomy is adopted and the surveillance task becomes more urgent, as shown in Fig. 4.35.

4.3.2.4 Discussion

Participants' Self-reported Workload

Both adaptive autonomy and low-maximum-speed autonomy can achieve a smaller

participant-reported workload compared with high-maximum-speed autonomy. The design principles can explain the performance of adaptive autonomy. In the design of the adaptive autonomy, the maximum speed limit is varied by estimated workload, steering torque, and the steering rate. When the subjects experience the surveillance task with low urgency, steering torque and the steering rate change reduce the maximum speed limit so that subjects can control the vehicle more easily when they experience difficulty in local conditions. It results in the fact that the adaptive autonomy has a lower average speed level and larger safety margin when compared to the high-maximum-speed autonomy. On the other hand, when subjects experience the surveillance task with high urgency, the adaptive autonomy reduces the speed due to the increased workload. Even if the participants do not encounter driving difficulties (torque or steering rate is 0), the maximum speed is reduced to provide extra safety margin. Therefore, the adaptive autonomy achieves a less self-reported workload compared with the high-maximum-speed autonomy.

Driving Task Performance

For the performance in the lane-keeping task, the adaptive autonomy can achieve a medium centerline tracking error compared to the centerline tracking error when both non-adaptive autonomy settings are applied. It is observed from Experiment 3 that the centerline tracking error increases when the maximum speed limit increases. Therefore, the value of the centerline tracking error under adaptive autonomy can result from the fact that the average speed of the adaptive autonomy lies between the two non-adaptive autonomy settings.

Participants' Control Effort During Lane Keeping

It is observed that the adaptive autonomy can achieve a minimum control effort during the centerline tracking mission among all three autonomy settings. It can be explained by the design principles. The speed reduction from workload and human torque under the over-loaded condition, as well as the speed reduction from steering rate and human torque under the moderate workload condition, makes the driving task easier when compared with the non-adaptive autonomy settings.

After considering the centerline tracking performance shown in the previous sec-

tion, it is shown that the adaptive autonomy can achieve a balanced centerline tracking performance with minimum control effort compared with the other two non-adaptive autonomy settings in the lane-keeping stage.

Emergency Maneuvering Performance

The deviation from the centerline under the adaptive autonomy setting lies between the deviation from the centerline when the other two non-adaptive autonomy settings are implemented. It can be seen as the extension of the conclusion from Experiment 3 as well. In Experiment 3, results show that greater maximum speed limits lead to a larger deviation from the centerline. Because the adaptive autonomy achieves a medium average speed, the deviation from the centerline under emergency is also at a medium level.

Participants' Control Effort Under Emergency

The steering control effort under emergency is at a medium level when adaptive autonomy is implemented. It can be explained by the conclusion from Experiment 3 as well. In Experiment 3, results show that greater maximum speed limits lead to a smaller steering control effort. The reduced steering control effort in the high-maximum-speed autonomy cases aims to achieve a gentle maneuver to avoid tire lift-off or roll-over. Compared with the high-maximum-speed autonomy, the adaptive autonomy reduces speed during the obstacle avoidance (through sensing the extra torque and steering rate change) so that the subjects can have extra room to control the vehicle, leading to increased human torque. Compared with the low-maximum-speed autonomy, the adaptive autonomy achieves a higher traveling speed at the cost of the safety margin of the obstacle avoidance.

Surveillance Task Performance

Only the surveillance task urgency impacts the surveillance task performance. It aligns with the previous result that the surveillance task performance worsens when participants experience the surveillance tasks with high urgency. It also shows that the detection accuracy of the adaptive autonomy under the current setting can achieve at least the same performance as the non-adaptive autonomy with different maximum speed limits.

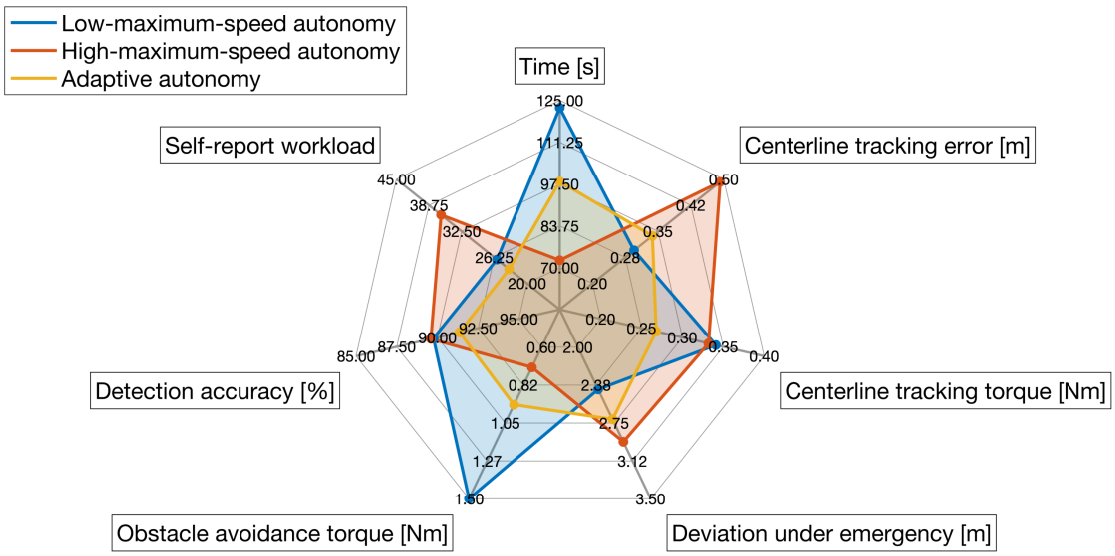

Figure 4.36: Spider plot showing all metrics in Experiment 4 when autonomy settings are different. The axis is the dimension of the metrics. The more away from the axis, the worse performance in that dimension. The one with a smaller coverage is considered a better design.

Conclusion on Overall Performance

In conclusion, the adaptive autonomy can achieve a workload closer to the low-maximum-speed autonomy and a reduced steering control effort in the lane-keeping duration. It balances the performance between driving task performance, emergency maneuvering performance, emergency steering control effort, and mission duration compared with the other two non-adaptive autonomy settings. A spider plot concludes these characteristics as shown in Fig. 4.36.

It is suggested to implement adaptive autonomy when the difference between the autonomy and human is not large, and the steering control effort is an important metric to consider.

Effect of Taking Workload into Consideration When Designing Adaptive Autonomy

The workload-adaptive autonomy considers three factors: the (estimated) workload w_t from the human operator, the human's torque τ_h, and the steering rate γ. This

subsection aims to analyze the impact of the workload, which is the major human factor considered in this dissertation. A new adaptive autonomy is created here, which assumes the human operator always has a moderate workload condition. Therefore, the calculation of its maximum speed limit, which is called the re-calculated maximum speed limit and labeled by $u_{x,max,n}$, assumes the workload $w_t = 50$ in Eq. 4.2 under all circumstances. Under the moderate workload condition, the re-calculated maximum speed limit $u_{x,max,n}$ has a similar value as the original maximum speed limit $u_{x,max}$. However, there is a difference between these maximum speed limits under the over-loaded condition. As shown in Fig. 4.37, the re-calculated maximum speed limit is always set at a higher speed than the original maximum speed limit. It will lead to a shorter mission duration and faster traveling speed. However, an increased traveling speed under the over-loaded condition leads to a worse driving task performance, as suggested by [48] and indicated by the results in Experiment 3 and Experiment 4. Therefore, the role of the workload in the over-loaded condition is to achieve a good mission performance at the cost of more mission duration when compared with the adaptive autonomy, which does not consider the workload. It is achieved by reducing the maximum speed limit, which provides more safety margin as indicated in [99].

4.4 Conclusion

In this chapter, the adaptation at the autonomy level is investigated. It is achieved by adapting maximum speed limit, the autonomy parameter that significantly impacts the human subject's workload. First, several candidates for the autonomy parameters are investigated in a pilot study. The maximum speed limit is selected as a result of this pilot study. In Experiment 3, a human subject study investigates the impact of the maximum speed limit on workload and other driving-performance-based metrics. This investigation is performed by implementing autonomy with two maximum speed limits in a dual-task shared control scenario. Results from 12 participants in Experiment 3 show that a higher maximum speed limit leads to a higher workload, shorter mission duration, and worse driving task performance. These conclusions

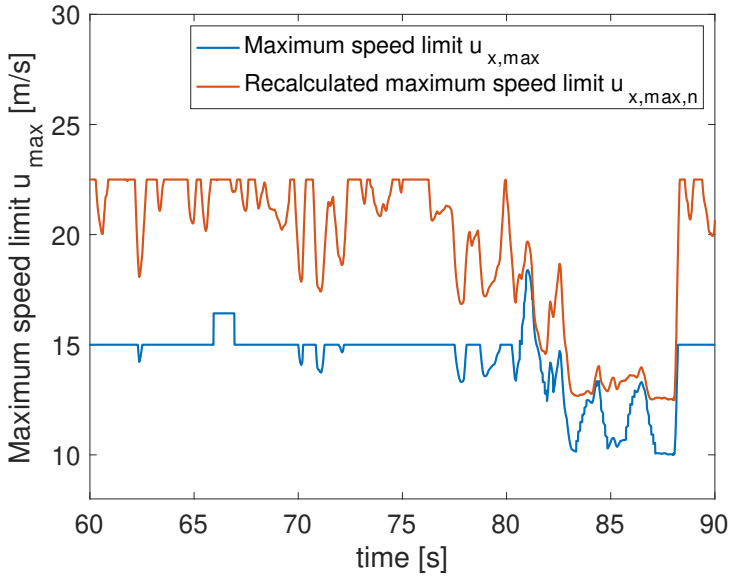

Figure 4.37: Difference between the maximum speed limit in workload-adaptive autonomy (original maximum speed limit $u_{x,max}$) and the maximum speed limit in an adaptive autonomy without workload (recalculated maximum speed limit $u_{x,max,n}$) under the over-loaded condition.)

are then used to design an adaptive autonomy, which considers workload, human steering torque, and steering rate. The benefits of the proposed adaptive autonomy are then evaluated in Experiment 4. The performance is evaluated by implementing three autonomy settings, including the proposed adaptive autonomy and the baseline non-adaptive autonomy with two maximum speed limits in a dual-task shared control driving mission. In this experiment, workload is controlled by the surveillance task urgency. A real-time Bayesian-Inference (BI)-based workload estimation algorithm is implemented to provide the estimated workload online. The results from 12 subjects indicate that adaptive autonomy leads to a balance between self-reported workload, driving task performance in both lane-keeping and obstacle-avoidance stage, steering control effort in the obstacle-avoidance stage, and time to finish the mission. Moreover, it helps reduce the steering control effort in the lane-keeping stage.

These results reveal the benefit of considering and adapting to workload in shared control problems at the autonomy level. Nevertheless, the combined effect of the workload-adaptive control consolidation and workload-adaptive autonomy is not dis-

covered. Therefore, in the next chapter, potential improvements are investigated when adaptation happens both at the control consolidation level and at the autonomy level.

Chapter 5

Combined Effect of the Workload-Adaptive Shared Control Consolidation and Workload-adaptive Autonomy Navigation Formulation

5.1 Introduction

In this chapter, the benefits of adaptation to workload at both control consolidation level and autonomy level are investigated by conducting a human subject study in a dual-task mission. There are 24 student subjects in this experiment. The mission goal is identical to the previous experiment, Experiment 4. During the mission, subjects need to perform both the driving and surveillance tasks. However, the driving task's control consolidation and autonomy settings are different from those used in previous experiments. On the one hand, two control consolidations, including the non-adaptive control consolidation and the adaptive control consolidation, are used for the control consolidation level. On the other hand, the non-adaptive high-maximum-speed and low-maximum-speed autonomy, along with the adaptive autonomy, are implemented for the autonomy level. Subjects experience all possible combinations of the control

consolidation and autonomy settings under different workload conditions. Therefore, the conclusion can be drawn based on the performance under these combinations of settings. The workload is controlled by the surveillance task urgency, similar to previous experiments. Like Experiment 4, the real-time workload estimation is achieved using the Bayesian Inference (BI) method [87].

5.2 Evaluation of the Combined Framework including Both Workload-adaptive Control Consolidation and Workload-adaptive Autonomy: Experiment 5

5.2.1 Method

Participants

There are a total of 26 university student subjects in this experiment. Data of one participant is discarded due to the wrong experiment setup. Data of another participant is discarded because the participant's vision is not qualified for the surveillance task. The average age of the participants is 22.54 years old ($SD = 3.43$ years). They hold a driving license for 4.25 years on average ($SD = 2.60$ years). All participants have a normal or corrected-to-normal vision, and the eye tracker can be calibrated on their eyes.

Apparatus and Stimuli

The dual-task shared control testbed (introduced in Chapter 2) with the Unreal-based visualization module (introduced in Sec. 2.2.3) is used in this experiment. Participants perform the driving task and the surveillance task simultaneously.

The goal of the driving task is similar to Experiment 4, which is shown in Sec. 4.3.2.2. In the driving task, the participant and the autonomy share the vehicle's steering control, while the vehicle's speed is controlled by autonomy only. The goal of the driving task is to complete a fixed-length track with minimal deviation from the centerline

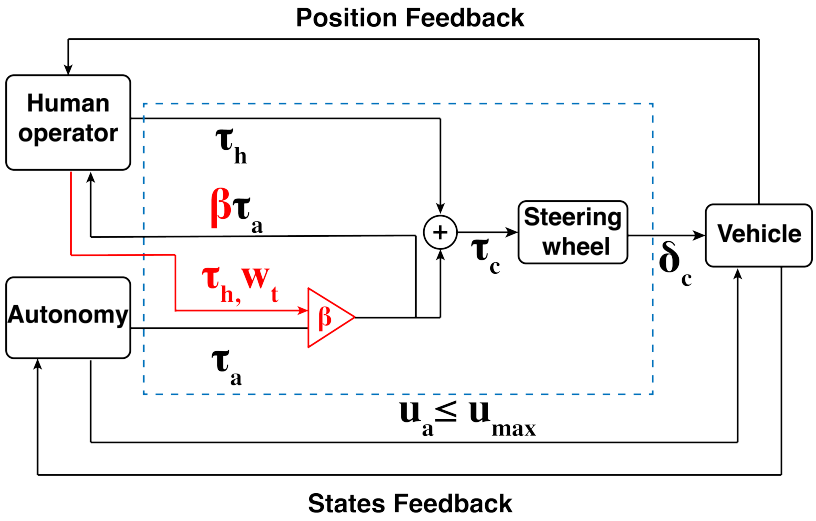

Figure 5.1: Control block diagram when different control consolidation and different autonomy maximum speed limits are implemented. The blue dashed lines highlight the control consolidation part. For the non-adaptive control consolidation, the assistance level β is always 1. The term u_a represents the speed of the vehicle is controlled by autonomy only. u_{max} can assume one of the three autonomy maximum speed limits: 12.5 m/s, 22.5 m/s and adaptive autonomy speed limit $u_{x,max}$.

while avoiding obstacles on the centerline. The autonomy has no obstacle avoidance capability. Unlike previous experiments where adaptive control consolidation and adaptive autonomy are evaluated in isolation, in this experiment, all combinations of the control consolidation and autonomy settings are investigated. There are two control consolidations used in this experiment: non-adaptive control consolidation and adaptive control consolidation. The non-adaptive control consolidation is introduced in Sec. 3.2.1.1. From the signal shown in Sec. 4.3.2.3, the real-time workload estimator can detect the slight workload increment caused by the surveillance task in the low urgency cases. Therefore, the adaptive control consolidation, which is introduced in Sec. 3.2.1.2, is implemented. In addition, three autonomy settings are presented, including the adaptive autonomy, which is introduced in Sec. 4.3.1, and the non-adaptive autonomy with a low maximum speed limit and a high maximum speed limit. The latter two are also called the low-maximum-speed autonomy and the high-maximum-speed autonomy and are introduced in Sec. 4.2.1.2. The control block diagram used in this experiment is shown in Fig. 5.1.

Participants also need to perform the surveillance task, whose setting is identical to Experiment 4 as described in Sec. 4.3.2.2. The goal of the surveillance task is to make the identification within the time limit as accurate as possible. The surveillance task urgency is used to control the subject's workload in this experiment. There are two surveillance task urgencies: 1.5 s pace and 6.5 s pace. They are labeled as high surveillance task urgency and low surveillance task urgency, respectively.

The real-time workload estimator based on Bayesian Inference and developed by our collaborators [87] is used in this experiment, which is the same as the one used in Experiment 4. For the workload estimation, the corresponding data from a 4 s time window captured by the eye tracker, Tobii Pro Glasses 2, (30 Hz sampling rate), are used to estimate participants' workload. The processing of the workload is similar to the method in Experiment 4, which is shown in Sec. 4.3.2.2. A moving average filter is applied with a 1 s time window, and w_t is down-sampled to 10 Hz. The processed signal of the real-time estimated workload can be found in Sec. 4.3.2.3.

Autonomy Formulation

The same autonomy formulation is used in this human subject study as in Experiment 4 (Sec. 4.3.2.2). The maximum speed limit $u_{x,max}$ is set to be 12.5 m/s, 22.5 m/s, and adaptive function $u_{x,max}(w_t, \tau_h, \hat{\gamma})$ for the low-maximum-speed autonomy, high-maximum-speed autonomy, and adaptive autonomy, respectively. The detailed information of the proposed adaptive autonomy maximum speed limit $u_{x,max}(w_t, \tau_h, \hat{\gamma})$ can be found in Sec. 4.3.1.

Experimental Design

The experiment uses a within-subject design. There are three independent variables: the autonomy setting, the control consolidation setting, and the surveillance task urgency. The autonomy setting includes adaptive autonomy, non-adaptive low-maximum-speed autonomy (12.5 m/s speed limit), and non-adaptive high-maximum-speed autonomy (22.5 m/s speed limit). The latter two are labeled as low-maximum-speed autonomy and high-maximum-speed autonomy in short. The control consolidation setting includes adaptive control consolidation and non-adaptive control consolidation. The surveillance task urgency includes the low urgency (6.5 s pace) and

Table 5.1: Twelve test conditions in Experiment 5

Condition	Surveillance task urgency	Autonomy setting (maximum speed limit)	Control consolidation setting
1	1.5 s	12.5 m/s	Non-adaptive
2	1.5 s	22.5 m/s	Non-adaptive
3	1.5 s	Adaptive	Non-adaptive
4	6.5 s	12.5 m/s	Non-adaptive
5	6.5 s	22.5 m/s	Non-adaptive
6	6.5 s	Adaptive	Non-adaptive
7	1.5 s	12.5 m/s	Adaptive
8	1.5 s	22.5 m/s	Adaptive
9	1.5 s	Adaptive	Adaptive
10	6.5 s	12.5 m/s	Adaptive
11	6.5 s	22.5 m/s	Adaptive
12	6.5 s	Adaptive	Adaptive

high urgency (1.5 s pace). In this experiment, subjects drive on 12 different tracks of the same length (around 1200 m). The subject experiences a combination of autonomy setting, control consolidation setting, and the surveillance task urgency on one track. The corresponding twelve combinations are shown in Table 5.1. To eliminate the potential order effects, the presentation of the twelve test cases follows a 12×12 Latin square design.

Measures

There are seven dependent variables collected in the experiment:

- Participants' self-reported workload
- Participants' steering control effort in the lane-keeping task
- Driving task performance
- Participants' steering control effort under emergency
- Emergency maneuvering performance
- Surveillance task performance
- Time to finish the task

In this experiment, the obstacle-avoidance stage has the same definition as in Experiment 1 (Sec. 3.2.2.2), Experiment 3 (Sec. 4.2.1.2), and Experiment 4 (Sec. 4.3.2.2). The obstacle-avoidance stage is defined as the period when the human subjects deviate at least 1 m from the centerline and avoid the obstacles. The remaining part is defined as the lane-keeping stage.

After completion of each track, participants report their workload using the NASA TLX survey [90]. The NASA TLX survey is presented to the participants before the experiment such that they understand the meaning of workload. Similar to methods in previous experiments given in Sec. 3.2.2.2, Sec. 3.3.2.2, Sec. 4.2.1.2 and Sec. 4.3.2.2, a participant's steering control effort in the lane-keeping task is calculated as the average value of the absolute human torque during the lane-keeping stage. Driving task performance is evaluated by lane-keeping error, calculated as the mean of the absolute deviation of the vehicle's position from the centerline during the lane-keeping stage. Steering control effort under emergency is calculated as the average of the absolute human torque that the participant applied on the steering wheel during the obstacle avoidance maneuver. Emergency maneuvering performance is evaluated by centerline deviation during the obstacle avoidance maneuver, which uses a similar calculation method as driving task performance but in the obstacle-avoidance stage. The torque from the participant is measured from a steering torque rotatory sensor. The collection rate of driving performance and steering control effort of the lane-keeping and obstacle-avoidance stages is 100 Hz. The surveillance task performance is measured using the detection accuracy of the surveillance task. The time to finish the mission is the time duration of the mission.

Experimental Procedure

Before the training session starts, participants provide a signed informed consent and fill in a demographic survey to report their age and driving experience. After that, they receive a training session.

During the training session, the participants first perform three trials of driving tasks only, with the low-maximum-speed autonomy, the high-maximum-speed autonomy, and the adaptive autonomy in order. The trial with the low-maximum-speed autonomy takes approximately 4 minutes, while the trial with the high-maximum-speed autonomy takes approximately 2 minutes. The trial with the adaptive autonomy takes approximately 2 minutes. Then the participants perform a training trial of the surveillance task only. It consists of two portions. The first portion is with the low surveillance task urgency, and it takes approximately 1 minute. The second portion is

with the high surveillance task urgency, and it takes approximately 2 minutes. After that, the participants perform three combined driving and surveillance task trials with different surveillance task urgencies and different autonomy settings. In the combined task, the surveillance task urgency of the first portion, which lasts for 1 minute, is low, and the surveillance task urgency of the second portion, which reaches the end of the training trial, is high. The order of the autonomy settings in these combined training tasks is the low-maximum-speed autonomy, the high-maximum-speed autonomy, and the adaptive autonomy. Except for the last training trial where the adaptive control consolidation is implemented, the non-adaptive control consolidation is used.

During the official experiment, participants perform the combined driving task and the surveillance task on twelve tracks with the test cases described in Table 5.1. In each trial, participants travel at a fixed distance (around 1200 m). After each trial, the participants are required to fill in a post-survey (NASA TLX) [90] to report the workload during the last track. If they hit the obstacle, the trial is restarted.

5.2.2 Results

Three-way repeated measures Analysis of Variance (ANOVA) is conducted with the surveillance task urgency, the consolidation setting, and the maximum allowed speed setting as the within-subjects variables. Results are reported as significant for $\alpha < .05$.

Table 5.2 summarizes the mean and standard error (SE) values of the participants' self-reported workload, centerline tracking error, centerline tracking torque, deviation under emergency, obstacle avoidance torque, time to finish the mission and detection accuracy.

5.2.2.1 Analysis of All Schemes

Participants' Self-reported Workload

Both surveillance task urgency and autonomy setting have a significant impact on participants' self-reported workload.

When the surveillance task is less urgent (6.5 s), participants report lower workload

Table 5.2: Mean and standard error (SE) of self-reported workload, centerline tracking error, centerline tracking torque, deviation under emergency, obstacle avoidance torque, time to finish the mission and detection accuracy in Experiment 5

Metrics	N	Surveillance task urgency					
		6.5 s					
		Non-adaptive control consolidation			Adaptive control consolidation		
		12.5 m/s	22.5 m/s	Adaptive autonomy	12.5 m/s	22.5 m/s	Adaptive autonomy
Workload	24	15.655 ± 2.619	27.976 ± 3.603	20.298 ± 2.891	12.470 ± 1.567	25.804 ± 3.002	18.869 ± 3.149
Centerline tracking error (m)	24	0.257 ± 0.016	0.408 ± 0.025	0.306 ± 0.015	0.250 ± 0.018	0.417 ± 0.021	0.330 ± 0.017
Centerline tracking torque (Nm)	24	0.342 ± 0.014	0.343 ± 0.009	0.279 ± 0.007	0.322 ± 0.011	0.317 ± 0.009	0.287 ± 0.019
Deviation under emergency (m)	24	2.411 ± 0.110	2.918 ± 0.104	2.801 ± 0.111	2.489 ± 0.108	2.947 ± 0.160	2.902 ± 0.133
Obstacle avoidance torque (Nm)	24	1.479 ± 0.045	0.755 ± 0.053	0.811 ± 0.052	1.025 ± 0.030	0.572 ± 0.032	0.661 ± 0.042
Time to finish the mission (s)	24	122.512 ± 0.009	72.400 ± 0.074	93.838 ± 0.976	122.518 ± 0.011	72.415 ± 0.067	90.959 ± 1.028
Detection accuracy (%)	24	90.931 ± 1.324	88.750 ± 2.505	92.827 ± 1.283	89.216 ± 1.828	93.030 ± 1.691	95.069 ± 1.020
Metrics	N	Surveillance task urgency					
		1.5 s					
		Non-adaptive control consolidation			Adaptive control consolidation		
		12.5 m/s	22.5 m/s	Adaptive autonomy	12.5 m/s	22.5 m/s	Adaptive autonomy
Workload	24	28.185 ± 3.602	42.440 ± 4.709	33.601 ± 3.722	32.589 ± 3.366	43.542 ± 4.110	32.440 ± 3.937
Centerline tracking error (m)	24	0.314 ± 0.013	0.513 ± 0.029	0.344 ± 0.020	0.306 ± 0.014	0.534 ± 0.034	0.348 ± 0.019
Centerline tracking torque (Nm)	24	0.354 ± 0.011	0.369 ± 0.012	0.285 ± 0.007	0.336 ± 0.009	0.333 ± 0.012	0.279 ± 0.009
Deviation under emergency (m)	24	2.392 ± 0.089	2.966 ± 0.141	2.582 ± 0.098	2.502 ± 0.126	3.156 ± 0.173	2.563 ± 0.145
Obstacle avoidance torque (Nm)	24	1.492 ± 0.040	0.770 ± 0.045	0.967 ± 0.054	1.374 ± 0.055	0.705 ± 0.041	0.855 ± 0.061
Time to finish the mission (s)	24	122.549 ± 0.016	72.371 ± 0.067	104.307 ± 0.568	122.547 ± 0.015	72.424 ± 0.062	103.675 ± 0.644
Detection accuracy (%)	24	90.388 ± 2.838	85.378 ± 1.976	88.157 ± 1.466	91.579 ± 2.575	86.494 ± 1.711	88.222 ± 1.287

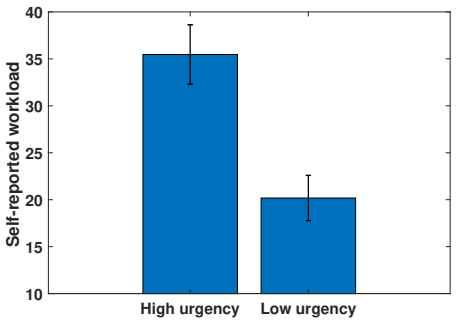

(a) Relationship between surveillance task urgency and self-reported workload in Experiment 5

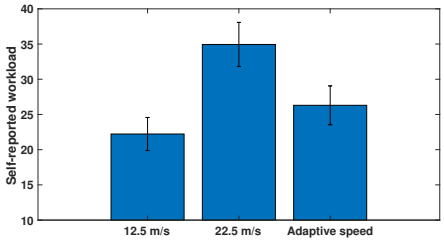

(b) Relationship between autonomy settings and self-reported workload in Experiment 5. The autonomy setting in the figure is represented by the maximum speed limit.

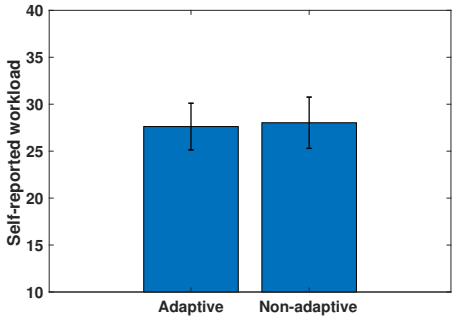

(c) Relationship between control consolidation settings and self-reported workload in Experiment 5

Figure 5.2: Relationship between self-reported workload and different independent variables in Experiment 5.

($F(1, 23) = 44.036,\ p < .001$), which is shown in Fig. 5.2a.

With different autonomy settings, participants report different workload levels ($F(2, 22) = 26.485,\ p < .001$), which is shown in Fig. 5.2b. Specifically, subjects report the lowest workload when the low-maximum-speed autonomy is implemented. When adaptive autonomy is implemented, the self-reported workload is at a medium level. When the high-maximum-speed autonomy is implemented, subjects report the highest workload. For the pairwise comparison, results report a significant difference in the self-reported workload between adaptive autonomy cases and low-maximum-speed autonomy cases ($p = 0.010$). A significant difference is observed between the self-reported workload under the low-maximum-speed cases and the high-maximum-speed cases ($p < 0.001$). The difference between the workload level reported under

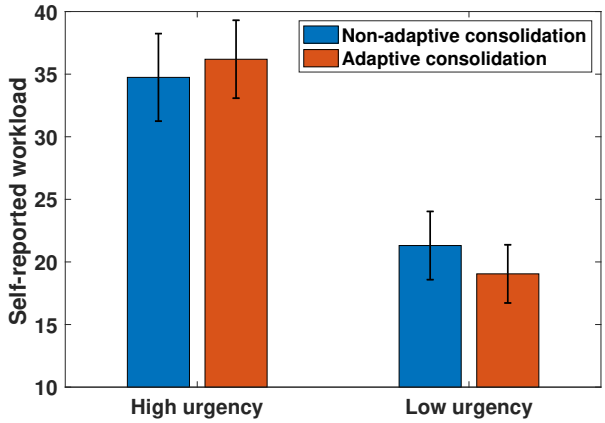

Figure 5.3: Relationship between self-reported workload and different control consolidation settings in Experiment 5 under different surveillance task urgencies

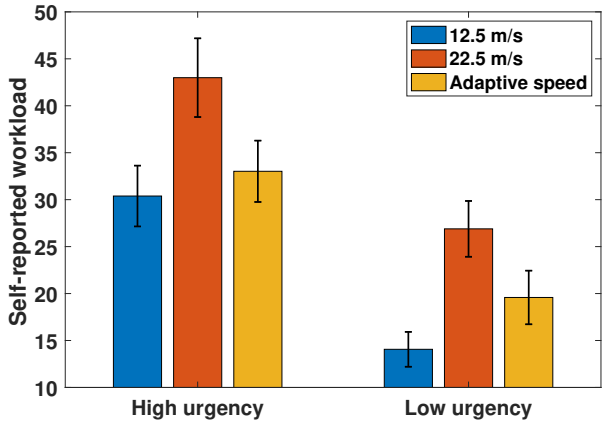

Figure 5.4: Relationship between self-reported workload and different autonomy settings in Experiment 5 under different surveillance task urgencies

the adaptive autonomy cases and the high-maximum-speed cases is also significant ($p < 0.001$).

When different control consolidation settings are implemented, the difference in corresponding self-reported workload is non-significant ($F(1, 23) = 0.167,\ p = 0.686$), which is shown in Fig. 5.2c.

In addition, no significant interaction effect is observed between surveillance task urgency and control consolidation settings ($F(1, 23) = 1.603,\ p = 0.218$), as shown in Fig. 5.3. There is also no significant interaction effect between surveillance task urgency and autonomy settings ($F(2, 22) = 0.479,\ p = 0.623$), as shown in Fig. 5.4.

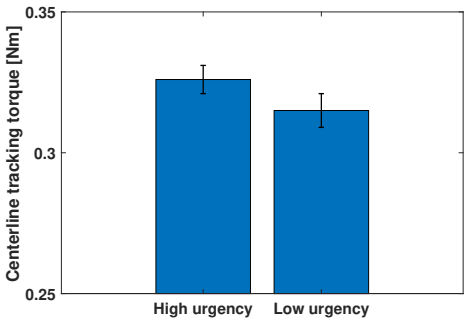

(a) Relationship between surveillance task urgency and centerline tracking torque in Experiment 5

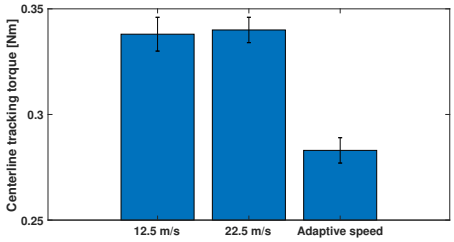

(b) Relationship between autonomy settings and centerline tracking torque in Experiment 5. The autonomy setting in the figure is represented by the maximum speed limit.

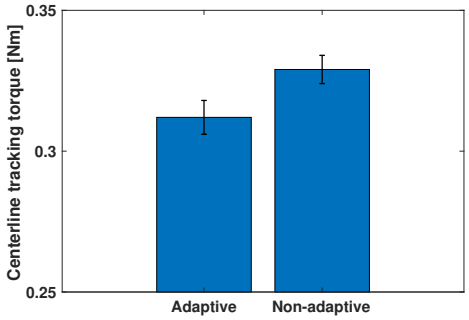

(c) Relationship between control consolidation settings and centerline tracking torque in Experiment 5

Figure 5.5: Relationship between centerline tracking torque and different independent variables in Experiment 5.

Participants' Steering Control Effort During Lane Keeping

Both control consolidation setting and autonomy setting impact participants' steering control effort in the lane-keeping task significantly.

There is a significant difference in steering control effort in the lane-keeping task when different control consolidations are implemented ($F(1, 23) = 6.926,\ p = .015$), as shown in Fig. 5.5c. The steering control effort in the lane-keeping task is significantly reduced when the adaptive control consolidation is implemented.

The autonomy setting significantly affects the steering control effort in the lane-keeping task ($F(2, 22) = 25.075,\ p < .001$), as shown in Fig. 5.5b. The steering control effort in the adaptive autonomy cases is significantly lower than the steering control effort when the low-maximum-speed autonomy or the high-maximum-speed

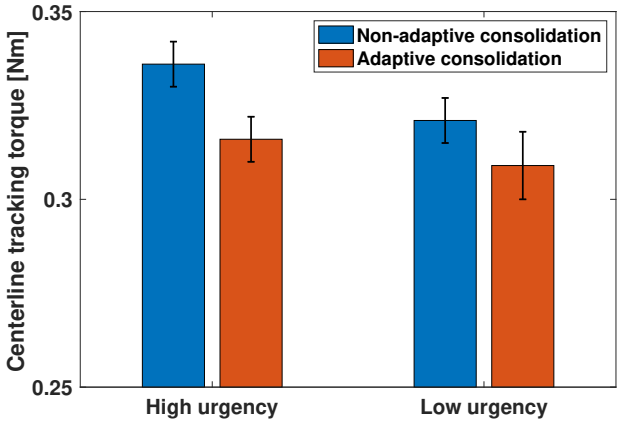

Figure 5.6: Relationship between centerline tracking torque and different control consolidation settings in Experiment 5 under different surveillance task urgencies

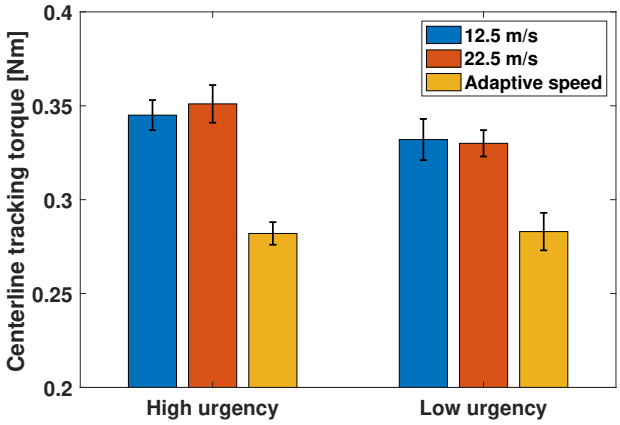

Figure 5.7: Relationship between centerline tracking torque and different autonomy settings in Experiment 5 under different surveillance task urgencies

autonomy is implemented, respectively. For the pairwise comparison, there is a significant difference in the steering control effort in the lane-keeping stage between the adaptive autonomy cases and the cases with the low-maximum-speed autonomy ($p < .001$). A significant difference is also observed between the lane-keeping steering control effort in adaptive autonomy cases and the cases with the high-maximum-speed autonomy ($p < .001$). The steering control effort difference in the lane-keeping task between the cases of the low-maximum-speed autonomy and the high-maximum-speed autonomy is not significant ($p = 0.841$).

The influence of the surveillance task urgency on participants' steering control

effort in the lane-keeping task is non-significant ($F(1, 22) = 3.332,\ p = 0.081$), as shown in Fig. 5.5a.

Moreover, there is a significant interaction effect between control consolidation setting and autonomy setting ($F(2, 22) = 3.906,\ p = 0.027$). The adaptive control consolidation reduces steering control effort in the lane-keeping task when non-adaptive autonomy settings are implemented, i.e., when the low-maximum-speed autonomy or the high-maximum-speed autonomy is implemented. When adaptive autonomy is implemented, the adaptive control consolidation cannot reduce the steering control effort significantly. These results and the corresponding figure are expanded in the next sub-sections (Sec. 5.2.2.2 and Sec. 5.2.2.3) in more detail.

In addition, no significant interaction effect is observed between surveillance task urgency and control consolidation settings ($F(1, 23) = 0.290,\ p = 0.595$), as shown in Fig. 5.6. There is no significant interaction effect between surveillance task urgency and autonomy settings ($F(2, 22) = 1.044,\ p = 0.360$), as shown in Fig. 5.7.

Driving Task Performance

The surveillance task urgency and autonomy settings significantly affect the driving task performance.

Participants have a better driving performance when the surveillance task is less urgent ($F(1, 23) = 53.255,\ p < 0.001$), as shown in Fig. 5.8a.

With the different autonomy settings, participants achieve different driving task performance ($F(2, 22) = 92.734,\ p < .001$), as shown in Fig. 5.8b. Participants achieve the best driving performance when the low-maximum-speed autonomy is implemented. The centerline tracking error is at a medium level when adaptive autonomy is utilized. Participants have the worst driving performance when the high-maximum-speed autonomy is implemented. For the pairwise comparison, the centerline tracking error in the cases when the low-maximum-speed autonomy is implemented is significantly lower compared with the adaptive autonomy cases ($p < .001$) and the high-maximum-speed autonomy cases ($p < .001$). The centerline tracking performance is significantly better when adaptive autonomy is implemented compared with the cases when the high-maximum-speed autonomy is implemented ($p < .001$).

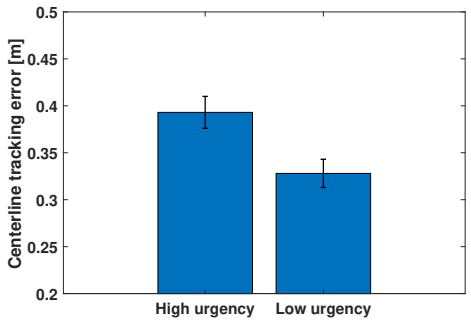

(a) Relationship between surveillance task urgency and centerline tracking error in Experiment 5

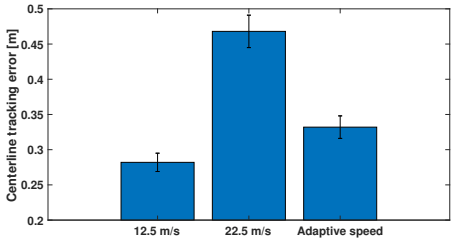

(b) Relationship between autonomy settings and centerline tracking error in Experiment 5. The autonomy setting in the figure is represented by the maximum speed limit.

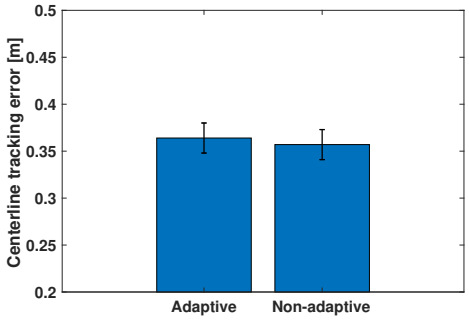

(c) Relationship between control consolidation settings and centerline tracking error in Experiment 5

Figure 5.8: Relationship between centerline tracking error and different independent variables in Experiment 5.

The difference in driving performance when different control consolidations are used is not significant ($F(1, 23) = 2.157,\ p = 0.155$), as shown in Fig. 5.8c.

Moreover, there is an interaction effect between surveillance task urgency and autonomy setting ($F(2, 22) = 8.185,\ p < .001$), as shown in Fig. 5.10. In general, the centerline tracking error is increased when the surveillance task urgency is high compared with cases when the surveillance task urgency is low. This increment is smaller when the adaptive autonomy is implemented compared with the non-adaptive autonomy with two different speed limits.

In addition, there is no interaction effect between surveillance task urgency and control consolidation setting ($F(1, 23) = 0.025,\ p = 0.875$), as shown in Fig. 5.9.

Participants' Steering Control Effort Under Emergency

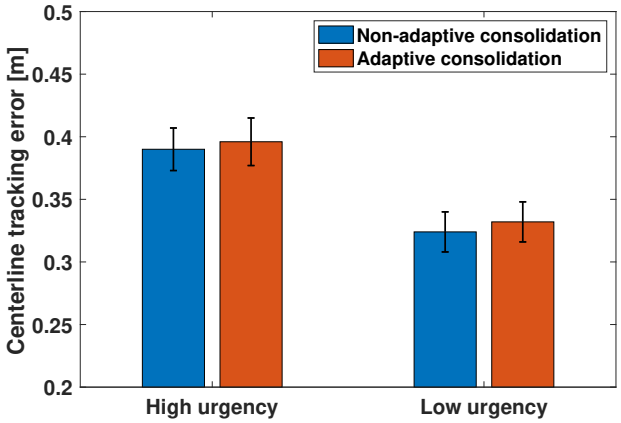

Figure 5.9: Relationship between centerline tracking error and different control consolidation settings in Experiment 5 under different surveillance task urgencies

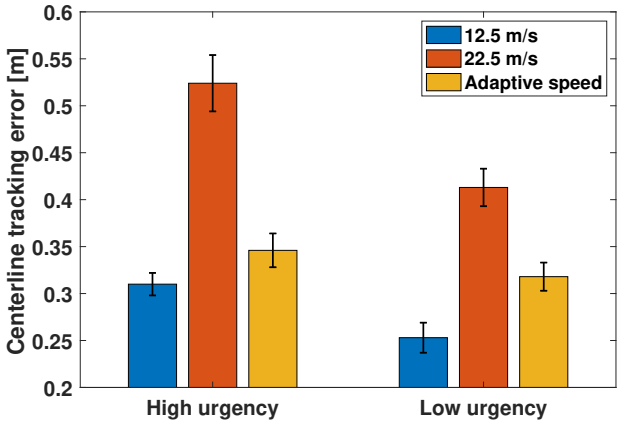

Figure 5.10: Relationship between centerline tracking error and different autonomy settings in Experiment 5 under different surveillance task urgencies

The surveillance task urgency, the control consolidation setting, and the autonomy setting all have a significant impact on the participants' steering control effort under emergency.

Participants exert less torque under emergency cases when the surveillance task is less urgent ($F(1, 23) = 55.505,\ p < 0.001$), as shown in Fig. 5.11a.

Participants spend less steering control effort under emergency cases when the adaptive control consolidation is implemented ($F(1, 23) = 70.308,\ p < 0.001$), as shown in Fig. 5.11c.

Different autonomy settings impact the participants' steering torque under emer-

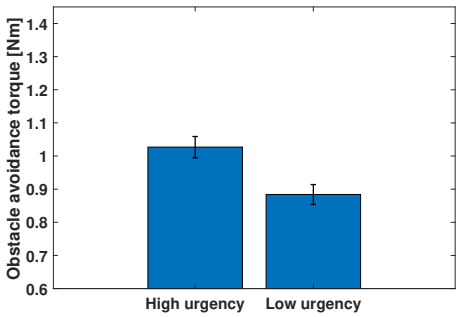

(a) Relationship between surveillance task urgency and obstacle avoidance torque in Experiment 5

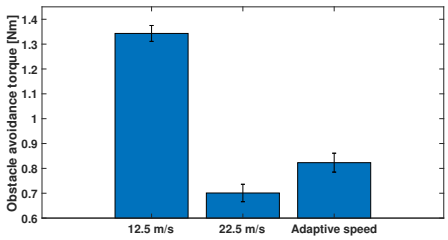

(b) Relationship between autonomy settings and obstacle avoidance torque in Experiment 5. The autonomy setting in the figure is represented by the maximum speed limit.

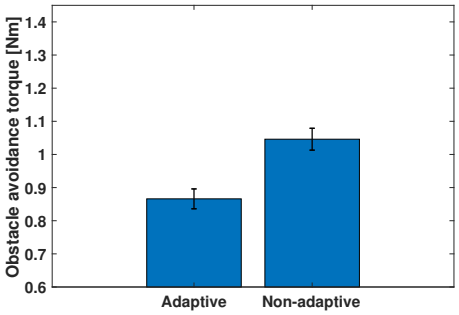

(c) Relationship between control consolidation settings and obstacle avoidance torque in Experiment 5

Figure 5.11: Relationship between obstacle avoidance torque and different independent variables in Experiment 5.

gency significantly ($F(2, 22) = 219.884,\ p < 0.001$), as shown in Fig. 5.11b. The steering torque exerted under emergency is at its lowest level when the high-maximum-speed autonomy is implemented. Participants exert a medium level of steering torque under emergency when the adaptive autonomy is implemented. The steering control effort of obstacle avoidance is highest when the low-maximum-speed autonomy is implemented. As for pairwise comparison, participants exert significantly less steering torque under emergency when the high-maximum-speed autonomy is implemented compared with the cases when adaptive autonomy is implemented ($p < 0.001$). The difference in the emergency steering torque is also significant between the cases when the high-maximum-speed autonomy is implemented and the cases when the low-maximum-speed autonomy is implemented ($p < 0.001$). In addition, partici-

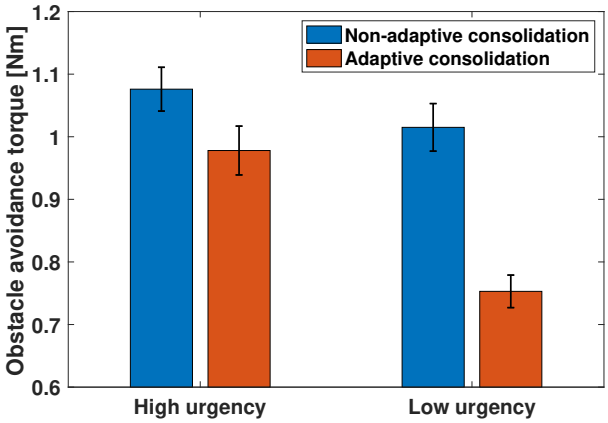

Figure 5.12: Relationship between obstacle avoidance torque and different control consolidation settings in Experiment 5 under different surveillance task urgencies

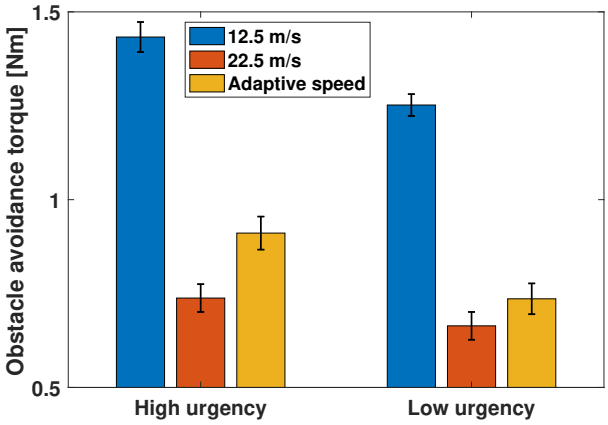

Figure 5.13: Relationship between obstacle avoidance torque and different autonomy settings in Experiment 5 under different surveillance task urgencies

pants exert more emergency steering torque when the low-maximum-speed autonomy is implemented than the steering torque when adaptive autonomy is implemented ($p < 0.001$).

In addition, several significant interaction effects are observed. Firstly, there is an interaction effect between the control consolidation setting and surveillance task urgency ($F(1, 23) = 11.333,\ p = 0.003$), as shown in Fig. 5.12. There is less reduced emergency torque from implementing the adaptive control consolidation when the surveillance task is more urgent. Secondly, there is a significant interaction effect between the surveillance task urgency and the autonomy setting ($F(2, 22) = 3.937$,

$p = 0.026$), as shown in Fig. 5.13. The human steering torque increment from switching to the surveillance task with high urgency is increased when the adaptive autonomy is implemented. Thirdly, there is an interaction effect between the control consolidation setting and autonomy setting ($F(2, 22) = 6.935,\ p = 0.002$). More human steering torque is reduced from implementing the adaptive control consolidation when the low-maximum-speed autonomy is implemented. Finally, there is an interaction effect between surveillance task urgency, the control consolidation setting, and the autonomy setting ($F(2, 22) = 3.892,\ p = 0.027$). More human steering torque reduction from implementing adaptive control consolidation happens when the surveillance task urgency is low and the low-maximum-speed autonomy is implemented. These results and the corresponding figures when both the control consolidation setting and the autonomy setting are involved are expanded in the next sub-sections (Sec. 5.2.2.2 and Sec. 5.2.2.3) in more detail.

Emergency Maneuvering Performance

The autonomy setting significantly impacts emergency maneuvering performance.

The deviation from the centerline under emergency has a significant difference when the autonomy settings are different ($F(2, 22) = 30.734,\ p < 0.001$), which is shown in Fig. 5.14b. The low-maximum-speed autonomy achieves the lowest deviation from the centerline under emergency. When adaptive autonomy is implemented, the deviation from the centerline under emergency is at a medium level. The emergency maneuvering performance is the worst when the high-maximum-speed autonomy is implemented. The pairwise comparison shows that less deviation is achieved when the low-maximum-speed autonomy is implemented compared to the other two autonomy settings with $p < 0.001$, respectively. The deviation is significantly lower when the adaptive autonomy is implemented than the deviation when the high-maximum-speed autonomy is implemented ($p = 0.001$).

Impacts from surveillance task urgency ($F(1, 23) = .990,\ p = .330$) and control consolidation setting ($F(1, 23) = 3.102,\ p = .091$) are not significant, which are shown in Fig. 5.14a and Fig. 5.14c, respectively.

In addition, there is an interaction effect between the surveillance task urgency and

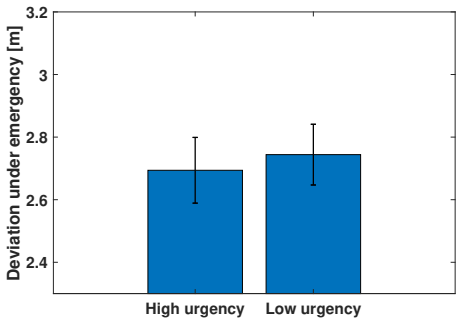

(a) Relationship between surveillance task urgency and emergency maneuvering performance in Experiment 5

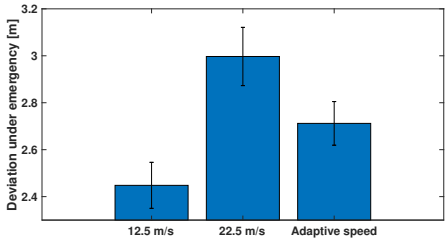

(b) Relationship between autonomy settings and emergency maneuvering performance in Experiment 5. The autonomy setting in the figure is represented by the maximum speed limit.

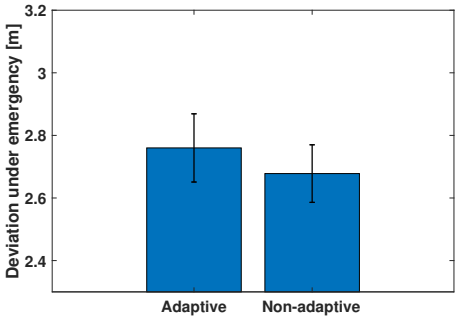

(c) Relationship between control consolidation settings and emergency maneuvering performance in Experiment 5

Figure 5.14: Relationship between emergency maneuvering performance and different independent variables in Experiment 5.

the autonomy setting ($F(2, 22) = 6.416,\ p = .003$), as shown in Fig. 5.16. Specifically, the deviation from the centerline under emergency is increased when the surveillance task urgency is high and the high-maximum-speed autonomy is implemented. The adaptive autonomy reduces the deviation when switching to surveillance tasks whose urgency is higher. There is no significant interaction effect between surveillance task urgency and control consolidation settings ($F(1, 23) = .055,\ p = .816$), as shown in Fig. 5.15.

Surveillance Task Performance

Both surveillance task urgency and autonomy setting have a significant impact on the surveillance task performance.

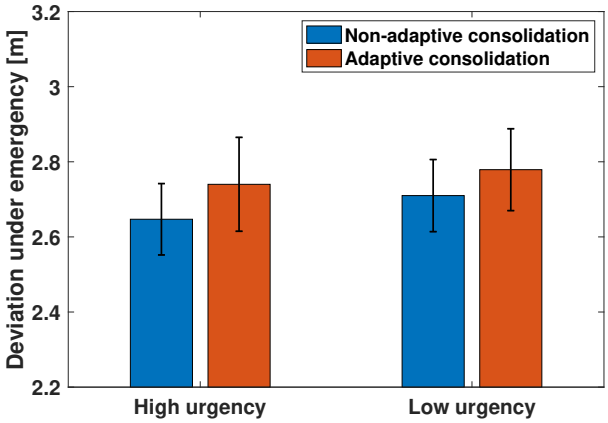

Figure 5.15: Relationship between emergency maneuvering performance and different control consolidation settings in Experiment 5 under different surveillance task urgencies

The detection accuracy is worse when the surveillance task urgency is high ($F(1, 23) = 8.619,\ p = .007$), as shown in Fig. 5.17a.

The detection accuracy is also significantly impacted when the autonomy setting is different ($F(2, 22) = 3.702,\ p = .032$), as shown in Fig. 5.17b. The detection accuracy is the lowest when the high-maximum-speed autonomy is implemented. Participants achieve the highest detection accuracy when adaptive autonomy is implemented. The detection accuracy is at a medium level when the low-maximum-speed autonomy is implemented. For the pairwise comparison, there is a significant difference between the detection accuracy in the cases when the adaptive autonomy is used and when the high-maximum-speed autonomy is implemented ($p = 0.004$). The difference in the detection accuracy is not significant between the adaptive autonomy cases and cases when the low-maximum-speed autonomy is implemented ($p = 0.569$). The difference between the low-maximum-speed autonomy and the high-maximum-speed autonomy is also not significant ($p = 0.112$).

The impact of the control consolidation setting on the surveillance task performance is not significant ($F(1, 23) = 1.122,\ p = .301$), as shown in Fig. 5.17c.

In addition, there is an interaction effect between the surveillance task urgency and autonomy setting ($F(2, 22) = 5.810,\ p = .006$), as shown in Fig. 5.19. Results show

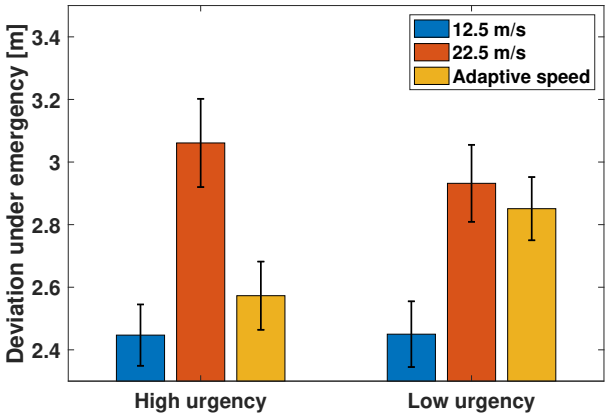

Figure 5.16: Relationship between emergency maneuvering performance and different autonomy settings in Experiment 5 under different surveillance task urgencies

that the detection accuracy in the cases with low-maximum-speed autonomy is more robust to the different surveillance task urgencies than in the other two autonomy settings. There is no significant interaction effect between surveillance task urgency and control consolidation settings ($F(1, 23) = 0.112,\ p = .741$), as shown in Fig. 5.18.

Time to Finish the Mission

The surveillance task urgency, the control consolidation setting, and the autonomy setting all have a significant impact on the time to finish the task.

It takes more time to finish the mission when the surveillance task is more urgent ($F(1, 23) = 206.249,\ p < .001$), which is shown in Fig. 5.20a.

The duration is slightly shorter when the adaptive control consolidation is used ($F(1, 23) = 8.732,\ p = .007$), as shown in Fig. 5.20c.

Autonomy setting significantly impacts the mission duration ($F(2, 22) = 4994.984$, $p < .001$), as shown in Fig. 5.20b. The mission duration is shortest when the high-maximum-speed autonomy is implemented. At the same time, the mission time is longest when the low-maximum-speed autonomy is implemented. The time to finish the mission is at a medium level when adaptive autonomy is utilized. For the pairwise comparison, every pair of autonomy settings significantly differ from each other ($p < .001$).

In addition, there are several significant interaction effects. Firstly, there is an

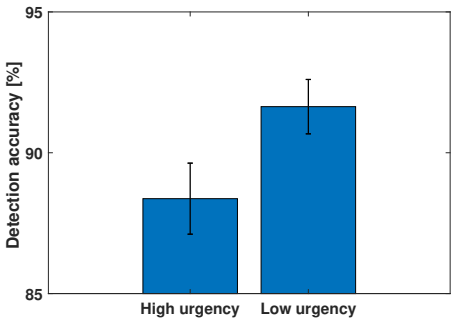

(a) Relationship between surveillance task urgency and surveillance task performance in Experiment 5

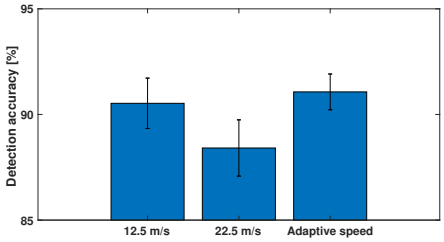

(b) Relationship between autonomy settings and surveillance task performance in Experiment 5. The autonomy setting in the figure is represented by the maximum speed limit.

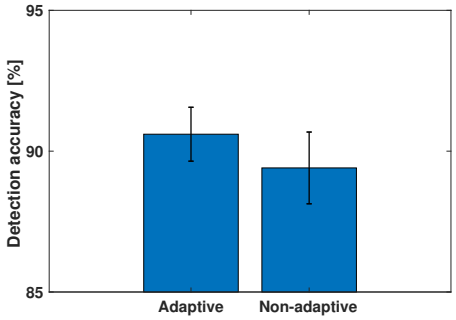

(c) Relationship between control consolidation settings and surveillance task performance in Experiment 5

Figure 5.17: Relationship between surveillance task performance and different independent variables in Experiment 5.

interaction effect between the surveillance task urgency and the control consolidation settings ($F(1, 23) = 6.636,\ p = .017$), as shown in Fig. 5.21. The adaptive control consolidation saves more mission time when the surveillance task is less urgent. Secondly, there is an interaction effect between the surveillance task urgency and the autonomy setting ($F(2, 22) = 202.544,\quad p < .001$), as shown in Fig. 5.22. When adaptive autonomy is implemented, the time to finish the mission increases with a higher surveillance task urgency. Thirdly, there is an interaction effect between the consolidation setting and the autonomy setting ($F(2, 22) = 8.449,\quad p < .001$). The adaptive control consolidation reduces mission time when the adaptive autonomy is implemented. Finally, there is an interaction effect between the surveillance task urgency, the control consolidation setting, and the autonomy setting ($F(2, 22) = 6.156,$

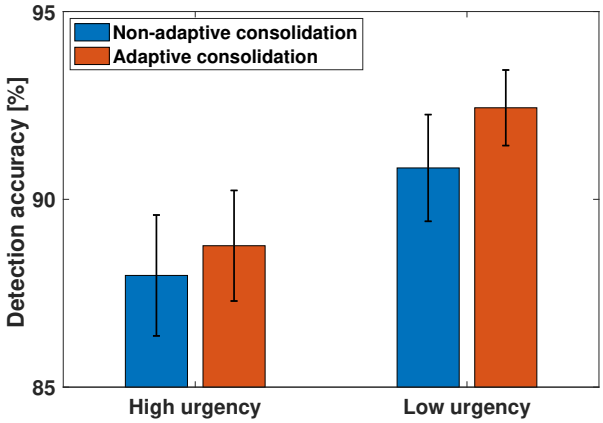

Figure 5.18: Relationship between surveillance task performance and different control consolidation settings in Experiment 5 under different surveillance task urgencies

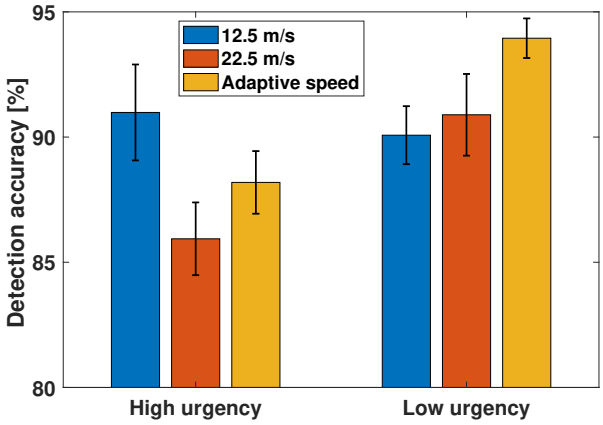

Figure 5.19: Relationship between surveillance task performance and different autonomy settings in Experiment 5 under different surveillance task urgencies

$p = .004$). The adaptive control consolidation saves more mission time when the surveillance task urgency is low and the adaptive autonomy is implemented. These results and the corresponding figures when both the control consolidation setting and the autonomy setting are involved are expanded in the next sub-sections (Sec. 5.2.2.2 and Sec. 5.2.2.3) in more detail.

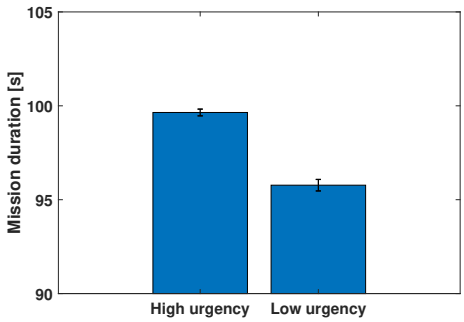

(a) Relationship between surveillance task urgency and mission duration in Experiment 5

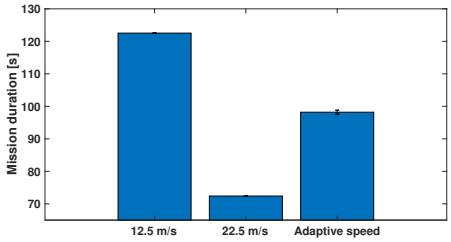

(b) Relationship between autonomy settings and mission duration in Experiment 5. The autonomy setting in the figure is represented by the maximum speed limit.

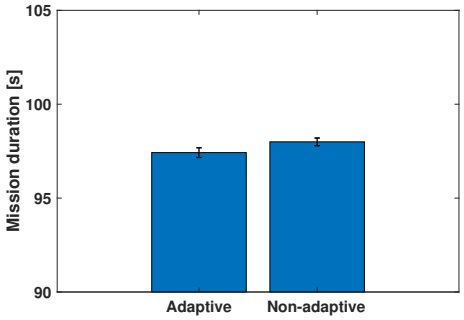

(c) Relationship between control consolidation settings and mission duration in Experiment 5

Figure 5.20: Relationship between mission duration and different independent variables in Experiment 5.

5.2.2.2 The Effect of Different Control Consolidations When Adaptive Autonomy Is Implemented

This sub-section aims to find the performance of different control consolidations when the adaptive autonomy is implemented. In addition, the baseline cases (i.e., the non-adaptive control consolidation and the non-adaptive autonomy) with different maximum speed limits are also included in this analysis to find out the benefit when both adaptation schemes are applied. An ANOVA analysis is conducted separately, whose data are extracted from Table 5.2. There are two independent variables: the surveillance task urgency and the schemes to compare. There are four schemes to compare in this analysis: the adaptive control consolidation and adaptive autonomy, the non-adaptive control consolidation and adaptive autonomy, the baseline scheme with

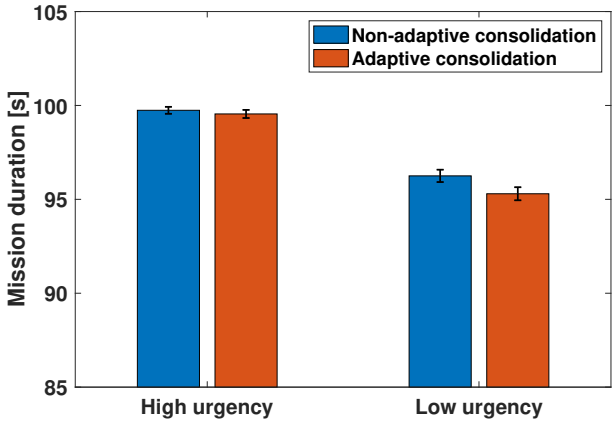

Figure 5.21: Relationship between mission duration and different control consolidation settings in Experiment 5 under different surveillance task urgencies

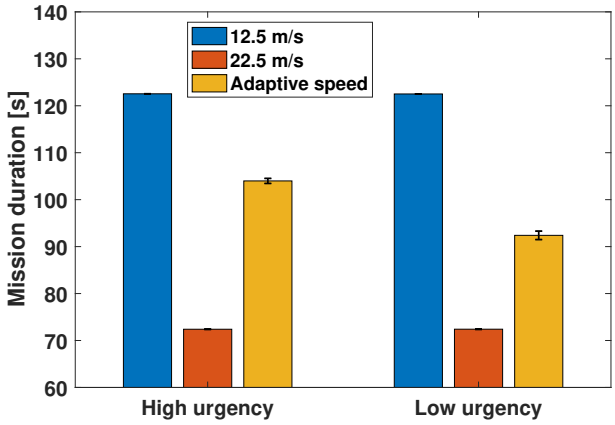

Figure 5.22: Relationship between mission duration and different autonomy settings in Experiment 5 under different surveillance task urgencies

low-maximum-speed autonomy, and the baseline scheme with the high-maximum-speed autonomy. The latter two are called the low-speed baseline and the high-speed baseline in short. Since the main effect of the surveillance task urgency is explored in the previous sub-section (Sec. 5.2.2.1), in this sub-section, only plots showing the impact of different schemes and the interaction effect between the scheme and the surveillance task urgency are demonstrated.

Participants' Self-reported Workload

There is a significant difference in participants' self-reported workload when different surveillance task urgencies are presented ($F(1, 23) = 26.416,\ p < 0.001$). An

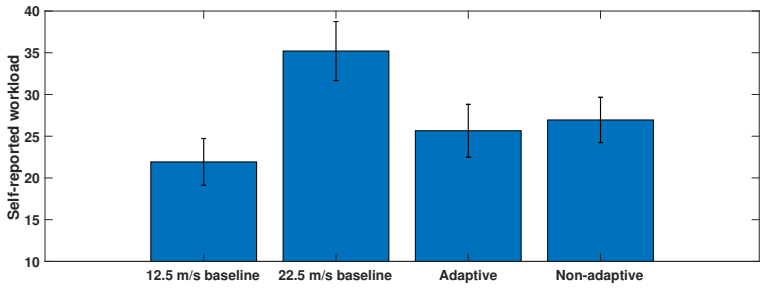

Figure 5.23: Relationship between self-reported workload and different schemes in Experiment 5. "Adaptive" represents the adaptive control consolidation with adaptive autonomy, while "Non-adaptive" means the non-adaptive control consolidation with adaptive autonomy.

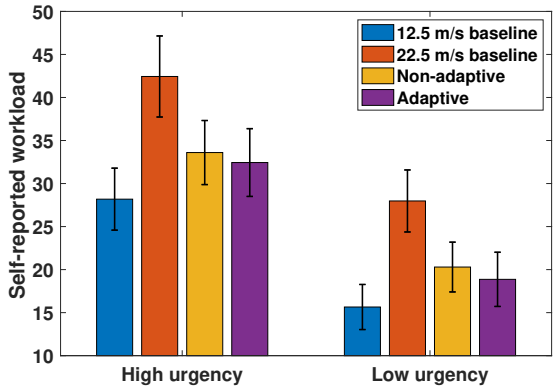

Figure 5.24: Relationship between self-reported workload and different schemes in Experiment 5 when different surveillance task urgency is presented. "Adaptive" represents the adaptive control consolidation with adaptive autonomy, while "Non-adaptive" means the non-adaptive control consolidation with adaptive autonomy.

urgent surveillance task leads to a higher self-reported workload. A significant difference is also observed when different schemes are used ($F(3, 21) = 13.012,\ p < 0.001$), which is shown in Fig. 5.23. The self-reported workload in the low-speed baseline scheme, two adaptive schemes, and high-speed baseline scheme is in ascending order. No significant interaction effect is found between urgency and scheme ($F(3, 21) = 0.071,\ p = 0.975$), as shown in Fig. 5.24.

In terms of the pairwise comparison of schemes, there is a difference between the two baseline schemes with different maximum speed limits ($p < 0.001$). The difference between the baseline schemes and the schemes with adaptive autonomy is also significant. Specifically, the differences between the low-speed baseline scheme

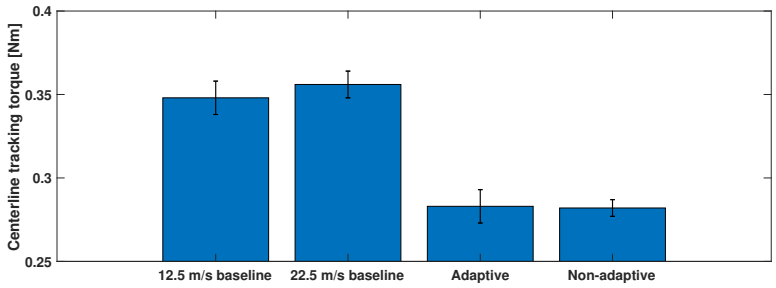

Figure 5.25: Relationship between steering control effort in the lane-keeping stage and different schemes in Experiment 5. "Adaptive" represents the adaptive control consolidation with adaptive autonomy, while "Non-adaptive" means the non-adaptive control consolidation with adaptive autonomy.

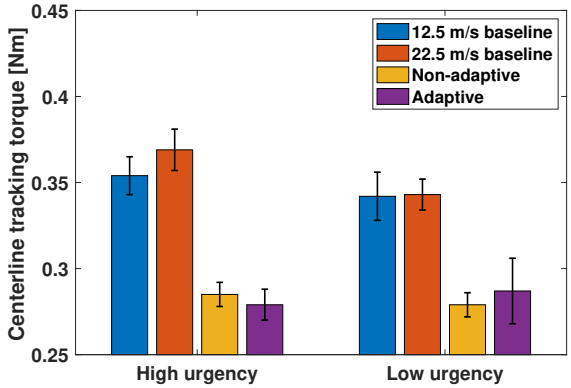

Figure 5.26: Relationship between steering control effort in the lane-keeping stage and different schemes in Experiment 5 when different surveillance task urgency is presented. "Adaptive" represents the adaptive control consolidation with adaptive autonomy, while "Non-adaptive" means the non-adaptive control consolidation with adaptive autonomy.

and adaptive cases ($p = 0.038$ for the one with non-adaptive control consolidation and $p = 0.050$ for the one with adaptive control consolidation) are significant. In addition, the differences between the high-speed baseline scheme and adaptive cases ($p < 0.001$ for both cases) are significant. There is no significant difference between the schemes with the adaptive autonomy but with different control consolidation settings ($p = 0.541$).

Participants' Steering Control Effort During Lane Keeping

There is a significant difference in participants' steering control effect in the lane-keeping stage when different schemes are used ($F(3, 21) = 23.109,\ p < 0.001$), which

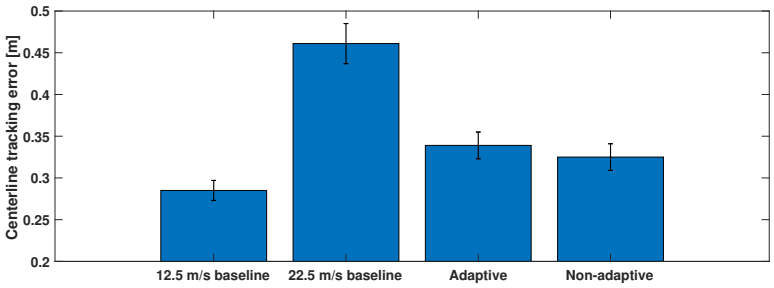

Figure 5.27: Relationship between centerline tracking error in the lane-keeping stage and different schemes in Experiment 5. "Adaptive" is the adaptive control consolidation with adaptive autonomy, while "Non-adaptive" is the non-adaptive control consolidation with adaptive autonomy.

is shown in Fig. 5.25. Schemes with adaptive autonomy have a lower steering control effort compared to baseline schemes. No significant effect is found when different surveillance task urgencies are presented ($F(1, 23) = 1.703,\ p = 0.205$). In addition, no interaction effect is found ($F(3, 21) = 0.763,\ p = 0.519$), as shown in Fig. 5.26.

In terms of the pairwise comparison of schemes, there is no significant difference between the two baseline schemes with different maximum speed limits ($p = 0.533$). The difference between the baseline schemes and the schemes with adaptive autonomy is significant ($p < 0.001$ for every pair of a baseline scheme and a scheme with adaptive autonomy). There is no significant difference between the schemes with the adaptive autonomy but with different control consolidation settings ($p = 0.902$).

Driving Task Performance

There is a significant difference in participants' centerline tracking error when different surveillance task urgencies are presented ($F(1, 23) = 30.974,\ p < 0.001$). An urgent surveillance task leads to a higher centerline tracking error during the lane-keeping stage. A significant difference is also observed when different schemes are used ($F(3, 21) = 54.577,\ p < 0.001$), which is shown in Fig. 5.27. The centerline tracking error in the low-speed baseline scheme, two adaptive schemes, and high-speed baseline scheme is in ascending order. In addition, there is an interaction effect between urgency and scheme ($F(3, 21) = 4.686,\ p = 0.005$), as shown in Fig. 5.28. The centerline tracking error increment from switching to an urgent surveillance task

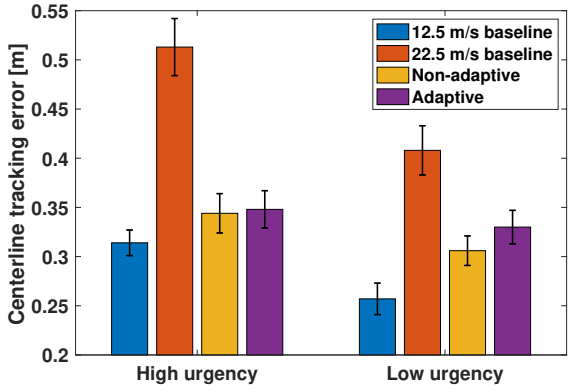

Figure 5.28: Relationship between centerline tracking error in the lane-keeping stage and different schemes in Experiment 5 when different surveillance task urgency is presented. "Adaptive" is the adaptive control consolidation with adaptive autonomy, while "Non-adaptive" is the non-adaptive control consolidation with adaptive autonomy.

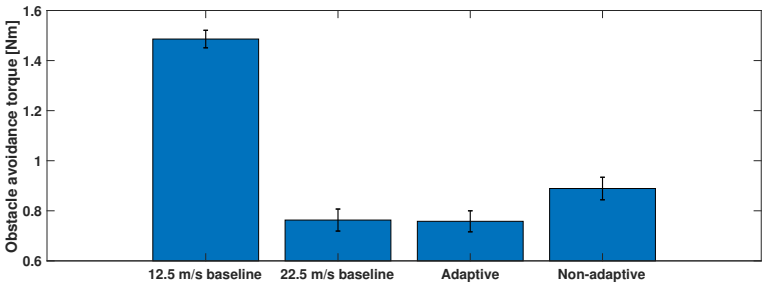

Figure 5.29: Relationship between human steering torque in the obstacle-avoidance stage and different schemes in Experiment 5. "Adaptive" is the adaptive control consolidation with adaptive autonomy, while "Non-adaptive" is the non-adaptive control consolidation with adaptive autonomy.

when the adaptive autonomy is used is less than in other schemes.

In terms of the pairwise comparison of schemes, a significant difference is found between the two baseline schemes with different maximum speed limits ($p < 0.001$). The difference between the baseline schemes and the schemes with adaptive autonomy is also significant ($p < 0.001$ for every pair of a baseline scheme and a scheme with adaptive autonomy). There is no significant difference between the schemes with the adaptive autonomy but with different control consolidation settings ($p = 0.104$).

Participants' Steering Control Effort Under Emergency

There is a significant difference in participants' steering control effort in the

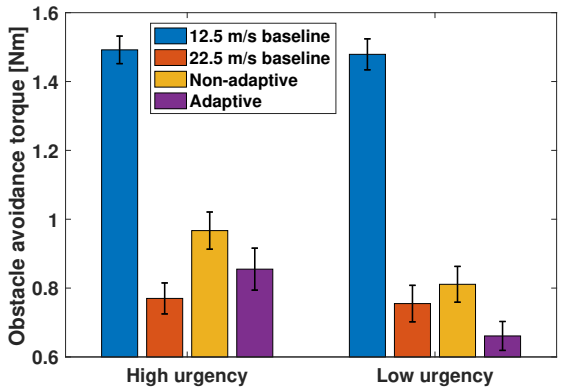

Figure 5.30: Relationship between human steering torque in the obstacle-avoidance stage and different schemes in Experiment 5 when different surveillance task urgency is presented. "Adaptive" is the adaptive control consolidation with adaptive autonomy, while "Non-adaptive" is the non-adaptive control consolidation with adaptive autonomy.

obstacle-avoidance stage when different surveillance task urgencies are presented ($F(1, 23) = 11.064,\ p = 0.003$). An urgent surveillance task leads to a larger human steering torque when subjects avoid obstacles. A significant difference is also observed when different schemes are used ($F(3, 21) = 135.007,\ p < 0.001$), which is shown in Fig. 5.29. In the order of adaptive scheme with adaptive control consolidation, high-speed baseline scheme, adaptive scheme with non-adaptive control consolidation, and low-speed baseline scheme, the human steering torque under emergency is ascending. There is an interaction effect between urgency and scheme ($F(3, 21) = 3.333,\ p = 0.024$), as shown in Fig 5.30. The emergency human steering torque increases when an urgent surveillance task and adaptive schemes are presented.

In terms of the pairwise comparison for difference schemes, there is a significant difference between the low-speed baseline and any other scheme ($p < 0.001$). A significant difference is also observed between the high-speed baseline and the adaptive scheme with non-adaptive control consolidation ($p = 0.013$). The difference between two adaptive schemes with different control consolidation settings is also significant ($p = 0.006$). There is no significant difference between the high-speed baseline and the adaptive scheme with adaptive control consolidation ($p = 0.907$).

Emergency Maneuvering Performance

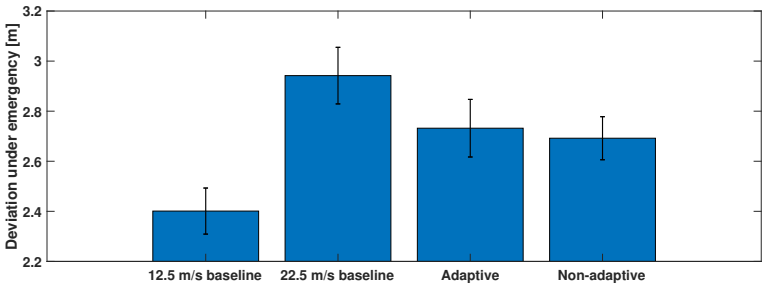

Figure 5.31: Relationship between deviation from the centerline in the obstacle-avoidance stage and different schemes in Experiment 5. "Adaptive" is the adaptive control consolidation with adaptive autonomy, while "Non-adaptive" is the non-adaptive control consolidation with adaptive autonomy.

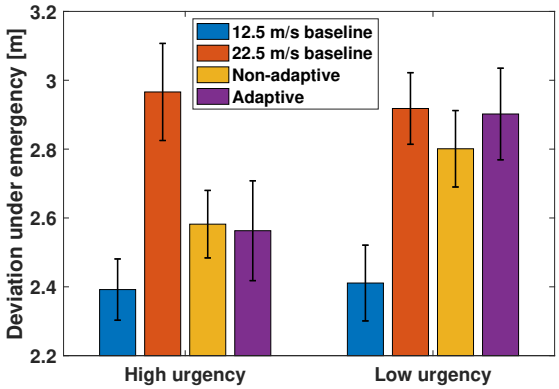

Figure 5.32: Relationship between deviation from the centerline in the obstacle-avoidance stage and different schemes in Experiment 5 when different surveillance task urgency is presented. "Adaptive" is the adaptive control consolidation with adaptive autonomy, while "Non-adaptive" is the non-adaptive control consolidation with adaptive autonomy.

There is a significant difference in deviation from the centerline in the obstacle-avoidance stage when different surveillance task urgencies are presented ($F(1, 23) = 5.497,\ p = 0.028$). An urgent surveillance task leads to a smaller deviation from the centerline when subjects avoid obstacles. A significant difference is also observed when different schemes are used ($F(3, 21) = 16.572,\ p < 0.001$), which is shown in Fig. 5.31. In the low-speed baseline scheme, two adaptive schemes, and the high-speed baseline scheme, the deviation from the centerline is in ascending order. In addition, the interaction effect between urgency and scheme is not significant ($F(3, 21) = 2.262,\ p = 0.089$), as shown in Fig. 5.32.

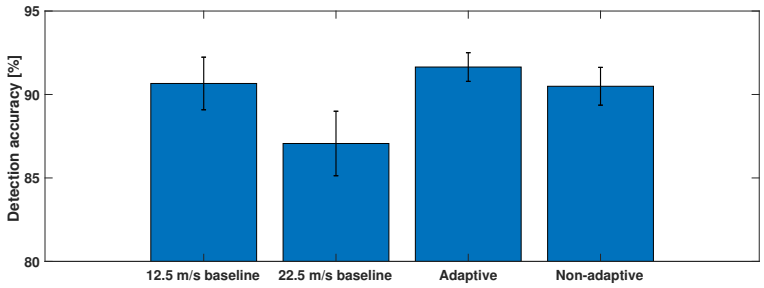

Figure 5.33: Relationship between surveillance task detection accuracy and different schemes in Experiment 5. "Adaptive" is the adaptive control consolidation with adaptive autonomy, while "Non-adaptive" is the non-adaptive control consolidation with adaptive autonomy.

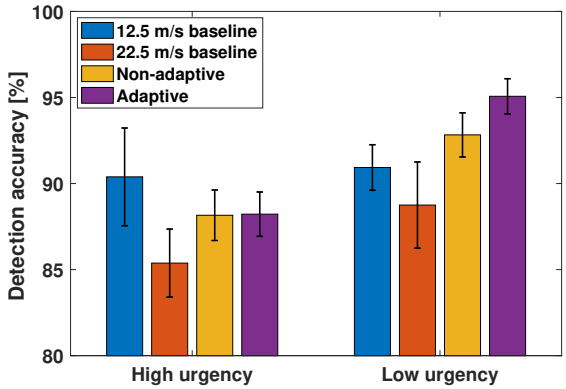

Figure 5.34: Relationship between surveillance task detection accuracy and different schemes in Experiment 5 when different surveillance task urgency is presented. "Adaptive" is the adaptive control consolidation with adaptive autonomy, while "Non-adaptive" is the non-adaptive control consolidation with adaptive autonomy.

In terms of the pairwise comparison for difference schemes, there is a significant difference between the low-speed baseline and any other scheme ($p < 0.001$). Significant differences are observed between the high-speed baseline and the adaptive schemes ($p = 0.002$ compared to the adaptive scheme with non-adaptive control consolidation and $p = 0.048$ compared to the adaptive scheme with adaptive control consolidation). The difference between two adaptive schemes with different control consolidation settings is not significant ($p = 0.631$).

Surveillance Task Performance

There is a significant difference in surveillance task accuracy when different surveillance task urgencies are presented ($F(1, 23) = 8.416,\ p = 0.008$). An urgent surveil-

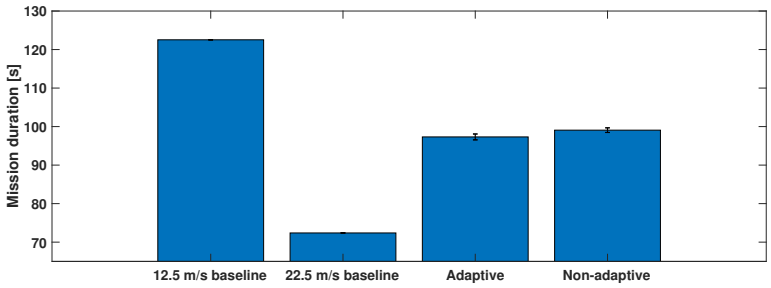

Figure 5.35: Relationship between time to finish the mission and different schemes in Experiment 5. "Adaptive" is the adaptive control consolidation with adaptive autonomy, while "Non-adaptive" is the non-adaptive control consolidation with adaptive autonomy.

lance task leads to a worse surveillance task performance. There is also a significant difference when different schemes are used ($F(3, 21) = 3.228,\ p = 0.028$), which is shown in Fig. 5.33. The surveillance task accuracy of the high-speed baseline scheme is significantly lower than the other schemes. In addition, no significant interaction effect is found between urgency and scheme ($F(3, 21) = 1.610,\ p = 0.195$), as shown in Fig. 5.34.

In terms of the pairwise comparison for difference schemes, no significant difference is found between the low-speed baseline and any other scheme ($p = 0.091$ compared to the high-speed baseline scheme; $p = 0.908$ compared to the adaptive scheme with non-adaptive control consolidation; $p = 0.545$ compared to the adaptive scheme with adaptive control consolidation). Significant differences are observed between the high-speed baseline and the adaptive schemes ($p = 0.015$ compared to the adaptive scheme with non-adaptive control consolidation and $p = 0.018$ compared to the adaptive scheme with adaptive control consolidation). The difference between two adaptive schemes with different control consolidation settings is not significant ($p = 0.297$).

Time to Finish the Mission

There is a significant difference in mission time when different surveillance task urgencies are presented ($F(1, 23) = 204.162,\ p < 0.001$). An urgent surveillance task leads to a longer mission duration. There is also a significant difference when different schemes are used ($F(3, 21) = 2259.019,\ p < 0.001$), which is shown in Fig. 5.35.

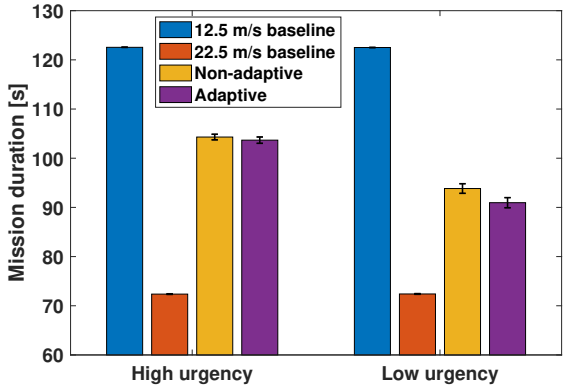

Figure 5.36: Relationship between time to finish the mission and different schemes in Experiment 5 when different surveillance task urgency is presented. "Adaptive" is the adaptive control consolidation with adaptive autonomy, while "Non-adaptive" is the non-adaptive control consolidation with adaptive autonomy.

The mission duration is in ascending order in the high-speed baseline scheme, two adaptive schemes, and the low-speed baseline scheme. The adaptive scheme with the adaptive control consolidation has shorter mission duration than the adaptive scheme with non-adaptive control consolidation. In addition, a significant interaction effect is found between urgency and scheme ($F(3, 21) = 129.561, p < 0.001$), as shown in Fig. 5.36. The mission duration increases when an urgent surveillance task and adaptive schemes are used.

In terms of the pairwise comparison for difference schemes, a significant difference is found in the mission duration between any two different schemes ($p = 0.007$ between two adaptive schemes and $p < 0.001$ between any other combination of the schemes).

5.2.2.3 The Effect of Different Autonomy Settings When Adaptive Control Consolidation Is Implemented

This sub-section aims to find the performance difference between adaptive autonomy and non-adaptive autonomy with different maximum speed limits when the adaptive control consolidation is implemented. In addition, the baseline cases (i.e., the non-adaptive control consolidation and the non-adaptive autonomy) with different maximum speed limits are also included in this analysis as a benchmark. An ANOVA

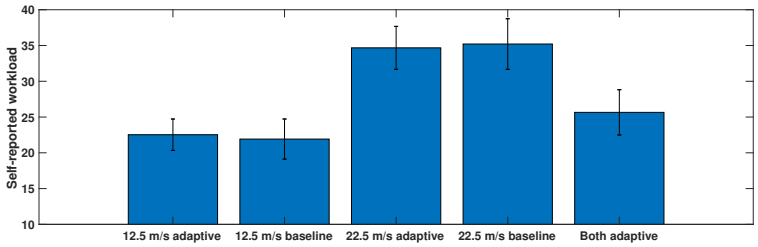

Figure 5.37: Relationship between self-reported workload and different schemes in Experiment 5. "12.5 m/s adaptive" and "22.5 m/s adaptive" represents the adaptive control consolidation with non-adaptive autonomy whose maximum speed limit is 12.5 m/s and 22.5 m/s, respectively.

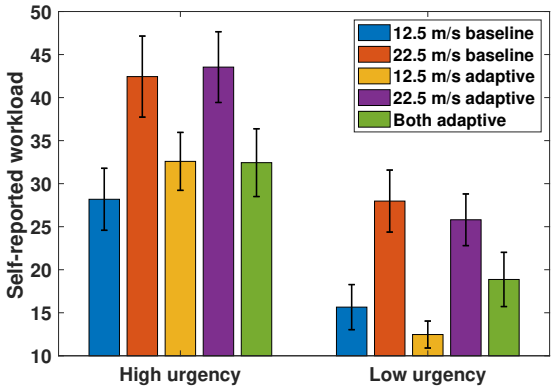

Figure 5.38: Relationship between self-reported workload and different schemes in Experiment 5 when different surveillance task urgency is presented. "12.5 m/s adaptive" and "22.5 m/s adaptive" represents the adaptive control consolidation with non-adaptive autonomy whose maximum speed limit is 12.5 m/s and 22.5 m/s, respectively.

analysis is conducted separately, whose data are extracted from Table 5.2. There are two independent variables: the surveillance task urgency and the schemes to compare. In this subsection, there are five different schemes to compare: the adaptive control consolidation with adaptive autonomy, the adaptive control consolidation with the low-speed autonomy, the adaptive control consolidation with the high-speed autonomy, the baseline with the low-speed autonomy, and the baseline with the high-speed autonomy.

Participants' Self-reported Workload

There is a significant difference in participants' self-reported workload when different surveillance task urgencies are presented ($F(1, 23) = 51.660,\ p < 0.001$). An

urgent surveillance task leads to a higher self-reported workload. A significant difference is also observed when different schemes are used ($F(4, 20) = 15.933,\ p < 0.001$), which is shown in Fig. 5.37. The self-reported workload values in the low-maximum-speed baseline scheme, adaptive control consolidation with the low-maximum-speed autonomy, adaptive control consolidation with adaptive autonomy, adaptive control consolidation with the high-maximum-speed autonomy, and high-maximum-speed baseline scheme are in ascending order. In addition, no significant interaction effect is found between urgency and scheme ($F(4, 20) = 1.005,\ p = 0.409$), as shown in Fig. 5.38.

In terms of the pairwise comparison for difference schemes, there is a difference between the low-maximum-speed autonomy schemes and high-maximum-speed autonomy schemes regardless of the control consolidation implemented ($p < 0.001$ for each pair of low-maximum-speed autonomy scheme and high-maximum-speed autonomy scheme). When the schemes both use the low-maximum-speed autonomy, the difference between two control consolidations is not significant ($p = 0.741$). When the schemes both use the high-maximum-speed autonomy, the difference between two control consolidations is also not significant ($p = 0.786$). The adaptive control consolidation with adaptive autonomy has a significant difference in self-reported workload with both schemes, including both control consolidation settings, when the high-maximum-speed autonomy is implemented ($p < 0.001$). The difference between adaptive control consolidation with adaptive autonomy and the low-maximum-speed baseline scheme is marginally significant ($p = 0.050$). In contrast, the difference is non-significant when compared with the adaptive control consolidation with the low-maximum-speed autonomy ($p = 0.104$).

Participants' Steering Control Effort During Lane Keeping

There is a significant difference in participants' steering control effect in the lane-keeping stage when different schemes are used ($F(4, 20) = 11.671,\ p < 0.001$), which is shown in Fig. 5.39. Schemes with adaptive control consolidation have a lower human steering control effort compared to baseline schemes. The adaptive control consolidation with adaptive autonomy achieves the smallest steering control effort.

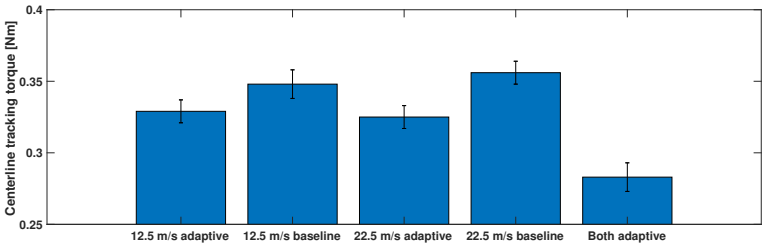

Figure 5.39: Relationship between steering control effort in the lane-keeping stage and different schemes in Experiment 5. "12.5 m/s adaptive" and "22.5 m/s adaptive" represents the adaptive control consolidation with non-adaptive autonomy whose maximum speed limit is 12.5 m/s and 22.5 m/s, respectively.

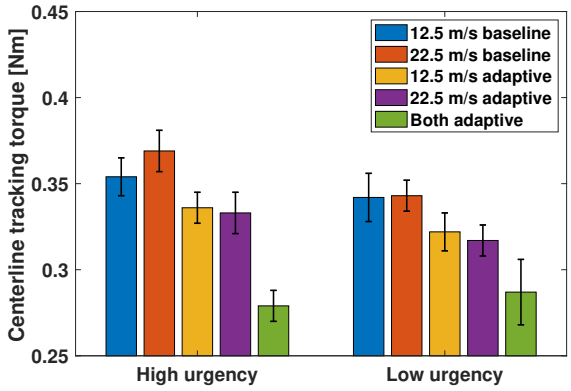

Figure 5.40: Relationship between steering control effort in the lane-keeping stage and different schemes in Experiment 5 when different surveillance task urgency is presented. "12.5 m/s adaptive" and "22.5 m/s adaptive" represents the adaptive control consolidation with non-adaptive autonomy whose maximum speed limit is 12.5 m/s and 22.5 m/s, respectively.

No significant effect is found when different surveillance task urgencies are presented ($F(1, 23) = 2.832,\ p = 0.106$). In addition, no significant interaction effect is observed ($F(4, 20) = 0.669,\ p = 0.615$), as shown in Fig. 5.40.

In terms of the pairwise comparison for difference schemes, there is a difference between two control consolidations when the low-maximum-speed autonomy is implemented ($p = 0.036$). There is also a difference between two control consolidations when the high-maximum-speed autonomy is implemented ($p = 0.001$). When using the same control consolidation, the difference between the low-maximum-speed autonomy and the high-maximum-speed autonomy is not significant ($p = 0.533$ for the non-adaptive control consolidation and $p = 0.748$ for the adaptive control con-

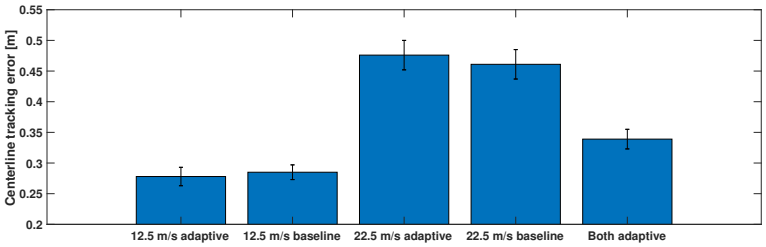

Figure 5.41: Relationship between driving performance in the lane-keeping stage and different schemes in Experiment 5. "12.5 m/s adaptive" and "22.5 m/s adaptive" represents the adaptive control consolidation with non-adaptive autonomy whose maximum speed limit is 12.5 m/s and 22.5 m/s, respectively.

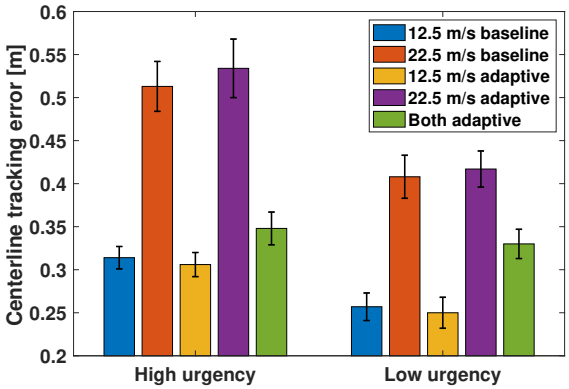

Figure 5.42: Relationship between driving performance in the lane-keeping stage and different schemes in Experiment 5 when different surveillance task urgency is presented. "12.5 m/s adaptive" and "22.5 m/s adaptive" represents the adaptive control consolidation with non-adaptive autonomy whose maximum speed limit is 12.5 m/s and 22.5 m/s, respectively.

solidation). The adaptive control consolidation with adaptive autonomy significantly differs from any other scheme ($p < 0.001$).

Driving Task Performance

There is a significant difference in participants' centerline tracking error in the lane-keeping stage when different surveillance task urgencies are presented ($F(1, 23) = 44.679,\ p < 0.001$). An urgent surveillance task leads to worse driving performance. A significant difference is also observed when different schemes are used ($F(4, 20) = 69.526,\ p < 0.001$), which is shown in Fig. 5.41. The centerline tracking error in schemes with the low-maximum-speed autonomy, adaptive control consolidation with adaptive autonomy, and schemes with the high-maximum-speed autonomy are in

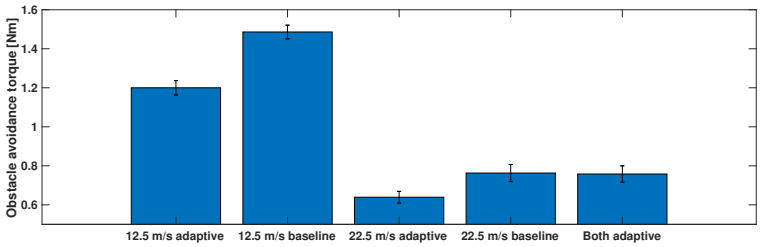

Figure 5.43: Relationship between steering control effort in the obstacle-avoidance stage and different schemes in Experiment 5. "12.5 m/s adaptive" and "22.5 m/s adaptive" represents the adaptive control consolidation with non-adaptive autonomy whose maximum speed limit is 12.5 m/s and 22.5 m/s, respectively.

ascending order. In addition, a significant interaction effect is found between urgency and scheme ($F(4, 20) = 4.369,\ p = 0.003$), as shown in Fig. 5.42. The centerline tracking error increment in the adaptive control consolidation with adaptive autonomy when switching to an urgent surveillance task is less than in other schemes.

In terms of the pairwise comparison for difference schemes, a significant difference is found between two baseline schemes with different maximum speed limits ($p < 0.001$). There is also a significant difference between two schemes with adaptive control consolidation while the autonomy has different maximum speed limits ($p < 0.001$). When using the same autonomy with a fixed maximum speed (i.e., both using the low-maximum-speed autonomy or the high-maximum-speed autonomy), the difference in implementing two different control consolidations is not significant ($p = 0.373$ for the low-maximum-speed autonomy and $p = 0.252$ for the high-maximum-speed autonomy). The adaptive control consolidation with adaptive autonomy significantly differs from any other scheme ($p < 0.001$).

Participants' Steering Control Effort Under Emergency

There is a significant difference in participants' steering control effort in the obstacle-avoidance stage when different surveillance task urgencies are presented ($F(1, 23) = 46.501,\ p < 0.001$). An urgent surveillance task leads to a larger human steering torque when subjects avoid obstacles. A significant difference is also observed when different schemes are used ($F(4, 20) = 181.225,\ p < 0.001$), which is shown in Fig. 5.43. There are two major observations. On the one hand, schemes with adap-

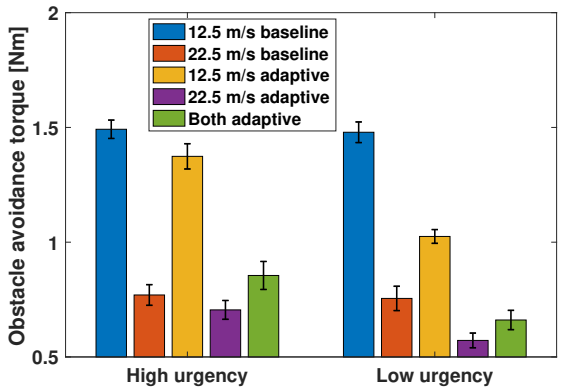

Figure 5.44: Relationship between steering control effort in the obstacle-avoidance stage and different schemes in Experiment 5 when different surveillance task urgency is presented. "12.5 m/s adaptive" and "22.5 m/s adaptive" represents the adaptive control consolidation with non-adaptive autonomy whose maximum speed limit is 12.5 m/s and 22.5 m/s, respectively.

tive control consolidation have less emergency human steering torque. On the other hand, the steering control effort during obstacle avoidance is in ascending order in schemes with the high-maximum-speed autonomy, the adaptive autonomy schemes, and schemes with the low-maximum-speed autonomy. In addition, there is an interaction effect between urgency and scheme ($F(4, 20) = 7.737,\ p < 0.001$), as shown in Fig. 5.44. The emergency torque drops more when a less urgent surveillance task and adaptive control consolidations are presented.

In terms of the pairwise comparison for difference schemes, a significant difference is found between two baseline schemes with different maximum speed limits ($p < 0.001$). There is also a significant difference between two schemes with adaptive control consolidation, while their autonomy has different maximum speed limits ($p < 0.001$). When using the same autonomy with a fixed maximum speed (i.e., both using the low-maximum-speed autonomy or the high-maximum-speed autonomy), the difference in different control consolidations is significant as well ($p < 0.001$). The adaptive control consolidation with adaptive autonomy significantly differs from other schemes with the low-maximum-speed autonomy ($p < 0.001$). The difference in the emergency human steering effort between the scheme using adaptive control consolidation with adaptive autonomy and the scheme using adaptive control consoli-

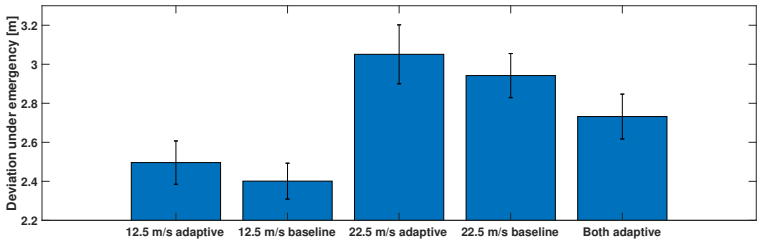

Figure 5.45: Relationship between emergency maneuvering performance and different schemes in Experiment 5. "12.5 m/s adaptive" and "22.5 m/s adaptive" represents the adaptive control consolidation with non-adaptive autonomy whose maximum speed limit is 12.5 m/s and 22.5 m/s, respectively.

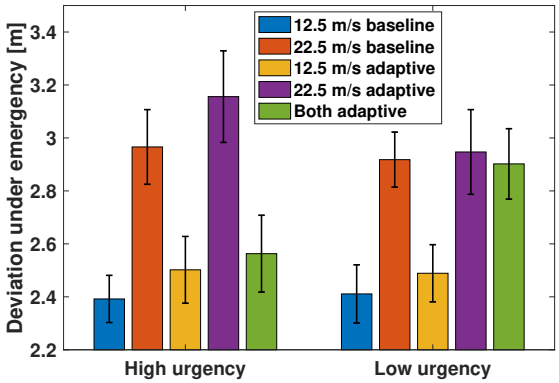

Figure 5.46: Relationship between emergency maneuvering performance and different schemes in Experiment 5 when different surveillance task urgency is presented. "12.5 m/s adaptive" and "22.5 m/s adaptive" represents the adaptive control consolidation with non-adaptive autonomy whose maximum speed limit is 12.5 m/s and 22.5 m/s, respectively.

dation with the high-maximum-speed autonomy is also significant ($p = 0.005$). However, the difference between adaptive control consolidation with adaptive autonomy and the baseline scheme with the high-maximum-speed autonomy is not significant ($p = 0.907$).

Emergency Maneuvering Performance

A significant difference is observed when different schemes are used ($F(4, 20) = 18.109,\ p < 0.001$), which is shown in Fig. 5.45. In schemes with the low-maximum-speed autonomy, the scheme with adaptation at both levels, and schemes with the high-maximum-speed autonomy, the deviation from the centerline is in ascending order. No significant difference in deviation from the centerline in the obstacle-

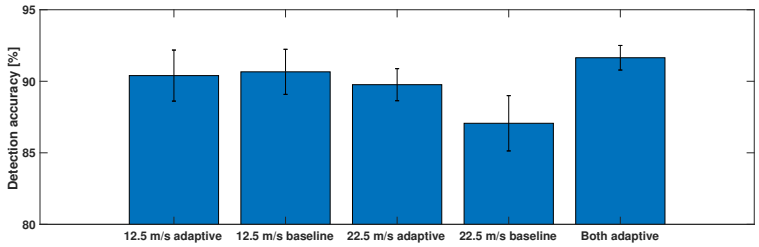

Figure 5.47: Relationship between detection accuracy and different schemes in Experiment 5. "12.5 m/s adaptive" and "22.5 m/s adaptive" represents the adaptive control consolidation with non-adaptive autonomy whose maximum speed limit is 12.5 m/s and 22.5 m/s, respectively.

avoidance stage when different surveillance task urgencies are presented ($F(1, 23) = 0.097,\ p = 0.758$). In addition, there is an interaction effect between urgency and scheme ($F(4, 20) = 3.193,\ p = 0.017$), as shown in Fig. 5.46. The deviation from the centerline drops significantly when an urgent surveillance task and the adaptive control consolidation with adaptive autonomy are presented.

In terms of the pairwise comparison for difference schemes, there is a significant difference between the low-maximum-speed baseline and the high-maximum-speed baseline ($p < 0.001$). There is also a significant difference between the adaptive control consolidation with low-maximum-speed autonomy and adaptive control consolidation with high-maximum-speed autonomy ($p < 0.001$). The difference between two control consolidation settings with the same autonomy setting is not significant ($p = 0.099$ for the low-maximum-speed autonomy and $p = 0.279$ for the high-maximum-speed autonomy). The adaptive control consolidation with adaptive autonomy differs from any other scheme significantly ($p = 0.001$ for the low-maximum-speed baseline, $p = 0.048$ for the high-maximum-speed baseline, $p = 0.034$ for the adaptive control consolidation and low-maximum-speed autonomy, and $p = 0.014$ for the adaptive control consolidation and high-maximum-speed autonomy).

Surveillance Task Performance

The results show a significant difference in surveillance task accuracy when different surveillance task urgencies are presented ($F(1, 23) = 5.985,\ p = 0.022$). An urgent surveillance task leads to a worse surveillance task performance. No signifi-

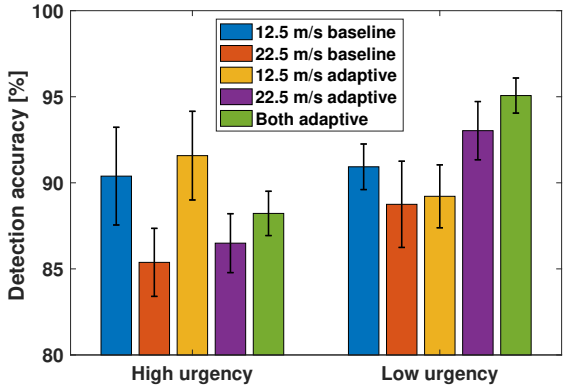

Figure 5.48: Relationship between detection accuracy and different schemes in Experiment 5 when different surveillance task urgency is presented. "12.5 m/s adaptive" and "22.5 m/s adaptive" represents the adaptive control consolidation with non-adaptive autonomy whose maximum speed limit is 12.5 m/s and 22.5 m/s, respectively.

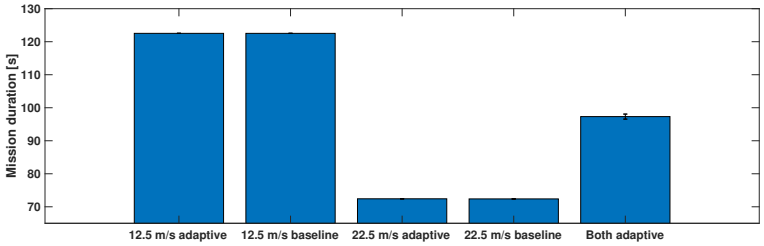

Figure 5.49: Relationship between mission duration and different schemes in Experiment 5. "12.5 m/s adaptive" and "22.5 m/s adaptive" represents the adaptive control consolidation with non-adaptive autonomy whose maximum speed limit is 12.5 m/s and 22.5 m/s, respectively.

cant difference when different schemes are used ($F(4, 20) = 1.794,\ p = 0.137$), which is shown in Fig. 5.47. A significant interaction effect is found between urgency and scheme ($F(4, 20) = 2.610,\ p = 0.041$), as shown in Fig. 5.48. The adaptive control consolidation with adaptive autonomy can achieve a better surveillance task detection accuracy when the surveillance task is less urgent than other schemes.

Time to Finish the Mission

There is a significant difference in mission time when different surveillance task urgencies are presented ($F(1, 23) = 256.411,\ p < 0.001$). An urgent surveillance task leads to a longer mission duration. There is also a significant difference when different schemes are used ($F(4, 20) = 5484.639,\ p < 0.001$), which is shown in Fig. 5.49.

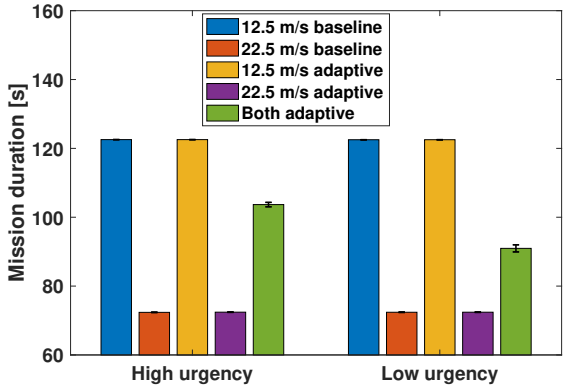

Figure 5.50: Relationship between mission duration and different schemes in Experiment 5 when different surveillance task urgency is presented. "12.5 m/s adaptive" and "22.5 m/s adaptive" represents the adaptive control consolidation with non-adaptive autonomy whose maximum speed limit is 12.5 m/s and 22.5 m/s, respectively.

The mission duration is in ascending order in the schemes with the high-maximum-speed autonomy, adaptive control consolidation with adaptive autonomy, and schemes with the low-maximum-speed autonomy. In addition, a significant interaction effect is found between urgency and scheme ($F(4, 20) = 252.047,\ p < 0.001$), as shown in Fig. 5.50. The mission duration increases when an urgent surveillance task and adaptive autonomy are used.

In terms of the pairwise comparison for difference schemes, when using autonomy whose maximum speed limit is the same, no significant difference between different control consolidations is found ($p = 0.814$ when the low-maximum-speed autonomy is used, and $p = 0.571$ when the high-maximum-speed autonomy is used). Compared with other cases, switching to adaptive autonomy will significantly change the mission duration ($p < 0.001$).

5.2.3 Discussion

5.2.3.1 Control Consolidation Settings: Main Effect

Participants' Control Effort During Lane Keeping

The control effort in the lane-keeping stage is reduced when the adaptive control consolidation is implemented. It can be seen as a result of the design principle. The

assistance level β is smaller than one when the human operator wants to intervene, and the control effort will drop correspondingly.

However, this reduction of the control effort is not effective when adaptive autonomy is also applied. From the Sec. 4.3.2.4, the adaptive autonomy also has the capability of reducing the human's torque in the lane-keeping stage. The control effort drops from two different adaptive schemes may be coupled together and thus, cannot further reduce the torque.

Participants' Control Effort Under Emergency

The torque in the obstacle-avoidance stage is reduced when the adaptive control consolidation is implemented. In addition, the adaptive control consolidation reduces more torque when the surveillance task is less urgent. It can be explained by the design principle of adaptive control consolidation. When the human operator exerts extra torque to intervene, the assistance level β drops. It drops more when the human operator experiences a moderate workload than the high workload cases, which aims to give the human operator more control authority to achieve an optimal human-machine teaming performance.

In addition, compared to the torque reduction in the lane-keeping stage, the adaptive control consolidation can reduce more torque in the obstacle-avoidance stage. It can be explained by the fact that the assistance level β drops more when there is a considerable difference between the autonomy and the human operator. It can be validated by the conclusion in Chapter 3 as well.

The adaptive control consolidation reduces more torque when the low-maximum-speed autonomy is implemented than in other autonomy settings. In cases with the low-maximum-speed autonomy, the human operator is likely to intervene more actively, i.e., exert more torque to intervene. Therefore, the assistance level β drops more according to the design principle. It can be observed more straightforward when the low surveillance task is implemented (when the human operator experiences a moderate workload).

Time to Finish the Mission

The adaptive control consolidation can reduce the mission duration from the re-

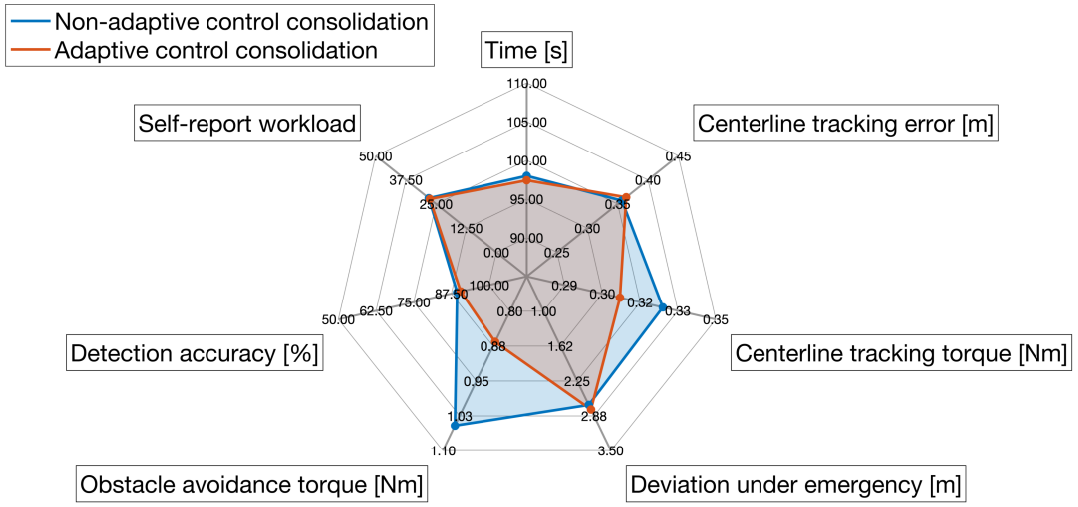

Figure 5.51: Spider plot showing all metrics in Experiment 5 when different control consolidations are used. The axis is the dimension of the metrics. The more away from the axis, the worse performance in that dimension. The one with a smaller coverage is considered a better design.

sults. It happens when adaptive autonomy is also implemented. From the design principle of adaptive autonomy, the maximum speed limit drops more if the human operator applies more torque. By implementing the adaptive control consolidation, humans exert less torque, leading to a higher autonomy's maximum speed limit and less mission time.

Conclusion For Adaptive Control Consolidation

The results show that adaptive control consolidation can reduce the control effort in lane-keeping and obstacle-avoidance stages. In addition, the mission performance with adaptive control consolidation is similar to the cases when non-adaptive control consolidation is applied. In conclusion, adaptive control consolidation can reduce the control effort without sacrificing mission performance when different autonomy settings are used. It is suggested to use the adaptive control consolidation when saving control effort is beneficial for the mission. A spider plot summarizes these characteristics as shown in Fig. 5.51.

5.2.3.2 Autonomy Settings: Main Effect

Participants' Self-reported Workload

Participants' self-reported workload is related to the autonomy settings. A higher average traveling speed leads to a higher reported workload. This result aligns with the previous finding in Sec. 4.2.1.3. However, in Experiment 4, which is shown in Sec. 4.3.2.3, the results show that there is no significance between the adaptive autonomy cases and the cases with the low-maximum-speed autonomy. The difference between these two experiments can explain it. The subjects experience the same autonomy setting twice in this experiment, while they only have one chance in Experiment 4. Therefore, this extra experience in this experiment may help them tell the difference between the adaptive autonomy cases and the cases with low-maximum-speed autonomy, which is challenging to differentiate in Experiment 4.

Participants' Steering Control Effort During Lane Keeping

The human steering control effort in the lane-keeping stage is reduced when the adaptive autonomy is implemented. With different non-adaptive autonomy settings, no significant difference in steering control effort in the lane-keeping stage is observed. This result aligns with the previous results, which are shown in Sec. 4.3.2.3 when adaptive autonomy is used. Moreover, it indicates a benefit of reducing the human steering control effort in the lane-keeping stage when adaptive autonomy is implemented regardless of the control consolidation setting.

In addition, as indicated by the interaction effect between the control consolidation setting and the autonomy setting, the control effort reduction from implementing the adaptive autonomy on top of the adaptive control consolidation decreases compared to the non-adaptive control consolidation cases with adaptive autonomy. The benefit of adaptive control consolidation, which leads to a smaller control effort, may prevent the benefit of adaptive autonomy because the control effort is already at a low level.

Driving Task Performance

The results indicate that a higher average speed leads to a higher centerline tracking error for the driving task performance in the lane-keeping stage. It aligns with

the previous finding in Sec. 4.3.2.3. The explanation is also similar: the human operator has more safety margin to maneuver the vehicle when the speed is lower. After considering this effect, the adaptive autonomy gives the human operator more room to lower the vehicle's speed when an intervention is observed by sensing the increasing human torque on the steering wheel. In addition, adaptive autonomy achieves a robust centerline tracking error when different surveillance task urgency is presented to the human operator. This result is not observed in Experiment 4 since there is an improvement in centerline tracking error when the surveillance task is less urgent. It can be explained by the difference in experiment design between these two experiments as well. The extra experience gives the human driver more experience to perform the driving task better in cases with low task urgency. In this point of view, the adaptive autonomy can directly achieve the robust driving mission performance regardless of the extra driving and testing experience in this experiment.

Participants' Steering Control Effort Under Emergency

The adaptive autonomy uses a medium level of the steering control effort in the obstacle-avoidance stage. It aligns with the previous finding in Sec. 4.3.2.3 that a faster average speed leads to a smaller steering control effort when avoiding the obstacles. One possible explanation is that the human driver intervenes more actively, given the extra safety margin to maneuver the vehicle provided by the vehicle's low traveling speed.

In addition, from the interaction effect between the control consolidation setting and the autonomy setting, the adaptive control consolidation helps reduce more steering control effort when the autonomy's maximum speed limit is lower. It can be explained by the design principle of adaptive control consolidation. When the human torque is larger, the assistance level β drops more. The lower assistance level leads to a larger drop in emergency steering control effort when the autonomy's maximum speed limit is low.

Emergency Maneuvering Performance

Adaptive autonomy can achieve a medium level of deviation from the centerline among three different autonomy settings. From the previous explanation shown in

Sec. 4.3.2.3, the deviation from the centerline when avoiding obstacles is related to the traveling speed. A lower speed limit gives the human operator more safety margin to maneuver the vehicle and adjust the behavior to prevent further deviation from the centerline. The average speed of adaptive autonomy is at a medium level, leading to a medium deviation from the centerline under emergency. It also explains why adaptive autonomy improves emergency maneuvering performance when the surveillance task urgency is high. The vehicle's traveling average speed is reduced when participants perform an urgent version of the surveillance task, leading to a lower deviation under emergency.

Surveillance Task Performance

The results of surveillance task urgency show that adaptive autonomy and non-adaptive autonomy with a low maximum speed limit achieve a better surveillance task urgency than the one with a high maximum speed limit. On the one hand, when a low maximum speed limit is set and the vehicle moves slowly, the human operator has more time and room to scan the surveillance screen and detect potential threats. On the other hand, adaptive autonomy reduces the speed when the human operator is over-loaded or engaged in an intervention, creating more room for the surveillance task than non-adaptive autonomy with a high maximum speed limit.

Time to Finish the Mission

The adaptive autonomy can achieve a medium mission duration compared with the other two non-adaptive autonomy settings. In addition, the mission duration increases when the surveillance task urgency is high. Both of these results align with the results in Sec. 4.3.2.3 and the design principles of adaptive autonomy.

Conclusion For Adaptive Control Consolidation

The results show that adaptive autonomy can reduce the steering control effort in lane-keeping stages. In addition, it balances the mission duration, workload, driving mission performance, emergency maneuvering performance, and emergency steering control effort. It is suggested to use the adaptive autonomy when the perception difference between the autonomy and human is not large, and the steering control effort is an important metric to consider. A spider plot summarizes these characteristics as

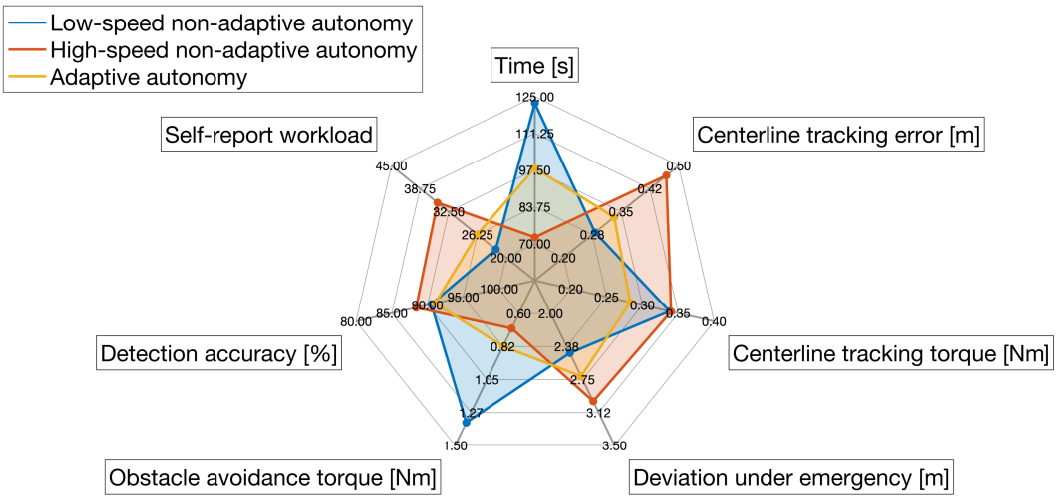

Figure 5.52: Spider plot showing all metrics in Experiment 5 when different autonomy settings are used. The axis is the dimension of the metrics. The more away from the axis, the worse performance in that dimension. The one with a smaller coverage is considered a better design.

shown in Fig. 5.52.

5.2.3.3 Adding Adaptive Control Consolidation When Adaptive Autonomy Is Implemented

In this sub-section, the benefit of adding the adaptive control consolidation on top of the adaptive autonomy is discussed based on the results shown in Sec. 5.2.2.2.

Participants' Self-reported Workload

While the adaptive autonomy can achieve a medium level of self-reported workload value, the adaptive control consolidation does not help reduce the self-reported workload value significantly. It is concluded that the average speed of the autonomy contributes to the self-reported workload significantly.

Participants' Control Effort During Lane Keeping

Adaptive autonomy alone can reduce the control effort during the lane-keeping stage to a low level. Adding the adaptive control consolidation on top of the adaptive autonomy does not help reduce the control effort significantly. The results imply that the control effort reduction from the adaptive autonomy creates a ceiling effect that

prevents the further benefit from using adaptive control consolidation.

Driving Task Performance

The driving task performance is affected by the average speed. Therefore, if using adaptive autonomy, the centerline tracking error will be at a medium level compared with the high-maximum-speed autonomy and low-maximum-speed autonomy cases. The effect of using adaptive control consolidation on driving task performance is not significant when the adaptive autonomy is implemented. It indicates that the adaptive control consolidation will not sacrifice the driving performance. In addition, the robustness of the centerline tracking error against the surveillance task urgency is also preserved when the adaptive control consolidation is implemented.

Participants' Control Effort Under Emergency

The adaptive autonomy requires more control effort than the baseline cases with the high-maximum-speed autonomy when implementing non-adaptive control consolidation. After implementing the adaptive control consolidation, the control effort of the adaptive autonomy will reduce to the same level as the baseline cases with the high-maximum-speed autonomy. Therefore, the adaptive control consolidation can further save control effort when avoiding obstacles, where a large difference between the human operator and autonomy exists.

Emergency Maneuvering Performance

The emergency maneuvering performance is affected by the average speed. Therefore, if using adaptive autonomy, the deviation from the centerline will be at a medium level compared with the high-maximum-speed autonomy and low-maximum-speed autonomy. The effect of using adaptive control consolidation on emergency maneuvering performance is not significant when adaptive autonomy is implemented. It indicates that the adaptive control consolidation will not sacrifice the driving performance when avoiding obstacles. In addition, when the surveillance task urgency is changed from low to high, the deviation from the centerline in adaptive autonomy cases is decreased. This deviation reduction from switching to the high surveillance task urgency is preserved when the adaptive control consolidation is implemented.

Surveillance Task Performance

The surveillance task detection accuracy is better in low-maximum-speed and adaptive autonomy cases than in high-maximum-speed cases. Implementing adaptive control consolidation does not significantly affect the detection accuracy when adaptive autonomy is also implemented.

Time to Finish the Mission

The average speed affects the mission duration, given that the length of the track is constant. Therefore, if using adaptive autonomy, the mission duration will be at a medium level compared with the high-maximum-speed autonomy and low-maximum-speed autonomy. Implementing adaptive control consolidation on top of adaptive autonomy will reduce the mission duration. The adaptive control consolidation aims to reduce the control effort throughout the entire mission, which will lead to a faster traveling speed based on the design principle of adaptive autonomy. Therefore, implementing adaptive control consolidation leads to faster average speed when adaptive autonomy is also implemented, resulting in a shorter mission duration.

Summary

In summary, the benefits of the adaptive control consolidation are listed below when the adaptive autonomy is implemented. By adding the adaptive control consolidation to the adaptive autonomy, the participants can finish the mission using less control effort in the obstacle-avoidance stage and shorter mission duration when compared with the adaptive autonomy cases with non-adaptive control consolidation without sacrificing other performance. Therefore, it suggests that the adaptive control consolidation should be implemented on top of the adaptive autonomy when the autonomy needs help from the human operator, such as to avoid the obstacles. When both control consolidation and autonomy levels are adaptive, they are able to achieve a balance between mission duration, driving performance, and surveillance task performance at lower steering control effort. A spider plot compares the two baseline schemes with different maximum speed limits and two schemes with adaptive autonomy and different control consolidations is shown in Fig. 5.53.

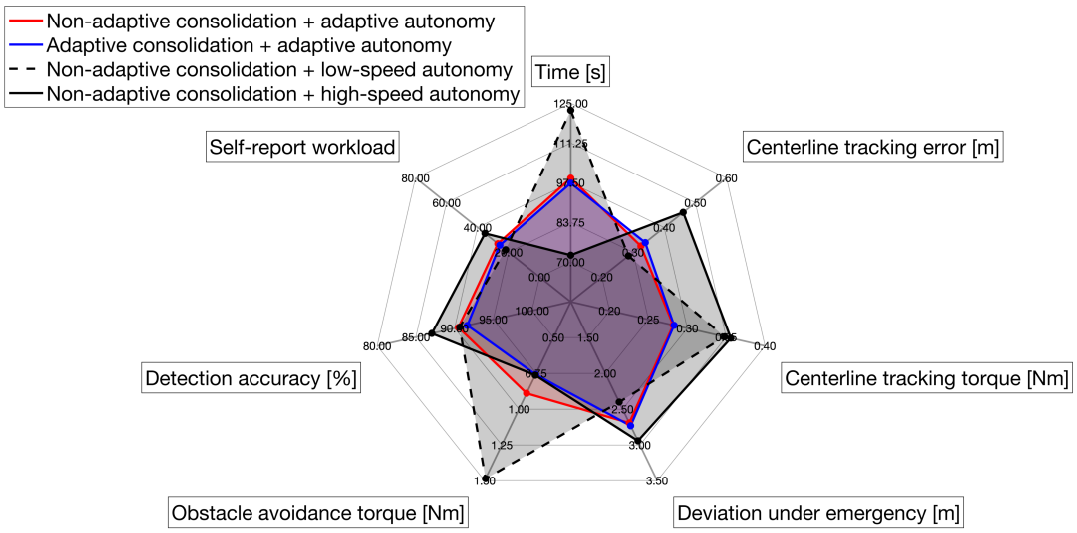

Figure 5.53: Spider plot showing all metrics in Experiment 5 when different schemes are used. There are four schemes in this plot, including two baseline schemes with different maximum speed limits and two schemes with adaptive autonomy and different control consolidations. The axis is the dimension of the metrics. The more away from the axis, the worse performance in that dimension. The one with a smaller coverage is considered a better design.

5.2.3.4 Adding Adaptive Autonomy When Adaptive Control Consolidation Is Implemented

In this sub-section, the benefit of adding adaptive autonomy on top of adaptive control consolidation is discussed based on the results shown in Sec. 5.2.2.3.

Participants' Self-reported Workload

By switching to adaptive autonomy when adaptive control consolidation is implemented, the self-reported workload remains the same level as the cases with the low-maximum-speed autonomy and adaptive control consolidation. The self-reported workload drops significantly when switching from the cases with the high-maximum-speed autonomy and adaptive control consolidation. It shows that using adaptive autonomy can achieve the lowest level of self-reported workload when adaptive control consolidation is implemented.

Participants' Control Effort During Lane Keeping

The control effort in the lane-keeping stage can be further reduced by switching to adaptive autonomy when adaptive control consolidation is implemented. In general, the adaptive control consolidation with adaptive autonomy can achieve a minimum level of control effort in the lane-keeping stage.

Driving Task Performance

Switching to adaptive autonomy leads to a medium level of driving performance in the lane-keeping stage. The centerline tracking error reduces when changing the autonomy from a high-maximum-speed one, and the error increases when changing the autonomy from a low-maximum-speed one. It is also worth noticing that the centerline tracking error becomes robust against surveillance task urgency when switching to adaptive autonomy.

Participants' Control Effort Under Emergency

Switching to adaptive autonomy leads to a medium level of control effort in the obstacle-avoidance stage. The value is greater than the cases when adaptive control consolidation and high-maximum-speed autonomy are both implemented. And it is smaller than the cases when adaptive control consolidation and the low-maximum-speed autonomy are both utilized. Although the value is greater than the cases where adaptive control consolidation and the high-maximum-speed autonomy are both applied, the control effort is at the same level as the baseline cases when the high-maximum-speed autonomy is applied.

Emergency Maneuvering Performance

Switching to adaptive autonomy leads to a medium level of emergency maneuvering performance. The deviation from the centerline in the obstacle-avoidance stage reduces when changing the autonomy from a high-maximum-speed one. In contrast, the deviation increases when changing the autonomy from a low-maximum-speed one. It is also worth noticing that the deviation reduces when the urgent surveillance task is presented in the adaptive autonomy case.

Surveillance Task Performance

Switching to adaptive autonomy does not significantly impact the surveillance task performance, though a marginal improvement from the high-maximum-speed

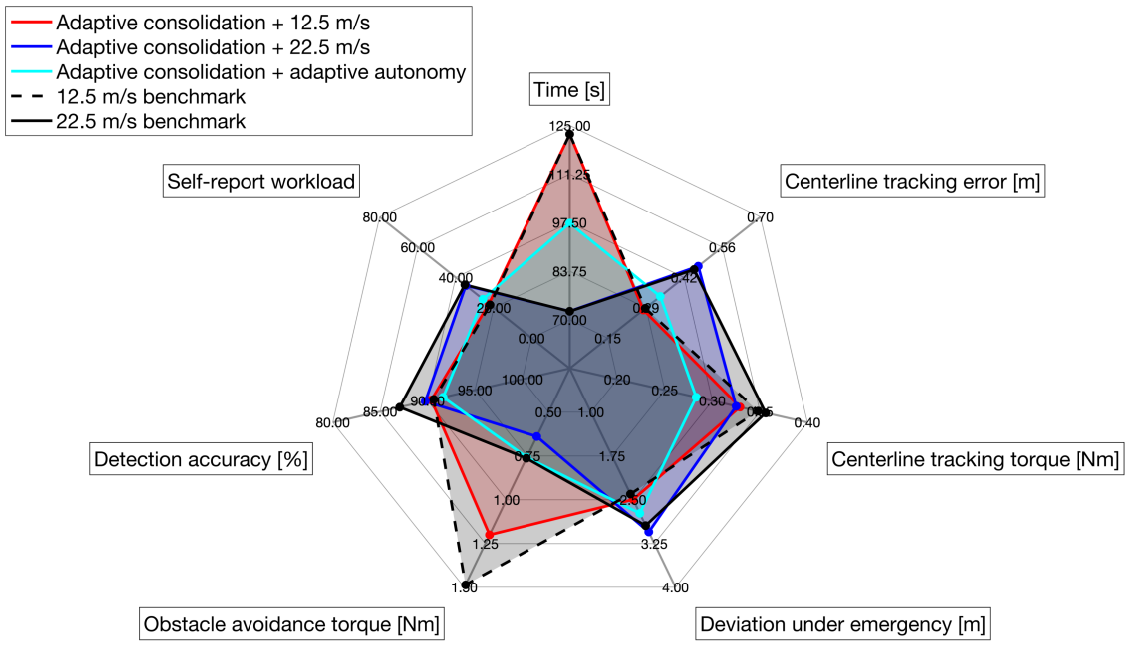

Figure 5.54: Spider plot showing all metrics in Experiment 5 when different schemes are used. There are five schemes in this plot, including two baseline schemes with different maximum speed limits, two schemes with adaptive control consolidations, and the scheme with both adaptive control consolidation and adaptive autonomy. The axis is the dimension of the metrics. The more away from the axis, the worse performance in that dimension. The one with a smaller coverage is considered a better design.

autonomy is obtained when adaptive control consolidation is implemented.

Time to Finish the Mission

Switching to adaptive autonomy achieves a medium level of mission duration. The adaptive cases finish faster than the low-maximum-speed autonomy cases while it takes longer than the high-maximum-speed autonomy cases.

Summary

In summary, the benefits of using adaptive autonomy are listed below when the adaptive control consolidation is also implemented. Adaptive autonomy can achieve the minimum self-reported workload, control effort during the lane-keeping task, and robust centerline tracking error. It balances the mission duration, driving task perfor-

mance, and emergency maneuvering performance compared to other adaptive control consolidation cases. Therefore, it suggests that adaptive autonomy should be implemented on top of the adaptive control consolidation when the mission is evaluated by the overall performance, including driving performance, control effort, and mission time. The adaptive control consolidation with the low-maximum-speed autonomy should be used when the lane-keeping performance and emergency maneuvering performance are weighted much higher than other metrics. The adaptive control consolidation with the high-maximum-speed autonomy should be used when the mobility or mission duration is the most important evaluation metric. A spider plot compares two baseline schemes with different maximum speed limits, two schemes with adaptive control consolidations and different autonomy maximum speed limits, and the scheme with both adaptive control consolidation and adaptive autonomy is shown in Fig. 5.54.

5.3 Conclusion

In this chapter, the adaptation at both adaptive control consolidation level and autonomy level is investigated by a human subject study. In Experiment 5, participants experience all possible combinations of control consolidation and autonomy settings in the dual-task shared control driving mission. The results of 24 participants indicate the following conclusions. First, the adaptive control consolidation can reduce the steering control effort without sacrificing the driving performance in the driving task, regardless of the autonomy setting. Second, the adaptive autonomy can balance the reported workload, mission duration, driving task performance, emergency maneuvering performance, and emergency steering control effort at the lowest steering control effort in the lane-keeping stage. Third, by adding the adaptive control consolidation to the adaptive autonomy, the participants can finish the mission using less steering control effort in the obstacle-avoidance stage and shorter mission duration than the one without adaptive control consolidation. Fourth, adding adaptive autonomy to schemes with adaptive control consolidation can achieve the minimum self-reported

workload, control effort during the lane-keeping task, and robust centerline tracking error. In addition, it balances the mission duration, driving task performance, and emergency maneuvering performance compared to other adaptive control consolidation cases. Adaptation at both levels can achieve the best surveillance task performance and least steering control effort in the lane-keeping and obstacle-avoidance stages. Meanwhile, it balances the self-reported workload, mission duration, and driving performance in the lane-keeping and obstacle-avoidance stages.

Chapter 6

Conclusions and Future Work

6.1 Dissertation Summary

This dissertation addresses the gap of adaption to an important human factor, workload, in haptic shared steering control of an autonomy-enabled vehicle. Adaptive schemes at both control consolidation and autonomy levels are developed and evaluated through human subject studies. First, in Chapter 3, two adaptive control consolidations are designed considering the human driver's workload and steering torque. Two experiments, Experiment 1 and Experiment 2, are conducted to assess the performance after the adaptive control consolidations are implemented compared to the baseline non-adaptive cases under different workload conditions. Second, in Chapter 4, autonomy maximum speed limit is assessed in a human subject study, Experiment 3, to confirm that it has a significant impact on the human driver's workload in a haptic shared control driving scenario. Third, in Chapter 4, a workload-adaptive autonomy is designed, which varies autonomy's maximum speed limit. The performance of adaptive autonomy is evaluated through a human subject study, Experiment 4, compared to the baseline non-adaptive autonomy with different maximum speed limits when subjects experience different workload conditions. Finally, in Chapter 5, the combined effect is investigated when both adaptive control consolidation and adaptive autonomy are applied through the human subject study Experiment 5. Unlike previous evaluations where the adaptive control consolidation and adap-

tive autonomy are assessed in isolation, all combinations of the control consolidation setting and the autonomy setting are presented to subjects who experience different workload conditions in Experiment 5.

As a result, this dissertation makes the following original contributions:

- Development of a workload-adaptive control consolidation and the evaluation of its performance.

  Two adaptive control consolidations are developed. The first one considers the human operator's workload and steering torque. The second one considers the estimated workload, human steering toque, and eyes-on-road. At a high level, these adaptive designs believe the human's decision under moderate workload condition and therefore reduces the assistance level from autonomy when there is a disagreement between the human operator and autonomy to give the human operator more control authority. It leverages the optimal human performance under the moderate workload condition as indicated in Sec. 1.1.2. Under other conditions, the control authority of autonomy increases to provide more support to the human operator. In addition, two methods that regulate the workload are proposed. They are based on the screen refresh rate and surveillance task urgency, respectively. The experiments validate the hypothesis that these methods can regulate the workload. Furthermore, the evaluation of the mission performance through the human subject studies shows that when there is little difference between the perception of the subject and autonomy with respect to the position of the centerline of the path is presented to the subject, the adaptive control consolidation can reduce the steering control effort without sacrificing the driving mission performance compared to the baseline non-adaptive control consolidation. When the perception difference is large, the adaptive control consolidation can reduce human workload, increase their trust in the system, improve driving performance, and reduce human steering control effort without sacrificing surveillance task performance. This original contribution is documented in the publications [86, 100, 75].

- Development of a workload-adaptive autonomy and evaluation of its performance.

  Through a human subject study, autonomy's maximum speed limit is confirmed as an autonomy parameter that significantly impacts the human driver's workload. The result of the human subject study indicates that a higher maximum speed limit leads to a higher workload, shorter mission duration, and worse driving task performance. The results also imply that the driving mission performance is reduced when the human operator is over-loaded, which reaffirms the inverted-U shape curve introduced in Sec. 1.1.2. These conclusions are then used to design an adaptive autonomy, which considers workload, human torque, and steering rate. At a high level, the adaptive autonomy is designed to reduce the maximum speed limit when the human operator is over-loaded, the vehicle is difficult to control, or there is a significant disagreement between the human operator and autonomy. Thus, the maximum speed reduction can help the human operator control the vehicle easily. The performance of the adaptive autonomy is evaluated through a human subject study compared to the non-adaptive autonomy with different maximum speed limits. Results indicate that adaptive autonomy balances self-reported workload, driving task performance in both lane-keeping and obstacle-avoidance stage, steering control effort in the obstacle-avoidance stage, and time to finish the mission. In addition, it can reduce the steering control effort in the lane-keeping stage. This original contribution is documented in the publications [87, 101].

- Evaluation of the combined framework which includes both workload-adaptive control consolidation and workload-adaptive autonomy.

  The combined performance of the adaptive control consolidation and the adaptive autonomy is examined by a human subject study. Subjects experience all possible combinations of control consolidation and autonomy settings. The results indicate two conclusions about the adaptive control consolidation and the autonomy by themselves and two interactive relationships between them.

For the main effect, the adaptive control consolidation can reduce the steering control effort without sacrificing the driving performance in the driving task, regardless of the autonomy setting. Therefore, it is said to reduce the steering control effort in the cases when the disagreement between agents is minor (lane-keeping stage) and significant (obstacle-avoidance stage). Furthermore, the effect of the adaptive control consolidation is more significant when the disagreement is large. Adaptive autonomy balances the reported workload, mission duration, driving task performance, emergency maneuvering performance, and emergency steering control effort at the lowest steering control effort in the lane-keeping stage. It can be achieved regardless of the control consolidation setting. Considering the interaction effect, by adding the adaptive control consolidation to the adaptive autonomy, the participants can finish the mission using less steering control effort in the obstacle-avoidance stage and less time duration than the one without adaptive control consolidation. Therefore, the adaptive control consolidation can further reduce the steering control effort when the disagreement between agents is significant. Nevertheless, the effect of adaptive consolidation is not significant because of the implementation of adaptive autonomy, which can also reduce the steering control effort when a minor disagreement exists between agents. Adding adaptive autonomy to schemes with adaptive control consolidation can achieve the minimum self-reported workload on top of the benefit of implementing adaptive autonomy compared to other adaptive control consolidation cases. The adaptation at both levels can achieve the best surveillance task performance and least steering control effort in the lane-keeping and obstacle-avoidance stages. It also balances the self-reported workload, mission duration, and driving performance in the lane-keeping and obstacle-avoidance stages. This original contribution is documented in the publications [87, 101].

6.2 Technology Transfer

The adaptive control consolidation developed in Chapter 3 has been transitioned to the Toyota Research Institute (TRI) and is implemented on their code-base. An ongoing human subject study is testing the performance in practical scenarios based on the simulation platform in TRI.

6.3 Limitations and Future Work

The following subsections describe some limitations and possible future directions to address these limitations.

6.3.1 Haptic Shared Speed Control

The current testbed, which is described in Chapter 2, does not provide the support for collaborative speed control of the vehicle due to the lack of a haptic pedal set. As a result, the speed of the vehicle is completely controlled by autonomy. However, the speed control authority of the human operator is also an important dimension to consider in the context of shared control. In [102, 103, 104], researchers have developed several longitudinal shared control systems for the haptic pedal set. Their results indicate that haptic speed control schemes can also benefit the mission performance. Therefore, one direction of future work to address this limitation is to include the haptic pedal set and investigate the performance when both human operator and adaptive autonomy are in the speed control loop.

6.3.2 Experimental Validation for Other Cases

The conclusions about the developed haptic schemes are limited to the vehicle, driving scenarios, and secondary tasks considered in this dissertation. First, the experiment relies on the simulation of a HMMWV, which provides a different driving experience from a standard passenger vehicle. For example, the high center of gravity of a HMMWV makes it more prone to tire lift-off and even rollover. The participants may

control a different vehicle more aggressively if the tire lift-off happens less frequently. Second, the simulation testbed adopts an off-road environment where no other vehicle is present. The participants may have different control patterns when driving, for example, on a highway with some surrounding vehicles. Finally, the secondary task used in this testbed is visual-based. The performance of the developed shared control schemes can be investigated with other types of secondary tasks. Several commonly-used secondary tasks are the n-back task (auditory-based) [105, 106, 107], phone task (auditory-based) [108, 109, 110, 111] and navigation tasks [110, 112]. Under different kinds of secondary tasks, the participants may perform differently. Therefore, the investigation of the developed haptic shared control schemes in other cases is another future direction.

6.3.3 Full Age Spectrum for Participants

Subjects of this work come from the University of Michigan College of Engineering students, whose age ranges from 18 to 27. The results can be different if a different age group is used as the pool of subjects. Research shows that the driving performance is different when elder subjects are driving [113, 114, 115, 116, 117]. Specifically, in [118], researchers show that compared to younger drivers, the older participants react slower, have a higher chance to collide, and have a slower driving speed in manual driving. The difference in performance between different age groups can be significant in the shared control mode as well. In [115], researchers find that under the takeover behavior from the L3 automated driving, the older participants have a longer reaction time and worse driving stability. Therefore, investigating the developed adaptive schemes when the participants have a variety of ages is considered to be one of the future directions to evaluate the generalizability of the developed scheme.

6.3.4 Investigation of Other Methods to Control Workload

Two methods are used in this dissertation to control the participants' workload in the experiments; namely, the refresh rate of the driving screen and the surveillance

task urgency. Both of these methods control workload in a binary manner; i.e., they create two workload scenarios, moderate and high workload, where the latter requires more resources to finish the mission than the former. These methods lead to two limitations.

First, the under-loaded condition, which has equal importance as the over-loaded condition, is not considered. Consider, as an example, using surveillance task urgency to control workload: the participants need to allocate some resources and focus on the surveillance task for the threat identification even when the urgency of the surveillance task is low. In addition, the images and the position of the threat may change between image sets. Therefore, the under-loaded condition is not likely to happen.

Second, because the designed methods are binary, the workload estimation algorithm treats it as a binary classification problem, as well. The outcome of the algorithm is a classification result indicating whether the human operator experiences a high workload or moderate workload. Although the continuous workload estimation signal shown in Sec. 4.3.2.3 is continuous, this is the result of the moving average filter mentioned in Sec. 4.3.2.2 and not a result of a workload classification on a continuous scale.

Therefore, one of the future directions is to find a better method to regulate the workload of the human subjects so that it can control a broader range of workload and have a better resolution. It then remains to be seen if such higher resolution would lead to a better workload-adaptive shared control performance.

6.3.5 Field Test for Developed Schemes

The experiment is conducted in a simulated environment. As a result, some feelings in the real driving are not emulated, which is a limitation of this work. An example of such missing feeling is the sense of the longitudinal acceleration [119]. When driving in a real vehicle, one can feel the acceleration in their body. However, in the fixed-base simulator used in this study, one can only tell if the vehicle is accelerating by visually estimating the speed change of the vehicle from the reference objects (like rock or grass) in the simulated environment. Other differences reported in the literature be-

tween simulated and real driving include the reaction time [120, 121], mean heart rate in response to unexpected events [122] and self-evaluation of sleepiness [121]. These differences in feeling may remind the participants that they are in a simulator rather than the real driving scenario, leading to a different driving performance compared to the real cases. As a result, conducting a field test that implements the developed haptic shared control schemes in a real driving scenario is one of the future directions.

6.3.6 Game-theory Based Shared Control Design

This dissertation studies the adaptation of the continuous negotiation between agents based on some design principles. An alternative approach to design can be taken. For example, in a shared control driving scenario, the human driver and autonomy can be treated as two players in a differential game. The inputs of these agents to the haptic steering wheel can be considered as the actions to interact with each other. In addition, the negotiation between two agents in the shared control can be regarded as delivering and receiving the other agent's information during the dynamic process. These characteristics make the haptic shared control driving scenario similar to a dynamic game problem.

Hence, researchers turn to the game theory framework to describe and analyze the haptic shared control [123]. Two types of games, namely the cooperative game and the noncooperative game, are implemented in haptic shared control, and the mission performance is investigated. In the noncooperative games, each player, either the human operator or the autonomy, is considered a rational individual and has an individual goal to achieve, i.e., each player has their own cost function to optimize considering the impact of other's action [124, 125, 126, 127, 128]. In the cooperative game, the actions of the agents are derived from a global cost function that represents both agents' common interest [124, 125]. These schemes are shown to achieve improvement in mission performance. These results point to a potential extension that adapting to workload in these game-theory-based frameworks could also be beneficial, which is one of the future directions.

6.3.7 Human Driver Model for Better Design of the Schemes

Critical values and connecting curve shape selections in the design of the adaptive schemes are obtained from the results of pilot studies conducted with a limited pool of subjects. This may lead to a biased design and thus a sub-optimal performance for the general population. A way to mitigate this issue is to design the adaptive schemes using a human model, which can help understand the human operators' behavior during the haptic shared control and provide a range of predictions for the humans' next actions. In addition, the human driver model would pave the way to design model-based workload-adaptation schemes, which may be beneficial.

Human driver models in the literature are control-theory based or cognitive-framework based models to predict the human driver's behavior. Control-theory based methods typically rely on the game-theory based framework. In [129], the human driver's input is modeled by a spring-mass-damper system based on the game theory framework in [125]. In [130, 131], the author applies the inverse optimal control method in a Linear-Quadratic path tracking game by assuming both human driver and autonomy are model predictive controller who has quadratic costs. The parameters of the human's cost function are derived by the Pontryagin Maximum Principle (PMP), given the prediction horizon is finite [130, 131] or infinite [130]. In contrast, a method called probabilistic Inverse Reinforcement Learning (pIRL) is adopted in [132, 133, 134]. Its goal is to estimate the parameters better, which can avoid the ill-conditioned estimation derived from the maximum principle. However, the models to control in pIRL cases are considered primitive and may not be able to handle a complex shared control scenario.

The cognitive-framework based methods seek a more general approach that can apply to a broader scope than the game theory framework. They typically deploy the principles in the Adaptive Control of Thought-Rational (ACT-R) cognitive architecture [135, 136]. A good example in [137] demonstrates that the developed human driver model can capture the human driver's behavior characterized by the Average Lane-Keeping Error (ALKE). By applying these models to different workload condi-

tions, different human driver models can be obtained whose parameters may differ from each other. These differences can provide essential clues for the adaptive scheme design. In conclusion, one potential future direction is to develop the human driver model.

Appendices

Pilot User Studies to Investigate the Role of Workload in Developed Adaptive Schemes

Introduction

In this appendix chapter, two pilot studies are presented to investigate the impact of workload in two workload-adaptive schemes as supplements to arguments in Sec. 3.2.2.4 and Sec. 4.3.2.4, respectively.

Impact of Workload in Workload-adaptive Control Consolidation: Pilot Study 1

Introduction of Pilot Study 1

In this pilot human subject study, namely Pilot Study 1, the impact of the workload as a parameter of adaptive control consolidation, shown in Sec. 3.2.1.2, is evaluated. There are 8 participants in this experiment. They are asked to perform a driving task mission. In the mission, the subject is required to achieve a centerline tracking with minimum deviation from the centerline with the help of autonomy. Sometimes autonomy perceives a different centerline to represent the cases where a continuous significant disagreement exists between agents. This case is called biased autonomy.

Two types of control consolidation are presented to the subject, including the developed workload-adaptive control consolidation and the torque-adaptive control consolidation, which is obtained by considering the workload in workload-adaptive control consolidation as moderate all the time. The screen refresh rate, which is introduced in Sec. 3.2.2.2, is used to control the workload of the participants. Because there is no difference between the two control consolidation settings under the moderate workload condition, only the high workload setting (i.e., the 2.5 Hz screen refresh rate) is presented to the participants to study the difference.

Method

Participants

There are 8 students participating in this experiment. All participants have a normal or corrected-to-normal vision, and the eye tracker can be calibrated on their eyes.

Apparatus and Stimuli

The shared control simulation platform introduced in Chapter 2 with the visualization module introduced in Sec. 2.2.2 is used in this experiment. Participants perform only the driving task. In the driving task, the participant and the autonomy share the vehicle's steering control, while the vehicle's speed is controlled by autonomy only. The goal of the driving task is to complete a track with minimal deviation from the centerline. In some cases, to emulate a perception difference, an offset is introduced such that the autonomy tracks a path that deviates from the centerline by 0.8 m, which is referred to as biased autonomy. The value of bias is selected to be large enough to differ from the unbiased case clearly, but not too large to render autonomy useless. Both workload-adaptive shared control consolidation and torque-adaptive shared control consolidation are used in this experiment. The workload-adaptive control consolidation is introduced in Sec. 3.2.1.2, while the torque-adaptive control consolidation is obtained by assuming the workload level of the workload-adaptive control consolidation is always moderate. The screen refresh rate is used to affect the participants' workload. Because there is no difference between the two control

consolidations under the moderate workload condition, only the 2.5 Hz screen refresh rate is presented in this experiment.

Autonomy Formulation

The same autonomy formulation as in Experiment 1 (Sec. 3.2.2.2) is used in this human subject experiment.

Experimental Design

The experiment uses a within-subjects design with two independent variables. The first one is the autonomy setting, i.e., biased autonomy vs. unbiased autonomy. The second one is the control consolidation setting, which includes the workload-adaptive control consolidation and the torque-adaptive control consolidation. Each participant experiences four tracks in the experiment where the screen refresh rate is 2.5 Hz.

Measures

There are two dependent variables collected in the experiment:

- Participants' steering control effort
- Driving task performance

Similar to previous methods in Sec. 3.2.2.2, Sec. 3.3.2.2, Sec. 4.2.1.2, Sec. 4.3.2.2 and Sec. 5.2.1, a participant's steering control effort is calculated as the average value of the absolute human torque. Driving task performance is evaluated by lane-keeping error, which is calculated as the mean of the absolute deviation of the vehicle's position from the centerline.

Experimental procedure

During the training session, the participants perform five trials of the driving task under different conditions: one trial with the 20 Hz refresh rate, non-adaptive control consolidation with an unbiased autonomy, and four trials with the 2.5 Hz refresh rate. They experience non-adaptive control consolidation with an unbiased autonomy, adaptive control consolidation with a biased autonomy, adaptive control consolidation with an unbiased autonomy, and non-adaptive control consolidation with a biased autonomy in order. Each trial takes approximately 2.5 min.

Table A.1: Mean and standard error (SE) of centerline tracking error and centerline tracking torque in Experiment Pilot Study 1

Metrics	N	Screen refresh rate			
		2.5 Hz			
		Unbiased autonomy		Biased autonomy	
		Workload-adaptive	Torque-adaptive	Workload-adaptive	Torque-adaptive
Centerline tracking error (m)	8	0.219 ± 0.010	0.321 ± 0.037	0.519 ± 0.022	0.670 ± 0.025
Centerline tracking torque (Nm)	8	0.396 ± 0.013	0.365 ± 0.009	0.823 ± 0.021	0.480 ± 0.015

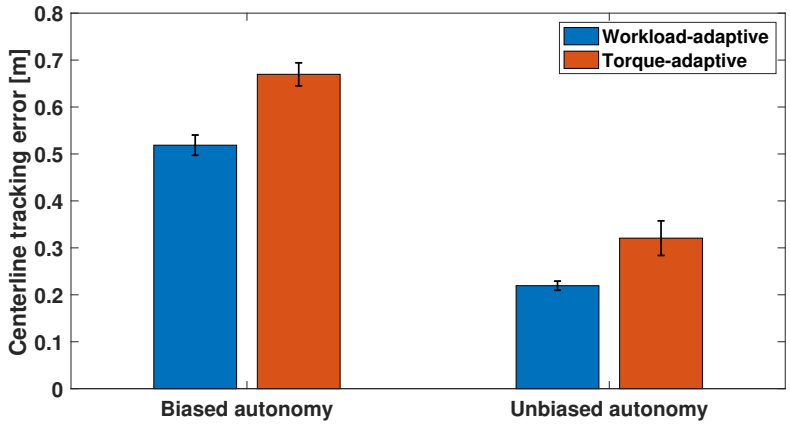

Figure A.1: Relationship between centerline tracking error and different control consolidation settings in Pilot Study 1

During the real experiment, participants perform the driving task on four different tracks with a different autonomy setting and control consolidation setting. Each trial takes approximately 1.5 min.

Results

Two-way repeated measures Analysis of Variance (ANOVA) is conducted with the control consolidation setting and the autonomy setting as the within-subjects variables. Results are reported as significant for $\alpha < .05$.

Table A.1 summarizes the mean and standard error (SE) values of the participants' driving task performance and their exerted torque during the mission.

Driving Task Performance

When unbiased autonomy is implemented, there is a significant difference ($p = 0.024$) in centerline tracking error between two control consolidations. When it comes to biased autonomy, a significant difference can also be found ($p < 0.001$). The

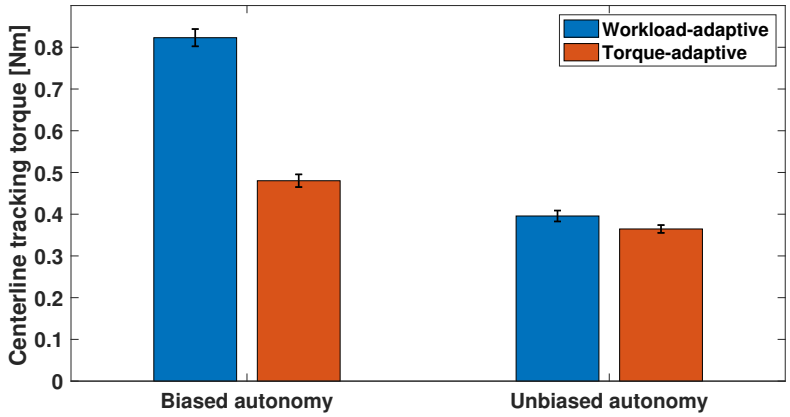

Figure A.2: Relationship between centerline tracking torque and different control consolidation settings in Pilot Study 1

workload-adaptive control consolidation achieves a smaller centerline tracking error, as shown in Fig. A.1.

Participants' Steering Control Effort

When unbiased autonomy is implemented, there is no significant difference ($p = 0.082$) in centerline tracking torque between two control consolidations. For biased autonomy, a significant difference is found ($p < 0.001$). The torque-adaptive control consolidation achieves a smaller centerline tracking torque. These results are illustrated in Fig. A.2.

Discussion

Driving Task Performance

Because the torque-adaptive control consolidation only considers the impact of the human torque and assumes the human operator always has a moderate level of workload, its assistance level β_{torque} is smaller than the assistance level of workload-adaptive control consolidation $\beta_{workload}$ (or β). The reduced assistance from autonomy leads to a worse mission performance when the autonomy is unbiased, which is also shown in Sec. 3.2.2.4. When the autonomy is biased, the workload-adaptive control consolidation still provides a better centerline tracking performance, which can be explained by the following reason. When the human operator is over-loaded, (s)he has

limited resources to control the vehicle compared to the moderate workload condition. It leads to a larger settling time for the vehicle after the human intervenes, which is not likely to happen under the moderate workload condition. Even if it is biased, the extra torque from autonomy helps stabilize the vehicle, which acts as a damper. As a result, it makes the vehicle easier to control and leads to better mission performance.

Steering Control Effort

As shown in the previous discussion, the assistance level from torque-adaptive control consolidation β_{torque} is smaller than the assistance level of workload-adaptive control consolidation $\beta_{workload}$ (or β). It will lead to a smaller control effort as per the discussion given in Experiment 1.

In conclusion, the role of adaptation to workload in the over-loaded condition is to achieve a good mission performance with more control effort compared with the consolidation that does not consider the workload. This result is achieved by providing more assistance from autonomy.

Impact of Workload in Workload-adaptive Autonomy: Pilot Study 2

Introduction of Pilot Study 2

In this pilot human subject study, namely Pilot Study 2, the impact of the workload as a parameter of adaptive autonomy design, shown in Sec. 4.3.1, is evaluated. There are 8 participants in this experiment. They are asked to perform a dual-task mission. In the driving task, the subject is required to achieve a centerline tracking with minimum deviation from the centerline with the help of autonomy. There are obstacles located at the centerline, which are invisible to autonomy. Therefore, the subject should intervene and avoid the obstacles. Two types of autonomy are presented to the subject, including the developed workload-adaptive autonomy and the torque-adaptive autonomy, which is obtained by considering the workload in workload-adaptive autonomy as moderate all the time. In addition to the driving task, the participants also need

to perform the surveillance task, whose task urgency, introduced in Sec. 2.5, controls the participants' workload. Because there is no difference between the two autonomy settings under the moderate workload condition, only the high workload setting (i.e., the high surveillance task urgency) is presented to the participants.

Method

Participants

8 students participated in this experiment. The 8 participants were on average 23.61 years old ($SD = 1.88$ years) and had an average of 4.42 years of driving experience ($SD = 2.25$ years). All participants had a normal or corrected-to-normal vision, and the eye tracker could be calibrated on their eyes.

Apparatus and Stimuli

The dual-task shared control simulation platform introduced in Chapter 2 with the visualization module introduced in Sec. 2.2.3 is used in this experiment. Participants perform two tasks, the driving task and the surveillance task, simultaneously. In the driving task, the participant and the autonomy share the vehicle's steering control, while the vehicle's speed is controlled by autonomy only. The goal of the driving task is to complete a track with minimal deviation from the centerline while avoiding obstacles on the centerline. The autonomy has no obstacle avoidance capability. There are two autonomy settings in this experiment: The workload-adaptive autonomy, which is introduced in Sec. 4.3.1 and the torque-adaptive autonomy, which is obtained by always assuming a moderate workload condition in the workload-adaptive autonomy. The impact on mission performance only comes from the different autonomy settings. The participants also need to perform the surveillance task. The goal of the surveillance task is to make the identification within the time limit as accurate as possible. The surveillance task urgency is used to control the subject's workload in this experiment. Because the design is identical for the workload-adaptive autonomy and torque-adaptive autonomy under the moderate workload condition, only the high workload condition is explored in this pilot study. There is only one surveillance task urgency: 1.5 s pace, which is labeled as high surveillance task urgency. A real-time

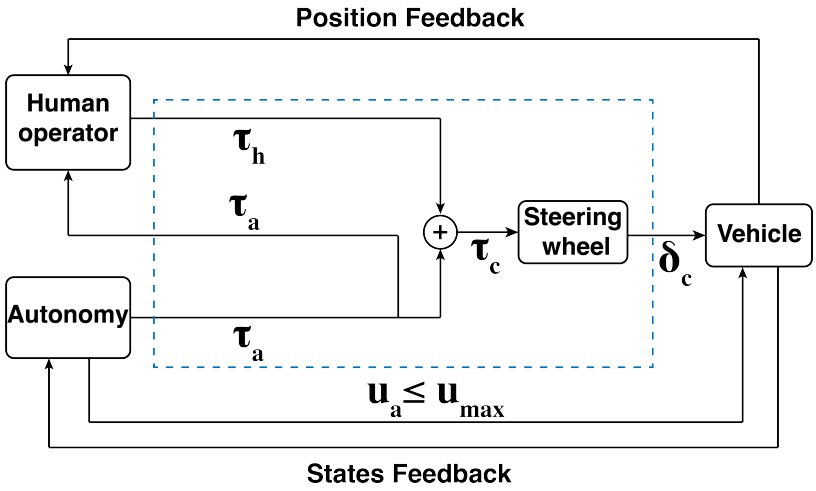

Figure A.3: Control block diagram when different maximum speed limits are implemented. The blue dashed lines highlight the control consolidation where non-adaptive control consolidation is implemented. The term u_a represents the speed of the vehicle is controlled by autonomy only. u_{max} can assume one of the two autonomy maximum speed limits: workload-adaptive autonomy speed limit $u_{x,max}$ and torque-adaptive autonomy speed limit $u_{x,max,torque}$.

workload estimator based on Bayesian Inference and developed by our collaborators is used [87]. For the workload estimation, the corresponding data from a 4 s time window captured by the eye tracker, Tobii Pro Glasses 2 (30 Hz sampling rate), are used to estimate participants' workload. A moving average filter is applied with a 1 s time window, and w_t is down-sampled to 10 Hz.

Autonomy Formulation

The same autonomy formulation compared to Experiment 4 (Sec. 4.3.2.2) is used in this human subject experiment. The control block diagram is shown in Fig. A.3.

Experimental Design

The experiment uses a within-subjects design with only one independent variable: the autonomy settings with different maximum speed limits, i.e., the workload-adaptive autonomy's maximum speed limit vs. the torque-adaptive autonomy's maximum speed limit. Each participant experiences two tracks in the experiment where the surveillance task urgency is always high.

Measures

There are seven dependent variables collected in the experiment:

- Participants' self-reported workload
- Participants' steering control effort in lane-keeping task
- Driving task performance
- Participants' steering control effort under emergency
- Emergency maneuvering performance
- Surveillance task performance
- Time to finish the task

In this experiment, the obstacle-avoidance stage has the same definition as in Sec. 3.2.2.2, Sec. 4.2.1.2, Sec. 4.3.2.2 and Sec. 5.2.1. The obstacle-avoidance stage is defined as the period when the human subjects deviate at least 1 m from the centerline and avoid the obstacles. The remaining part is defined as the lane-keeping stage.

After each track, participants report their workload using the NASA TLX survey [90]. The NASA TLX survey is presented to the participants before the experiment such that they understand the meaning of workload. Similar to previous methods in Sec. 3.2.2.2, Sec. 3.3.2.2, Sec. 4.2.1.2, Sec. 4.3.2.2 and Sec. 5.2.1, a participant's steering control effort in the lane-keeping task is calculated as the average value of the absolute human torque during the lane-keeping stage. Driving task performance is evaluated by lane-keeping error, which is calculated as the mean of the absolute deviation of the vehicle's position from the centerline during the lane-keeping stage. Steering control effort under emergency is calculated as the average of the absolute human torque that the participant applied on the steering wheel during the obstacle avoidance maneuver. Emergency maneuvering performance is evaluated by centerline deviation during the obstacle avoidance maneuver, which uses a similar calculation method as driving task performance but in the obstacle-avoidance stage. The torque from the participant is measured from a steering torque rotatory sensor. The collection rate of driving performance and steering control effort of the lane-keeping and obstacle-avoidance stages is 100 Hz. The surveillance task performance is measured

using the detection accuracy of the surveillance task. The time to finish the mission is the mission duration.

Experimental procedure

Before the training session starts, participants provide a signed informed consent and fill in a demographic survey to report their age and driving experience.

During the training session, the participants first perform three trials of driving tasks only, with the non-adaptive low-maximum-speed autonomy, the non-adaptive high-maximum-speed autonomy, and the workload-adaptive autonomy in order. The trial with the low-maximum-speed autonomy takes approximately 4 minutes, while the trial with the high-maximum-speed autonomy takes approximately 2 minutes. The trial with the adaptive autonomy takes approximately 2 minutes. Then the participants perform a training trial of the surveillance task only. It consists of two portions. The first portion is with the low surveillance task urgency, and it takes approximately 1 minute. The second portion is with the high surveillance task urgency, and it takes approximately 2 minutes. After that, the participants perform three combined driving and surveillance task trials with different surveillance task urgencies and different autonomy settings. The training session is designed to increase the mission difficulty gradually and help participants understand how to control the vehicle in a shared control scenario. As a result, participants experience the low-maximum-speed autonomy and low surveillance task urgency in the training phase, even though these conditions do not appear in the testing phase. On the other hand, the high-maximum-speed autonomy is used as the alternative for torque-adaptive autonomy during the training phase. It also helps participants notice the speed difference in different autonomy settings.

During the official experiment, participants perform the combined driving task and the surveillance task on two tracks with the workload-adaptive autonomy and torque-adaptive autonomy. The surveillance task urgency is always high. In each trial, participants travel a fixed distance (around 1200 m). After each trial, the participants are required to fill in a post-survey (NASA TLX) [90] to report the workload during the last track. If they hit the obstacle, the trial is restarted.

Table A.2: Mean and standard error (SE) of workload, centerline tracking error, centerline tracking torque, deviation under emergency, obstacle avoidance torque, time to finish the mission and detection accuracy in Experiment Pilot Study 2

Metrics	N	Surveillance task urgency	
		1.5 s (High surveillance task urgency)	
		Autonomy's setting	
		Workload-adaptive	Torque-adaptive
Workload	8	29.107 ± 7.950	35.982 ± 8.064
Centerline tracking error (m)	8	0.445 ± 0.080	0.566 ± 0.089
Centerline tracking torque (Nm)	8	0.273 ± 0.018	0.234 ± 0.025
Deviation under emergency (m)	8	2.756 ± 0.271	3.736 ± 0.181
Obstacle avoidance torque (Nm)	8	0.964 ± 0.106	0.391 ± 0.083
Time to finish the mission (s)	8	104.689 ± 0.397	79.693 ± 1.110
Detection accuracy (%)	8	81.868 ± 3.211	84.216 ± 2.807

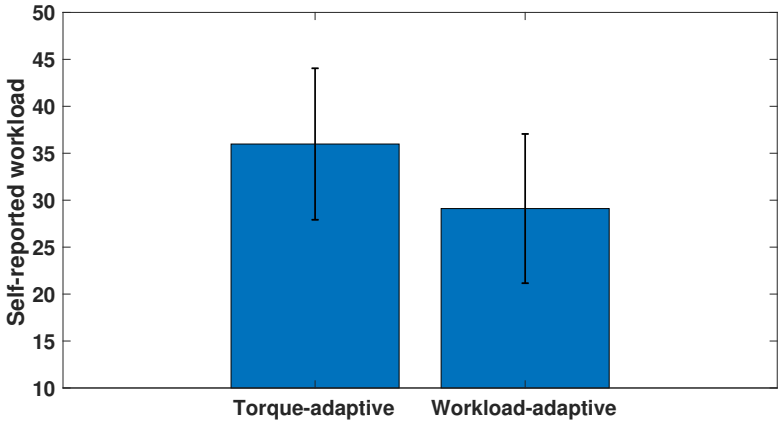

Figure A.4: Relationship between self-reported workload and different autonomy settings in Pilot Study 2

Results

One-way repeated measures Analysis of Variance (ANOVA) is conducted with the autonomy setting as the only within-subjects variable. Results are reported as significant for $\alpha < .05$.

Table A.2 summarizes the mean and standard error (SE) values of the participants' self-reported workload, driving task performance, their exerted torque during the lane-keeping stage, emergency maneuvering performance, participants' control effort under emergency, surveillance task performance, and time to finish the mission.

Participants' Self-reported Workload

There is no significant impact of autonomy settings on the participants' reported workload ($F(1, 7) = 1.669,\ p = 0.237$). Participants report a similar level of workload

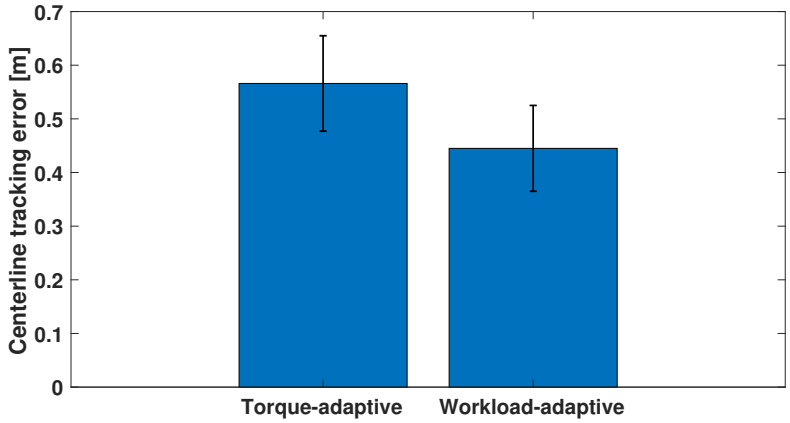

Figure A.5: Relationship between centerline tracking error and different autonomy settings in Pilot Study 2

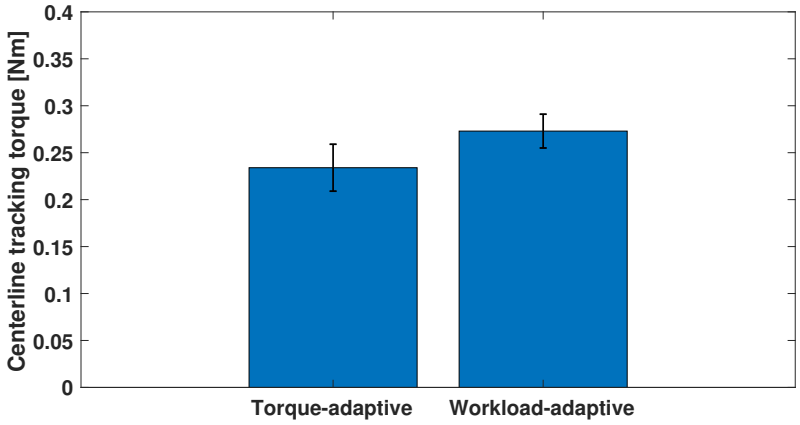

Figure A.6: Relationship between centerline tracking torque and different autonomy settings in Pilot Study 2

when workload-adaptive autonomy and torque-adaptive autonomy are implemented respectively, as shown in Fig. A.4.

Driving Task Performance

The autonomy setting has a significant impact on the driving task performance in the lane-keeping stage ($F(1,7) = 14.832,\ p = 0.006$). When workload-adaptive autonomy is implemented, the centerline tracking error is significantly reduced compared to the cases when torque-adaptive is used. Fig. A.5 shows the centerline tracking error in the lane-keeping stage when two autonomy settings are implemented.

Participants' Steering Control Effort During Lane Keeping

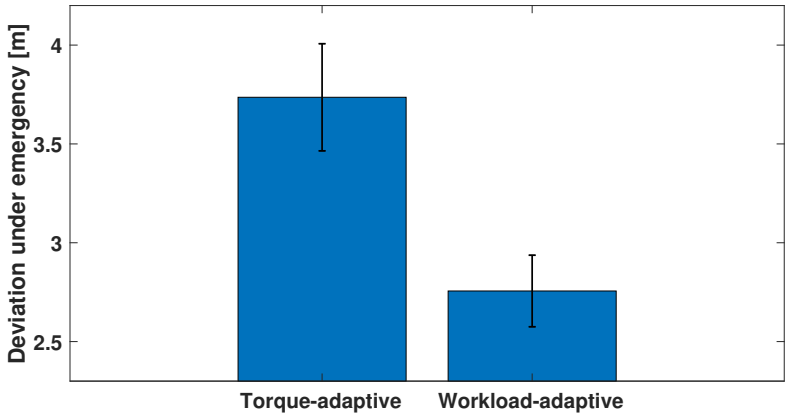

Figure A.7: Relationship between deviation from the centerline and different autonomy settings in Pilot Study 2

There is no significant impact of autonomy settings on the participants' steering control effort during the lane-keeping stage ($F(1,7) = 2.607,\ p = 0.150$). Participants exert a similar level of torque when workload-adaptive autonomy and torque-adaptive autonomy are implemented respectively, as shown in Fig. A.6.

Emergency Maneuvering Performance

The autonomy setting has a significant impact on the emergency maneuvering performance in the obstacle-avoidance stage ($F(1,7) = 17.962,\ p = 0.004$). When workload-adaptive autonomy is implemented, the deviation from the centerline is significantly reduced compared to the cases when torque-adaptive is used. Fig. A.7 shows the deviation from the centerline in the obstacle-avoidance stage when two autonomy settings are implemented.

Participants' Steering Control Effort Under Emergency

The autonomy setting has a significant impact on the steering control effort under emergency ($F(1,7) = 38.725,\ p < 0.001$). When torque-adaptive autonomy is implemented, the torque from participants during the obstacle-avoidance stage is significantly reduced compared to the cases when workload-adaptive is used. Fig. A.8 shows the human torque in the obstacle-avoidance stage when two autonomy settings are implemented.

Surveillance Task Performance

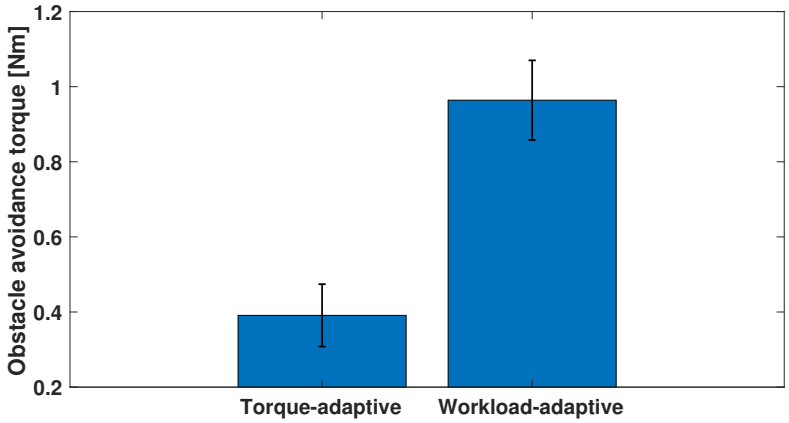

Figure A.8: Relationship between emergency steering control effort and different autonomy settings in Pilot Study 2

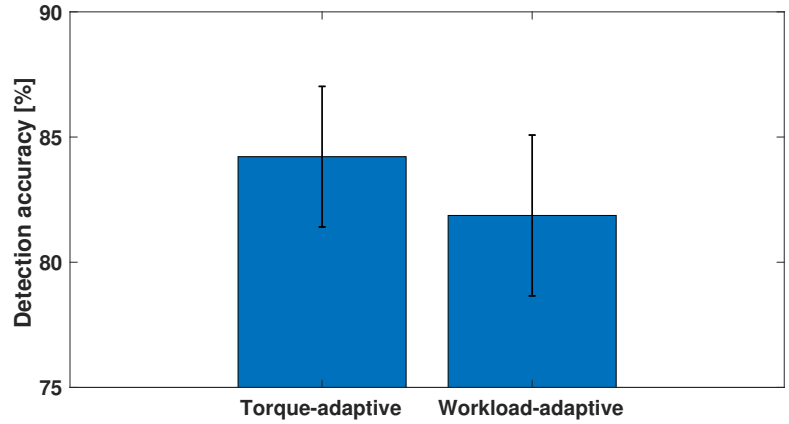

Figure A.9: Relationship between surveillance task detection accuracy and different autonomy settings in Pilot Study 2

There is no significant impact of autonomy settings on the surveillance task detection accuracy ($F(1,7) = 0.538,\ p = 0.487$). Participants have a similar level of detection accuracy when workload-adaptive autonomy and torque-adaptive autonomy are implemented respectively, as shown in Fig. A.9.

Time to Finish the Mission

The autonomy setting has a significant impact on the time to finish the mission ($F(1,7) = 614.785,\ p < 0.001$). When torque-adaptive autonomy is implemented, the time to finish the mission is significantly shortened compared to the cases when workload-adaptive is used. Fig. A.10 shows the mission duration when two autonomy

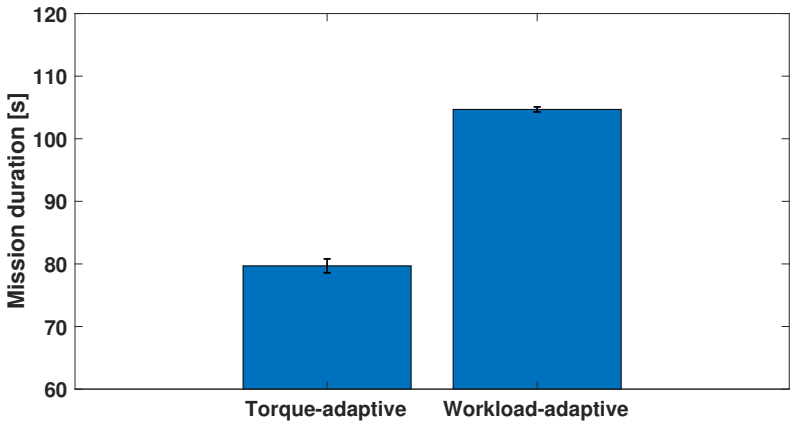

Figure A.10: Relationship between mission duration and different autonomy settings in Pilot Study 2

settings are implemented.

Discussion

Participants' Steering Control Effort in Lane-keeping Stage

The workload-adaptive autonomy does not have a significant difference in center-line tracking torque compared to the torque-adaptive autonomy. Even if the vehicle's speed is higher, the steering control effort is not decreased, which can be explained by the minor disagreement between agents.

Driving Task Performance

When high urgency is used for the surveillance task, the workload-adaptive autonomy achieves a significantly better driving task performance. It can be explained by the design principle of workload-adaptive autonomy. When the human operator experiences the over-loaded condition, the workload-adaptive autonomy reduces the speed limit, which will lead to a speed drop. The speed drop provides additional safety margin and operation room so that the human operator can handle the mission in an easier way. This extra safe margin is proved to be beneficial in this pilot study by improving the driving performance.

Participants' Steering Control Effort Under Emergency

The workload-adaptive autonomy has a higher level of the steering control effort

in the obstacle-avoidance stage compared to the torque-adaptive autonomy cases. It aligns with the previous finding in Sec. 4.3.2.3 that a faster average speed leads to a smaller steering control effort when avoiding the obstacles. The reason is similar: the human driver intervenes more actively, given the extra safety margin to maneuver the vehicle provided by the vehicle's low traveling speed.

Emergency Maneuvering Performance

From the previous explanation, a lower speed limit gives the human operator more safety margin to maneuver the vehicle and adjust the behavior to prevent further deviation from the centerline. The design principle of workload-adaptive autonomy reduces the speed limit while the torque-adaptive autonomy does not provide the speed reduction as much as workload-adaptive autonomy. This difference explains why workload-adaptive autonomy outperforms torque-adaptive autonomy in terms of emergency maneuvering performance.

Time to Finish the Mission

The workload-adaptive autonomy reduces the maximum speed limit when the participants experience the over-loaded condition, which happens more often when the surveillance task urgency is high. As a result, the time to finish the mission is longer than the torque-adaptive autonomy, whose maximum speed does not drop significantly in the over-loaded condition.

Conclusion For Adaptive Control Consolidation

The results show that adapting to workload provides additional safety margin by reducing the maximum speed limit. It leads to an improvement in driving performance, including the lane-keeping stage and the obstacle-avoidance stage at the cost of time and steering control effort in the obstacle-avoidance stage. These characteristics are summarized in Fig. A.11.

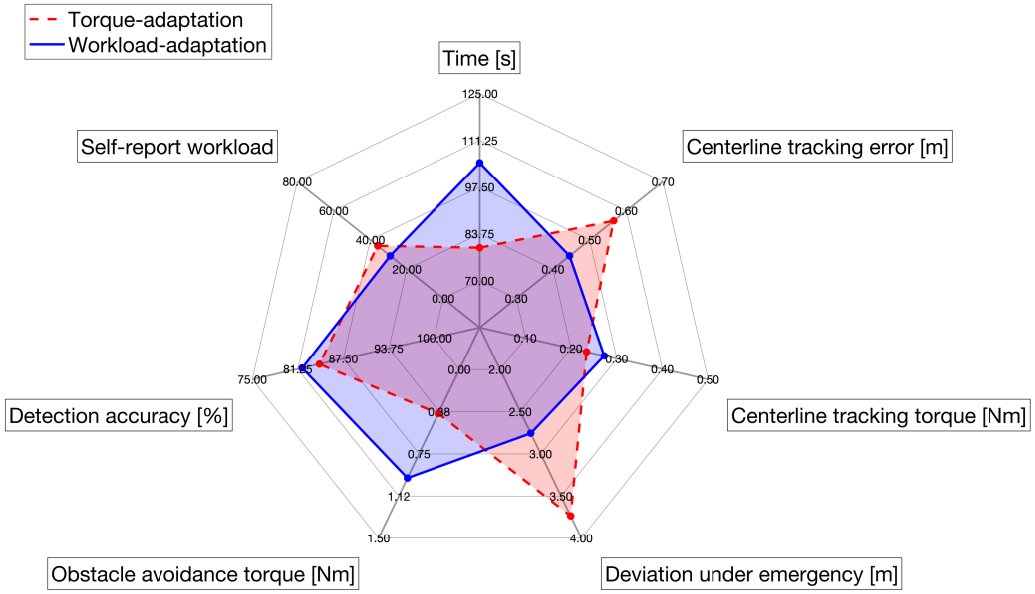

Figure A.11: Spider plot showing all metrics in Experiment Pilot Study 2 when different autonomy settings are used. The axis is the dimension of the metrics. The more away from the axis, the worse performance in that dimension. The one with a smaller coverage is considered a better design.

Bibliography

[1] S. A. Bagloee, M. Tavana, M. Asadi, and T. Oliver, "Autonomous vehicles: challenges, opportunities, and future implications for transportation policies," *Journal of Modern Transportation*, vol. 24, no. 4, p. 284–303, 2016.

[2] Y. Chen, J. Gonder, S. Young, and E. Wood, "Quantifying autonomous vehicles national fuel consumption impacts: A data-rich approach," *Transportation Research Part A: Policy and Practice*, vol. 122, pp. 134–145, 2019.

[3] A. Vahidi and A. Sciarretta, "Energy saving potentials of connected and automated vehicles," *Transportation Research Part C: Emerging Technologies*, vol. 95, pp. 822–843, 2018.

[4] A. Olia, S. Razavi, B. Abdulhai, and H. Abdelgawad, "Traffic capacity implications of automated vehicles mixed with regular vehicles," *Journal of Intelligent Transportation Systems*, vol. 22, no. 3, pp. 244–262, 2018.

[5] J. Carbaugh, D. N. Godbole, and R. Sengupta, "Safety and Capacity Analysis of Automated and Manual Highway Systems," tech. rep., Institute of Transportation Studies, UC Berkeley, Nov. 1999.

[6] J. M. Anderson, N. Kalra, K. D. Stanley, P. Sorensen, C. Samaras, and T. A. Oluwatola, *Autonomous Vehicle Technology: A Guide for Policymakers*. Santa Monica, CA: RAND Corporation, 2016.

[7] A. T. Ben Husch, "Regulating autonomous vehicles, national conference of state legislatures." `https://www.ncsl.org/research/transportation/regulating-autonomous-vehicles.aspx`.

[8] S. Zang, M. Ding, D. Smith, P. Tyler, T. Rakotoarivelo, and M. A. Kaafar, "The impact of adverse weather conditions on autonomous vehicles: How rain, snow, fog, and hail affect the performance of a self-driving car," *IEEE Vehicular Technology Magazine*, vol. 14, no. 2, pp. 103–111, 2019.

[9] R. L. McCarthy, "Autonomous Vehicle Accident Data Analysis: California OL 316 Reports: 2015–2020," *ASCE-ASME J Risk and Uncert in Engrg Sys Part B Mech Engrg*, vol. 8, 09 2021. 034502.

[10] C. Urmson, J. Anhalt, D. Bagnell, C. Baker, R. Bittner, M. N. Clark, J. Dolan, D. Duggins, T. Galatali, C. Geyer, M. Gittleman, S. Harbaugh, M. Hebert, T. M. Howard, S. Kolski, A. Kelly, M. Likhachev, M. McNaughton, N. Miller, K. Peterson, B. Pilnick, R. Rajkumar, P. Rybski, B. Salesky, Y.-W. Seo, S. Singh, J. Snider, A. Stentz, W. R. Whittaker, Z. Wolkowicki, J. Ziglar, H. Bae, T. Brown, D. Demitrish, B. Litkouhi, J. Nickolaou, V. Sadekar, W. Zhang, J. Struble, M. Taylor, M. Darms, and D. Ferguson, "Autonomous driving in urban environments: Boss and the urban challenge," *Journal of Field Robotics*, vol. 25, no. 8, pp. 425–466, 2008.

[11] S. Zilberstein, "Building strong semi-autonomous systems," in *Proceedings of the Twenty-Ninth AAAI Conference on Artificial Intelligence*, AAAI'15, p. 4088–4092, AAAI Press, 2015.

[12] *Taxonomy and Definitions for Terms Related to Driving Automation Systems for On-Road Motor Vehicles*, Sep 2016.

[13] S. M. Erlien, S. Fujita, and J. C. Gerdes, "Shared steering control using safe envelopes for obstacle avoidance and vehicle stability," *IEEE Transactions on Intelligent Transportation Systems*, vol. 17, no. 2, pp. 441–451, 2016.

[14] W. Schwarting, J. Alonso-Mora, L. Pauli, S. Karaman, and D. Rus, "Parallel autonomy in automated vehicles: Safe motion generation with minimal intervention," in *2017 IEEE International Conference on Robotics and Automation (ICRA)*, pp. 1928–1935, May 2017.

[15] W. Schwarting, J. Alonso-Mora, L. Paull, S. Karaman, and D. Rus, "Safe nonlinear trajectory generation for parallel autonomy with a dynamic vehicle model," *IEEE Transactions on Intelligent Transportation Systems*, vol. 19, no. 9, pp. 2994–3008, 2018.

[16] J. Storms, K. Chen, and D. Tilbury, "A shared control method for obstacle avoidance with mobile robots and its interaction with communication delay," *The International Journal of Robotics Research*, vol. 36, no. 5-7, pp. 820–839, 2017.

[17] F. Altché, X. Qian, and A. de La Fortelle, "An algorithm for supervised driving of cooperative semi-autonomous vehicles," *IEEE Transactions on Intelligent Transportation Systems*, vol. 18, no. 12, pp. 3527–3539, 2017.

[18] W. Schwarting, J. Alonso-Mora, L. Pauli, S. Karaman, and D. Rus, "Parallel autonomy in automated vehicles: Safe motion generation with minimal intervention," in *2017 IEEE International Conference on Robotics and Automation (ICRA)*, pp. 1928–1935, 2017.

[19] S. J. Anderson, S. C. Peters, T. E. Pilutti, and K. Iagnemma, "Design and development of an optimal-control-based framework for trajectory planning,

threat assessment, and semi-autonomous control of passenger vehicles in hazard avoidance scenarios," in *Robotics Research* (C. Pradalier, R. Siegwart, and G. Hirzinger, eds.), (Berlin, Heidelberg), pp. 39–54, Springer Berlin Heidelberg, 2011.

[20] S. J. Anderson, S. B. Karumanchi, and K. Iagnemma, "Constraint-based planning and control for safe, semi-autonomous operation of vehicles," in *2012 IEEE Intelligent Vehicles Symposium*, pp. 383–388, 2012.

[21] S. J. Anderson, J. M. Walker, and K. Iagnemma, "Experimental performance analysis of a homotopy-based shared autonomy framework," *IEEE Transactions on Human-Machine Systems*, vol. 44, no. 2, pp. 190–199, 2014.

[22] M. Yue, C. Fang, H. Zhang, and J. Shangguan, "Adaptive authority allocation-based driver-automation shared control for autonomous vehicles," *Accident Analysis & Prevention*, vol. 160, p. 106301, 2021.

[23] Y. Lu, J. Liang, G. Yin, L. Xu, J. Wu, J. Feng, and F. Wang, "A shared control design for steering assistance system considering driver behaviors," *IEEE Transactions on Intelligent Vehicles*, pp. 1–1, 2022.

[24] R. Li, Y. Li, S. E. Li, E. Burdet, and B. Cheng, "Driver-automation indirect shared control of highly automated vehicles with intention-aware authority transition," in *2017 IEEE Intelligent Vehicles Symposium (IV)*, pp. 26–32, 2017.

[25] M. Li, H. Cao, X. Song, Y. Huang, J. Wang, and Z. Huang, "Shared control driver assistance system based on driving intention and situation assessment," *IEEE Transactions on Industrial Informatics*, vol. 14, no. 11, pp. 4982–4994, 2018.

[26] F. Flemisch, A. Schieben, J. Kelsch, and C. Löper, "Automation spectrum, inner / outer compatibility and other potentially useful human factors concepts for assistance and automation," in *Annual Meeting Human Factors & Ergonomics Society, European Chapter* (D. de Waard, F. Flemisch, B. Lorenz, H. Oberheid, and K. Brookhuis, eds.), Shaker Publishing, 2008.

[27] P. G. Griffiths and R. B. Gillespie, "Sharing control between humans and automation using haptic interface: Primary and secondary task performance benefits," *Human Factors*, vol. 47, no. 3, pp. 574–590, 2005.

[28] S. M. Petermeijer, D. A. Abbink, and J. C. F. de Winter, "Should drivers be operating within an automation-free bandwidth? evaluating haptic steering support systems with different levels of authority," *Human Factors*, vol. 57, no. 1, pp. 5–20, 2015.

[29] A. Bhardwaj, A. Ghasemi, Y. Zheng, H. Febbo, P. Jayakumar, T. Ersal, J. L. Stein, and B. Gillespie, "Who's the boss? arbitrating control authority between a human driver and automation system," *Transportation Research Part F: Psychology and Behaviour*, vol. 68, pp. 144–160, 2020.

[30] S. Tada, K. Sonoda, and T. Wada, "Simultaneous achievement of workload reduction and skill enhancement in backward parking by haptic guidance," *IEEE Transactions on Intelligent Vehicles*, vol. 1, no. 4, pp. 292–301, 2016.

[31] Z. Ercan, A. Carvalho, H. E. Tseng, M. Gökaşan, and F. Borrelli, "A predictive control framework for torque-based steering assistance to improve safety in highway driving," *Vehicle System Dynamics*, vol. 56, no. 5, pp. 810–831, 2018.

[32] T. Brandt, T. Sattel, and M. Bohm, "Combining haptic human-machine interaction with predictive path planning for lane-keeping and collision avoidance systems," in *2007 IEEE Intelligent Vehicles Symposium*, pp. 582–587, 2007.

[33] B. Forsyth and K. Maclean, "Predictive haptic guidance: intelligent user assistance for the control of dynamic tasks," *IEEE Transactions on Visualization and Computer Graphics*, vol. 12, no. 1, pp. 103–113, 2006.

[34] Z. Wang, R. Zheng, T. Kaizuka, K. Shimono, and K. Nakano, "The effect of a haptic guidance steering system on fatigue-related driver behavior," *IEEE Transactions on Human-Machine Systems*, vol. 47, no. 5, pp. 741–748, 2017.

[35] M. Mulder, D. A. Abbink, and E. R. Boer, "The effect of haptic guidance on curve negotiation behavior of young, experienced drivers," in *2008 IEEE International Conference on Systems, Man and Cybernetics*, pp. 804–809, Oct 2008.

[36] H. M. Zwaan, S. M. Petermeijer, and D. A. Abbink, "Haptic shared steering control with an adaptive level of authority based on time-to-line crossing," *IFAC-PapersOnLine*, vol. 52, no. 19, pp. 49–54, 2019. 14th IFAC Symposium on Analysis, Design, and Evaluation of Human Machine Systems (HMS) 2019.

[37] N. A. Oufroukh and S. Mammar, "Integrated driver co-pilote approach for vehicle lateral control," in *2014 IEEE Intelligent Vehicles Symposium Proceedings*, pp. 1163–1168, 2014.

[38] A.-T. Nguyen, C. Sentouh, and J.-C. Popieul, "Sensor reduction for driver-automation shared steering control via an adaptive authority allocation strategy," *IEEE/ASME Transactions on Mechatronics*, vol. 23, no. 1, pp. 5–16, 2018.

[39] A.-T. Nguyen, C. Sentouh, and J.-C. Popieul, "Driver-automation cooperative approach for shared steering control under multiple system constraints: Design and experiments," *IEEE Transactions on Industrial Electronics*, vol. 64, no. 5, pp. 3819–3830, 2017.

[40] M. Benloucif, C. Sentouh, J. Floris, P. Simon, and J.-C. Popieul, "Online adaptation of the level of haptic authority in a lane keeping system considering the driver's state," *Transportation Research Part F: Traffic Psychology and Behaviour*, vol. 61, pp. 107–119, 2019.

[41] C. Sentouh, A.-T. Nguyen, M. A. Benloucif, and J.-C. Popieul, "Driver-automation cooperation oriented approach for shared control of lane keeping assist systems," *IEEE Transactions on Control Systems Technology*, vol. 27, no. 5, pp. 1962–1978, 2019.

[42] D. A. Abbink, D. Cleij, M. Mulder, and M. M. v. Paassen, "The importance of including knowledge of neuromuscular behaviour in haptic shared control," in *2012 IEEE International Conference on Systems, Man, and Cybernetics (SMC)*, pp. 3350–3355, 2012.

[43] A. D.A. and M. M., "Neuromuscular analysis as a guideline in designing shared control," in *Advances in Haptics* (M. H. Zadeh, ed.), ch. 27, Rijeka: IntechOpen, 2010.

[44] D. Waard, "The measurement of drivers' mental workload," *PhD thesis*, 01 1997.

[45] R. D. O'donnell and F. T. Eggemeier, *Workload assessment methodology.* 1986.

[46] R. Parasuraman, T. B. Sheridan, and C. D. Wickens, "Situation awareness, mental workload, and trust in automation: Viable, empirically supported cognitive engineering constructs," *Journal of Cognitive Engineering and Decision Making*, vol. 2, no. 2, pp. 140–160, 2008.

[47] P. C. Schutte, "How to make the most of your human: Design considerations for single pilot operations," in *Engineering Psychology and Cognitive Ergonomics* (D. Harris, ed.), (Cham), pp. 480–491, Springer International Publishing, 2015.

[48] F. Flemisch, F. Nashashibi, N. Rauch, A. Schieben, S. Glaser, G. Temme, P. Resende, B. Vanholme, C. Löper, G. Thomaidis, H. Mosebach, J. Schomerus, S. Hima, and A. Kaußner, "Towards highly automated driving: Intermediate report on the haveit-joint system," in *Proc. 3rd Eur. Road Transp. Res. Arena*, 2010.

[49] P. H. Seong, H. G. Kang, M. G. Na, J. H. Kim, G. Heo, and Y. Jung, "Advanced mmis toward substantial reduction in human errors in npps," *Nuclear Engineering and Technology*, vol. 45, no. 2, pp. 125–140, 2013.

[50] B. Mekdeci and M. L. Cummings, "Modeling multiple human operators in the supervisory control of heterogeneous unmanned vehicles," in *Proceedings of the 9th Workshop on Performance Metrics for Intelligent Systems*, PerMIS '09, (New York, NY, USA), p. 1–8, Association for Computing Machinery, 2009.

[51] P. A. Hancock, "A dynamic model of stress and sustained attention," *Human Factors*, vol. 31, no. 5, pp. 519–537, 1989. PMID: 2625347.

[52] R. M. Yerkes and J. D. Dodson, "The relation of strength of stimulus to rapidity of habit-formation," *Journal of Comparative Neurology and Psychology*, vol. 18, no. 5, pp. 459–482, 1908.

[53] B. Mehler, B. Reimer, J. F. Coughlin, and J. A. Dusek, "Impact of incremental increases in cognitive workload on physiological arousal and performance in young adult drivers," *Transportation Research Record*, vol. 2138, no. 1, pp. 6–12, 2009.

[54] S. Lu, M. Y. Zhang, T. Ersal, and X. J. Yang, "Workload management in teleoperation of unmanned ground vehicles: Effects of a delay compensation aid on human operators' workload and teleoperation performance," *International Journal of Human–Computer Interaction*, pp. 1–11, 2019.

[55] G. F. Briggs, G. J. Hole, and M. F. Land, "Emotionally involving telephone conversations lead to driver error and visual tunnelling," *Transportation Research Part F: Traffic Psychology and Behaviour*, vol. 14, no. 4, pp. 313–323, 2011.

[56] N. Li and C. Busso, "Detecting drivers' mirror-checking actions and its application to maneuver and secondary task recognition," *IEEE Transactions on Intelligent Transportation Systems*, vol. 17, no. 4, pp. 980–992, 2016.

[57] Y. Hwang, D. Yoon, H. S. Kim, and K.-H. Kim, "A validation study on a subjective driving workload prediction tool," *IEEE Transactions on Intelligent Transportation Systems*, vol. 15, no. 4, pp. 1835–1843, 2014.

[58] G. Matthews, "Individual differences in driver stress and performance," *Proceedings of the Human Factors and Ergonomics Society Annual Meeting*, vol. 40, no. 12, pp. 579–583, 1996.

[59] G. Matthews, T. J.Sparkes, and H. M.Bygrave, "Attentional overload, stress, and simulate driving performance," *Human Performance*, vol. 9, no. 1, pp. 77–101, 1996.

[60] J. D. Lee, C. D. Wickens, Y. Liu, and L. N. Boyle, *Designing for people: an introduction to human factors engineering*. CreateSpace, 2017.

[61] M. Cummings and S. Guerlain, "Developing operator capacity estimates for supervisory control of autonomous vehicles," *Human Factors*, vol. 49, no. 1, pp. 1–15, 2007. PMID: 17315838.

[62] N. Du, J. Kim, F. Zhou, E. Pulver, D. M. Tilbury, L. P. Robert, A. K. Pradhan, and X. J. Yang, "Evaluating effects of cognitive load, takeover request lead time, and traffic density on drivers' takeover performance in conditionally automated driving," in *12th International Conference on Automotive User Interfaces and Interactive Vehicular Applications*, AutomotiveUI '20, (New York, NY, USA), p. 66–73, Association for Computing Machinery, 2020.

[63] F. N. Biondi, M. Lohani, R. Hopman, S. Mills, J. M. Cooper, and D. L. Strayer, "80 mph and out-of-the-loop: Effects of real-world semi-automated driving on driver workload and arousal," *Proceedings of the Human Factors and Ergonomics Society Annual Meeting*, vol. 62, no. 1, pp. 1878–1882, 2018.

[64] A. Broad, T. Murphey, and B. Argall, "Highly parallelized data-driven mpc for minimal intervention shared control," *arXiv preprint arXiv:1906.02318*, 2019.

[65] A. Broad, I. Abraham, T. Murphey, and B. Argall, "Data-driven koopman operators for model-based shared control of human–machine systems," *The International Journal of Robotics Research*, vol. 39, no. 9, pp. 1178–1195, 2020.

[66] A. H. Ghasemi, M. Johns, B. Garber, P. Boehm, P. Jayakumar, W. Ju, and R. B. Gillespie, "Role negotiation in a haptic shared control framework," in *Adjunct Proceedings of the 8th International Conference on Automotive User Interfaces and Interactive Vehicular Applications*, AutomotiveUI '16 Adjunct, (New York, NY, USA), p. 179–184, Association for Computing Machinery, 2016.

[67] M. Johns, B. Mok, D. Sirkin, N. Gowda, C. Smith, W. Talamonti, and W. Ju, "Exploring shared control in automated driving," in *2016 11th ACM/IEEE International Conference on Human-Robot Interaction (HRI)*, pp. 91–98, 2016.

[68] M. A. Benloucif, A.-T. Nguyen, C. Sentouh, and J.-C. Popieul, "A new scheme for haptic shared lateral control in highway driving using trajectory planning," *IFAC-PapersOnLine*, vol. 50, no. 1, pp. 13834–13840, 2017. 20th IFAC World Congress.

[69] A. Benloucif, A.-T. Nguyen, C. Sentouh, and J.-C. Popieul, "Cooperative trajectory planning for haptic shared control between driver and automation in highway driving," *IEEE Transactions on Industrial Electronics*, vol. 66, no. 12, pp. 9846–9857, 2019.

[70] H. S. Kim, Y. Hwang, D. Yoon, W. Choi, and C. H. Park, "Driver workload characteristics analysis using eeg data from an urban road," *IEEE Transactions on Intelligent Transportation Systems*, vol. 15, no. 4, pp. 1844–1849, 2014.

[71] K. Fitzpatrick, S. Chrysler, E. S. Park, A. Nelson, J. Robertson, and V. Iragavarapu, "Driver workload at higher speeds," 2010.

[72] Y. Zheng, M. J. Brudnak, P. Jayakumar, J. L. Stein, and T. Ersal, "An experimental evaluation of a model-free predictor framework in teleoperated vehicles," in *IFAC Workshop on Time Delay Systems*, vol. 49, pp. 157–164, 2016.

[73] J. Liu, P. Jayakumar, J. L. Overholt, J. L. Stein, and T. Ersal, "The Role of Model Fidelity in Model Predictive Control Based Hazard Avoidance in Unmanned Ground Vehicles Using LIDAR Sensors," vol. 3 of *Dynamic Systems and Control Conference*, 10 2013. V003T46A005.

[74] MathWorks, "Simulink desktop real-time." `https://www.mathworks.com/products/simulink-desktop-real-time.html`.

[75] R. Luo, Y. Weng, Y. Wang, P. Jayakumar, M. J. Brudnak, V. Paul, V. R. Desaraju, J. L. Stein, T. Ersal, and X. J. Yang, "A workload adaptive haptic shared control scheme for semi-autonomous driving," *Accident Analysis & Prevention*, vol. 152, p. 105968, 2021.

[76] MathWorks, "Simulink 3d animation." `https://www.mathworks.com/products/3d-animation.html`.

[77] Epic Games, "Unreal engine 4." `https://www.unrealengine.com`.

[78] V. GAMES, "Landscape auto material." `https://www.unrealengine.com/marketplace/en-US/product/landscape-auto-material`.

[79] Defect, "Rusty barrels vol.1." `https://www.unrealengine.com/marketplace/en-US/product/rusty-barrels`.

[80] J. Liu, P. Jayakumar, J. L. Stein, and T. Ersal, "Combined speed and steering control in high speed autonomous ground vehicles for obstacle avoidance using model predictive control," *IEEE Transactions on Vehicular Technology*, vol. 66, no. 10, pp. 8746–8763, 2017.

[81] H. Febbo, J. Liu, P. Jayakumar, J. L. Stein, and T. Ersal, "Moving obstacle avoidance for large, high-speed autonomous ground vehicles," in *2017 American Control Conference (ACC)*, pp. 5568–5573, IEEE, 2017.

[82] J. Liu, P. Jayakumar, J. L. Stein, and T. Ersal, "A study on model fidelity for model predictive control-based obstacle avoidance in high-speed autonomous ground vehicles," *Vehicle System Dynamics*, vol. 54, no. 11, pp. 1629–1650, 2016.

[83] H. Febbo, "Nloptcontrol.jl." `https://github.com/JuliaMPC/NLOptControl.jl`, 2017.

[84] A. Wächter and L. T. Biegler, "On the implementation of an interior-point filter line-search algorithm for large-scale nonlinear programming," *Mathematical Programming*, vol. 106, no. 1, pp. 25–57, 2006.

[85] J. Liu, P. Jayakumar, J. L. Stein, and T. Ersal, "A nonlinear model predictive control formulation for obstacle avoidance in high-speed autonomous ground vehicles in unstructured environments," *Vehicle System Dynamics*, vol. 56, no. 6, pp. 853–882, 2018.

[86] R. Luo, Y. Wang, Y. Weng, V. Paul, M. J. Brudnak, P. Jayakumar, M. Reed, J. L. Stein, T. Ersal, and X. J. Yang, "Toward real-time assessment of workload: A bayesian inference approach," *Proceedings of the Human Factors and Ergonomics Society Annual Meeting*, vol. 63, no. 1, pp. 196–200, 2019.

[87] R. Luo, Y. Weng, P. Jayakumar, M. J. Brudnak, V. Paul, V. R. Desaraju, J. L. Stein, T. Ersal, and X. J. Yang, "Real-time workload estimation using eye tracking: A bayesian inference approach," *International Journal of Human-Computer Interaction*, Under Review.

[88] W. Wang, J. Xi, C. Liu, and X. Li, "Human-centered feed-forward control of a vehicle steering system based on a driver's path-following characteristics," *IEEE Transactions on Intelligent Transportation Systems*, vol. 18, no. 6, pp. 1440–1453, 2017.

[89] D. Tran, J. Du, W. Sheng, D. Osipychev, Y. Sun, and H. Bai, "A human-vehicle collaborative driving framework for driver assistance," *IEEE Transactions on Intelligent Transportation Systems*, vol. 20, no. 9, pp. 3470–3485, 2019.

[90] S. G. Hart and L. E. Staveland, "Development of nasa-tlx (task load index): Results of empirical and theoretical research," in *Human Mental Workload* (P. A. Hancock and N. Meshkati, eds.), vol. 52 of *Advances in Psychology*, pp. 139 – 183, North-Holland, 1988.

[91] B. M. Muir and N. Moray, "Trust in automation. Part II. Experimental studies of trust and human intervention in a process control simulation," *Ergonomics*, vol. 39, pp. 429–460, mar 1996.

[92] X. J. Yang, V. V. Unhelkar, K. Li, and J. A. Shah, "Evaluating effects of user experience and system transparency on trust in automation," in *2017 12th ACM/IEEE International Conference on Human-Robot Interaction (HRI)*, pp. 408–416, IEEE, 2017.

[93] N. Du, K. Y. Huang, and X. J. Yang, "Not All Information Is Equal: Effects of Disclosing Different Types of Likelihood Information on Trust, Compliance and Reliance, and Task Performance in Human-Automation Teaming," *Human Factors*, vol. 62, no. 6, pp. 987–1001, 2020.

[94] J.-Y. Jian, A. M. Bisantz, and C. G. Drury, "Foundations for an empirically determined scale of trust in automated systems," *International Journal of Cognitive Ergonomics*, vol. 4, no. 1, pp. 53–71, 2000.

[95] Y. Guo and X. J. Yang, "Modeling and Predicting Trust Dynamics in Human–Robot Teaming: A Bayesian Inference Approach," *International Journal of Social Robotics*, 2020.

[96] B. L. Hooey, D. B. Kaber, J. A. Adams, T. W. Fong, and B. F. Gore, "The underpinnings of workload in unmanned vehicle systems," *IEEE Transactions on Human-Machine Systems*, vol. 48, no. 5, pp. 452–467, 2017.

[97] H. Zhang, Y. Zhang, Y. Xiao, and C. Wu, "Analyzing the influencing factors and workload variation of takeover behavior in semi-autonomous vehicles," *International Journal of Environmental Research and Public Health*, vol. 19, no. 3, 2022.

[98] "Armor: The hmmwv built for hard time." https://strategypage.com/htmw/htarm/articles/20140530.aspx, 2014.

[99] D. W. J. Van Der Wiel, M. M. van Paassen, M. Mulder, M. Mulder, and D. A. Abbink, "Driver adaptation to driving speed and road width: Exploring parameters for designing adaptive haptic shared control," in *2015 IEEE International Conference on Systems, Man, and Cybernetics*, pp. 3060–3065, 2015.

[100] Y. Weng, R. Luo, P. Jayakumar, M. J. Brudnak, V. Paul, V. R. Desaraju, J. L. Stein, X. J. Yang, and T. Ersal, "Design and evaluation of a workload-adaptive haptic shared control framework for semi-autonomous driving," in *2020 American Control Conference (ACC)*, pp. 4369–4374, 2020.

[101] Y. Weng, R. Luo, P. Jayakumar, M. J. Brudnak, V. Paul, V. R. Desaraju, J. L. Stein, X. J. Yang, and T. Ersal, "A workload adaptive autonomy formulation for semi-autonomous driving," In preparation.

[102] D. A. Abbink, M. Mulder, F. C. T. Van der Helm, M. Mulder, and E. R. Boer, "Measuring neuromuscular control dynamics during car following with continuous haptic feedback," *IEEE Transactions on Systems, Man, and Cybernetics, Part B (Cybernetics)*, vol. 41, no. 5, pp. 1239–1249, 2011.

[103] M. Mulder, D. A. Abbink, M. M. van Paassen, and M. Mulder, "Design of a haptic gas pedal for active car-following support," *IEEE Transactions on Intelligent Transportation Systems*, vol. 12, no. 1, pp. 268–279, 2011.

[104] S. Mosbach, M. Flad, and S. Hohmann, "Cooperative longitudinal driver assistance system based on shared control," in *2017 IEEE International Conference on Systems, Man, and Cybernetics (SMC)*, pp. 1776–1781, 2017.

[105] C. Herff, D. Heger, O. Fortmann, J. Hennrich, F. Putze, and T. Schultz, "Mental workload during n-back task—quantified in the prefrontal cortex using fnirs," *Frontiers in Human Neuroscience*, vol. 7, 2014.

[106] M. J. Kane, A. R. A. Conway, T. K. Miura, and G. J. H. Colflesh, "Working memory, attention control, and the n-back task: a question of construct validity.," *Journal of experimental psychology. Learning, memory, and cognition*, vol. 33 3, pp. 615–622, 2007.

[107] S. M. Jaeggi, M. Buschkuehl, W. J. Perrig, and B. Meier, "The concurrent validity of the n-back task as a working memory measure," *Memory*, vol. 18, no. 4, pp. 394–412, 2010. PMID: 20408039.

[108] D. Shinar, N. Tractinsky, and R. Compton, "Effects of practice, age, and task demands, on interference from a phone task while driving," *Accident Analysis & Prevention*, vol. 37, no. 2, pp. 315–326, 2005.

[109] T. Ranney, J. Harbluk, and I. Noy, "The effects of voice technology on test track driving performance: Implications for driver distraction," *Proceedings of the Human Factors and Ergonomics Society Annual Meeting*, vol. 46, pp. 1814–1818, 09 2002.

[110] T. A. Ranney, E. N. Mazzae, W. R. Garrott, and F. S. Barickman, "Development of a test protocol to demonstrate the effects of secondary tasks on closed-course driving performance," *Proceedings of the Human Factors and Ergonomics Society Annual Meeting*, vol. 45, no. 23, pp. 1581–1585, 2001.

[111] B. H. Kantowitz, R. J. Hanowski, and L. Tijerina, "Simulator evaluation of heavy-vehicle driver workload: Ii: Complex secondary tasks," *Proceedings of the Human Factors and Ergonomics Society Annual Meeting*, vol. 40, no. 18, pp. 877–881, 1996.

[112] P. C. Burns, P. L. Trbovich, T. McCurdie, and J. L. Harbluk, "Measuring distraction: Task duration and the lane-change test (lct)," *Proceedings of the Human Factors and Ergonomics Society Annual Meeting*, vol. 49, no. 22, pp. 1980–1983, 2005.

[113] R. Toups, T. J. Chirles, J. P. Ehsani, J. P. Michael, J. P. K. Bernstein, M. Calamia, T. D. Parsons, D. B. Carr, and J. N. Keller, "Driving Performance in Older Adults: Current Measures, Findings, and Implications for Roadway Safety," *Innovation in Aging*, vol. 6, 01 2022. igab051.

[114] M. Karthaus and M. Falkenstein, "Functional changes and driving performance in older drivers: Assessment and interventions," *Geriatrics*, vol. 1, no. 2, 2016.

[115] J. Gong, X. Guo, L. Pan, C. Qi, and Y. Wang, "Impact of age on takeover behavior in automated driving in complex traffic situations: A case study of beijing, china," *Sustainability*, vol. 14, no. 1, 2022.

[116] Y. Zhu, M. Jiang, and T. Yamamoto, "Analysis on the driving behavior of old drivers by driving recorder gps trajectory data," *Asian Transport Studies*, vol. 8, p. 100063, 2022.

[117] Y. Zhao and T. Yamamoto, "Review of studies on older drivers' behavior and stress—methods, results, and outlook," *Sensors*, vol. 21, no. 10, 2021.

[118] S. Doroudgar, H. M. Chuang, P. J. Perry, K. Thomas, K. Bohnert, and J. Canedo, "Driving performance comparing older versus younger drivers," *Traffic Injury Prevention*, vol. 18, no. 1, pp. 41–46, 2017. PMID: 27326512.

[119] M. Pinto, V. Cavallo, and T. Ohlmann, "The development of driving simulators: Toward a multisensory solution," *Le Travail Humain*, vol. 71, no. 1, pp. 62–95, 2008.

[120] A. Riener and J. Kepler, "Reaction time differences in real and simulated driving," in *2009 Adjunct Proceedings of the First International Conference on Automotive User Interfaces and Interactive Vehicular Applications (2009 AutomotiveUI)*, 2009.

[121] P. Philip, P. Sagaspe, J. Taillard, C. Valtat, N. Moore, T. Åkerstedt, A. Charles, and B. Bioulac, "Fatigue, Sleepiness, and Performance in Simulated Versus Real Driving Conditions," *Sleep*, vol. 28, pp. 1511–1516, 12 2005.

[122] M. J. Johnson, T. Chahal, A. Stinchcombe, N. Mullen, B. Weaver, and M. Bédard, "Physiological responses to simulated and on-road driving," *International Journal of Psychophysiology*, vol. 81, no. 3, pp. 203–208, 2011. PROCEEDINGS OF THE 15TH WORLD CONGRESS OF PSYCHOPHYSIOLOGY of the International Organization of Psychophysiology (I.O.P.) Budapest, Hungary September 1-4, 2010.

[123] W. Wang, X. Na, D. Cao, J. Gong, J. Xi, Y. Xing, and F.-Y. Wang, "Decision-making in driver-automation shared control: A review and perspectives," *IEEE/CAA Journal of Automatica Sinica*, vol. 7, no. 5, pp. 1289–1307, 2020.

[124] X. Na and D. J. Cole, "Game-theoretic modeling of the steering interaction between a human driver and a vehicle collision avoidance controller," *IEEE Transactions on Human-Machine Systems*, vol. 45, no. 1, pp. 25–38, 2015.

[125] X. Na and D. J. Cole, "Linear quadratic game and non-cooperative predictive methods for potential application to modelling driver–afs interactive steering control," *Vehicle System Dynamics*, vol. 51, no. 2, pp. 165–198, 2013.

[126] X. Na and D. J. Cole, "Application of open-loop stackelberg equilibrium to modeling a driver's interaction with vehicle active steering control in obstacle avoidance," *IEEE Transactions on Human-Machine Systems*, vol. 47, no. 5, pp. 673–685, 2017.

[127] M. Flad, L. Fröhlich, and S. Hohmann, "Cooperative shared control driver assistance systems based on motion primitives and differential games," *IEEE Transactions on Human-Machine Systems*, vol. 47, no. 5, pp. 711–722, 2017.

[128] X. Ji, K. Yang, X. Na, C. Lv, and Y. Liu, "Shared steering torque control for lane change assistance: A stochastic game-theoretic approach," *IEEE Transactions on Industrial Electronics*, vol. 66, no. 4, pp. 3093–3105, 2019.

[129] A. H. Ghasemi, "Game Theoretic Modeling of a Steering Operation in a Haptic Shared Control Framework," vol. 2 of *Dynamic Systems and Control Conference*, 09 2018.

[130] S. Rothfuß, J. Inga, F. Köpf, M. Flad, and S. Hohmann, "Inverse optimal control for identification in non-cooperative differential games," *IFAC-PapersOnLine*, vol. 50, no. 1, pp. 14909–14915, 2017. 20th IFAC World Congress.

[131] M. Lemmer, F. Köpf, S. Schwab, M. Flad, and S. Hohmann, "Modeling of human-centered cooperative control by means of tracking in discrete time linear quadratic differential games," in *2018 IEEE First International Conference on Artificial Intelligence and Knowledge Engineering (AIKE)*, pp. 156–161, 2018.

[132] J. J. Inga Charaja, *Inverse Dynamic Game Methods for Identification of Cooperative System Behavior*. PhD thesis, Karlsruher Institut für Technologie (KIT), 2021.

[133] F. Köpf, J. Inga, S. Rothfuß, M. Flad, and S. Hohmann, "Inverse reinforcement learning for identification in linear-quadratic dynamic games," *IFAC-PapersOnLine*, vol. 50, no. 1, pp. 14902–14908, 2017. 20th IFAC World Congress.

[134] J. Inga, F. Köpf, M. Flad, and S. Hohmann, "Individual human behavior identification using an inverse reinforcement learning method," in *IEEE International Conference on Systems, Man and Cybernetics (SMC), Banff, AB, Canada, 5–8 October 2017*, p. 99–104, Institute of Electrical and Electronics Engineers (IEEE), 2017.

[135] J. R. Anderson, *The architecture of cognition*. Psychology Press, Taylor and Frances Group, 2009.

[136] J. R. Anderson, D. Bothell, M. D. Byrne, S. Douglass, C. Lebiere, and Y. Qin, "An integrated theory of the mind.," *Psychological review*, vol. 111, no. 4, p. 1036, 2004.

[137] C. Li, M. P. Cole, P. Jayakumar, and T. Ersal, "Modeling human steering behavior in haptic shared control of autonomy-enabled unmanned ground vehicles," *Human Factors*, Under review.